University of Alberta

The Role of the MUC1/ICAM-1 Interaction in Promoting Breast Cancer Cell Migration

by

Jennifer Joy Rahn

A thesis submitted to the Faculty of Graduate Studies and Research in partial fulfillment of the requirements for the degree of Doctor of Philosophy

Medical Sciences - Laboratory Medicine and Pathology

Edmonton, Alberta
Fall 2004

Library and Archives Canada

Published Heritage Branch

395 Wellington Street
Ottawa ON K1A 0N4
Canada

Bibliothèque et Archives Canada

Direction du Patrimoine de l'édition

395, rue Wellington
Ottawa ON K1A 0N4
Canada

Your file Votre référence
ISBN: 0-612-96007-2
Our file Notre référence
ISBN: 0-612-96007-2

The author has granted a non-exclusive license allowing the Library and Archives Canada to reproduce, loan, distribute or sell copies of this thesis in microform, paper or electronic formats.

The author retains ownership of the copyright in this thesis. Neither the thesis nor substantial extracts from it may be printed or otherwise reproduced without the author's permission.

L'auteur a accordé une licence non exclusive permettant à la Bibliothèque et Archives Canada de reproduire, prêter, distribuer ou vendre des copies de cette thèse sous la forme de microfiche/film, de reproduction sur papier ou sur format électronique.

L'auteur conserve la propriété du droit d'auteur qui protège cette thèse. Ni la thèse ni des extraits substantiels de celle-ci ne doivent être imprimés ou aturement reproduits sans son autorisation.

In compliance with the Canadian Privacy Act some supporting forms may have been removed from this thesis.

While these forms may be included in the document page count, their removal does not represent any loss of content from the thesis.

Conformément à la loi canadienne sur la protection de la vie privée, quelques formulaires secondaires ont été enlevés de cette thèse.

Bien que ces formulaires aient inclus dans la pagination, il n'y aura aucun contenu manquant.

Canada

Acknowledgements

This work would not have been possible without the support of the Alberta Cancer Board, the Canadian Breast Cancer Foundation and the Alberta Cancer Foundation.

Many thanks to my supervisors, Dr. Judith Hugh and Dr. Linda Pilarski, for all their guidance and patient instruction.

Thank you to Dr. Manijeh Pasdar, for Journal Club, my solid introduction to cell biology and moral support.

Thank you to Dr. Hanne Ostergaard for her intellectual support on the overall direction of this thesis.

Special reagents and cell lines, without which this work would have been incomplete, were generously provided by ICOS Corporation, Biomira Inc., Dr. Sandra Gendler, Dr. Joanne Emerman and Dr. Ken Dimock.

Thank you to Mr. John Hanson for help with the more complicated statistical analyses.

Thank you to Dr. Xuejun Sun, Dr. Michael Hendzel, Dr. Andy Shaw, Dr. Christi Andrin, Ms. Gerry Baron, Ms. Juanita Wizniak, Ms. Sophia Adamia, and Mr. Jon Keats for helping me with valuable technical advice and instruction.

Thank you to Dr. Wendy Gati, Dr. Bob Stinson, Dr. Qiang Shen, Mr. Rob Dupuit, Ms. Jean Melax and Ms. Adira Zefram for friendship, moral support and helping me get started.

Thank you to Dr. Greg Tyrrell and the Department of Laboratory Medicine and Pathology.

Table of Contents

	Page
Chapter 1: Introduction	1
1.0 Thesis Overview	2
1.1 Breast Cancer Pathology and Metastasis	4
1.1.1 The Normal Breast	4
1.1.2 The Cancerous Breast	5
1.1.2.1 Carcinogenesis	5
1.1.2.2 Breast Cancer Subtypes and Stages of Metastatic Progression	7
1.1.3 The Microenvironment and Metastasis	8
1.1.3.1 The Contribution of Fibroblasts to Metastasis	8
1.1.3.2 The Contribution of Endothelial Cells to Metastasis	10
1.1.3.2.1 Homing or Specific Extravasation	10
1.1.3.2.2 Seed vs. Soil	11
1.1.4 Similarities Between Leukocyte Extravasation During Inflammation and Tumour Extravasation During Metastasis	12
1.2 Structure and Function of the MUC1 and ICAM-1 Molecules	15
1.2.1 The MUC1 Physical Entity	15
1.2.1.1 Nomenclature	15
1.2.1.2 The Extracellular Domain	17
1.2.1.3 The Transmembrane Domain	20
1.2.1.4 The Cytoplasmic Domain	21
1.2.1.5 Splice Variants	23

Page

1.2.2 MUC1 in Normal and Malignant Breast Epithelia 24

1.2.3 MUC1 Functions 24

1.2.3.1 MUC1 and Disruption of Adherens Junctions and Matrix Adhesions 24

1.2.3.2 MUC1 Signalling 25

1.2.3.2.1 MUC1, EGFR and the MAPK Pathway 25

1.2.3.2.2 MUC1 as a "Sensor" of the Microenvironment 26

1.2.3.3 MUC1 May Be Involved in Motility and/or Directional Growth 27

1.2.3.4 Other Putative Functions 30

1.2.4 Basic Physiology of ICAM-1 30

1.2.5 ICAM-1 Function in Leukocyte Adhesion to Endothelia and Transendothelial Migration 34

1.3 Study Objectives 36

Chapter 2: Intracellular Distribution of MUC1 38

2.0 Introduction 39

2.1 Methods and Materials 40

2.1.1 Tumour Sections 40

2.1.2 Cells 41

2.1.3 Antibodies and Reagents 41

2.1.4 Immunohistochemical Staining of Paraffin Embedded Breast Tumours 42

2.1.5 Evaluation of Immunohistochemically Stained Tumours 43

2.1.6 Plasmid Construction 43

Page

2.1.6.1 PCR of the MUC1 and ICAM-1 Gene Inserts and Addition of Engineered Cut Sites. 44

2.1.6.2 Insertion of the PCR Products and Selection of Clones with the Correct Orientation of Gene Insert 46

2.1.6.3 Insertion of Synthetic Signal Sequences 47

2.1.7 Transfection and Subcloning 48

2.1.8 Confocal Microscopy of Fluorescently Labelled Cell Lines 49

2.1.8.1 MUC1 and β-Catenin Double Immunostain 49

2.1.8.2 MUC1 and ICAM-1 Fluorescent Detection 49

2.1.9 FRET 50

2.1.9.1 FRET by Acceptor Fluorescence Increase 50

2.1.9.2 FRET by Acceptor Photobleach 51

2.1.10 Statistical Analysis 51

2.2 Results 52

2.2.1 Literature Review Findings 52

2.2.2 Clinical Distribution of MUC1 in Breast Cancer 52

2.2.2.1 Normal Glandular Epithelia 52

2.2.2.2 Ductal Carcinoma 52

2.2.2.3 Invasive Lobular Carcinoma 58

2.2.2.4 MUC1 and β-Catenin 58

2.2.2.5 MUC1 and Nuclear Grade 61

2.2.3* In Vitro *Distribution of MUC1 in Cell Lines 68

2.2.3.1 MUC1 and β-Catenin in Breast Cancer Cell Lines 68

2.2.3.2 MUC1 and ICAM-1 in Heterotypic Co-Culture 66

2.2.3.3 MUC1 Distribution in Transfected Cell Lines 68

2.2.3.3.1 Characterisation of the YFP-MUC1 and CFP-ICAM-1 Transfectants 68

2.2.3.3.2 Fluorescent Microscopy of Transfectants 71

Page

2.2.3.4 MUC1 and ICAM-1 in Co-Cultured Transfectants 71

2.2.3.4.1 Three Dimensional Reconstructions 71

2.2.3.4.2 FRET by Acceptor Fluorescence Increase 76

2.2.3.4.3 FRET by Acceptor Photobleaching 79

2.3 Discussion 79

2.3.1 Intracellular Localisation of MUC1 is Important in Prognosis 79

2.3.2 MUC1 and Disruption of Cell-Cell Adhesion 83

2.3.3 MUC1 and Intracellular Localisation of β-Catenin 84

2.3.4 MUC1 and ICAM-1 Co-Localisation at Points of Heterotypic Cell Contact 84

2.3.5 Overview 86

Chapter 3: MUC1/ICAM-1 Interactions and Tumour Cell Migration 87

3.0 Introduction 88

3.1 Methods and Materials 89

3.1.1 Assay Development 89

3.1.2 Reagents 90

3.1.3 Primary Cells and Cell Lines 93

3.1.4 Transendothelial Migration Assay 93

3.1.5 Western Blotting and Band Density Analysis 95

3.1.6 Statistical Methods 95

3.1.7 Ethics 95

Page

3.2 Results 96

3.2.1 Cytokine Stimulation of ICAM-1 Expression Increased TEM_E in the Developmental Model 96

3.2.2 Synergy Between HUVECs and Primary Fibroblasts in Promoting TEM_E 99

3.2.3 Synergy is Specific to a Particular Microenvironment 101

3.2.4 Synergy is a Combination of the Physical Presence of ICAM-1 and Fibroblast Secreted Factors Acting on HUVECs 101

3.2.5 The Effect of Fibroblast Secreted Factors on HUVECs is to Further Upregulate ICAM-1 Expression 105

3.2.6 Cell Line Specific Migratory Responses are Influenced by the Level of MUC1 Expression 106

3.2.7 The MUC1/ICAM-1 Requirement for TEM_E Holds True with Generic Cell Types 112

3.3 Discussion 112

3.3.1 Both MUC1 and ICAM-1 are Involved in Epithelial Cell TEM_E 115

3.3.2 Specific Microenvironmental Factors Can Further Promote TEM_E in an ICAM-1-Dependent Manner 115

3.3.3 Endothelial Cell TEM_E Bears Resemblance to Leukocyte TEM_E 116

3.3.4 Overview 116

Chapter 4: Microenvironmental Influences on MCF-7 Integrin Expression 119

4.0 Introduction 120

Page

4.1 Methods and Materials 123

4.1.1 Reagents 123

4.1.2 Cells 124

4.1.3 Co-Culture 124

4.1.4 Flow Cytometry 126

4.2 Results 126

4.2.1 MCF-7 Cells Do Not Express Significant Levels of Surface β4-Integrins, Regardless of Culture Conditions 126

4.2.2 Decreases in MCF-7 Surface Expression of β1-Integrins is Independent of ICAM-1 Unless both Cytokines and Fibroblast Conditioned Media are Present 129

4.3 Discussion 131

4.3.1 The Potential Significance of the β1-Integrin Drop 131

4.3.2 Overview 132

Chapter 5: MUC1/ICAM-1 Interactions and Calcium Signalling 133

5.0 Introduction 134

5.1 Methods and Materials 134

5.1.1 Assay Development 134

5.1.2 Reagents 135

5.1.3 Cells 135

5.1.4 Calcium Oscillation Assay 137

5.1.5 Data Analysis 140

5.1.6 Western Blotting 140

Page

5.1.7 Flow Cytometry 142

5.1.8 Statistical Analysis 142

5.2 Results 142

5.2.1 Human ICAM-1 Transfected NIH 3T3 Cells can Induce Calcium Oscillations in Human Breast Cancer Cell Lines 142

5.2.2 Human ICAM-1 Transfected NIH 3T3 Cells can Induce Calcium Oscillations in Human MUC1-Transfected 293T Cells 143

5.2.3 Antibodies Against the MUC1 Extracellular Domain that are Known to Block Interaction with ICAM-1 can Diminish the Oscillatory Response 147

5.2.4 MUC1 Positive Cells can Induce a Mild Oscillatory Response in HUVECs Stimulated with Cytokines Known to Upregulate ICAM-1 Expression 147

5.3 Discussion 150

5.3.1 The MUC1/ICAM-1 Triggered Signal is Calcium Based, Oscillatory, Specific and Bi-Directional 150

5.3.2 Possible Signal Mediators and Downstream Targets 152

5.3.3 Overview 156

Chapter 6: Discussion 157

6.0 Thesis Overview 158

6.1 Properties of MUC1 that May be Related to Metastasis 159

6.1.1 Distribution 159

6.1.2 Adhesion and Dysadhesion 161

Page

6.1.3 Signalling 162

6.2 Possible Contributions of Endothelial and Stromal Cells to Metastasis 162

6.3 Relative Importance of the MUC1/ICAM-1 Interaction to Metastasis 164

6.4 Closing Remarks 165

References 166

Appendix I: The FRET Technique 187

Appendix II: Transwell Development Data 194

Appendix III: Calcium Oscillation Development Data 210

List of Tables

	Page
Table 1.1: Endothelial surface adhesion molecules involved in interactions with cancer cells	14
Table 2.1: Studies of MUC1 in Patients with Breast Carcinoma using Percent Positive Staining	53
Table 2.2: Studies of MUC1 in Patients with Breast Carcinoma with Subcellular Localisation	55
Table 3.1: Optimization of the Final Transwell Model Parameters	91
Table 3.2: Comparison of MCF-7 Migration Using the Transwell Method.	117
Table 4.1: β1-Integrins Show a Tendency to Decrease Expression as Transformed Epithelia Develop into Invasive Carcinomas	122
Table 5.1: Development of the Calcium Oscillation Assay	136

List of Figures

	Page
Figure 1.1: Normal Breast Architecture	6
Figure 1.2: Several adhesion molecules are involved in leukocyte to endothelial cell binding	13
Figure 1.3: The presence of MUC1 mRNA transcript in adult human tissues	16
Figure 1.4: Schematic of MUC1 and the MUC Family	18
Figure 1.5: Diagram of O- and N-linked glycosylations	19
Figure 1.6: Main features of the MUC1 cytoplasmic tail	22
Figure 1.7: MUC1 may complex with p120ctn to promote cell migration	29
Figure 1.8: Speculative diagram of how MUC1 may complex with β-catenin and APC to control the direction of cell growth	31
Figure 1.9: Schematic diagram of how MUC1 may be involved in β-catenin nuclear translocation and signalling	32
Figure 1.10: Schematic diagram of how MUC1 might be involved in γ-catenin nuclear translocation and signalling	33
Figure 1.11: The ICAM-1 Molecule	35
Figure 2.1: High overall MUC1 expression increases probability of survival (as described in the literature)	54
Figure 2.2: High cytoplasmic MUC1 expression corresponds to a decreased probability of survival (as described in the literature)	56
Figure 2.3: Staining of MUC1, β-Catenin and E-Cadherin in normal, glandular human breast epithelia	57
Figure 2.4: Staining of MUC1, β-Catenin and E-Cadherin in human breast ductal carcinoma	59
Figure 2.5: Staining of MUC1, β-Catenin and E-Cadherin in human breast lobular carcinoma	60

Page

Figure 2.6: Comparison of MUC1 and β-Catenin localisation in human breast carcinomas 62

Figure 2.7: Nuclear staining of the MUC1 cytoplasmic domain and β-Catenin in carcinomas of different human tissues 64

Figure 2.8: The mean nuclear grades of invasive ductal carcinomas according to the levels of MUC1 expression 65

Figure 2.9: MUC1 and β-Catenin staining in ZR-75-1 and MCF-7 human breast cancer cell lines 67

Figure 2.10: Endothelial ICAM-1 appears to cap at regions of cell-cell contact with MCF-7 cells 69

Figure 2.11: The SYM and SCI Constructs 70

Figure 2.12: Western Blot analysis of the SYM and SCI 293T subclones 72

Figure 2.13: Confocal and Fluorescent Microscopy analyses of SYM and SCI transfected cells 74

Figure 2.14: A co-localisation signal for YFP-MUC1 and CFP-ICAM-1 is visible with transfected 293T cells 75

Figure 2.15: Three dimensional projections of an SYM25 cell migrating through SCI4 cells 77

Figure 2.16: Images taken during the Acceptor Increase FRET experiment 78

Figure 2.17: Example of FRET attempt made using the SCI4 and SYM25 cells in the Acceptor Photobleaching experiments 80

Figure 2.18: Example of FRET attempt made using transiently SCI transfected EAhy926 cells and SYM25 cells in the Acceptor Photobleaching experiments 81

Figure 2.19: Negative control used in the EAhy926 Acceptor Photobleaching FRET Experiment 82

Figure 3.1: Optimized Transwell set up 92

Page

Figure 3.2: Addition of ICAM-1-Upregulating cytokines increases MCF-7 migration through an EAhy926 monolayer supported by a Transwell membrane 97

Figure 3.3: Larger numbers of MCF-7 subclones with higher MUC1 expression migrate through a cytokine-stimulated EAhy926 monolayer in comparison to subclones with lower expression 98

Figure 3.4: The combination of HUVECs and primary human fibroblasts synergistically promote MCF-7 cell TEM_E that is MUC1 and ICAM-1 dependent 100

Figure 3.5: The synergy effect is specific to the combination of HUVECs + primary human fibroblasts 102

Figure 3.6: The highest levels of MCF-7 TEM_E were observed in the presence of high ICAM-1 expressing cells on either side of the Transwell membrane, inflammatory cytokines, and fibroblast conditioned media 103

Figure 3.7: Inclusion of inflammatory cytokines and fibroblast conditioned media in co-culture systems results in increased endothelial ICAM-1 and corresponds to high MCF-7 TEM_E 107

Figure 3.8: Human breast cancer cell lines migrate though gelatin in a cell type-specific manner 109

Figure 3.9: MUC1-expressing cell lines have higher migratory responses in culture-conditions shown to increase endothelial ICAM-1 expression 110

Figure 3.10: Basal rates of migration through a gelatin-coated Transwell membrane appear to be subclone specific 113

Figure 3.11: The migratory responses of MUC1-expressing 293T subclones appear to be sensitive to ICAM-1 expression 114

Figure 4.1: Integrin expression profile of MCF-7 cells 121

Page

Figure 4.2: Schematic diagram of the co-culture model 125

Figure 4.3: Mode of flow cytometry data collection 127

Figure 4.4: MCF-7 cells cultured under conditions that resulted in high levels of transendothelial migration in the Transwell assay show decreased surface β1-integrin expression 128

Figure 4.5: Line graphs of surface β1-integrin expression on MCF-7 cells with statistical analyses done on specific data pairs 130

Figure 5.1: The calcium oscillation assay experimental set up 139

Figure 5.2: The Oscillation Factor Calculation 141

Figure 5.3: Contact with ICAM-1 expressing cells induces calcium oscillations in MUC1-expressing human breast cancer cell lines 144

Figure 5.4: Contact with ICAM-1 expressing cells induces calcium oscillations in MUC1-expressing 293T transfectants 145

Figure 5.5: Antibody Blockade of the ICAM-1 binding site on the MUC1 molecule inhibits the calcium-based oscillatory response 148

Figure 5.6: MUC1 positive cells can induce an ICAM-1 dependent, intracellular calcium-based response in HUVECs, with minor oscillations 149

Figure 5.7: Schematic of selected calcium-sensitive migratory processes 154

Figure 5.8: Schematic of how the MUC1/ICAM-1 initiated signal may occur 155

List of Abbreviations

aa	amino acid
2-APB	2-Aminoethoxydiphenylborane
AChR	Acetylcholine receptor
ADAM	A disintegrin and metalloprotease
APC	Adenomatous polyposis coli
Asn	Asparagine
ATCC	American Type Culture Collection
ATP	Adenosine triphosphate
BCECF-AM	2',7'-bis-(2-carboxyethyl)-5-(and-6)- carboxyfluorescein, acetoxymethyl ester
bFGF	Basic fibroblast growth factor
BRCA	Breast Cancer Gene
BTT	2% BSA in PBS with 0.05% Tween 20
Ca	Calcium
CaM	Calmodulin
CaMK	Calmodulin-dependent protein kinase
cAMP	Cyclic adenosine monophosphate
CAMs	Cell adhesion molecules
CCL	Cytokine Ligand for CCR
CCR	Cytokine Receptor containing a double cysteine motif
CD	Cluster of differentiation
CEA	Carcinoembryonic antigen
CFP	Cyan fluorescent protein
CM	Conditioned media
CO	Carbon dioxide
CSF1-R	Colony stimulating factor 1 receptor
CXCL	Cytokine Ligand for CXCR
CXCR	Cytokine Receptor containing a specific motif: Cysteine-any amino acid-cysteine
DAB	Diaminobenzidine tetrahydrochloride

DMEM	Dulbecco's Modified Eagle Media
DMSO	Dimethyl sulfoxide
DNA	Deoxyribose nucleic acid
dNTP	Deoxyribose nucleotide phosphate
DPBS	Dulbecco's phosphate buffered saline
ECGS	Endothelial cell growth supplement
ECL	Enhanced chemiluminescence
EDTA	Ethylenediaminetetraacetic acid
EGF	Epidermal growth factor
EGFR	Epidermal growth factor receptor
EMA	Epithelial membrane antigen
EMT	Epithelial to mesenchymal transition
ER	Endoplasmic reticulum
ERK	Extracellular-signal-regulated kinase
ESA	Epithelial specific antigen
ETA	Epithelial tumour antigen
FAK	Focal adhesion kinase
FBS	Fetal bovine serum
FCM	Fibroblast conditioned media
FITC	Fluorescein isothiacyanate
FRET	Fluorescence resonance energy transfer
Gal	Galactose
GalNAc	N-acetyl galactosamine
GC	Guanidine-cytidine
GFPv	Green fluorescent protein variant
GHR	Growth hormone receptor
GlcNAc	N-acetyl glucosamine
Grb2	Growth receptor binding protein 2
GSK3β	Glycogen synthase kinase 3 β
HBS	HEPES buffered saline
HCl	Hydrochloride

HEPES	4-(2-hydroxyethyl)-1-piperazineethanesulfonic acid
HGF	Hepatocyte growth factor
HMEV	Human mammary epithelial cells
HUVECs	Human umbilical vein endothelial cells
ICAM-1	Intercellular adhesion molecule-1
IL	Interleukin
IP3	Inositol (1,4,5) triphosphate
IP3R	Inositol triphosphate receptor
kB	Kilobase
LCA	Leukocyte common antigen
LEF	Lymphoid enhancer binding factor
LFA-1	Lymphocyte function-associated antigen
MAdCAM-1	Mucosal addressin cell adhesion molecule-1
MAPK	Mitogen activated protein kinase
MCA	Mammary carcinoma antigen
MCF	Michigan Cancer Foundation
MCS	Multiple cloning site
MDCK	Madin Darby canine kidney
MIP-1	Macrophage inflammatory protein
mRNA	Messenger ribonucleic acid
MUC1 CT	MUC1 cytoplasmic tail
NBT/BCIP	Nitro blue tetrazolium chloride/ 5-Bromo-4-chloro-3-indolyl phosphate toluidine salt
NCBI	National Center for Biotechnology Information
NeuNAc	N-acetylneuraminic acid (sialic acid)
NIH	National Institutes of Health
NMR	Nuclear Magnetic Resonance
NSAIDs	Non-steroidal anti-inflammatory drugs
PBS	Phosphate buffered saline
PCNA	Proliferating cell nuclear antigen
PCR	Polymerase chain reaction

PDGF	Platelet derived growth factor
PDGF-R	Platelet derived growth factor receptor
PEM	Polymorphic epithelial mucin
PH	Plecstrin homology
PHEC	Primary human endothelial cell
PI3K	Phosphoinositol 3 kinase
PIP2	Phosphoinositol (4,5) diphosphate
PIP3	Phosphoinositol (3,4,5) triphosphate
PKCγ	Protein kinase C γ
PLC	Phospholipase C
PP2	3-(4-chlorophenyl) 1-(1,1-dimethylethyl)-1H-pyrazolo [3,4-d]pyrimidin-4-amine
Pro	Proline
PUM	Peanut-reactive urinary mucin
RANTES	Regulated on activation normal T-cell expressed
RIPA	Radioimmunoprecipitation assay
ROI	Region of interest
RPMI	Roswell Park Memorial Institute
SCI	Signal sequence CFP ICAM-1
SDS	Sodium dodecyl sulfate
SDS-PAGE	Sodium dodecyl sulfate - polyacrylamide gel electrophoresis
SEA	Sea urchin sperm protein, enterokinase, agrin
SEC	Secreted
SEM	Standard error of the mean
Ser	Serine
SH	Src homology
sLe	Sialylated Lewis antigen
Sos	Son of Sevenless
SYM	Signal sequence YFP MUC1
TACE	Tumor necrosis factor-alpha converting enzyme
TCF	T-cell specific transcription factor

TDLU	Terminal duct lobular unit
TEM_E	Transendothelial migration, specifically extravasation
TGF-β	Transforming growth factor-β
Thr	Threonine
Tn	Thomsen-Friedenreich related antigen (GalNAc)
TNF	Tumour necrosis factor
TR	Tandem repeat
uPA	Urokinase-like plasminogen activator
uPAR	Urokinase-like plasminogen activator receptor
VE	Vascular endothelial
VEGF	Vascular endothelial growth factor
VNTR	Variable numbers of tandem repeats
YFP	Yellow fluorescent protein

List of Cell Lines

Cell Line	Origin	Molecular Expression
293T (HEK 293T)	Human embryonic kidney epithelium	MUC1 negative ICAM-1 negative E-cadherin positive β-catenin positive
410.4	Murine mammary adenocarcinoma	No human proteins expressed
A549	Human lung carcinoma	Low MUC1 positive ICAM-1 positive E-cadherin positive β-catenin positive
DH5α	E. Coli	n/a
EAhy926	Fusion hybrid between HUVECs and A549 lung carcinoma	MUC1 negative ICAM-1 positive
1°Fibroblasts	Human breast tissue; ductal carcinoma *in situ*	Low MUC1 positive ICAM-1 positive
1°HMEC	Human normal breast epithelium (reduction mammoplasty)	Low MUC1 positive ICAM-1 negative E-cadherin positive β-catenin positive
Hs578T	Human mammary carcinoma	MUC1 negative ICAM-1 positive E-cadherin negative β-catenin positive
HUVECs	Human umbilical vein endothelial cells; primary cell culture.	MUC1 negative ICAM-1 positive VE-cadherin positive β-catenin positive
MCF-7	Human mammary adenocarcinoma; pleural effusion	MUC1 positive ICAM-1 low positive E-cadherin positive β-catenin positive

Cell Line	Origin	Molecular Expression
MDA-MB-468	Human mammary adenocarcinoma	MUC1 low positive ICAM-1 positive E-cadherin negative β-catenin positive
MDCK	Canine normal kidney epithelium	No human proteins expressed
Mesothelial	Human mesothelial lining; pleural effusion	MUC1 positive ICAM-1 positive E-cadherin positive β-catenin positive
MRC-5	Human normal lung fibroblast	ICAM-1 positive
NIH3T3	Murine embryonic fibroblast	No human proteins expressed
NIH3T3 ICAM-1	NIH3T3 cells transfected with the pBOS-ICAM-1 plasmid	MUC1 negative human ICAM-1 positive
NIH3T3 Mock	NIH3T3 cells transfected with the pBOS plasmid	No human proteins expressed
Panc	Human pancreatic adenocarcinoma	Low MUC1 positive ICAM-1 positive E-cadherin positive β-catenin positive
SCI	293T cells transfected with CFP-ICAM-1	MUC1 negative ICAM-1 positive
SYM	293T cells transfected with YFP MUC1	MUC1 positive ICAM-1 negative
T47D	Human mammary ductal carcinoma; pleural effusion	MUC1 positive ICAM-1 positive E-cadherin positive β-catenin positive
ZR-75-1	Human mammary ductal carcinoma; ascites	MUC1 positive ICAM-1 positive E-cadherin positive β-catenin positive

List of Antibodies

Antibody	Binding Specificity	Host Species	Detection Concentration	Blockade Concentration	Supplier
B27.29	MUC1 tandem repeat	Mouse	1 μg/mL	60 – 120 μg/mL	Biomira
CAT-5H10	β-catenin	Mouse	4 μg/mL	n/a	Zymed
HECD-1	E-cadherin	Mouse	5 μg/mL	n/a	Zymed
18E3D	ICAM-1	mouse	1 μg/mL	20 μg/mL	ICOS
CT1	MUC1 cytoplasmic tail	Rabbit (polyclonal)	5 μg/mL	n/a	Dr. Sandra Gendler (Mayo Clinic Scottsdale)
CT2	MUC1 cytoplasmic tail	Armenian Hamster	5 μg/mL	n/a	Dr. Sandra Gendler
MOPC 31C	n/a – IgG1 isotype control	mouse	5 μg/mL	60-120 μg/mL	Sigma Aldrich
B-5-1-2	Tubulin	mouse	5 μg/mL	n/a	Sigma Aldrich
B67.4	sLe^a	mouse	n/a	20 μg/mL	Biomira
JB1A	β1-integrin	mouse	5 μg/mL	20 μg/mL	Dr. John Wilkins (U Manitoba)
ICR5	ICAM-3	mouse	1 μg/mL	20 μg/mL	ICOS
HUTS-21	Activated β1-integrin	mouse	20 μg/mL	n/a	BD Biosciences
A9	β4-integrin	mouse	8 μg/mL	n/a	Santa Cruz Biotechnology

Chapter 1: Introduction

1.0 Thesis Overview

The MUC1 glycoprotein has long been associated with the development of breast carcinoma. Early pathology studies discovered that this mucin, which is normally restricted to the apical surface of breast epithelia, has increased expression and depolarized or cytoplasmic distribution as carcinomas progress [1,9-13]. It was also found that MUC1 is less glycosylated in many carcinomas: the truncated carbohydrates and partially exposed protein core create tumour-specific epitopes which could theoretically allow immune differentiation between malignant and benign epithelia [14-18]. The most immunogenic protein epitope is in the tandem repeat region of the extracellular domain, thereby providing 21-125 copies per MUC1 molecule [19]. The repeated epitope is thought to be highly immunogenic because of its teritiary structure, which forms a protruding knot [20,21]. This fuelled over ten years of research into creating a MUC1-based "therapeutic vaccine" [9,20,22-26].

MUC1 was initially thought to have very simple, passive functions, perhaps having no application other than protecting epithelia by providing hydration, lubrication, and a barrier to pathogens [27-35]. However, as MUC1 is found so commonly in both primary and secondary tumour sites, many questions of its possible contribution to metastatic spread have arisen. The theories surrounding MUC1 function have evolved gradually, starting with the steric hindrance theory, which proposed that the relatively long, rigid protein backbone of MUC1 (~500nm [29,36], compared to 10-50 nm for the remainder of the glycocalyx [37-39]), with its many negatively charged O-glycosylations [29], was responsible for providing repulsive forces, and sterically interfering with the functions of E-cadherin and integrins, thus minimizing cell-cell and cell-matrix interactions, and encouraging dissemination of the primary tumour [39-45]. The idea that MUC1 function was passive held predominance in the field, despite evidence that MUC1 contained sequences homologous to cytokine receptors, and could be differentially phosphorylated [46,47]. Since 1995, several molecules related to signal transduction have been found to physically associate with the tyrosine phosphorylated cytoplasmic tail of MUC1 (MUC1 CT), including src [48], protein kinase C [49], β-catenin [50] and Grb2/Sos [51]. The real breakthrough in demonstrating MUC1 as an active signalling

participant came in 2000 with a series of papers showing that aggregation of a MUC1 CT/CD8 chimera [52,53], or association of MUC1 with EGF-stimulated EGFR [54,55], resulted in MUC1 CT phosphorylation and activation of MAPK.

Studies examining MUC1 signalling have used either CD8 antibody, or EGF, which do not appear to interact with the tandem repeat domain of MUC1. Previous research in our laboratory has identified a physiologically relevant, extracellular binding partner of MUC1. In 1996, Regimbald et al. [2] demonstrated that tumour-cell MUC1 could bind to endothelial-cell ICAM-1, mediating heterotypic adhesion in a static assay. This was followed by a study by Kam et al. in 1998 [3], which showed that it was the peptide core of MUC1 that bound to ICAM-1, and that a peptide fragment long enough to adopt the normal tertiary structure [56] was required for binding. Finally, Horne showed that the strength of this adhesion was able to withstand shear stresses equivalent to physiologic blood flow [5]. Confirmation of the MUC1/ICAM-1 interaction has since been performed in other laboratories [57-59], and evidence has been found that underglycosylated MUC1 binds better to ICAM-1 [58].

The current thesis project examines how the MUC1/ICAM-1 interaction may be responsible for triggering migratory behaviours in human breast cancer cells. We performed an immunohistochemical review of MUC1 distribution and its correlation with nodal metastases in clinical specimens of human breast cancer [1], as well as fluorescent three-dimensional imaging of MUC1 and ICAM-1 expressing cells in co-culture. This was complemented by a functional study measuring the migratory responses of MUC1-positive cells when exposed to cell-bound ICAM-1, an examination MUC1/ICAM-1-induced integrin turn over, and a preliminary characterisation of calcium-based signalling triggered by the MUC1/ICAM-1 interaction [8].

The sum of this work suggests that on contact with ICAM-1 on an adjacent cell, MUC1 initiates a calcium-based promigratory signal in epithelial cells. The extent of migration can be modulated by the microenvironmental context. As ICAM-1 is present throughout the entire expected migratory track of a metastasizing tumour cell, this signal could facilitate stromal/transendothelial migration in the primary and secondary tumour sites. It also illuminates the vast diversity of MUC1 as a signalling molecule; it clearly can no longer be thought of as a simple mucin, and appears to be more than only a

docking site for other signalling participants.

1.1 Breast Cancer Pathology and Metastasis

1.1.1 The Normal Breast

Breast tissue begins to develop in the embryo (reviewed in [60,61]). From the fourth week of gestation, the mammary anlage, or primordial clustering of cells from which the breast develops, is detectable. These cells thicken into a 'milk streak' that forms on both sides of the embryonic midventral line. By the end of gestation, the mammary parenchyma has invaded the underlying stroma, and rudimentary ducts with small, club-like ends have formed.

Mammary glands grow at the same rate as the rest of the body until the peripubertal stage, when there is an allometric change in both the epithelia and surrounding stroma, and the ducts elongate and branch. Ductal elongation is directed by estrogen, growth hormone, insulin-like growth factor-1 and epidermal growth factor, and ductal branching and alveolar budding is influenced by additional factors, including progesterone, prolactin and thyroid hormone [60]. The site of active proliferation is a terminal end bud-like structure (a bulbous, invasive structure located at the tip of the mammary duct [62]). There is a cytochemically distinct compartment of division-competent cells in the mammary epithelium that are 'structurally undifferentiated' (unpolarised with few organelles). These cells possess the ability to regenerate as well as differentiate into epithelium and myoepithelium, and do not retain commonly used stains [63]. As such, they are referred to as 'light' or 'pale' cells, and are believed to be a mixture of epithelial stem cells and their primary progenitors. These cells tend to be located at the 'cap' of terminal end buds, and can give rise to partially differentiated 'transitional units', which are clusters of cells found every ~250 nm along the ducts [62] and may be initiation points for branching or the formation of new ductal trees.

Glandular development is accompanied by distinct epithelial-stromal interactions, which stimulate the deposition of a loose intralobular stroma around the epithelial structures and a denser, collagenous interlobular stroma outside of this compartment

(Figure 1.1). By the first menses, the terminal duct may give rise to ~11 surrounding alveolar buds, collectively referred to as a terminal duct lobular unit (TDLU). With each menstrual cycle, there is new budding until the gland reaches a growth plateau, around age 35. The degree of lobular complexity varies greatly, where the number of alveolar buds within a TDLU can number anywhere from 11 to 80. Functional differentiation occurs during pregnancy to support lactation, followed by involution (a decrease in size and function) when nursing ceases [60].

Other cells present in the breast include the myoepithelial cells, which form a 'basket-like' net around alveoli, and respond to oxytocin by contracting to eject milk during suckling [61]. A basement membrane, consisting of specific extracellular matrix proteins (reviewed in [64,65]), separates the TDLUs and myoepithelial cells from the surrounding stromal matrix. Fibroblasts are present in the stromal compartments, and can differentiate into myofibroblasts in response to injury, thus attaining contractile properties to facilitate closure of a wound bed [66]. Fibroblasts may share origins with vascular smooth muscle cells and pericytes (stromal cells that surround capillaries) [67], and can influence ductal morphogenesis via secretion of matrix proteins [68] and paracrine factors [61]. Finally, adipose tissue is found within the interlobular stroma, in a distinct compartment, and may contribute to glandular development by the production of estrogen [69].

1.1.2 The Cancerous Breast

1.1.2.1 Carcinogenesis

Breast carcinoma is believed to arise from the divisional compartment of the mammary epithelium, that is, the stem cells [70-72]. Two groups have independently isolated these primordial cancer cells. One group has isolated a $MUC1^-$/epithelial specific antigen $(ESA)^+$ breast epithelial cell line which can regenerate itself as well as luminal $MUC1^+/ESA^+$ cells and myoepithelial cells [73]. Another group has found that sorted cells from eight different patients which are $CD44^+/CD24^{low}$ form a tumourigenic subpopulation which consistently form tumours in mice even after serial passage [74]. Carcinogenesis is generally thought to begin with a single mutation or loss of

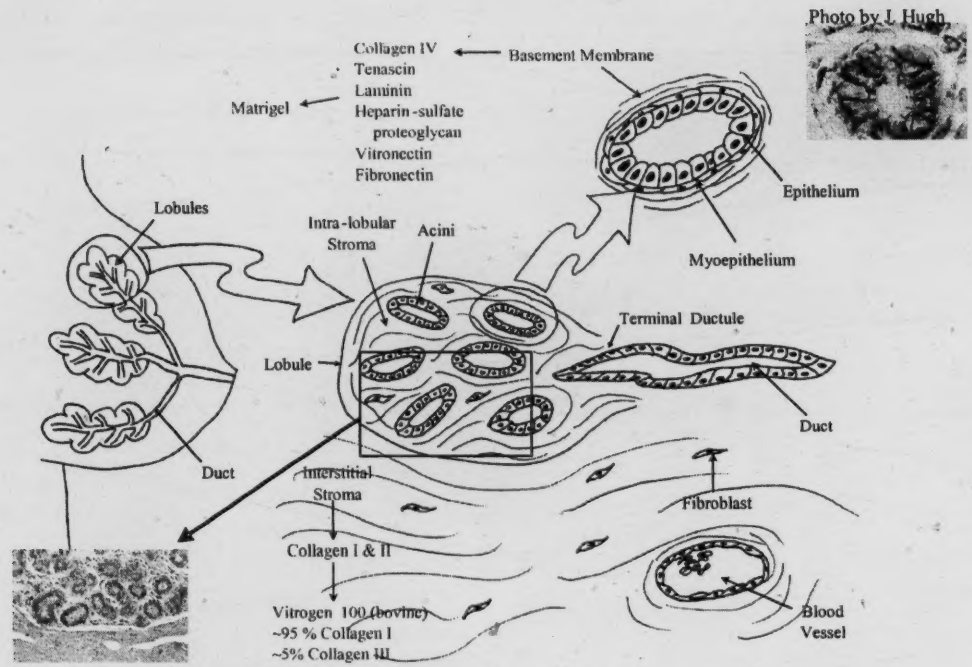

Photo from http://pathology.mc.duke.edu/research/Histo_course/breast1.jpg

Figure 1.1: Normal Breast Architecture. In the human breast, the adipose tissue, stromal matrix and intralobular matrix are in separate compartments (they are intermixed in murine breast). The ducts branch into alveolar structures, or lobules. Each lobule has three layers; the epithelium, myoepithelium and basement membrane. The basement membrane contains specific proteins that can send polarisation signals into the cells via integrins. The stromal matrix is less complex, comprised mainly of collagens I and II. The upper insert shows a cross-sectioned lobule stained for β-catenin (brown) and the nuclei counterstained with hematoxylin (blue). The lower insert shows a cross-sectioned terminal duct lobular unit and the partitioning of the stromal compartments, the proteins stained with eosin (pink) and the nuclei with hematoxylin (blue).

heterozygosity in a gene that is involved in growth control, which then increases the probability that this cell will over proliferate. Like other solid tumours, breast cancer appears to follow the "multi-hit" hypothesis, which is that a series of mutations must occur before a transformed cell can overcome all the barriers erected by tumour suppressor and cell-cycle checkpoint proteins. Candidate 'initiator' genes in breast cancer include BCRA1, BCRA2 (~5% of all breast cancers, hereditary), her2/c-erb-B2/neu, c-myc, EGFR and p53 (generally associated with sporadic breast cancers) [75,76]. Uncontrolled proliferation of cells already carrying mutations in genes whose function is to ensure repair or destruction of cells with damaged DNA, results in a propensity to accumulate other mutations. Some of these may give the tumour cell the ability to ignore the signals from the surrounding tissues and matrix, which instruct the epithelial cells to adopt a polarized phenotype, and become quiescent within the epithelial monolayer [77-79].

1.1.2.2 Breast Cancer Subtypes and Stages of Metastatic Progression

Genetically aberrant or malignant cells which have proliferated abnormally without digesting through the basement membrane are referred to as ***in situ***. Those which have digested through the basement membrane and accessed the stroma are referred to as **invasive**. Once stromal invasion has occurred, the presence of **vascular invasion** is taken as a bad prognostic sign, as the circulation of blood or lymph throughout the body is believed to carry tumour cells to the secondary organs that become colonized during metastasis. Ultimately, it is the spread of the malignant cells to vital organs and the disruption of organ function that leads to mortality.

Low grade tumours are prognostically better than high grade tumours. Grading is generally assigned by assessment of tumor appearance in three categories; (i) the percentage of the carcinoma composed of tubular structures (suggestive of functional differentiation; >75% scores as 1, <10% scores as 3) (ii) the frequency of mitosis in a high powered field (suggestive of proliferative rate; <7 scores as 1, >15 scores as 3), and (iii) nuclear pleomorphism, or the change in nuclear size and uniformity (suggestive of carcinogenic transformation; small and uniform scores as 1, marked variation scores as 3). Values falling between the stated limits are scored as 2 [80].

The two most prevalent types of breast cancer are "ductal" (~80%) and "lobular" (~10%). These designations are based on the appearance of the cancers, and the early assumption that they arose from either the ducts or lobules. Ductal carcinomas tend to grow and migrate in clusters while maintaining cell-cell adhesion; lobular carcinomas are E-cadherin negative and migrate through the stroma in lines of single cells. The remainder of breast cancers are referred to as tubular, papillary, colloid or mucinous, and medullary, again based on appearance [81,82].

1.1.3 The Microenvironment and Metastasis

Although genetic transformation is absolutely required for cancer to develop, metastasis appears to require a specific environment in order to occur. Weaver et al. have put forth the idea that "Tissue structure appears to determine the phenotype, which in turn overrides the cellular genotype" [79]. In the same report, this group showed that manipulation of outside-in signalling by β1 and β4 integrins could inhibit (β1-integrin blocking antibody) and promote (β4-integrin "function altering" antibody) disorganised growth, respectively. Other work by Bissell and Ronnov-Jessen specifically implicate fibroblasts in promoting outgrowths of primary tumours, suggesting that these stromal cells create a microenvironment that specifically favours metastasis [83-85]. Endothelial cells are also very much subjected to microenvironmental influences [86-88], and in our studies, we found that fibroblasts and endothelial cells could act synergistically to promote migration of tumour cells (Chapter 3). The mechanisms by which fibroblasts and endothelial cells may contribute to metastasis are outlined below.

1.1.3.1 The Contribution of Fibroblasts to Metastasis

Characterization of the microenvironment over the last decade has revealed that physiological extracellular components can dramatically influence the behaviour of tumour cells [70], and that these interactions bear a striking resemblance to wound healing [89]. It may be that fibroblasts, which maintain the stroma, respond to a tumour as a "wound that will not heal". In their normal capacity, fibroblasts respond to the release of PDGF by platelets that have integrated into a clot covering damage in an

epithelial monolayer. They become "activated" or transform into actin-expressing myofibroblasts, as they migrate towards the wound. They then release a number of growth and motogenic factors (e.g. HGF), as well as deposit a "provisional matrix" into the wound bed. This matrix is rich in splice variants of fibronectin which contain the ED-A and ED-B regions of this protein, and is capable of sending integrin-mediated signals into the epithelial cells, encouraging migration over the wound bed. Some of the secreted factors stimulate angiogenesis towards this healing region. The myofibroblasts use their contractile properties to pull the wound shut, then replace the transitory stroma with a more "mature" form as the healing completes [66,90,91].

When a tumour is forming within the breast tissue, fibroblasts again transform into myofibroblasts, migrate towards the tumour, release mitogenic and motogenic factors, and deposit the "oncofetal" ED-A and ED-B forms of fibronectin [92-94]. The similarities between wound and tumour stroma are functionally parallel, as tumour cells do tend to metastasize to wound sites when injected into animals (reviewed in [85]). Fibroblasts also secrete matrix metalloproteinases, normally used by cells such as leukocytes, to assist in transit through the stroma. The secretion of uPA (urokinase-like plasminogen activator) provides a substrate for uPAR on the tumour cells, initiating a proteolytic cascade. In addition to causing degradation of the extracellular matrix, uPAR/uPA activation of plasmin can result in proteolytic activation of TGF-β, which is also secreted by fibroblasts [66,95]. This particular substance has a unique function in breast cancer, as it appears to inhibit growth of normal or well differentiated cancers, but promotes growth in poorly differentiated cancers [96-99]. Thus, the normal actions of fibroblasts to promote the healing of the cancerous lesion, appear to inadvertently assist in metastatic spread.

Fibroblasts can also influence the behaviour of overlying endothelial cells. For example, rat skin fibroblasts can influence EAhy926 cells to upregulate their expression of decorin [87], a protein involved in angiogenesis, and bFGF can influence HUVECs to downregulate junctional adhesion complex proteins, while increasing VE-Cadherin dependent leukocyte migration [88]. Either of these events may favour metastatic spread, either by promoting growth of blood vessels to the tumour site, or creating "leaky" vessels that may be easier for tumour cells to intravasate (discussed below).

1.1.3.2 The Contribution of Endothelial Cells to Metastasis

Primary tumours spread to distant organs via the lymphvascular system. This could occur by tumour cells migrating through the stroma until they encounter a lymph or blood vessel, however, many reports have described tumour secretion of angiogenic factors (e.g. VEGF) which encourages the growth of blood vessels into the tumour [94]. This not only provides solid carcinomas with a nutrient and oxygen supply, but also access to blood vessels, enabling dissemination from the primary site.

The mechanism of tumour cell intravasation remains enigmatic. Tumours may digest their way into blood vessels [100], use some co-operative process in which the endothelial cells facilitate entry [101], induce "leaky" blood vessel growth into the tumour [102,103], or engage in vasculogenic mimicry [104-106]. This last proposal suggests that solid tumours are able to form channels within themselves that connect to the vasculature and are capable of hosting blood flow, an idea that is controversial [107,108].

Once circulating within the vasculature, breast cancer metastasizes preferentially to specific target organs, namely bone, brain, lungs and liver. It is generally agreed that blood-borne tumour cells can adhere to the vasculature within these organs by specific adhesion molecules, however at this point, the theories become divergent.

1.1.3.2.1 Homing or Specific Extravasation

It has been well established that the complement of proteins expressed on the surface of endothelial cells is specific to, and influenced by, the stroma of the organ housing them. This expression is plastic, as cardiac tissue transplanted to the liver will cause the liver vasculature which grows into that tissue to convert to the cardiac endothelia phenotype [86-88]. The idea of organ vasculature having an "address system" is further supported by studies using a bacterial phage library of randomly generated proteins, in which specific adhesion "codes" were identified for the vasculature of different organs, allowing the generation of a map. One clear example of this are "addressins" such as MAdCAM-1, an immunoglobulin-like, mucin-containing adhesion molecule involved in the homing of leukocytes to lymphoid tissues [4,109,110]. Thus, tumour cells with specific co-receptors for the "address" proteins on the organ-

conditioned endothelial cells would home to those sites in particular [6,86,111]. It has also been demonstrated that tumour cells can and will adhere to vessels with a diameter larger than that of the tumour cells, requiring no physical restriction based on size [112]. Finally, the CXCR4 and CCR7 chemokine receptors are upregulated in many clinical specimens of breast cancer, and their ligands, CXCL12 and CCL21, are found in the preferential metastasis sites, with the exception of brain. Since ligation of CXCR4 and CCR7 trigger diapedesis and cytoskeletal restructuring in tumour cells, and blocking of CXCR4 could inhibit metastasis in mice, it appears that this is a system where tumour cells extravasate and enter organs specifically based on whether their "key" fits the "lock" on the organ [113].

1.1.3.2.2 Seed vs. Soil

Quantitative *in vivo* videomicroscopy studies have demonstrated that the extravasation step in metastasis is relatively efficient, and not organ-dependent (reviewed in [114]). It was the growth of these cells (the seeds) after extravasation which was rate-limiting, and dependent on the particular growth factor milieu of the target organ (the soil). Critics of this theory say that interpretation of these results is hampered by the artificial infusion of large numbers of cultured cells which may not accurately reflect the clinical situation, as these cells have undergone an artificial selection process in establishing them in culture, and the process of intravasation is completely excluded [115]. Other intravital microscopy studies have produced diametrically opposite results, suggesting that tumour extravasation is rare, and adhesion of tumour cells to the vasculature may be the critical step for metastasis to occur [116].

As both of the preceding theories have shown validity in their respective experimental models, it is entirely probable that each phenomenon contributes to metastatic spread cooperatively.

1.1.4 Similarities Between Leukocyte Extravasation During Inflammation and Tumour Extravasation During Metastasis.

Tissue damage, or the presence of a pathogen, generally leads to the activation of macrophages and the release of cytokines that have multiple downstream effects (reviewed in [4]). Endothelial cells within the range of influence of these cytokines respond by upregulation of adhesion molecules, and the secretion and entrapment of cytokines on their luminal surfaces. Leukocytes are initially recruited by a series of transient adhesions to cytokine-activated endothelia, mediated by endothelial E- and P-selectins, and sialylated Lewis (sLe) a and x carbohydrate-containing ligands on the leukocyte. These adhesions result in the leukocyte appearing to roll along the endothelial lining of a blood vessel after an apparently random impaction caused by physiological blood flow. Selectin-mediated adhesions are only preliminary, however, as the expression of these molecules peaks at 4 hours, and declines to <20% of peak levels by 24 hours. During "rolling", the leukocyte comes into contact with cytokines bound to the luminal endothelial surfaces and becomes activated, a process that includes a conformational shift in the β2-integrins LFA-1 and Mac-1, exposing ICAM-1 binding sites (Figure 1.2). Ligation of ICAM-1 facilitates firm adhesion of the leukocyte to the endothelium, and is followed by leukocyte spreading, diapedesis and transendothelial migration.

Many reports have linked inflammation to the spread of cancer. In addition to the trophic and chemotactic effects of the milieu of soluble factors released during inflammation, and reports that metastasis can be inhibited by anti-inflammatory agents [117-120], many types of carcinoma have been reported to bind to activated endothelia, which could theoretically increase the probability of these cells extravasating into the stroma of a secondary target organ and forming a distant tumour site. Several of the molecules involved in leukocyte interactions with endothelial cells have also been implicated in tumour-to-endothelial cell adhesive interactions (Table 1.1), strongly suggesting that tumour cells opportunistically use mechanisms in place for leukocyte transendothelial migration for metastatic spread. The mechanisms through which MUC1

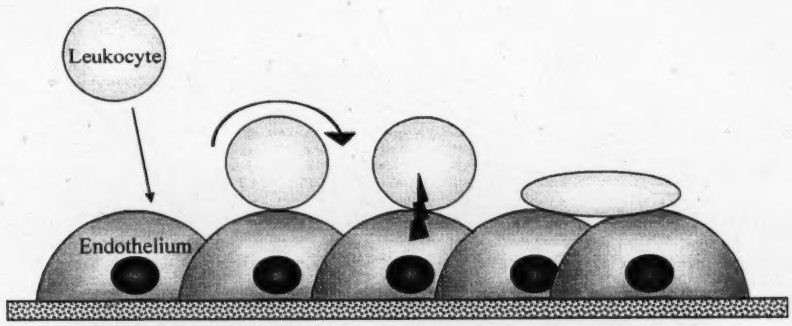

Event:	Tethering	Rolling	Activation	Arrest
Involved molecules on leukocyte:	sLe^x antigens on glycoproteins, glycolipids, PSGL-1	L-selectin α4β7 integrin α4β1 integrin	7 TMR	LFA-1, Mac-1 α4β7 integrin VLA-4
(Interstitial:)			Chemoattractants Chemokines C5a, PAF, LTB4 Formyl peptides	
Involved molecules on endothelium:	E-selectin P-selectin	PNAd MAdCAM-1 VCAM-1		ICAM-2, ICAM-1 MAdCAM-1, VCAM-1

Figure 1.2: Several adhesion molecules are involved in leukocyte to endothelial cell binding. Initial interactions between leukocyte Lewis antigens and endothelial selectins are transient and of low avidity, resulting in leukocyte rolling along activated endothelium. Firm adhesion is mediated by endothelial CAMs and leukocyte integrins that have been activated by local cytokines.

Based on [121].

Table 1.1: Endothelial surface adhesion molecules involved in interactions with cancer cells.

Endothelial Cell Surface Molecule	Tumour Cell Surface Molecule (co-receptor)	Known Cell Types
Selectin family		
E-selectin	sLe^a	Colon carcinoma
	sLe^x	Renal cell carcinoma
Immunoglobulin family		
CEA	CEA	Breast cancer
		Colon cancer
ICAM-1	β2 integrins	C6 glioma
VCAM-1	α4 integrins	Renal carcinoma
	α4β6	Melanoma
		Sarcoma
MUC18	MUC18	Melanoma
MAdCAM-1	α4 integrins	Speculated
Integrins		
α6 integrins	α6β1	B16/129 melanoma
β1 integrins		Small cell carcinoma
αvβ3	?	Multiple tumours
Other		
Thrombospondin	Thrombospondin and receptors	MCF-7 cells
Heparin Sulfate	NCAM	
Fibronectin-binding protein		
Specific to lung endothelium (dipeptidyl dipeptidase)		

Based on [122].

can mediate binding of tumour cells to activated endothelium, initially involves the sialylated Lewis$^{a/x}$ antigens present on the carbohydrate moieties of MUC1, which are known to bind to E- and P-selectins. Thus, as with leukocytes, tumour cells have been shown to engage in "rolling", mediated by the same molecular pair [123,124].

The demonstration that MUC1 and ICAM-1 were binding partners [2,3], and that the adhesion they mediated was sufficiently strong to withstand shear stresses equivalent to physiological blood flow [5], raised the question of whether the MUC1/ICAM-1 interaction could also mediate extravasation, and/or trigger signalling cascades linked to endothelial retraction and tumour cell pro-migratory behaviours, furthering the notion that tumour cell transendothelial migration mimicks that of leukocytes.

1.2 Structure and Function of the MUC1 and ICAM-1 Molecules

1.2.1 The MUC1 Physical Entity

Mucins in general are found on the apical surfaces of epithelia, and are thought to have protective functions, such as maintaining hydration, providing lubrication, and forming a barrier against digestive enzymes and pathogens. Their basic structure consists of a protein backbone, which carries multiple glycosylations. Some of these mucins can form a mesh via cross-linking at specific cysteine residues [29,125].

1.2.1.1 Nomenclature

MUC1 (also known as CD227, PEM or polymorphic epithelial mucin, EMA or epithelial membrane antigen, CA15-3, MCA or mammary carcinoma antigen, episialin, H23Ag, MAM6, DF3, ETA or epithelial tumour antigen, PUM or peanut-reactive urinary mucin, epitectin, and Muc-1; mouse homologue) was the first cloned human mucin, found at gene locus 1q22 [126]. mRNA transcripts for MUC1 have been found in virtually all epithelial tissues [127] (Figure 1.3). There are 14 members of the MUC1 family of mucin-type glycoproteins, both secreted and membrane bound [128], which are reported to have variable numbers of tandem repeats (VNTR) [126], however, their classification as a family has recently been challenged [128], on the basis of lack of

Cerebral cortex +1	Amygdalia +2	Heart +2	Esophagus +5	Kidney +6	Lung +7	Liver +2
Frontal lobe +1	Caudate nucleus +3	Aorta +3	Stomach +7	Skeletal muscle +1	Placenta +4	Pancreas +7
Parietal +1	Hippocampus +2	Atrium +3	Duodenum +6	Spleen +2	Bladder +4	Adrenal +2
Occipital +1	Medulla oblongata +2	Ventricle +2	Jejunum +4	Thymus +2	Uterus +4	Thyroid +4
Temporal lobe +1	Putamen +3	Septum +2	Ileum +3	PBLs +2	Prostate +4	Salivary gland +5
Pons +1	Substania nigra +1	Apex +2	Ilocecum +5	Lymph node +3	Testis +5	Breast +5
Cerebellum +3	Accumbens nucleus +1	Transverse colon +5	Appendix +5	Bone marrow +3	Ovary +3	
Corpus callosum +3	Thalamus +1	Descending colon +5	Rectum +5	Trachea +6		
Spinal cord +3	Pituitary +3	Ascending colon +6				

Examples of the relative intensities of probe signals: +1 +2 +3 +4 +5 +6 +7

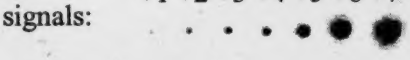

Figure 1.3: The presence of MUC1 mRNA transcript in adult human tissues. The information is from a commercial multiple tissue expression array assayed for MUC1 transcript using a probe to the tandem repeat reation. The numeric values refer to the relative intensities of the probe signals.
Based on Correa, I. et al., [127].

sequence homology, and the fact that there are many other glycoproteins on endothelial cells and leukocytes which are also described as mucins, but have historically been placed in different groups with different functions. Additionally, most of the MUC-type mucins have no common function on which to base this terminology, and are found at completely separate gene loci (Figure 1.4).

1.2.1.2 The Extracellular Domain

MUC1 is a heterodimer that consists of three domains: an extracellular domain, a transmembrane domain, and a highly conserved cytoplasmic tail. The extracellular portion has non-repetitive sequences flanking VNTR's which can number from 20-120. Each tandem repeat is comprised of a 20 amino acid sequence, containing 5 serine and threonine residues each of which can be O-glycosylated [29]. The juxtamembrane region of the extracellular domain (120 amino acids long) contains a SEA domain, named for the proteins in which it was first identified (sea urchin sperm protein, enterokinase, agrin) [129,130]. This is the site at which the MUC1 gene product is cleaved in the ER, and subsequently mediates a tight, non-covalent, SDS-labile reassociation of the two cleavage products prior to export to the Golgi [131]. Although the function of SEA domains is not yet clearly delineated, all known proteins that contain it are heavily glycosylated, and the N-terminal part of SEA domains are thought to bind to extracellular matrix proteins, specifically laminin [129,130]. Close to the SEA domain, is a region that shows up to 44% homology with the ligand binding sites of cytokine receptors, including IL-7R, GHR, and IL-3R [47].

N-glycosylation (Figure 1.5) of MUC1 occurs in the ER [132]. In general, N-glycosylations are used by the chaperone proteins calnexin and calreticulin to retain proteins in the ER until they are properly folded, and have also been implicated in intracellular trafficking, as they can target proteins to the apical side of cells [133] or to lysosomes [132]. O-glycosylation occurs in golgi compartments, and requires several rounds of MUC1 recycling between the cell surface and golgi to be completed. MUC1 has been demonstrated to recycle with a total intracellular residence time of 66 minutes, with 30% of all MUC1 intracellular at all times [134].

O-linked carbohydrates are generally made of three regions, the core (close to the

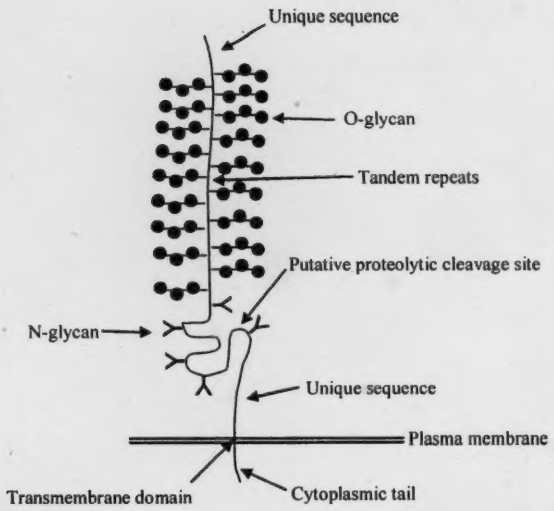

Mucin	Gene Locus	Tandem Repeats	VWF-D-like Domain	Cysteine-rich Domain	SEA Domain	Transmembrane
MUC6	11p15	~3500 amino acids (aa)	3 regions	None	No	No
MUC2	11p15	~2500 aa	4 regions	2 regions	No	No
MUC5B	11p15	~2300 aa	4 regions	7 regions	No	No
MUC5AC	11p15	~2300 aa	4 regions	9 regions	No	No
MUC4	3q29	~2300 to 6300 aa	1 region	No	No	Yes
MUC12	7q22	Variable	No	No	Yes	Yes
MUC13	3q13	~130 aa	No	No	Yes	Yes
MUC3A	7q22	Variable	No	No	Yes	Yes
MUC3B	7q22	Variable	No	No	Yes	Yes
MUC1	1q21	~600 to 2400 aa	No	No	Yes	Yes
MUC16	17q21	Variable	No	No	No	Yes
MUC7	4q13-q21	~130 aa	No	No	No	No
MUC8	12q24	Variable	No	No	No	No
MUC11	7q22	Variable	No	No	No	No

Figure 1.4: Schematic of MUC1 and the MUC Family. There are 14 mucin-type glycoproteins, both secreted and membrane bound, which have variable numbers of tandem repeats.

Based on Dekker J, et al., [135].

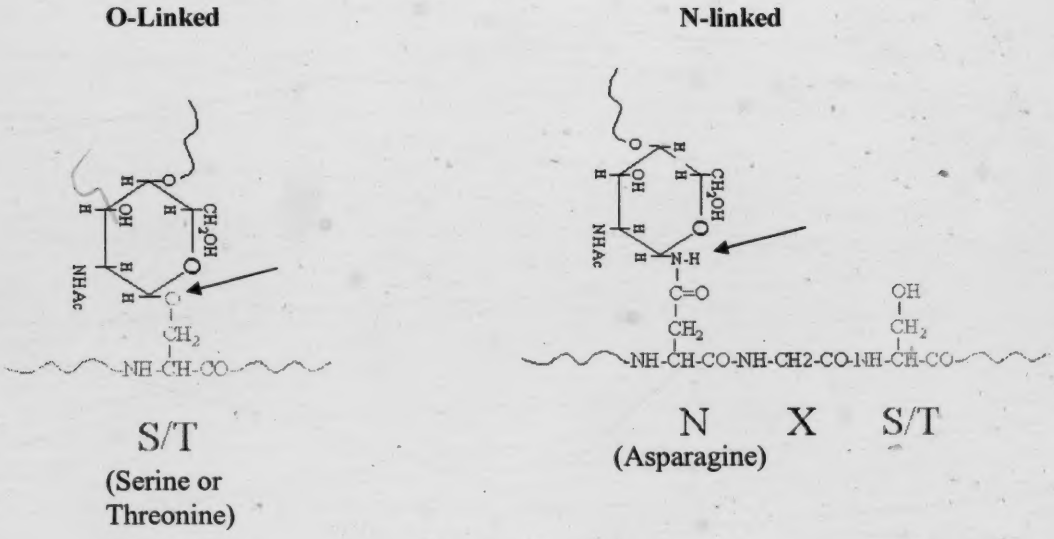

Figure 1.5: Diagram of O- and N-linked glycosylations. O-linked carbohydrates link from N- Acetylgalactosamine to a serine or threonine residue. An O-linked amino acid consensus sequence has not been defined. N-linked carbohydrates link from N-Acetylglucosamine to an asparagine residue. The N-linked amino acid consensus sequence is Asn-any AA- Ser or Thr. The middle amino acid can not be proline (Pro). Based on http://www.ionsource.com/Card/carbo/nolink.htm.

peptide backbone), the backbone, and the periphery. Sialyl Lewis^a antigens (NeuNAc or sialic acid) are normally found at the periphery of these carbohydrate structures, Tn (GalNAc or N-acetyl galactosamine) and T (Gal or galactose) are restricted to the core, and are usually covered up by further glycosyltransferase activity [126]. In breast tumour cells [136], these carbohydrates are truncated, less branched and have higher sialic acid content, along with a correspondingly high sialyl transferase activity (3 fold above normal). The lack of branching appears to be caused by an inability to synthesize part of the carbohydrate core, due to low levels of β6-GlcNAc-transferase activity, which for unknown reasons, is decreased at the mRNA level in breast carcinomas, or epimerase [137], which has been shown to completely block O-linked glycosylation and prevent maturation of N-linked glycans. O-glycosylations have also been implicated in apical targeting, and alterations in these structures can not only stimulate dynamin-1-dependent endocytosis of MUC1, but can result in intracellular accumulation of this protein without enhancing its degradation; the stability of MUC1 on the cell surface is absolutely dependent on the addition of O-linked glycans, and is increased with increasing size and number of these carbohydrates [137].

The peptide core of the MUC1 extracellular domain is rigid, and can extend up to 500 nm from the cell surface, far above the ~30nm glycocalyx. Early analyses attributed the rigidity to the many O-linked glycosylations, however, ^{1}H-NMR correlation spectroscopy has shown that the MUC1 protein core is not a random coil, but rod-shaped. This secondary structure is of the polyproline beta turn helix type, and is conferred by the presence of three tandem repeats. It is not dependent on, or disrupted by, the addition of glycosylations [56]. The first proline in the PDTRPAP part of the tandem repeat (entire sequence: GSTAPPAHGVTSAPDTRPAP) forms the major immunodominant epitope, and actually folds into a "knob-like" structure that extends out from this protein backbone.

1.2.1.3 The Transmembrane Domain

The transmembrane domain appears to have three key functions. It tethers the extracellular domain, and it trafficks MUC1 to the cell membrane via its C-Q-C motif at the junction of the cytoplasmic and transmembrane domains. Alteration of this sequence,

regardless of glycosylation, resulted in cytoplasmic rather than surface expression of MUC1 [138]. The third possible function of the transmembrane domain may be partitioning of MUC1 into lipid rafts. Pemberton et al. [138] have shown that despite deletion of all but three amino acids of the cytoplasmic tail, MUC1 still could not be extracted from the membranes of transfected *Panc* cells, demonstrating that these engineered proteins were detergent insoluble, the hallmark of lipid raft association.

1.2.1.4 The Cytoplasmic Domain

The cytoplasmic domain is alternatively reported as being 69 or 72 amino acids in length (depending on whether the C-Q-C motif is believed to be part of the transmembrane domain or cytoplasmic tail), and is thought to bind to actin, as cytochalasin D has been shown to disrupt normal apical localization of MUC1 in epithelial cells [139], and it is also co-localised with ezrin, a known linker of membrane proteins to the cytoskeleton [140]. Internalization of MUC1 can be inhibited by hypertonic media, which is typical of proteins internalized by clathrin-coated pits, and it has been suggested that the cytoplasmic domain of MUC1 may bind adaptors that recruit clathrin to the plasma membrane [132]. There are 7 highly conserved tyrosine residues within the MUC1 cytoplasmic domain, 4 of which are confirmed phosphorylation sites. Three of these are within known motifs for binding of phosphatidylinositol 3-kinase, phospholipase Cγ, and src family kinases (Figure 1.6) [141]. 70-90% of all phosphates present in ^{32}P-labelled MUC1 cytoplasmic tail were associated with tyrosine, whereas there was very little phosphoserine, and undetectable levels of phosphothreonine [47]. MUC1 has no intrinsic kinase. As such, many groups have investigated the ability of MUC1 to associate with molecules already implicated in signalling. Thus far, EGFR, erbB2, erbB3, erbB4 [54,55], PKC [49], Grb2/Sos [51], GSK3β [142], β-catenin [48-50,55,142,143], p120-catenin [144], γ-catenin [145] APC [146] and src [48,143,147] have been found physically associated with MUC1. Of these, src, GSK3β and EGFR have been shown to phosphorylate the cytoplamic tail of MUC1, and it is assumed that the erbB2, 3 and 4 proteins require the presence of EGFR in order to complex with MUC1.

The other notable feature of the MUC1 cytoplasmic domain, is that it contains a

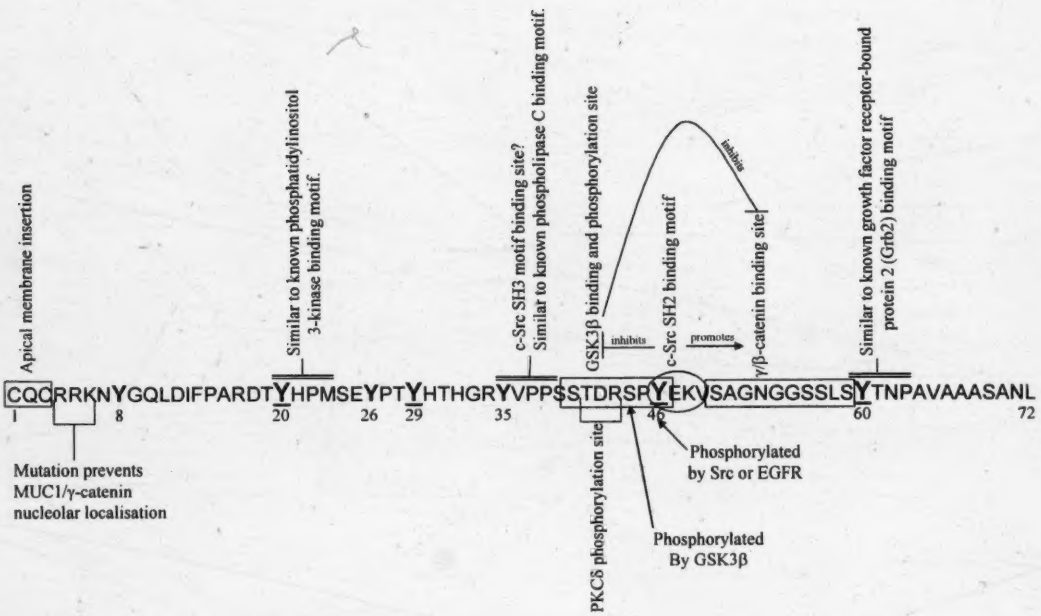

Figure 1.6: Main features of the MUC1 cytoplasmic tail. There are seven tyrosine residues in the cytoplasmic tail sequence. Four of these (underlined) are known to become phosphorylated on forced clustering of a MUC1-CT/CD8 chimera.

Based on [48,50,51,54,55,138,141-143,145].

DTYHPMS sequence similar to the autophosphorylation sites of certain cytokine receptors [148]. These include PDGF-R (IDYVPM), CSF1-R (DTYVEM), and AChR (TYHPMS). This, and the reported homology with cytokine receptors in the extracellular domain, has led to speculation that MUC1 may be a distant relative of the cytokine receptors, as two splice variants, MUC1/Y and MUC1/Zs, have been described as a putative cytokine receptor and cytokine respectively [47,149-151].

1.2.1.5 Splice Variants

There appear to be several MUC1 splice variants, however the nomenclature is somewhat inconsistent, and some of these reports have yet to be confirmed. MUC1/Y was first described, and is a 42-45kDa variation of MUC1 that is missing the tandem repeats and part of the SEA domain. It does not undergo cleavage itself, however, it has been shown to bind to MUC1/SEC (the secreted extracellular domain of MUC1), which results in phosphorylation of the MUC1/Y cytoplasmic tail. MUC1/SEC can be found in the sera of breast cancer patients [46]. To date, the only enzyme known to cleave the extracellular domain of MUC1 is the metalloprotease (TACE)/ADAM17 [152]. This demonstration was made in uterine cells during embryonic implantation, however the presence of this enzyme has also been documented in mammary tumours [153]. The next splice variant to be described is MUC1/X, which has 18 more amino acids in its extracellular domain than MUC1/Y, but again lacks the tandem repeats [154]. MUC1/Z [155] was reported a few months later, however, from its description, it appears to be the same as MUC1/X. Despite this, Croce et al. managed to detect both MUC1/X and /Z in breast cancer specimens, although their definition of these proteins differed from the initial reports [13]. Finally, MUC1/Zs is a secreted form of MUC1 that lacks the tandem repeats, while MUC1/A and /B are "tumour" and "normal" full-length MUC1 variants identified in thyroid carcinoma, and MUC1/C and /D are novel tandem repeat containing isoforms identified in cervical carcinoma [156]. The NIH review of the MUC1 protein and its isoforms cautions that the putative functions and characterizations of these proteins should be considered preliminary [157].

1.2.2 MUC1 in Normal and Malignant Breast Epithelia

In normal breast tissue, MUC1 is typically found only at the apical surface of the ductal and lobular epithelia. As such, it is a component of the milk fat globules that are secreted by pinching off of the apical membrane during lactation.

Clinical investigations have shown that MUC1 expression levels and patterns are related to prognosis in breast cancer [1,158], or other epithelial derived tumour lesions [159-162]. There are two possible mechanisms for the upregulation of MUC1 expression that occurs during carcinogenesis. Bieche et al. [10], examined 32 primary human breast cancers and found that there was a correlation between the presence of additional copies of the long arm of chromosome 1 (1q21-24) and high levels of MUC1 mRNA, suggesting a gene dosage effect may be involved in breast pathogenesis. A second mechanism would involve the underglycosylation of MUC1, which has been shown to result in defective trafficking and intracellular accumulation of this protein, without corresponding degradation ([137]; please see section 1.2.1.2).

Several experimental studies have demonstrated the link between MUC1 expression and the promotion of tumourigenesis. MUC1 knock-out mice, which are developmentally and reproductively normal, show a decreased growth rate in primary mammary tumours induced by polyoma middle T antigen [36]. However, MUC1 signalling has not been correlated with increased PCNA activation (a marker of cell proliferation, [54], please see section 1.2.3.2.1). MUC1 may also function in tumour cell motility, as transfection of this mucin into a human gastric cancer cell line conferred greater ability to migrate into Matrigel and mouse muscle after subcutaneous injection, and increased motility in a gold particle phagokinetic track assay [163].

1.2.3 MUC1 Functions

1.2.3.1 MUC1 and Disruption of Adherens Junctions and Matrix Adhesions

MUC1 can actively affect E-cadherin and integrin mediated adhesions; it has been reported that the cytoplasmic tail of MUC1 binds β-catenin [50,55], a dual signalling and structural protein, which is part of the link between E-cadherin and the cytoskeleton in

polarized, well-differentiated epithelial cells. During events such as wound healing, development and formation of certain types of carcinoma, β-catenin can complex with the TCF/LEF transcription factor, and move into the nuclear compartment, where it modulates regulation of genes such as c-myc [164], cyclin D1 [165] and E-cadherin [166]. Although nuclear β-catenin is not detectable in human breast cancer [1,55], it may be competitively inhibited from binding to E-cadherin by the MUC1 cytoplasmic tail, thus facilitating cell-cell detachment [50].

Active modulation of integrin function was demonstrated in MDA-MB-468 and MDA-MB-231 cells, to which peptides corresponding to specific regions of the MUC1 cytoplasmic tail were cytoplasmically introduced with the BioPorter reagent. These peptides co-localised with β-catenin and vinculin at focal adhesions, and peptides containing phosphorylation sites for binding of both β-catenin and $GSK_3\beta$, resulted in the maximum promotion of cell migration in a Transwell assay [55]. In this scenario, the cytoplasmic domain of MUC1 may be acting as a scaffolding to bring together the necessary kinases for focal adhesion turn over, thus loosening the attachment to the matrix.

1.2.3.2 MUC1 Signalling

1.2.3.2.1 MUC1, EGFR and the MAPK Pathway

Indirect stimulation of MUC1 has included the use of CD8/MUC1 CT chimeras, which are forcibly clustered by the addition of anti-CD8 antibody [52,53], and EGF, which leads to the association of EGFR with MUC1 [54,55]. In either scenario, phosphorylation of the MUC1 CT and ERK1/2 occurred. The latter phosphorylations could be inhibited by dominant negative ras (N17;[53]), suggesting that ERK1/2 activation is downstream of phosphorylated MUC1 CT. At this point, the final consequences of MUC1 signalling become ambiguous. Traditionally, activation of the Ras/Raf pathway is considered to be a proliferative signal, and the generation of MUC1 null mice which formed breast tumours on the addition of polyoma middle T antigen, has shown that these tumours display a decreased growth rate [167]. Despite clear indications that ERK1/2 are phosphorylated after MUC1 CT "activation", Schroeder et

al. demonstrated that this was not concurrent with increased PCNA activation [54], suggesting that the downstream consequence of MUC1 CT phosphorylation is not proliferation. This suggests that the results seen in the MUC1 null mice may have been caused by other microenvironmental factors, such as differential requirements for oxygenation and nutrients. If MUC1 is proven to be chemotactic for fibroblasts [168], the decreased growth rate of these tumours may be attributable to the lack of fibroblast-secreted trophic factors and extracellular matrix proteins, which would normally stimulate the directional growth of tumour cells, as well as vasculature, which would thus provide increased oxygenation and nutrients to the developing tumour.

1.2.3.2.2 MUC1 as a "Sensor" of the Microenvironment

MUC1 CT phosphorylation also occurs when there is a lack of cell-cell contacts, as Quin et al. have shown that phosphorylation is increased in low density cultures of ovarian carcinoma cell lines, or during the initial adhesion of these cells after trypsinization [169]. It is possible that this phosphorylation is part of a signal that is turned off once cells reach confluency. In this scenario, however, MUC1 was not forcibly clustered and EGF was not deliberately added, indicating that MUC1 "activation" can occur by other means. Thus far, the only identified ligand of the MUC1 extracellular domain that has possible physiological relevance is ICAM-1 [2,3,57,58]. It may be that excess MUC1, in the presence of other mutations, initiates loosening of lateral membrane adhesions, then loses polarity and modulates integrin function by interaction with the focal adhesions. Any putative ICAM-1-induced signals would then become important during stromal migration and entry and/or exit of the vasculature, as ICAM-1 is expressed on both fibroblasts and vascular endothelium. It has been suggested that MUC1 is involved in "transient cell structures of migrating cells that are involved in transient cell adhesions" [140], as MUC1 is found predominantly on microvilli and at the tips of filopodia, where it co-localises with ezrin, a known membrane-to-cytoskeleton linker. Thus, MUC1 is ideally positioned to "sense" pro-migratory signals during initial cell-cell contacts with adjacent cells also present in the microenvironment.

1.2.3.3 MUC1 May Be Involved in Motility and/or Directional Growth.

Early observations of MUC1 transfectants revealed that this mucin confers certain non-adhesive properties to cells. It was initially thought that the MUC1 effect was passive, and due to steric hindrance, that is, the multiple, negatively charged O-glycosylations were alleged to generate repulsive forces that reduced E-cadherin mediated cell-cell and integrin mediated cell-matrix adhesions, thus breaking apart a primary tumour, and facilitating metastasis [43-45]. However, this theory does not offer explanation for MUC1-bearing tumour cells adhering to the endothelia and matrix in the secondary target organ. Furthermore, the demonstration that MUC1 transfection into MDCK cells resulted in a non-adherent phenotype was performed in the MDCK-ras-e subclone [43,44], which are ras-transformed, and high E-cadherin expressors [170]. Transfection of MUC1 into the MDCK parental cell line did not result in loss of adhesion [138], supporting the idea that multiple changes must occur in a cell before it adopts malignant characteristics. Furthermore, steric hindrance does not appear to affect integrin binding to the extracellular matrix, as treatment of MUC1-transfected cells with a β1-integrin activating antibody could abolish the purported steric effects [43].

Functional studies involving transfection of MUC1 have shown that this mucin can cause a higher number of lung metastases in nude mice injected with a pancreatic cell line [171]. One possible explanation for this is related to the demonstration that a mucin suspected to be MUC1 has shown to be chemotactic and chemokinetic for skin and lung fibroblasts [168]. Thus, MUC1 could possibly take part in initiating the desmoplastic reaction, by encouraging the recruitment of fibroblasts, which would subsequently not only encourage angiogenesis, but support epithelial-to-mesenchymal transition (EMT) and growth of transformed epithelial cells. MUC1 may also function in tumour cell motility, as transfection of this mucin into a human gastric cancer cell line conferred greater ability to migrate into Matrigel and mouse muscle after subcutaneous injection, and increased motility in a gold particle phagokinetic track assay [163], and it could also increase migration of MDCK or 410.4 cells through collagen I-coated Transwells [172]. This may involve p120ctn, which can be involved in mediating the stability of E-cadherin at the cell membrane (reviewed in [173]), moduating cytoskeletal restructuring via Rho, Rac and Cdc42 [174-177], and lifting Kaiso-mediated transcriptional repression once

translocated to the nucleus [174,178]. Nuclear localisation of p120ctn has been associated with a branched cell morphology that precedes cell motility [176,178,179]. As the MUC1 CT has been known to bind to p120ctn [144], and can be observed either at the cell membrane or nucleus, there exists the possibility that it may be involved in the described functions of p120ctn (Figure 1.7).

Transfection of MUC1 into epithelial cells also changed the cellular morphology in three dimensional collagen I gels. 410.4 cells, which usually grew as undifferentiated spheres, grew instead as branched tubules. MDCK cells, which usually grew as hollow spheres, changed their growth pattern to elongated tubules with a lumen. Thus, it appears that in these cells, MUC1 stimulated directional growth, without disruption of cellular organization. As the MUC1 gene was put under the control of the β-actin promoter, these studies also demonstrated that high MUC1 expression by itself was insufficient to cause dispersion of cells, and appeared to be influenced by the normal tissue patterns of the respective cell types (i.e. kidney vs. breast) [172].

If MUC1 activation of the Ras/Raf pathway is not associated with proliferation, and the primary function(s) of MUC1 and its splice variants appear(s) to be related to modulation of cell-cell and cell-matrix adhesion, coupled with the gain of motile properties, is it possible that the Ras/Raf pathway could be triggering motility? Indeed, recent studies have shown that MAPK/ERK can regulate not only matrix degradation, but also enhance myosin light-chain kinase activity and subsequent myosin light chain phosphorylation, all favouring migratory behaviour (reviewed in [180]). Additionally, since MUC1 associates with EGFR, there is the possibility that it may participate in any of the Ca^{++}-related pro-migratory signals that are initiated by EGFR (reviewed in [181]).

Another possible way MUC1 might be influencing directional growth could involve binding to β-catenin and APC. It has been shown in drosophila male germline stem cells that an armadillo/APC/DE-cadherin complex functions to orient mitotic spindles, controlling the direction of cell division and maintaining proper tissue architecture [182]. Directional growth of three-dimensional MCF-7 colonies has been observed when these cells are co-cultured with fibroblasts [83]. Since MUC1 has also been reported to bind to β-catenin [50] and APC [146], perhaps MUC1 and E-cadherin

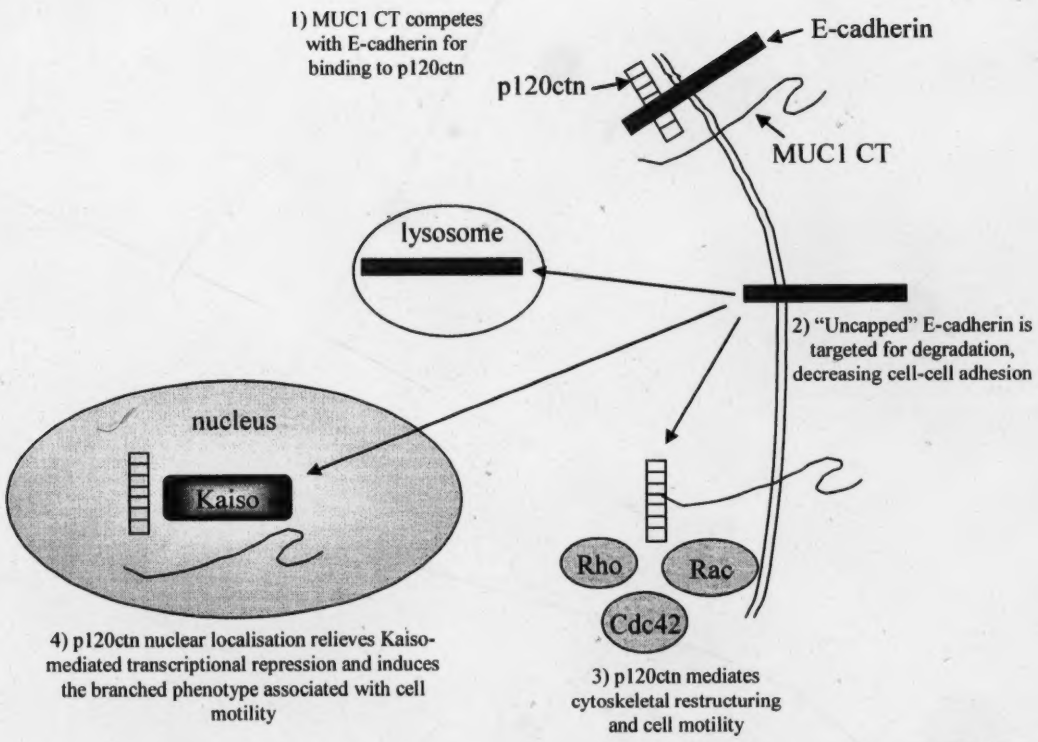
1) MUC1 CT competes with E-cadherin for binding to p120ctn
E-cadherin
p120ctn
MUC1 CT
lysosome
2) "Uncapped" E-cadherin is targeted for degradation, decreasing cell-cell adhesion
nucleus
Kaiso
Rho
Rac
Cdc42
4) p120ctn nuclear localisation relieves Kaiso-mediated transcriptional repression and induces the branched phenotype associated with cell motility
3) p120ctn mediates cytoskeletal restructuring and cell motility

Figure 1.7: MUC1 may complex with p120ctn to promote cell migration. MUC1 has been shown to compete with E-cadherin for binding to β-catenin. As MUC1 can also bind to p120ctn, there is the possibility that it may also competitively inhibit binding between p120ctn and E-cadherin. This may facilitate the known interaction of p120ctn with mediators of cytoskeletal restructuring, such as Rho, Rac and Cdc42, or with Kaiso, a transcription repressor. MUC1 CT facilitates nuclear localisation of p120ctn. Nuclear p120ctn has been associated with branching cell morphology and increased cell motility. Based on [173-179,183].

could orient mitotic spindles in a similar manner, with the direction being mediated by E-cadherin on the end of the cell facing the MCF-7 colony, and MUC1 on the side of the cell extending along the body of a fibroblast (Figure 1.8).

1.2.3.4 Other Putative Functions

It has been reported that complexes of the MUC1 CT and β-catenin have been found in the nuclei of multiple myeloma [184] and pancreatic cancer cells [185], however, we [1,186] and others [55] have determined that this does not occur in breast cancer. There are preliminary hints that MUC1 may be involved in regulating gene transcription, as three separate groups have located the cytoplasmic tail in the nucleus [13,145,185], and work by Huang et al., has suggested that a MUC1 CT/β-catenin complex can activate the cyclin D1 promoter [187]. This may be triggered by EGF, which has been shown to encourage association of MUC1 and β-catenin [145] (Figure 1.9). MUC1 is also reported to attenuate levels of intracellular reactive oxygen species, by upregulating superoxide dismutase, catalase and glutathione peroxidase, thus diminishing an apoptotic response [188]. Alternately, MUC1 may protect cells against apoptosis by increasing intracellular levels of phosphorylated AKT, Bad and Bcl-x_L [189]. This might be regulated by an alternative pairing between MUC1 and γ-catenin, since the latter molecule has been shown to upregulate Bcl-2 under different circumstances [190]. It may be that the presence of MUC1 may modulate the function of γ-catenin, in terms of whether it influences Bcl-2 or Bcl-x_L expression levels (Figure 1.10).

1.2.4 Basic Physiology of ICAM-1

ICAM-1 (CD54) is a 19 nm long transmembrane glycoprotein belonging to the immunoglobulin superfamily (reviewed in [191]). It has a highly charged 28 amino acid cytoplasmic tail, which connects to the cytoskeleton via a protein complex containing α-actinin [192] and ezrin [193,194], a 24 amino acid transmembrane domain, and a 453 amino acid extracellular domain. There are five immunoglobulin-like regions in the extracellular domain, and a free cysteine residue close to the membrane, which is

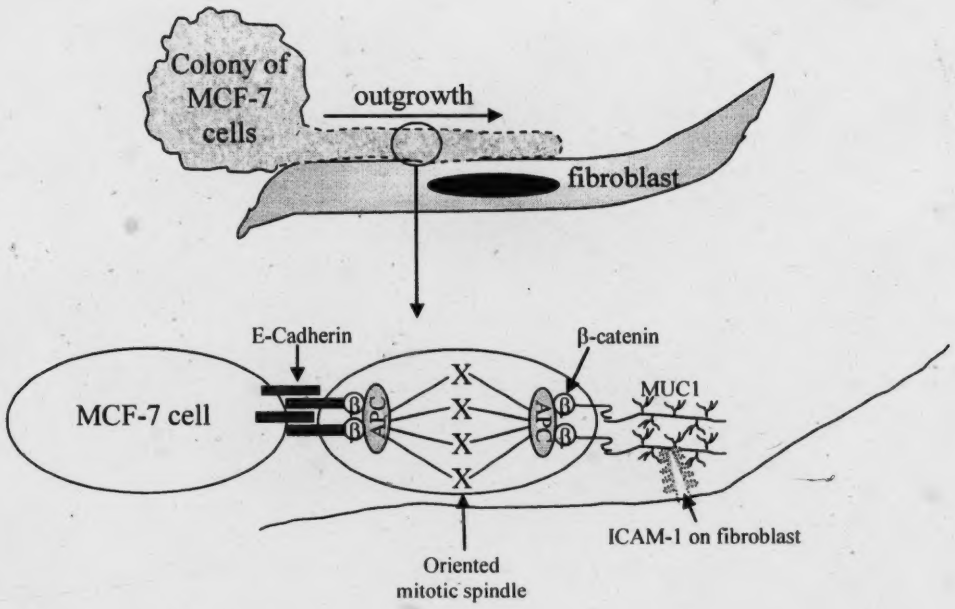

Figure 1.8: Speculative diagram of how MUC1 may complex with β-catenin and APC to control the direction of cell growth. Three dimensional colonies of MCF-7 cells are known to grow directionally along the body of co-cultured fibroblasts. Because both E-cadherin and MUC1 can complex with β-catenin and APC, it could be speculated that such complexes might mediate directional growth of MCF-7 colonies along the surface of an ICAM-1 expressing cell.
Based on [50,83,146,182].

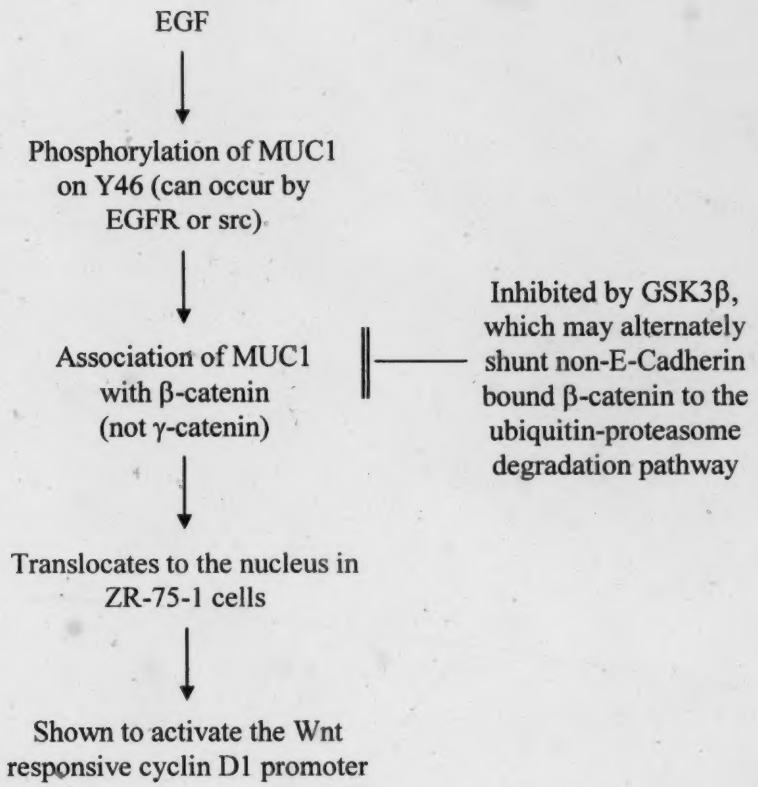
EGF
Phosphorylation of MUC1 on Y46 (can occur by EGFR or src)
Association of MUC1 with β-catenin (not γ-catenin)
Inhibited by GSK3β, which may alternately shunt non-E-Cadherin bound β-catenin to the ubiquitin-proteasome degradation pathway
Translocates to the nucleus in ZR-75-1 cells
Shown to activate the Wnt responsive cyclin D1 promoter

Figure 1.9: Schematic diagram of how MUC1 may be involved in β-catenin nuclear translocation and signalling. Based on [48,50,55,142,143,185,187,195].

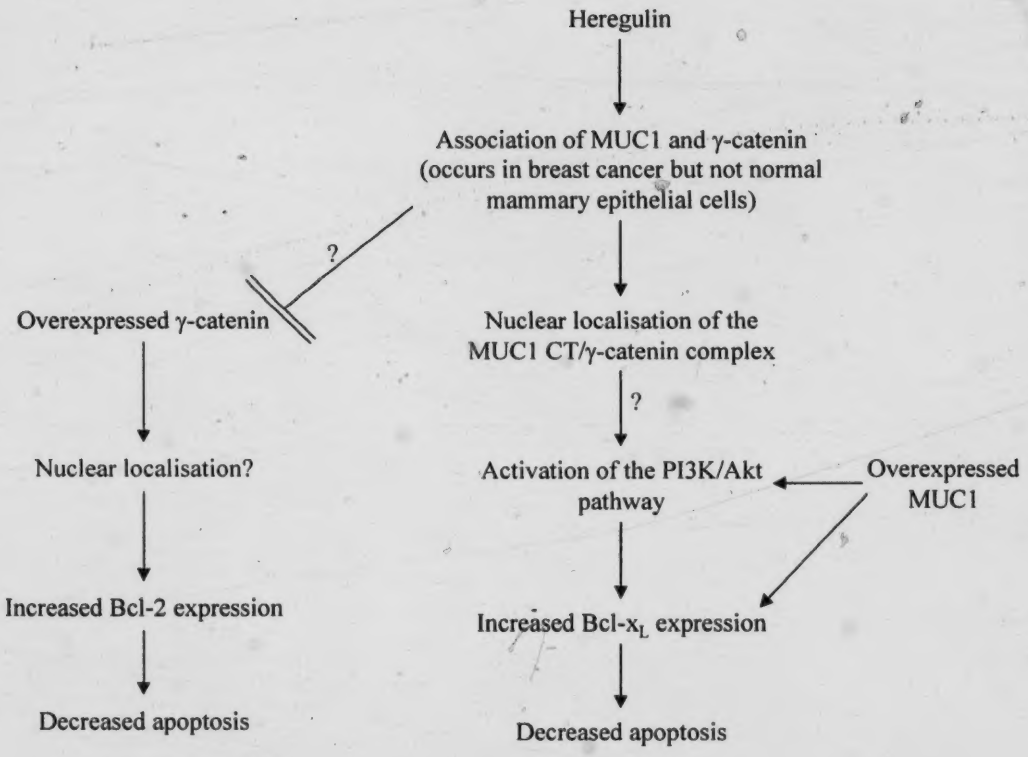

Figure 1.10: Schematic diagram of how MUC1 might be involved in γ-catenin nuclear translocation and signalling. Overexpression of MUC1 can activate the PI3K/Akt pathway, increase Bcl-x_L expression (but not Bcl-2 expression) and prevent apoptosis. It is also involved in nuclear translocation of γ-catenin. Since γ-catenin is also involved in regulating apoptotic responses, the MUC1 CT may influence which Bcl protein is affected by γ-catenin. Based on [145,189,190].

believed to mediate homodimerisation of the molecule [191,196-198], assisted by a "dimerisation interface" on Domain 1 (Figure 1.11) [197]. ICAM-1 is glycosylated in a tissue-dependent manner, and while the unglycosylated form is 60 kDa, it usually appears as 75-155 kDa on a Western blot.

ICAM-1 is expressed in several tissues, including leukocytes, endothelium and epithelium. It is an inducible molecule, most notably on endothelium, where it can be upregulated by inflammatory cytokines, such as TNF-α and IL-1β, which cause ICAM-1 mRNA to peak at 3 hours, and protein levels to peak at 18-24 hours, and remains at peak levels for at least 72 hours, or as long as the cytokine stimulus is present. Its expression on endothelial cells can also be increased in non-immunological situations, for example shear stress, reperfusion injury and ischemia [191,199-201].

There are several ligands for the extracellular domain, which include LFA-1 and Mac-1 on leukocytes, CD43, soluble fibrinogen, hyaluronin [191] and MUC1 [2,3,57]. Dimerization of ICAM-1 is essential for binding to LFA-1 and MUC1, and contact with LFA-1 results in the clustering of ICAM-1 to the point of cell-cell contact [196-198]. The patterns and levels of glycosylation have been suggested as mechanisms for cell type specificity, as the binding site for Mac-1 can be shielded by carbohydrate chains, which have no effect on binding of LFA-1. The signals initiated by ICAM-1 are again cell type specific, and may involve protein kinase C, cAMP, Ca^{++}, and/or phospholipase A2, depending on the cellular context [191].

1.2.5 ICAM-1 Function in Leukocyte Adhesion to Endothelia and Transendothelial Migration

As described in section 1.1.4, ICAM-1 is upregulated during inflammation to recruit leukocytes from the circulation. ICAM-1 plays a more complex role than simply providing firm anchorage after leukocyte rolling, however, as on ligation, ICAM-1 tends to cluster at the point of cell-cell contact, increasing the avidity of the binding [191]. This clustering triggers a series of signalling events. Early responses include an increase in cytosolic calcium [201-204], activation of src, and tyrosine phosphorylation of several proteins [205], including FAK, paxillin, p130cas, myosin light chain kinase and cortactin

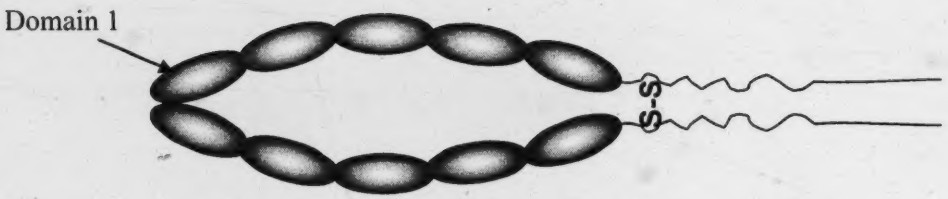

Figure 1.11: The ICAM-1 Molecule. The extracellular domain consists of five immunoglobulin-like domains, with a dimerisation interface on domain 1. Dimerisation is also mediated by a cysteine residue close to the transmembrane domain. Domain 1 is also involved in cation-dependent adhesion to integrin molecules.
Based on Jun CD, et al. [197].

[202,205-207], a protein that acts in conjunction with Dynamin 2 to remodel the actin cytoskeleton. There is also a Rho-dependent change in stress fibres and activation of c-Jun N-terminal kinase, as well as degradation of focal adhesion kinase, all leading to localised detachment of focal adhesions and endothelial retraction [203,206,208]. These events appear to occur preferentially at "tricellular corners", the point where three endothelial cells share cell-cell junctions [209,210]. The tight junctions are discontinuous at these corners, which perhaps facilitates the observed endothelial retraction that occurs on clustering of ICAM-1, either by addition of a cross-linking antibody, or an activated leukocyte. ICAM-1 itself is normally distributed evenly across the apical membrane of endothelial cells, however after 24 hours of cytokine stimulation, it redistributes to cell junctions [199]. Other proteins, such as junctional adhesion molecule and platelet endothelial cell adhesion molecule-1, appear to act in concert with ICAM-1 to guide migrating leukocytes towards tricellular corners [211]. Tumour cells also appear to be able to trigger similar responses in endothelial cells, as MCF-7 human breast adenocarcinoma cells, but not normal mammary epithelial cells, could trigger increases in intracellular calcium [204] and retraction in HUVECs [203].

Taken together, these observations suggest that transendothelial migration is a cooperative process, where the endothelial "barrier" actually facilitates the process if the transmigrating cell has an appropriate ICAM-1 ligand.

1.3 Study Objectives

This thesis is focussed on the functional and intracellular results of MUC1 ligation by ICAM-1, specifically at the transendothelial migration event of metastasis. It builds on earlier work done in this laboratory, showing that the protein core of the MUC1 tandem repeat domain can bind to dimerised ICAM-1. As such, MUC1 present on tumour cells can mediate firm adhesion to ICAM-1-expressing endothelial cells, with sufficient avidity to withstand shear stresses equivalent to physiological blood flow. The specific objectives of this study can be stated thus:

i) To determine if a correlation exists between MUC1 localisation in clinical specimens and the propensity to metastasize

ii) To determine if MUC1 and ICAM-1 can co-localise *in vitro* during heterotypic interactions between cells expressing either MUC1 or ICAM-1

iii) To determine if the functional consequence of MUC1 expression in an environment where adjacent cells express ICAM-1 is the adoption of a migratory phenotype

iv) To determine if a specific microenvironmental context can impact the migratory behaviour of MUC1-expressing cells

v) To begin characterising the intracellular events within the MUC1 expressing cell that may connect the initiation of the putative ICAM-1 induced signal at the cell surface to the actual motility of the cell.

Chapter 2: Intracellular Distribution of MUC1[1]

[1] Versions of parts of this chapter have been published. Rahn JJ, et al. 2001. Cancer. 91:1973-82. Rahn JJ and Hugh JC. 2001. Eur J Cancer. 37:668-70.

2.0 Introduction

Since 1981, several articles have been published documenting the presence and possible significance of MUC1 in breast carcinoma. However, the use of diverse antibodies and grading systems made direct comparisons between reports difficult, and no definite conclusions had previously been made about the significance of MUC1 quantity or staining patterns, or if these two parameters had any clinical significance. To clarify the distribution of MUC1 in the different histologic presentations of breast carcinoma, the literature was reviewed with special attention to the immunostaining conditions, and where possible the distribution of MUC1 within the cells, and combined with our own observations from 71 additional cases [1].

A secondary objective was to relate clinically observed MUC1 patterns to MUC1 behaviour observed in our functional studies. The intracellular positioning of MUC1, the relationship of a MUC1-expressing cell to surrounding cells, and proximity of MUC1 to other molecules such as E-cadherin and β-catenin was useful in assessing previously published theories on the role of MUC1 in promoting metastasis and guided the design of our later experiments. Much of the investigations completed in our lab have implicated the interaction between MUC1 and ICAM-1 in heterotypic cell adhesions. There is the potential that depolarised positioning of MUC1 on the plasma membrane may increase the probability of the MUC1 being ideally positioned to interact with ICAM-1 on adjacent cells. We speculated that cell surface MUC1 at the leading edge of a migrating cell, or at the initial point of heterotypic cell-cell contact may be important in setting off the cascade of events that leads to migration, perhaps by an ICAM-1 triggered signal.

Specifically, the questions investigated in this chapter were:

i) Did the intracellular distribution of MUC1 correlate with prognosis?

ii) Was there any evidence of MUC1 sterically or electrostatically inhibiting the function of adhesion molecules, thereby promoting liberation of cells from a primary tumour?

iii) Since MUC1 reportedly competes with E-cadherin for binding to β-catenin, was there an inverse relationship between co-localisation of β-catenin with E-cadherin vs. β-catenin with MUC1?

iv) Were MUC1 expression levels affecting β-catenin intracellular localization, perhaps influencing nuclear levels of β-catenin, which could increase cell proliferation, as observed in colon cancer (reviewed in [212])?

v) Was there any evidence that MUC1 and ICAM-1 localise preferentially at points of heterotypic cell contact?

These questions were addressed by immunostaining clinical breast specimens and breast cell lines for MUC1 and E-Cadherin/β-catenin. Cell lines in heterotypic co-culture were immunostained for MUC1 and ICAM-1, or transfected with YFP-MUC1 and CFP-ICAM-1, to examine potential interactions between these two molecules in cells exhibiting migratory behaviour.

2.1 Methods and Materials

2.1.1 Tumour Sections

Seventy-one current, consecutive specimens from patients with breast carcinoma that were submitted for routine processing were used in this study. The specimens were unselected and, thus, represented a random sampling of tumours with no follow-up data. The pathologic material was anonymized with only lymph node status available from most but not all patients. This handling of the specimens was in accordance with the ethics approval for this study, which was obtained from the Research Ethics Committee of the Alberta Cancer Board. Serial sections were immunostained for MUC1, β-catenin, and E-cadherin. Of 71 specimens, 33 were invasive ductal carcinoma not otherwise specified, 16 were invasive classical or variant subtypes of lobular carcinoma, and 21 were mixed ductal-lobular carcinoma. One specimen was ductal carcinoma in situ only. Of 71 specimens, 55 contained adjacent regions of normal glandular tissue on the same section.

2.1.2 Cells

Primary human umbilical vein endothelial cells (HUVECs) were harvested within 24 hours from freshly collected umbilical cords, by washing the veins with DPBS (0.9mM $CaCl_2$, 2.67mM KCl, 1.47mM KH_2PO_4, 0.5mM $MgCl_2 \cdot 6H_2O$, 138mM NaCl, 8.1mM $Na_2HPO_4 \cdot 7H_2O$, 5.6mM D-glucose, 0.333mM sodium pyruvate, pH 7.2), followed by 3mM $CaCl_2$ in DPBS, then filling the vein with freshly prepared collagenase at 1mg/mL in DPBS and allowing the cord to incubate at 37°C for 15 minutes. Detached endothelial cells were flushed out of the vein with warmed PHEC media (M199 media, 20% FBS, 10U penicillin, 10U streptomycin and 2mM L-glutamine), centrifuged and plated in a 0.1% gelatin-coated T25 flask with PHEC media + 1% ECGS-heparin (stock solution contains 10mg/mL heparin and 5mg/mL endothelial cell growth supplement). HUVEC identity was confirmed by phenotyping the cells with a panel of antibodies against CD31, CD34, FVIII, ICAM-1 and LCA. HUVECs were trypsinized and passaged 1:3 when confluent, and not used past the fifth passage. EAhy926 cells, which are a fusion hybrid of HUVECs and the A549 human lung carcinoma cell line, were kindly provided by Dr. Cora Jean S. Edgell, Department of Pathology, University of North Carolina at Chapel Hill, and maintained in RPMI media + 10% FBS, 2mM L-glutamine. 293T embryonic human kidney epithelial cells, ZR-75-1 and MCF-7 human breast adenocarcinoma cells were from the ATCC, and were maintained in DMEM + 10% FBS, RPMI +10% FBS + 2mM L-glutamine and DMEM + 10% FBS + 0.1mg/mL insulin, respectively. 293T cells transfected with SCI or SYM plasmids (described below) were selected and subcloned in media containing 1100 μg/mL G418, and maintained in media containing 200 μg/mL G418.

2.1.3 Antibodies and Reagents

Monoclonal antibody (mAb) B27.29 (gift from Biomira, Inc., Edmonton, Alberta, Canada) was used to detect MUC1. Cy3-B27.29 direct labelled antibody was prepared using a Cy3-NHS direct labelling kit from Amersham. This immunoglobulin G1 (IgG1) mAb is directed against the MUC1 epitope PDTRPAP on the tandem repeat. Anti-β-

catenin CAT-5H10 mAb and anti-E-cadherin HECD-1 mAb were purchased from Zymed. 18E3D mouse anti-human ICAM-1 monoclonal antibody was a gift of ICOS Corporation, and goat anti-mouse FITC secondary antibody was from Southern Biotechnology Associates, Inc. Antibodies were diluted in antibody dilution buffer (DAKO; for clinical immunohistochemistry) or 2% BSA + 0.02% Tween20 (fluorescent immunostaining) as follows: HECD-1 (1 mg/mL), 1:200 dilution; CAT-5H10 (1 mg/mL), 1:250 dilution; B27.29 (5 mg/mL), 1:5000 dilution; 18E3D (1.8 mg/mL), 1:2000 dilution; and goat anti-mouse FITC, 1:200 dilution. Biotin-labeled polyclonal antimouse/rabbit/goat IgGs (LINK), peroxidase-conjugated streptavidin, and diaminobenzidine tetrahydrochloride (DAB) buffer-substrate/chromogen system were from DAKO. Recombinant human cytokines, Tumour Necrosis Factor α (TNFα), and Interleukin 1β (IL-1β) were purchased from CedarLane Laboratories. T4 ligase was from New England Biolabs. Platinum High Fidelity Taq Polymerase was from Invitrogen, the dNTP mixture was from Roche, and Q-Solution was from Qiagen. pEYFP-N1 and pECFP-N1 plasmids were from Clontech. The pC1NeoTR+ FLAG plasmid carrying the MUC1 gene was a gift from Dr. Sandra Gendler, Mayo Clinic, Scottsdale, and the pBOS ICAM-1 plasmid (originally from Dr. Darren Shafren) was a gift of Dr. Ken Dimock, University of Ottawa.

2.1.4 Immunohistochemical Staining of Paraffin Embedded Breast Tumours

Formalin fixed, paraffin embedded sections were deparaffinized in xylene and rehydrated in an ethanol/water gradient. After microwave epitope retrieval in 1mM EDTA for 10 minutes, sections were incubated with the appropriate primary antibody for 1 hour at room temperature. A negative control with no primary antibody was performed for each specimen. The sections were then incubated in biotin LINK for 30 minutes. Endogenous peroxidase activity was abolished by incubating the sections for 2 minutes in 65% MeOH, 10.5% H_2O_2, and 24.5% H_2O before incubating with peroxidase-conjugated streptavidin for 30 minutes and DAB buffer-substrate/chromogen for 5 minutes. The slides were counterstained with hematoxylin and coverslipped using Entellan™ mounting media.

2.1.5 Evaluation of Immunohistochemically Stained Tumours

Staining patterns were enumerated separately for normal glands, in situ carcinoma, and invasive carcinoma. The proportions of cells positively stained in each subcellular location, i.e., apical, cytoplasmic, intracytoplasmic canaliculi, and nonapical membrane, were recorded for each antibody by two investigators (J.J.R and J.C.H.). Discrepancies were resolved after discussion at a dual occular microscope. The proportions were recorded as a percentage of the reference cell population, and the intensities were scored on a scale of 3, where 3 = dark, well-defined staining that was equal to or darker than that seen in normal tissue, 2 = moderate staining, 1 = only a faint stain, and 0 = no staining. In sections in which more than one type of tumour was noted (e.g., ductal-lobular admixed), each tumour type was scored and recorded separately. Histologic subtyping and nuclear grading were performed on a slide cut from the same block. Nuclear grading was assessed according to the nuclear grade component of the modified Scarff–Bloom–Richardson system. Briefly, nuclei which were regular in shape and size, and showed little variation were accorded one point. Marked variations, often with prominent nucleoli, were scored as 3 points, and moderate variation was given 2 points. There was general agreement between the two investigators. The exclusive use of nuclear grade for characterizing the tumours was employed to remove the influence of architectural grade or gland formation on our correlations between staining and grade (differentiation). Material for the literature review was abstracted from 25 articles in the English literature. The majority of these were found through cross-referencing bibliographies in the various articles.

2.1.6 Plasmid Construction

It was intended to make MUC1 and ICAM-1 proteins tagged at their N-terminals (extracellular) with CFP and YFP. The basic design was to insert synthetic signal sequences, specific to MUC1 or ICAM-1, into the MCS regions of the pEYFP-N1 and pECFP-N1 (Clontech) vectors, and the gene sequences of these molecules (derived from gene sequences already cloned into plasmids; ICAM-1 from Dr. Ken Dimock, University

of Ottawa, and MUC1 from Dr. Sandra Gendler, Mayo Clinic, Scottsdale) after the YFP or CFP sequences.

2.1.6.1 PCR of the MUC1 and ICAM-1 Gene Inserts and Addition of Engineered Cut Sites.

The MUC1 primers were designed to result in "sticky" ends compatible with a 5' Bsr G1 restriction enzyme cut, and a Not I restriction enzyme cut at the 3' end, to allow directional insertion into the pEYFP-N1 plasmid after the YFP gene. The forward primer was also designed to pick up the MUC1 gene after the signal sequence, as this was to be inserted separately, before the YFP gene. The final sequence was 5'ATATTGTACATTACAGGTTCTGGTCATGC3'. The reverse primer was 5'ATATGCGGCCGCTCTACAAGTTGGCAGAAG3'. The pC1NeoTR+ FLAG plasmid was digested with Not I, then the 3.5kB band (the MUC1 insert) was purified on a low melting point agarose gel, and the appropriate band was cut out after staining with ethidium bromide. The gel slice was melted at ~75°C, and 1µL was used as a PCR template. This was necessary, as early attempts to perform PCR on the entire plasmid after linearization resulted in multiple, non-specifically primed products. The MUC1 gene fragment is 82% GC, and has multiple tandem repeats, which made amplification problematic. To compensate, the final PCR reaction contained 5% DMSO and "Q-Solution" from the Qiagen PCR kit (proprietary, but most likely betaine) to ensure that the GC interactions were weakened sufficiently to allow accurate template priming, and avoid hairpin formation within the tandem repeat section of the template during amplification. Invitrogen Platinum® Taq DNA Polymerase High Fidelity was used, as Clontech and Qiagen Taq polymerases and PWO polymerase (Roche) produced unsatisfactory results. The final reaction mixture was:

5 µL Invitrogen 10X reaction buffer
2µL Invitrogen Mg^{++} solution
4µL primer mix
1µL dNTP mix (Roche)
2.5µL DMSO

0.5μL Invitrogen Platinum High Fidelity Taq Polymerase
24μL ddH_2O
10μL Qiagen Q-solution
1μL template

The best matched melting temperatures for these primers was ~57°C, however, as the engineered sticky ends would not be incorporated into the template until the first few rounds of replication, the initial annealing temperature had to be dropped to 30°C, which only took into consideration the part of the primer that actually corresponded to the original MUC1 gene sequence. The cycling parameters were as follows:

-94°C for 3 minutes (initial denature)
-25 cycles
    94°C for 30 seconds (denature)
    30°C for 1 minute (anneal)
    52°C for 3.5 minutes (extension)
-52°C for 10 minutes (final extension)

The ICAM-1 forward and reverse primers were both designed to have Bsr G1 cut site compatible sticky ends, as changing one to Not I resulted in melting temperatures that were too diverse. Thus, directional insertion was not possible, but the ICAM-1 gene has a Bgl II cut site towards the 3' end of the gene, which was later used to check directionality in the resulting bacterial clones. The forward primer sequence was 5'ATATTGTACAGCAATGCCCAGACATCTGTG3' and the reverse primer was 5'ATATTGTACAGTCAGGGAGGCGTGGCTTG3'. The PCR was much less problematic, and worked without special manipulations. The absence of the engineered cut sites on the template was taken into consideration when setting the annealing temperatures. The same Invitrogen Taq was used as for MUC1, without DMSO or Q-Solution, with the following cycle parameters:

-94°C for 3 minutes (initial denature)

-25 cycles

94°C for 30 seconds (denature)

22°C for 1 minute (anneal)

42°C for 2 minutes (extension)

-42°C for 10 minutes (final extension)

2.1.6.2 Insertion of the PCR Products and Selection of Clones with the Correct Orientation of Gene Insert.

The PCR products were 'picked up' using the Qiagen pDrive Cloning Vector, which comes with its own ligase in the provided reaction buffer. The manufacturer's protocol was followed. This allowed confirmation of the specificity of the cut sites for gene insertion into the Clontech vector by digesting the gene fragment out of the pDrive vector. The cloning vector also provided a larger region of DNA for the restriction enzymes to adhere to, and could be used to prepare a large culture of bacteria carrying the PCR product, thus ensuring a high concentration of insert for the subsequent ligation with the Clontech vector. Several attempts were made to insert the PCR products into the Clontech vectors without using the pDrive vector first. None were successful.

After isolating a pDrive transformed colony that released an insert of the correct size upon digestion with BsrG1 ± Not I, that insert was purified on a low melting point agarose gel, along with a BsrG1 ± Not I digested Clontech vector (the CFP vector was also dephosphorylated to prevent re-ligation, as the cut site at both ends of the ICAM-1 insert were the same) the appropriate bands were cut out, recovered by melting the gel slices in a 75°C waterbath, snap freezing in a dry ice/acetone bath for five minutes, then thawing the slices and pelleting the precipitated agarose at 14000 rpm for 5 minutes. The supernatants contained the DNA fragments, which were then ligated using T4 ligase (New England Biolabs), and vector:insert molar ratios of 1:10. Colonies carrying the desired vectors were identified by the digestion of mini-prep DNA with enzymes that would confirm the identity and direction of the inserts (Kpn I for MUC1, and Bgl II for ICAM-1).

2.1.6.3 Insertion of Synthetic Signal Sequences.

The MUC1 signal sequence was taken from the gene map provided to us by Dr. Sandra Gendler, and modified so that the 5' end conformed to the restriction sequence for Sal I, and the 3' end for Bam H1. This was done to allow directional insertion after cutting the MCS region of the pEYFP-N1 plasmid with the same enzymes. A Stu I diagnostic cut site was also engineered close to the 5' end to allow confirmation of insertion after the plasmid construct was completed. The final sequence was 5'TCGACTAGGCCTATGACACCGGGCACCCAGTCTCCTTTCTT CCTGCTGCTGCTCCTCACAGTGCTTACAGTTGTTACG3'. The ICAM-1 signal sequence was taken from the NCBI Nucleotide Database, entry # X06990, which identified the signal peptide encoding region as nucleotides 13 to 87, and modified to also have the sticky ends corresponding to Sal I and Bam H1 restriction cut sites, and an Afl II diagnostic cut site to confirm insertion. The final sequence was 5'TGCACA CTTAAGAGTGCTCCCAGCAGCCCCCGGCCCGCGCTGCCCGCACTCCTGGTCCT GCTCGGGGCTCTGTTCCCAGGACCTGGCAAG3'. These were synthesized by the DNA Core Services Laboratory, Biochemistry Department, University of Alberta. Insertion of the signal sequences was performed by our (then) Honours/Summer student, Jeffrey Chow. Equimolar amounts (200nmol/mL) of the sense and antisense strands of the signal sequence oligonucleotides were dissolved in annealing buffer (10mM Tris pH 8.0, 50mM NaCl, 1mM EDTA), and heated to 94°C. These were annealed by letting them cool slowly to room temperature overnight. The recipient vectors were digested with Sal I and Bam H1. Both the annealed oligos and digested plasmids were purified on a low melting point agarose gel, and the appropriate bands cut out after staining with ethidium bromide. The DNA was recovered from the gel slices as described in section 2.1.6.2. Digested plasmids and annealed oligos were mixed at a 1:20 vector:insert molar ratio, and ligated with T4 ligase, overnight at 16°C. The reaction mixtures were used to transform DH5α E. Coli, which were grown on Kanamycin antibiotic agar plates. A minimum of 6 colonies were selected for each plasmid preparation and minipreps (Qiagen Kit) were screened by digestion with either Stu I or Afl II. The final plasmids were designated as either SYM (signal sequence, YFP, MUC1) or SCI (signal sequence, CFP, ICAM-1), and MaxiPreps (Qiagen Kit) were made for later transfections.

2.1.7 Transfection and Subcloning

The final MUC1 plasmid, SYM, was transfected into HEK 293T cells, as this is a MUC1-null epithelial cell line. This was initially attempted with the traditional calcium phosphate method, electroporation, and the Qiagen Effectene Kit (the supplied manufacturer's protocol was followed). Cells were subcloned by treating the orginal transfection culture with DMEM + 10% FBS + 1100μg/mL G418 selection antibiotic for one week, then trypsinizing the cells and diluting them to 0.5 cells/200μL, and plating 200μL of cell suspension into individual wells on a 96 well plate. Each well was visually inspected to ensure there was only one colony per well. Wells with no colonies, or more than one colony, were marked and excluded. Out of these trials, only one stable, G418 resistant colony expressing MUC1 (as determined by Western Blotting) was attained through the Effectene method, however the expressed protein did not have the YFP tag (possibly due to a random recombination event).

The transfection was repeated using the Effectene Kit, this time incorporating a DMSO shock (10% DMSO in DMEM + 10% FBS, warmed to 37°C and incubated with cells at room temperature for 5 minutes, followed by a 1X wash with fresh media, addition of fresh media and return of the cells to the incubator) the following day, and inclusion of 2mM sodium butyrate in the media for 24 hours to "kick start" expression of the transfected gene. This resulted in 36 stably fluorescent, G418 resistant colonies.

The ICAM-1 plasmid, SCI, was also transfected in 293T cells, this time using the Invitrogen Lipofectamine 2000 reagent, followed by the addition of 2mM sodium butyrate to the media. This resulted in eighteen G418 resistant sublcones, four of which appeared fluorescent under the CFP filter on a fluorescent microscope.

EAhy926 cells and HUVECs were also transfected with the SCI plasmid, however, subclones could not be obtained, as transfected EAhy926 cells only survived for about 3 days, while >95% of the transfected HUVECs died within 24 hours.

2.1.8 Confocal Microscopy of Fluorescently Labelled Cell Lines

2.1.8.1 MUC1 and β-Catenin Double Immunostain

Cells were grown on glass slides, fixed for 15 minutes in 2% formaldehyde in PBS, and permeabilized for 15 minutes in 0.5% Triton X-100 in PBS. Slides were then washed in PBS, and incubated sequentially with CAT-5H10 (1 hour), goat-anti-mouse-FITC IgG (30 minutes), Cy3-direct labelled B27.29 (1 hour), then coverslipped using Fluoromount-G. Three PBS washes were performed after each step. The cells were visualized with a Zeiss Axiovert 100M confocal microscope, and Z-stacks were digitally recorded.

2.1.8.2 MUC1 and ICAM-1 Fluorescent Detection

EAhy926 cells were seeded on a glass slide and after adhesion, were stimulated with 20 U/mL each of TNF-α and IL-1β for 24 hours. MCF-7 cells were layered on top of the EAhy926 monolayer and incubated at 37°C overnight. Slides were fixed in 2% formaldehyde/PBS for 15 minutes, permeabilized in 0.5% Triton X-100/PBS for 15 minutes, then immunolabelled with 18E3D (mouse anti-human ICAM-1), goat anti-mouse FITC secondary antibody, then Cy3-labelled B27.29 (mouse anti-human MUC1 tandem repeats). Z-stacks of multiple focal planes through immunolabelled cells were imaged on a Zeiss Axiovert confocal microscope. In experiments using SCI and SYM transfectants, coverslips had been prepared earlier by pipetting a 100μL drop of 70μg/mL collagen onto a coverslip, and dried by incubation in a 60°C dry oven for one hour, then sterilized by exposure to UV light for 30 minutes. SCI cells were allowed to adhere for 4-5 hours, then the media was removed and a 100μL drop of SYM cells in suspension was added. The cells were co-cultured for 20 minutes in a 37°C incubator, 5% CO_2, for 20 minutes, then fixed using a modified formaldehyde/methanol technique [213]. Briefly, cells were washed twice in HBS (135mM NaCl, 10mM KCl, 0.4mM $MgCl_2$, 1mM $CaCl_2$, 10mM Na·HEPES, pH 7.4), incubated in 3.5% formaldehyde in HBS for 5 minutes at 4°C, then 10 minutes at room temperature, washed 3 X 5 minutes in HBS, incubated in methanol at -20°C for 6 minutes, washed again in HBS, then mounted in PBS-buffered glycerol.

2.1.9 FRET

Background information on the FRET technique appears in Appendix I.

2.1.9.1 FRET by Acceptor Fluorescence Increase

MatTek glass bottomed dishes where coated with 0.1% (w/v) gelatin in water (a 100µL drop was spread over the glass surface, dried in a 60°C oven, then UV irradiated for 30 minutes), and 100µL of SCI4 cells at 1 x 10^5/mL were plated and allowed to equilibrate overnight. The cells were rinsed with OptiMEM phenol red reduced media (Gibco) the next day, and covered with OptiMEM. SYM2 cells were trypsinized and suspended at ~1.2 x 10^7/mL in OptiMEM. After ~45 minutes (time required to set up microscope) the SCI cells were placed in a stage warmer set to 37°C, and over a 40X immersion oil objective (performed on the MJH Digital Imaging Microscope). Images were taken on three channels for each time point: CFP; YFP-FRET (YFP excitation); FRET-CFP/YFP. The CFP channel was set to a 25ms exposure, and the YFP channel set to 100ms. The SYM2 cells were pipetted over the SCI4 cells and the objective was focussed as near as possible to the interface between the two cell types. Z-stacks were taken every minute for 30 minutes. To analyse the images, the background was manually subtracted from each image (CFP, YFP and FRET channels), then the "Donor signal in Acceptor channel" was calculated by dividing the corrected YFP image by the CFP corrected image. An ROI (region of interest) marking where the two cell types were coming into contact was transferred to the "divided" image, and the region statistics displayed for the ROI was manually recorded. This was repeated to calculate the "Acceptor signal in Donor channel", "Donor signal in FRET channel" and "Acceptor signal in FRET channel". Then the FRET value was calculated using the FRET application in the Metamorph Software package, where under the "Set Up" tab, Source = Component, FRET method = Specified Bleed Through; Donor + Acceptor, Donor = the CFP corrected image, Acceptor = the YFP corrected image, and RawFRET = the FRET corrected image. Under the "Image Correction" tab, Background Subtraction = Regions, and Spectral Bleedthrough Coefficients = Bleed Through Correction. The numbers manually recorded for "Donor in Acceptor", "Acceptor in Donor", "Donor in FRET" and

"Acceptor in FRET" were entered into the appropriate boxes. After clicking on "Apply", an ROI indicating the region of cell-cell contact to be examined was transferred to the final FRET image, and the region statistics for the average grey level intensity was manually recorded. This number, or FRET value, corresponded to one time point in one focal plane in the z-stack. In order for spatial or temporal comparisons to be made, this analysis was repeated at the point of comparison. Then the final FRET values were compared.

2.1.9.2 FRET by Acceptor Photobleach

SCI4 or SCI transiently transfected EAhy926 cell and SYM2 or SYM25 cell co-culture specimens were prepared as described in section 2.1.8.2. Using the 2-photon Zeiss Axioscope microscope and the 40X oil immersion objective, fields were scanned for regions of obvious heterotypic cell-cell contact. The best focal plane was selected, the visual field was zoomed in on the cells of interest, and a "before" image capturing both fluorophores was saved after the image was adjusted to ensure there was no pixel saturation. The red laser was then disabled, and a bleach area corresponding to the region of cell-cell contact was defined. Two images on the CFP channel were recorded, the defined region was photobleached using the red laser at high intensity, then three more images were recorded on the CFP channel. The Zeiss software package automatically graphed the CFP fluorescence intensity over time, within the defined region. No mathematical manipulations were necessary, as no bleed through was expected in the CFP channel.

2.1.10 Statistical Analysis

Statistical correlations in the clinical immunohistochemical study were determined using the SAS program (release 6.12; SAS Institute Inc., Cary, NC). Comparisons of nuclear grade between two populations were made with a two-tailed, unpaired Student *t* test.

2.2 Results

2.2.1 Literature Review Findings

Higher levels of MUC1 staining were associated with a good prognosis and high probability of survival, as these tumours tended to also stain positively for estrogen receptor (such tumours respond well to anti-estrogen therapy), and be of low grade (Table 2.1 and Figure 2.1). Taken by itself, this information seems to suggest that heavy MUC1 staining is prognostically good. However, on examination of the subcellular localisation of MUC1, it becomes apparent that in these tumours the MUC1 is predominantly apical, and is perhaps better viewed as an indicator of functional differentiation. These cells are probably still capable of responding to polarisation signals, behaving as differentiated epithelia, and are not likely to be metastatically aggressive. Increased cytoplasmic staining of MUC1 was associated with decreased probability of survival (Table 2.2 and Figure 2.2), suggesting that these poorly differentiated cells are no longer capable of proper MUC1 targeting.

2.2.2 Clinical Distribution of MUC1 in Breast Cancer

2.2.2.1 Normal Glandular Epithelia

MUC1 showed strong apical staining in all normal glandular units. β-catenin and E-cadherin showed identical staining patterns with positive lateral membrane staining, and no detectable staining on the apical membrane. Rare epithelial cells also showed β-catenin in perinuclear and cytoplasmic sub-apical granules (Figure 2.3).

2.2.2.2 Ductal Carcinoma

In situ and invasive ductal carcinomas showed similar staining patterns. All tumours expressed MUC1, with 44 specimens (81%) showing > 50% of tumour cells stained. There was considerable heterogeneity in the cellular localization of MUC1. All eight samples (13%) with gland formation showed strong staining of the apical

Table 2.1: Studies of MUC1 in Patients with Breast Carcinoma using Percent Positive Staining

Reference	mAb Clone	Number of Patients	Positive Criteria (% Positive)	P value ≤ 0.06		
				Relation to Low Grade	Relation to ER positivity	Relation to good Prognosis
[214]	MAM3b	194	>10% (54)	significant	significant	significant
[215]	NCRC11	126	>50% (45)	significant	trend	significant
[216]	DF3	46	>10% (60)	significant	significant	not done
[217]	NCRC11	136	>25% (84)	not done	significant	not signif.
[218]	IIID5	80	>50% (56)	not done	not done	significant
[219]	IIID5	74	>50% (49)	not done	significant	not done
[220]	NCRC11	444	>50% (78)	significant	significant	significant
[221]	NCRC11	93	>25% (47)	not done	not signif.	not signif.
[222]	IIID5	85	>10% (70)	significant	significant	not done
[223]	NCRC11	63	>50% (67)	not done	not done	not signif.
[224]	HMFG1	168	>20% (52)	significant	significant	significant
[225]	NCRC11	115	>50% (70)	significant	not done	significant
[226]	NCRC11	483	>50% (65)	significant	significant	significant
[227]	CA15.3	39	>60% (73)	not done	not signif.	significant

Based on [1].

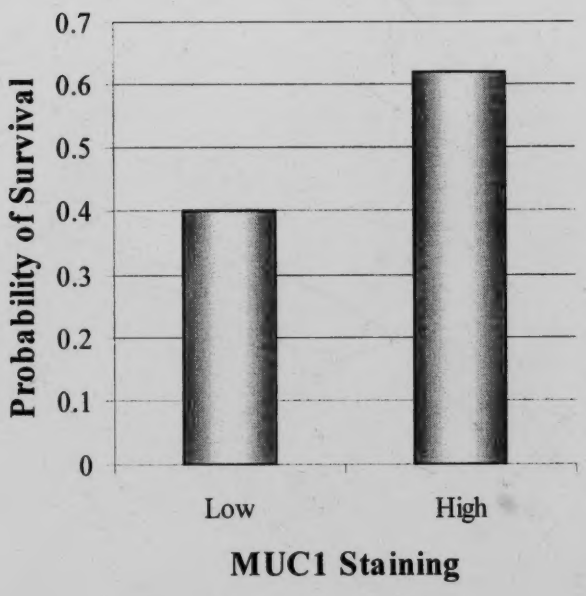

Figure 2.1: High overall MUC1 expression increases probability of survival (as described in the literature). Data were abstracted from the literature, and survival probabilities were compared in samples with low levels and high levels of overall MUC1 expression (e.g., site non-specific staining).

Based on: [1]

Table 2.2: Studies of MUC1 in Patients with Breast Carcinoma with Subcellular Localization

Reference	mAb Clone	Number of Patients	Relation to Prognosis	
			Better	Worse
[228]	HMFG1	175	Extracellular deposits of MUC1	Negative for MUC1
[229]	HMFG1	93	Negative for MUC1	Not done
[230]	DF3	28	Not done	Cytoplasmic MUC1
[231]	HMFG1	82	Not signif.	Not signif.
[232]	BRST-1	84	Not signif.	Not signif.
[233]	DF3	215	Overall MUC1 or Apical MUC1	Cytoplasmic MUC1
[234]	BrE-3	227	Membrane MUC1	Cytoplasmic MUC1
[235]	BC2	171	Not done	Overall MUC1 or Cytoplasmic MUC1

Based on [1].

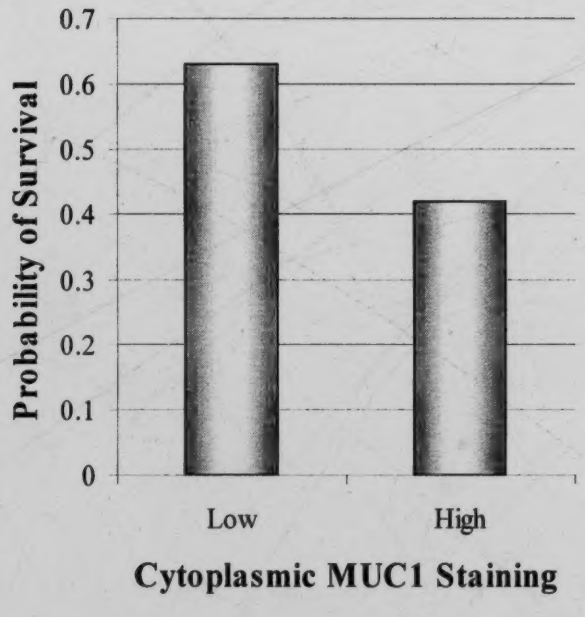

Figure 2.2: High cytoplasmic MUC1 expression corresponds to a decreased probability of survival (as described in the literature). Data were abstracted from the literature, and survival probabilities were compared in samples with low levels and high levels of cytoplasmic MUC1 expression.

Based on: [1]

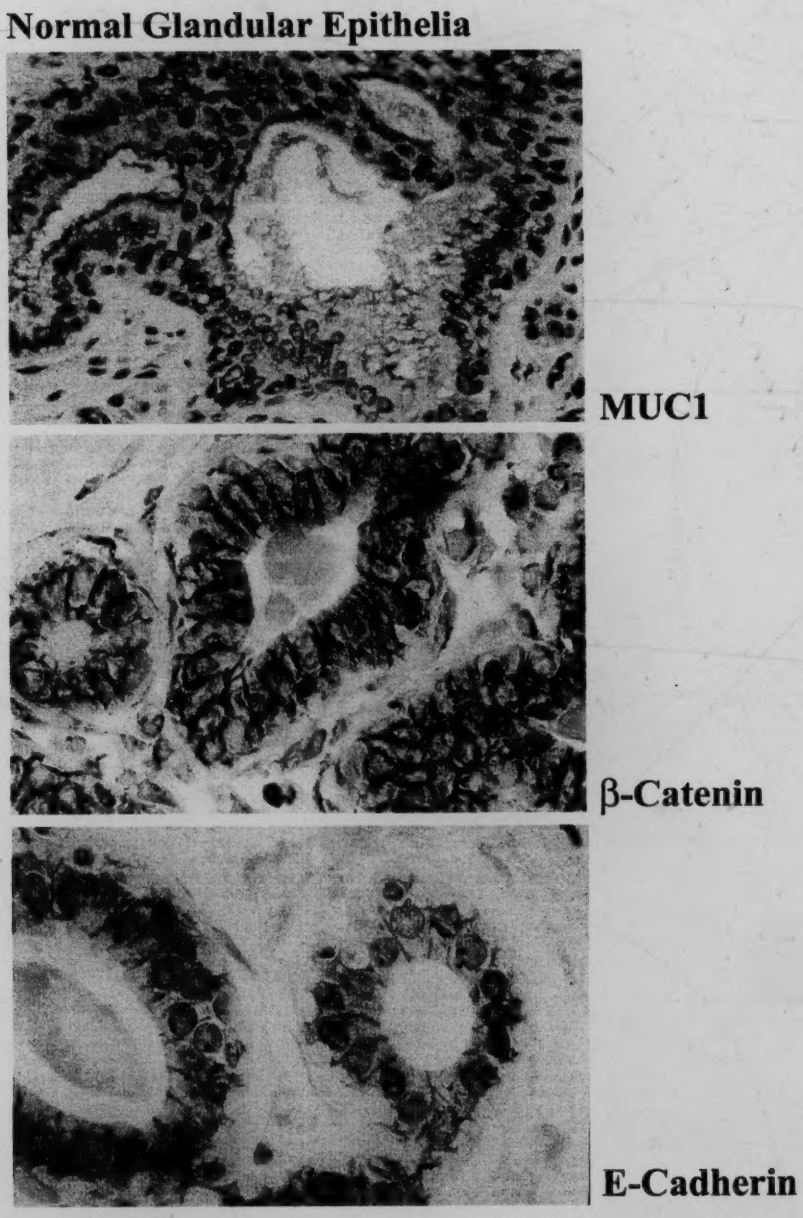

Figure 2.3: Staining of MUC1, β-Catenin and E-Cadherin in normal, glandular human breast epithelia. Specific molecular markers are stained brown (DAB), and cell nuclei are counterstained blue (alkaline hematoxylin). MUC1 appears on the apical luminal surfaces, while β-catenin and E-cadherin are along the lateral cell membranes. Based on [1].

membrane, whereas 19% showed exclusively cytoplasmic staining. The majority of samples (81%) showed some combination of membrane (apical, microcanaliculi, and nonapical membrane) and cytoplasmic staining. In 4% of in situ carcinoma samples and in 13% of invasive ductal carcinoma samples, the MUC1 staining was membranous around the entire cell circumference, even at the interface between two tumour cells. In these eight samples, there was prominent cytoplasmic staining in the remaining tumour cells.

Regardless of tumour differentiation, lateral membrane staining was seen exclusively for β-catenin in 80% of cases, and E-cadherin in 84% of cases examined. In one third of cases, there was also cytoplasmic staining for β-catenin which was usually coarse granular or perinuclear. Three cases (5.5%) showed prominent apical granules in a majority of the tumour cells (Figure 2.4).

2.2.2.3 Invasive Lobular Carcinoma

Approximately 50% of samples showed strong cytoplasmic MUC1 staining. No "circumferential" (over the entire cell membrane; appears circumferential on sectioned cells) membrane staining was seen, although this was sometimes difficult to discriminate from cytoplasmic staining. All intracellular canaliculi showed strong MUC1 staining along the rim of the canaliculus.

E-cadherin was present near the plasma membrane in only 9% of lobular cases. β-catenin was found at the plasma membrane in 33% of the cases. In 16 (48%) of the cases, particularly in regions of solid growth, a large, single perinuclear aggregate of β-catenin was detected. In three of these cases (8%), in addition to the perinuclear aggregates, β-catenin was also distributed at the lateral membranes (Figure 2.5).

2.2.2.4 MUC1 and β-Catenin

In those cases where MUC1 staining appeared circumferential, there was co-distribution of MUC1 and β-catenin. This occurred in 4% of in situ and 13% of invasive ductal carcinomas, with all of the tumours having a nuclear grade of 2 or 3. Typically, regions of MUC1/β-catenin co-distribution were focal in any given tumour. Of note is that in all areas showing membrane co-distribution of MUC1 and β-catenin, there was

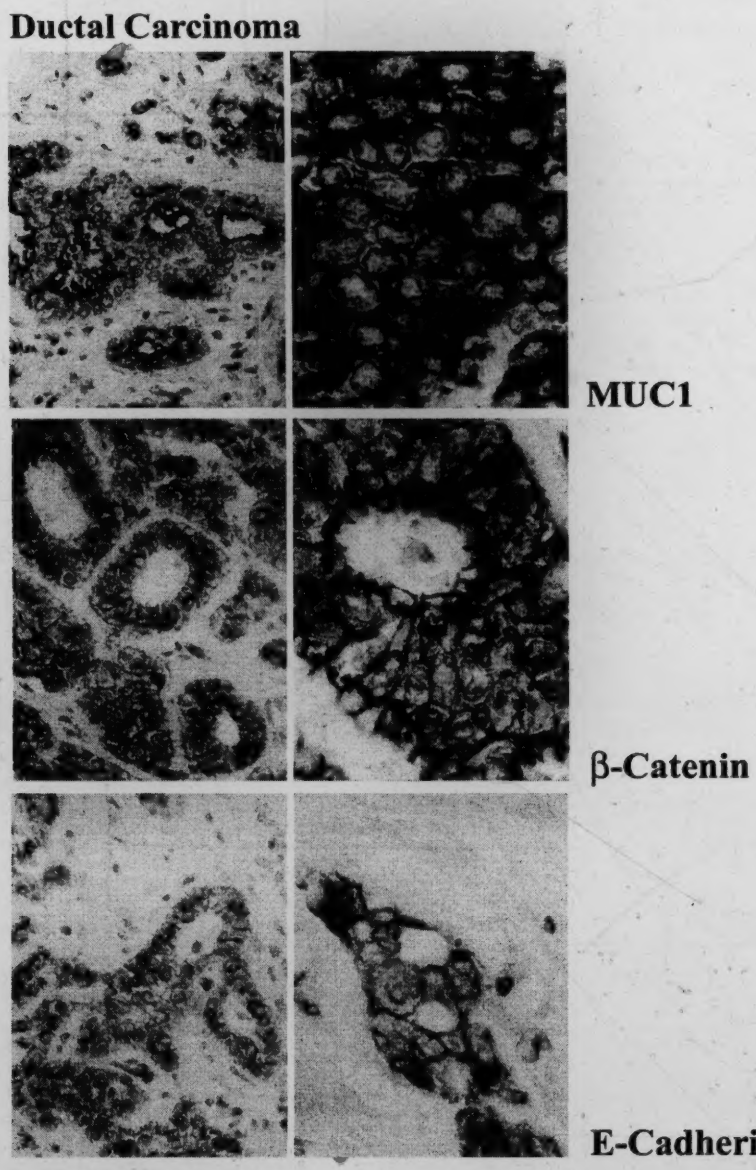

Figure 2.4: Staining of MUC1, β-Catenin and E-Cadherin in human breast ductal carcinoma. Specific molecular markers are stained brown (DAB), and cell nuclei are counterstained blue (alkaline hematoxylin). MUC1 appears on the apical luminal surfaces in relatively well differentiated carcinoma, and cytoplasmically or over the entire membrane surface in poorly differentiated carcinoma. β-catenin frequently appeared along the lateral cell membranes and in peri-nuclear granules. E-cadherin, when detectible, usually appeared along the lateral cell membranes.

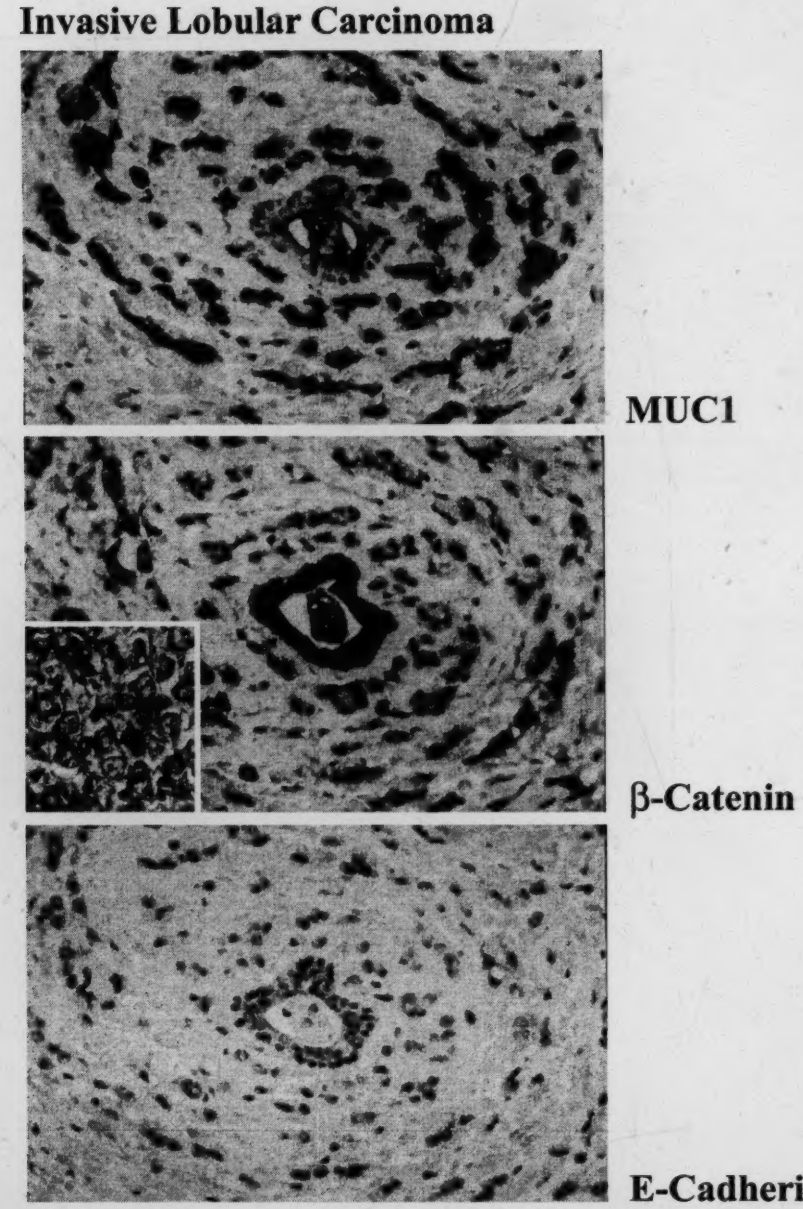

Figure 2.5: Staining of MUC1, β-Catenin and E-Cadherin in human breast lobular carcinoma. Specific molecular markers are stained brown (DAB), and cell nuclei are counterstained blue (alkaline hematoxylin). MUC1 typically appeared cytoplasmically and possibly over the entire cell membranes. β-Catenin frequently appeared at the plasma membrane, despite virtual absence of E-Cadherin at the membrane, and as perinuclear granules. The inset shows typical perinuclear β-Catenin staining.

also co-distribution with strongly staining E-cadherin. In those cases where nodal status was known, 5 of 6 (83%) of the cases showing membrane β-catenin and MUC1 co-distribution were node positive, compared to 10 of 34 (29%) in cases negative for co-distribution. This was shown to be statistically significant, with a Pearson Correlation of 0.4 and a p-value of 0.011. Using a multivariate logistic regression model, MUC1/β-catenin co-distribution remained an independent predictor of positive nodes even in the presence of grade (p-value of 0.022). No co-distribution between MUC1 and β-catenin was seen on any of the membranes of microcanuliculi, regardless of tumour type. Cytoplasmic co-distribution of these molecules was either minimal, or the staining patterns were distinct in any of the circumstances examined (Figure 2.6).

Nuclear β-catenin was not detected in any of the breast cancers examined. To confirm that this staining protocol was capable of detecting nuclear β-catenin, we examined two cases of colon cancer and one case of ovarian cancer, all of which showed strong nuclear staining restricted to the tumour cells. Unexpectedly, nuclear staining was detected in two cases of invasive ductal carcinoma using the polyclonal anti-MUC1 antibody directed against the cytoplasmic portion of MUC1 (Figure 2.7). Benign glandular elements in the same section showed the classical apical pattern of staining, as seen with the B27.29 antibody against the MUC1 extracellular domain.

2.2.2.5 MUC1 and Nuclear Grade

The 54 invasive ductal carcinoma samples initially were divided into those with low MUC1 expression (≤ 50% of tumour cells positive) and high MUC1 expression (> 50% of tumour cells positive), regardless of the intracellular location of the stain. The mean nuclear grade for specimens with high and low expression was 2.2 and 2.7, respectively, with a difference that was statistically significant ($P = 0.01$, Figure 2.8A).

The samples were then analyzed for differences in nuclear grade by cellular localization of MUC1 expression. High levels (> 50%) of cytoplasmic staining were present in 33 samples, and low levels (< 50%) were present in 21 samples. Comparison of the mean nuclear grade of the two groups, 2.2 and 2.4, respectively, was not statistically significant ($P = 0.3$, Figure 2.8B). There were too few samples for meaningful statistical comparisons for staining in other sites; however, some trends were

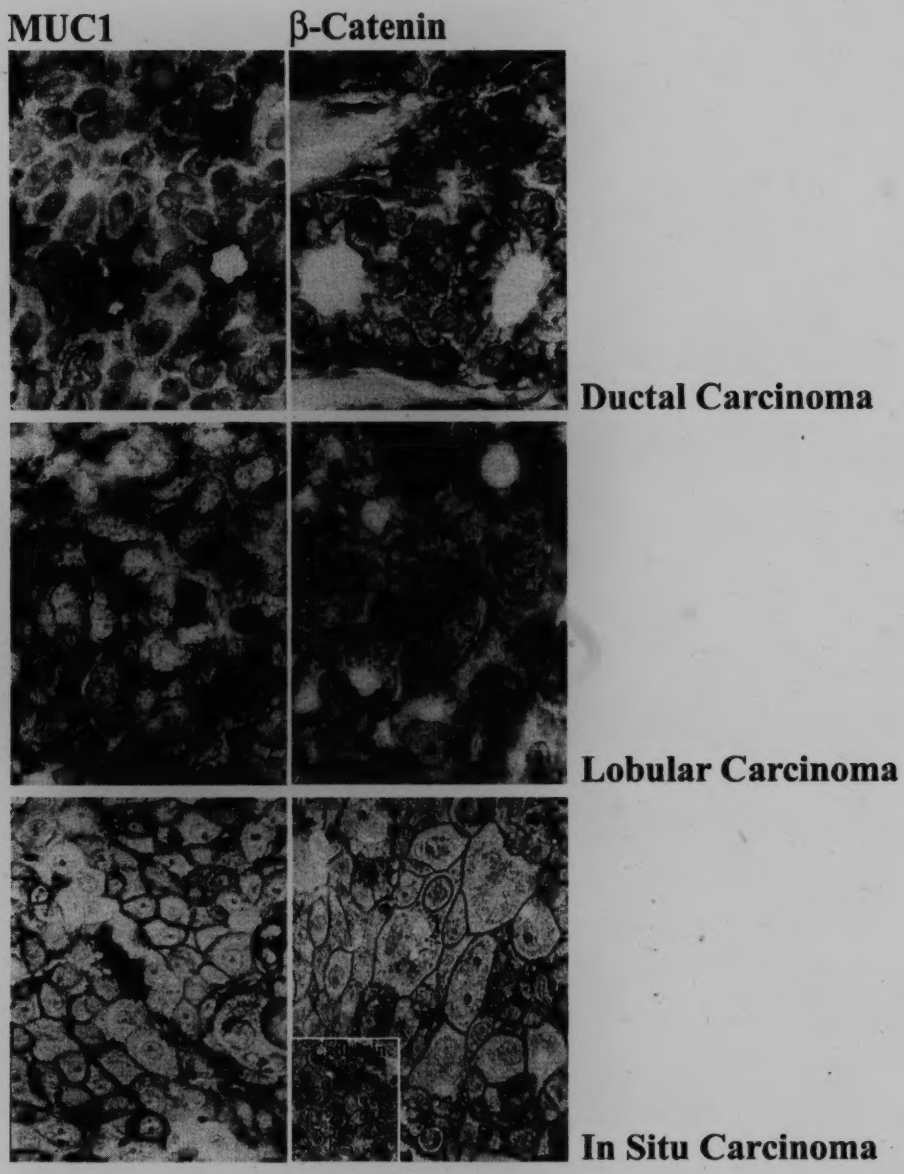

Figure 2.6: Comparison of MUC1 and β-Catenin localisation in human breast carcinomas. Specific molecular markers are stained brown (DAB), and cell nuclei are counterstained blue (alkaline hematoxylin). In ductal carcinoma, no obvious examples of MUC1 and β-catenin co-distribution were found. In cases where there was heavy staining for both molecules, MUC1 appeared on the luminal surfaces of microcannuliculi, while β-catenin appeared along the basolateral membranes. Similar observations were

Figure 2.6 (Continued): made in lobular carcinoma, and the cytoplasmic distribution of MUC1 makes possible co-distribution with β-catenin difficult to determine. MUC1 and β-catenin were seen to co-localise within the same subset of cells in *in situ* carcinoma, however in these cases, E-Cadherin staining was also clearly stained along the plasma membrane, making it difficult to predict if the β-catenin was associated with MUC1 or E-Cadherin. The inset shows typical E-Cadherin staining seen in ductal and *in situ* tumours. Based on [1].

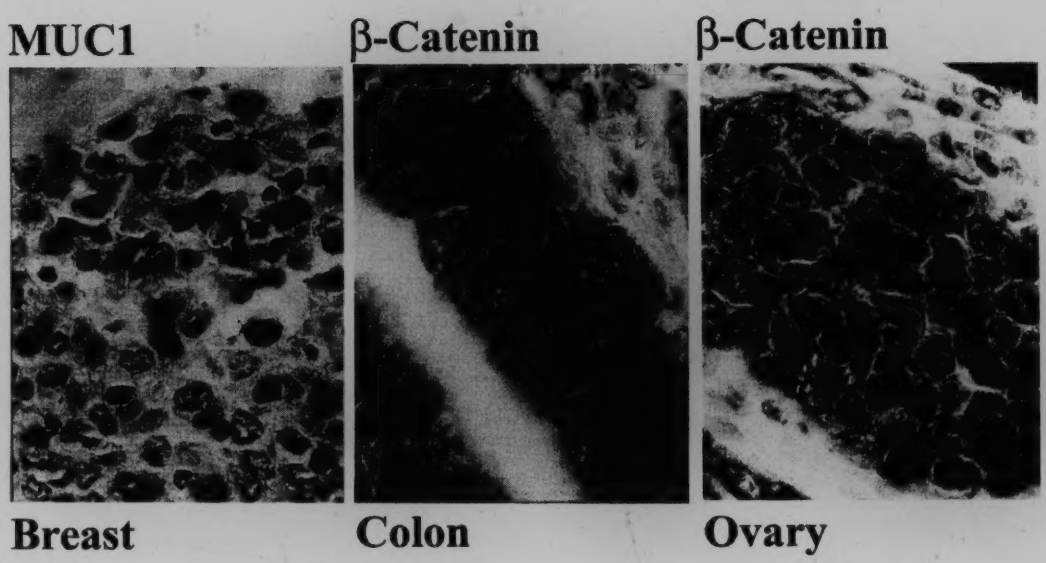

Figure 2.7: Nuclear staining of the MUC1 cytoplasmic domain and β-Catenin in carcinomas of different human tissues. Specific molecular markers are stained brown (DAB), and cell nuclei are counterstained blue (alkaline hematoxylin). The cytoplasmic tail of MUC1 was rarely observed in the nuclei of breast carcinomas. β-catenin was never seen in any of the 71 cases examined, however it was easily detected in a control section of colon carcinoma, and in one case of ovarian carcinoma. Based on [1,186].

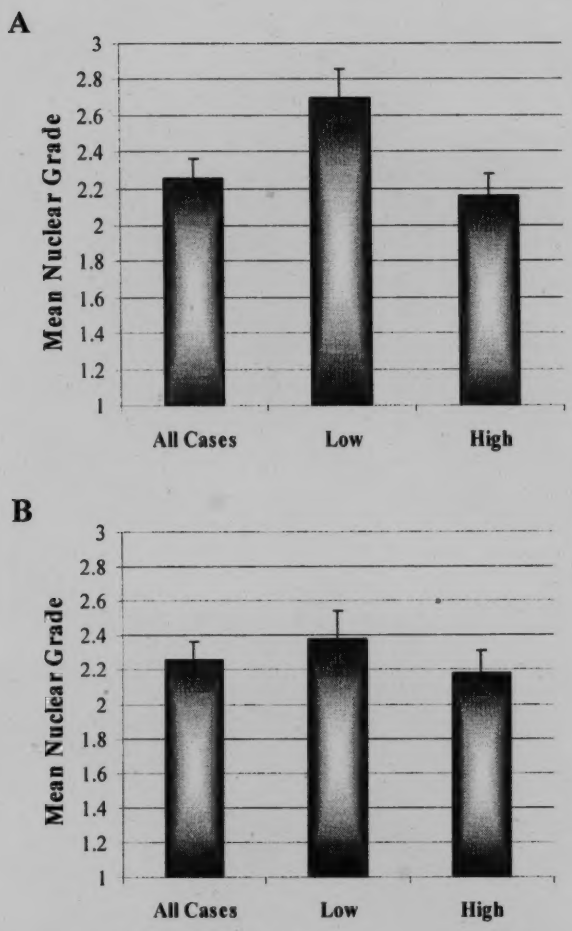

Figure 2.8: The mean nuclear grades of invasive ductal carcinomas according to the levels of MUC1 expression. (A) Overall MUC1 expression refers to the number of tumour cells with any immunoreactivity (site non-specific) expressed as a percentage of the total tumour cell population. The difference between low and high mean nuclear grades was statistically different ($P = 0.01$). (B) The number of tumour cells with positive staining for MUC1 in the cytoplasm were enumerated as percentage of the total tumour cell population. Low expression refers to ≤50%, and high expression to >50% positively staining cells. The difference between low and high nuclear grades was not statistically significant ($P > 0.3$). The data are presented as mean ± SEM. Based on [1].

evident. Predominantly apical staining was associated with a lower mean nuclear grade (1.8), whereas circumferential staining was associated with a higher mean nuclear grade (2.7) compared with the total population (2.3).

2.2.3 In Vitro *Distribution of MUC1 in Cell Lines*

2.2.3.1 MUC1 and β-Catenin in Breast Cancer Cell Lines

MUC1 association with β-catenin has been reported in the ZR-75-1 cell line, and in MUC1-transfected HEK 293T cells [50]. This was based on immunoprecipitation experiments, with no accompanying microscopy. Fluorescent immunostaining and confocal analysis of the ZR-75-1 cell line showed heterogenous MUC1 staining, depending on the amount of free membrane space, as determined by the individual cell position within a given colony (Figure 2.9). Colonies generally consisted of a non-confluent, flat layer adherent to the glass, from which extended loose aggregates of cells. MUC1 immunostained the most intensely within cytoplasmic vesicles. A minority of cells present at the top of the loose aggregates showed circumferential MUC1 staining, mainly along regions of free membrane. β-catenin showed strong linear staining along the intercellular membranes between adjacent cells, and in the loose aggregates, there was circumferential granular staining of β-catenin along the free membranes similar to the pattern seen with MUC1. Merging the two channels showed co-distribution of the fluorophores in this minority of the cell population.

These findings differed from those seen in the MCF-7 cell line which grows as tightly packed clusters of adherent cells. These showed MUC1 staining only on the outer edges of the colony, while β-catenin was found in areas of cell-cell contact and at low levels as granules, in the cytoplasm. Co-distribution of MUC1 and β-catenin in these cells appeared to be minimal, and may have been coincidental.

2.2.3.2 MUC1 and ICAM-1 in Heterotypic Co-Culture

We initially approached visualisation of the MUC1/ICAM-1 interaction by dual-colour confocal microscopy after staining MUC1 and ICAM-1 with Cy3 and FITC labelled

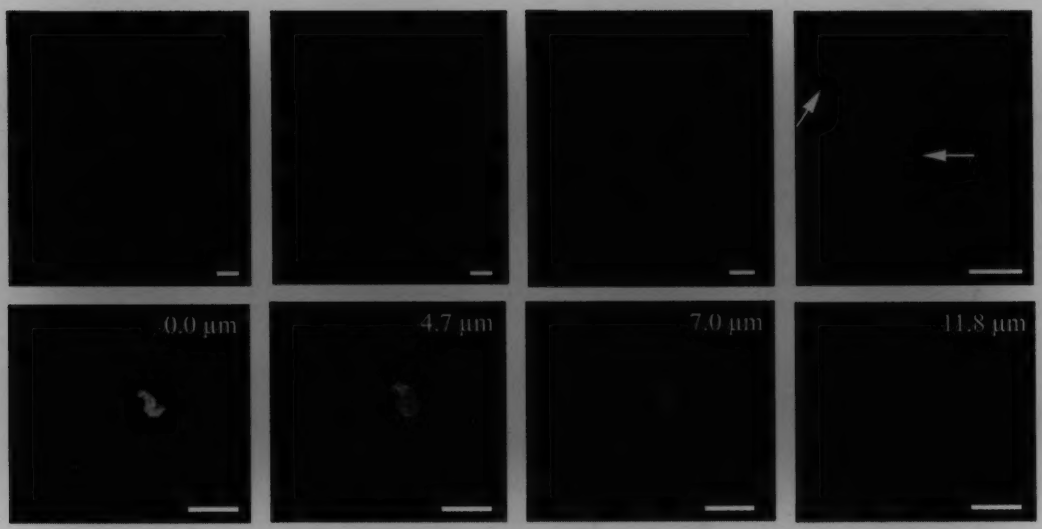

Figure 2.9: MUC1 and β-Catenin staining in ZR-75-1 and MCF-7 human breast cancer cell lines. ZR-75-1 cells appear in the top row, with MUC1 stained red, and β-catenin stained green, within a single optical section. The last two panels show the overlay. White arrows indicate where there may be co-distribution of the two molecules. MCF-7 cells appear in the bottom row, in a Z-stack of optical sections. There were no instances of apparent co-distribution in these cells. The white bar represents 20μm.

antibodies, respectively. Figure 2.10 shows a series of optical sections taken through co-cultured MCF-7 (MUC1-expressing human breast carcinoma cells) and cytokine stimulated EAhy926 cells (hybrid endothelial cell line that upregulates ICAM-1 expression on cytokine stimulation). A cluster of MCF-7 cells show heavy MUC1 expression (red) over the entire plasma membrane, where cells are not in contact with each other. The EAhy926 cells show relatively low ICAM-1 expression (green) however, the staining is more intense where ICAM-1 appears to be capping at points of cell-cell contact. There appears to be co-distribution with MUC1 (yellow co-localisation signal), however, there is very little apparent preferential distribution of MUC1 to these points, suggesting that although MUC1 is known to bind to ICAM-1, such binding does not trigger MUC1 capping. It should also be noted, that this observation was rare, as several fields on several slides had to be searched to locate this set of images. It may be that the initial MUC1/ICAM-1 interaction is transient, and is subsequently released in order to allow MCF-7 cell migration. Alternately, it may be that the MUC1/ICAM-1 interaction is an initial event that triggers or facilitates the interactions of other molecular adhesion pairs, and/or possibly initiates early signalling events involved in motility.

2.2.3.3 MUC1 Distribution in Transfected Cell Lines

To ensure relatively high and constant expression levels of fluorescently labelled MUC1 and ICAM-1, constructs of these proteins were made with YFP and CFP tags, respectively. This approach also eliminated any question of which cells were expressing which molecule, as ICAM-1 can be expressed on multiple cell types [191]. Figure 2.11 shows the plasmid maps and intended protein constructs.

2.2.3.3.1 Characterisation of the YFP-MUC1 and CFP-ICAM-1 Transfectants

When analysed by Western Blotting, two of the SYM subclones (SYM2 and 25) contained intensely staining epitopes for antibodies CT2 (the cytoplasmic domain of MUC1), B27.29 (the extracellular domain of MUC1), and A.v. (recognizes all GFP variants) at the same molecular weight as the B27.29 reactive band, indicating that the YFP was most likely at the N-terminus of the MUC1 extracellular domain, as expected

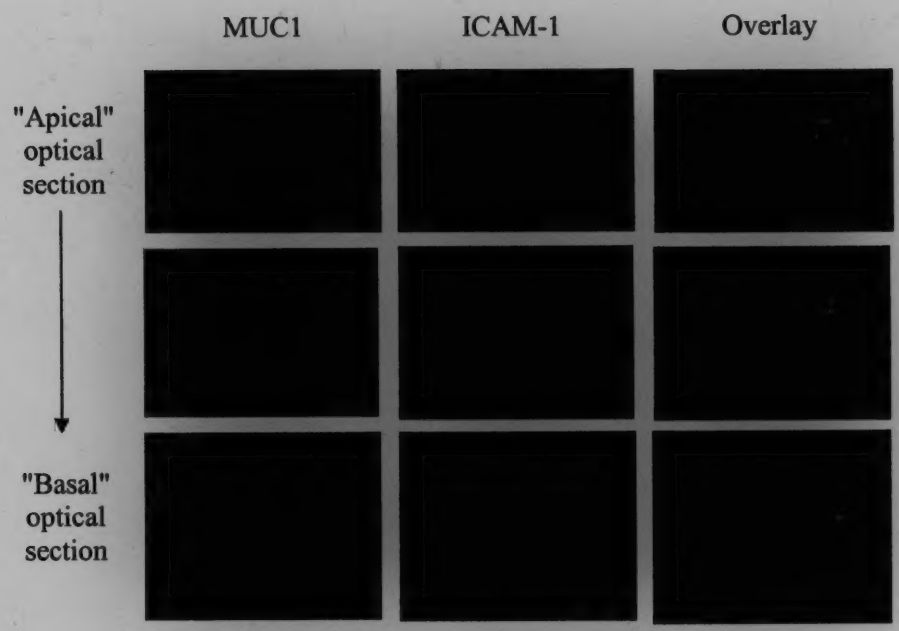

Figure 2.10: Endothelial ICAM-1 appears to cap at regions of cell-cell contact with MCF-7 cells. EAhy926 cells were seeded on a glass slide and after adhesion, were stimulated with TNF-α and IL-1β for 24 hours. MCF-7 cells were layered on top of the EAhy926 monolayer and incubated at 37°C overnight with no further cytokine stimulation. Slides were fixed in 2% formaldehyde/PBS for 15 minutes, permeabilized in 0.5% Triton X-100/PBS for 15 minutes, then double stained for MUC1 (Cy3) and ICAM-1 (FITC). Some co-distribution (yellow pseudocolour) appears to show ICAM-1 capping on a subset of EAhy926 cells where in contact with MCF-7 cells.

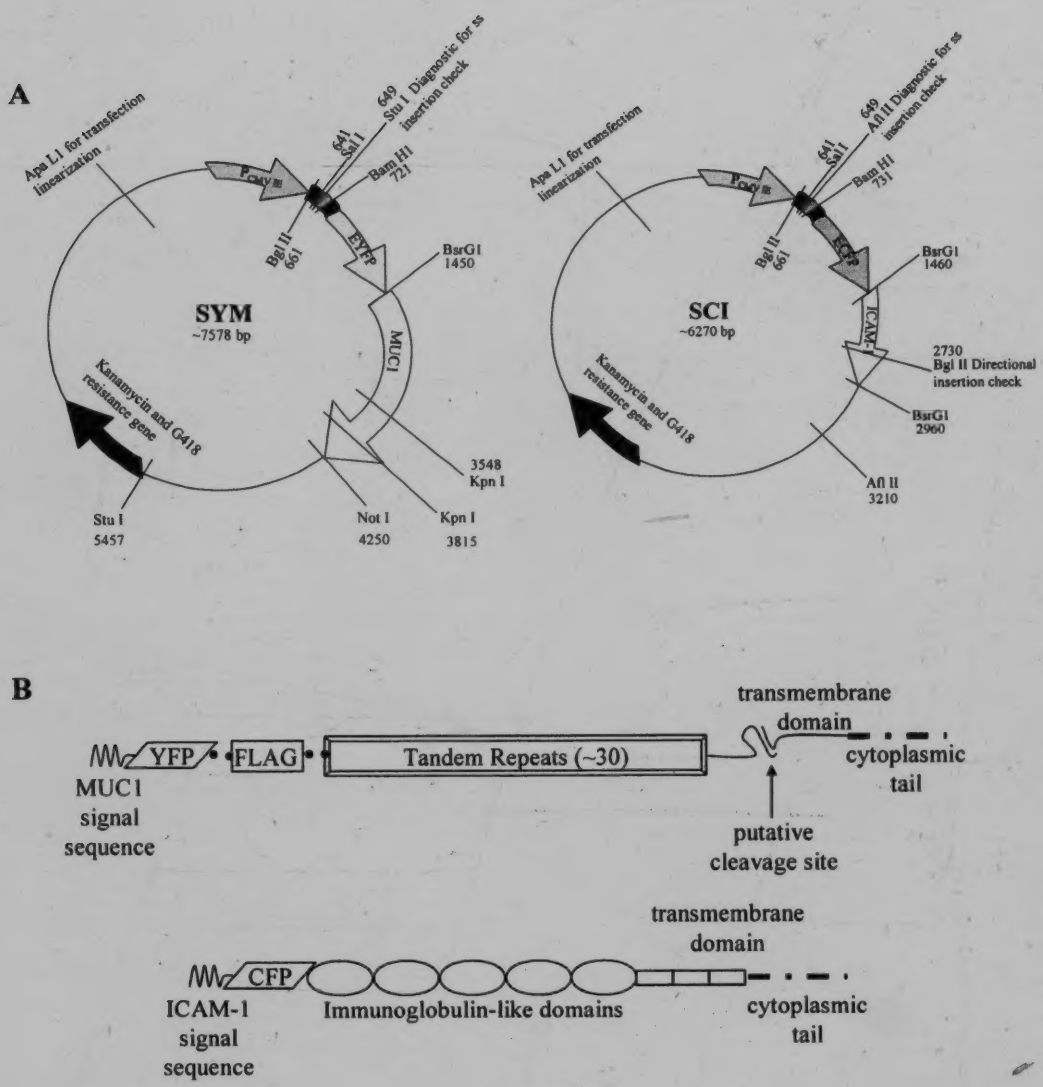

Figure 2.11: The SYM and SCI Constructs. (A) Schematic showing the construction of the SYM and SCI plasmids. A MUC1-specific signal sequence (ss) was directionally inserted in the multiple cloning site (MCS) of the pEYFP-N1 plasmid, and the PCR amplified MUC1 gene containing engineered BsrG1 and Not I cut sites was directionally inserted after the YFP gene. Directionality of the ICAM-1 insert in the final plasmid was checked by digestion with Bgl II, which cuts the ICAM-1 gene towards the 3' end. (B) Schematics of the final gene constructs. The signal sequences are expected to have been cleaved off during processing in the endoplasmic reticulum.

(Figure 2.12A). SYM1 appeared to have the MUC1 protein without the YFP tag, and SYM33 appeared to have low staining of the full construct. SYM3 showed staining barely above that of the parental cell line, and possibly of a lower molecular weight than the MUC1 extracellular band in the other subclones, and was negative for CT2 staining. With the SCI subclones, SCI1, 2 and 4, had highly expressed CFP labelled ICAM-1, however SCI1 and 2 may have altered the transfected gene, as they also contained a ~27kDa band that was reactive to the A.v. antibody (Figure 2.12B). This might be GFP cleaved from the ICAM-1 protein. SCI4 had A.v. reactivity only at the same position as the ICAM-1 band when the same membrane was probed for this protein.

2.2.3.3.2 Fluorescent Microscopy of Transfectants

Confocal analysis of the SYM25 subclone showed that the protein was distributed on the plasma membrane of the cell, as well as in what may be the Golgi (Figure 2.13A). In the SCI4 transfectants the CFP-ICAM-1 construct was over the entire plasma membrane, even when in contact with adjacent cells (Figure 2.13B). Transiently transfected EAhy926 cells (viable for 3 days post transfection) tended to be spread in a flat shape over the coverglass, and were not suitable for z-stack imaging by themselves. Transfection efficiencies were around 30 – 40% (Figure 2.13C).

2.2.3.4 MUC1 and ICAM-1 in Co-Cultured Transfectants

2.2.3.4.1 Three Dimensional Reconstructions

EAhy926 transiently transfected with SCI did not show clear membranous localisation of the CFP-ICAM-1 molecule, and in regions of obvious heterotypic cell contact with SYM25 cells, the co-localisation signal was weak at best (Figure 2.14A).

Similar results were seen with the SYM2 subclone (not shown). The SCI4 293T subclone did show clear membranous CFP-ICAM-1 expression, and as these cells tended to be cuboidal rather than flat like the EAhy926 cells, "transmigration" of the SYM25 cells, which had been layered over top of the SCI4 cells, was easily visualised (Figure 2.14B). In this particular field, the co-localisation signal could easily be seen where the two cell types contacted each other. Also, the SYM cells tended to show "migratory

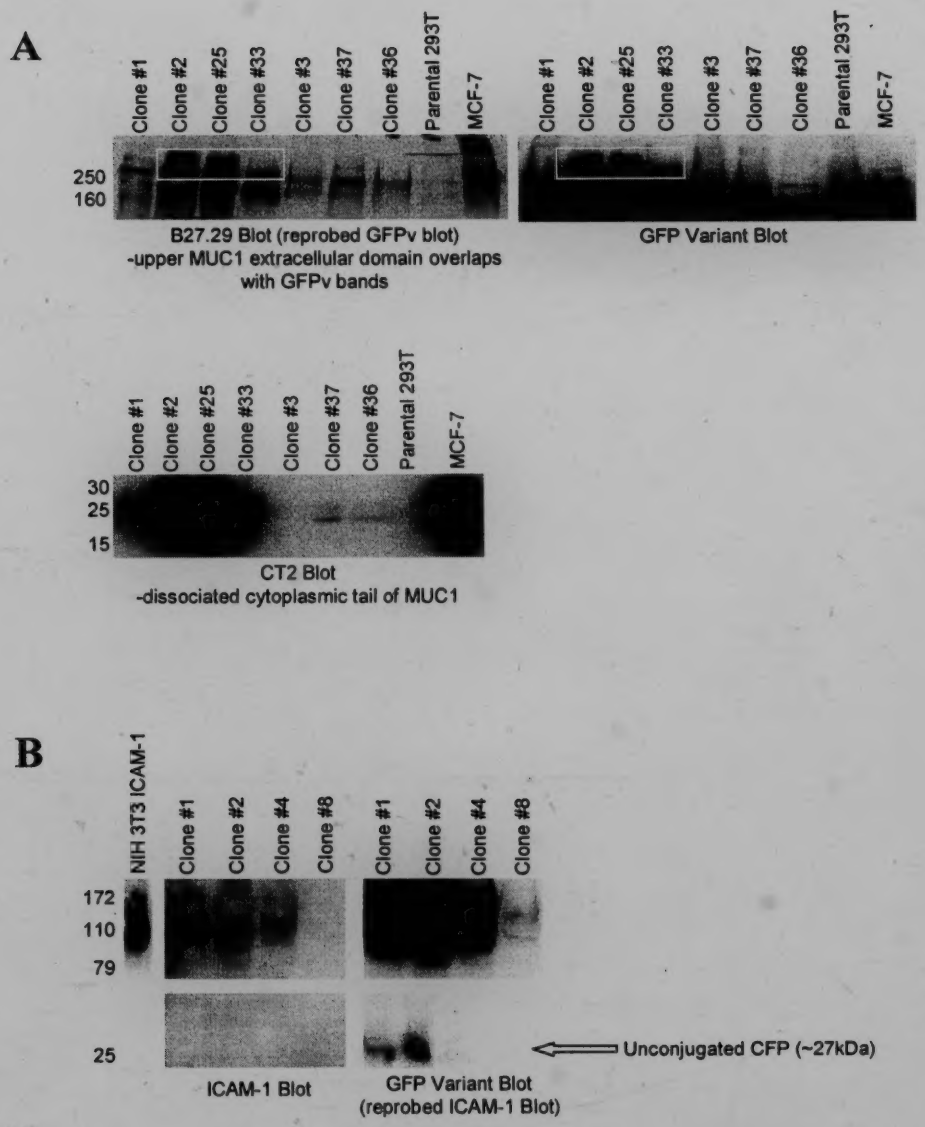

Figure 2.12: Western blot analysis of the 293T SYM and SCI subclones. (A) The SYM subclones. The first panel shows immunodetection of the tandem repeat portion of the transfected MUC1 protein, and the panel to the right shows the same membrane blotted for YFP. The white box highlights bands that appear to be positive for both MUC1 and YFP immunostaining, indicating a MUC1-YFP fusion protein. The lower panel shows confirmation that the entire molecule is expressed, as this is

Figure 2.12 (Continued): immunodetection of the cytoplasmic tail of MUC1. MCF-7 cells are included to show the molecular weight of the unconjugated protein. (B) The SCI subclones. All subclones, except for SCI8 appear to have an ICAM-1-CFP fusion protein. Only SCI4 has the fusion protein without an apparent CFP cleavage product. ICAM-1 transfected NIH 3T3 cells are included to show the molecular weight of the unconjugated protein.

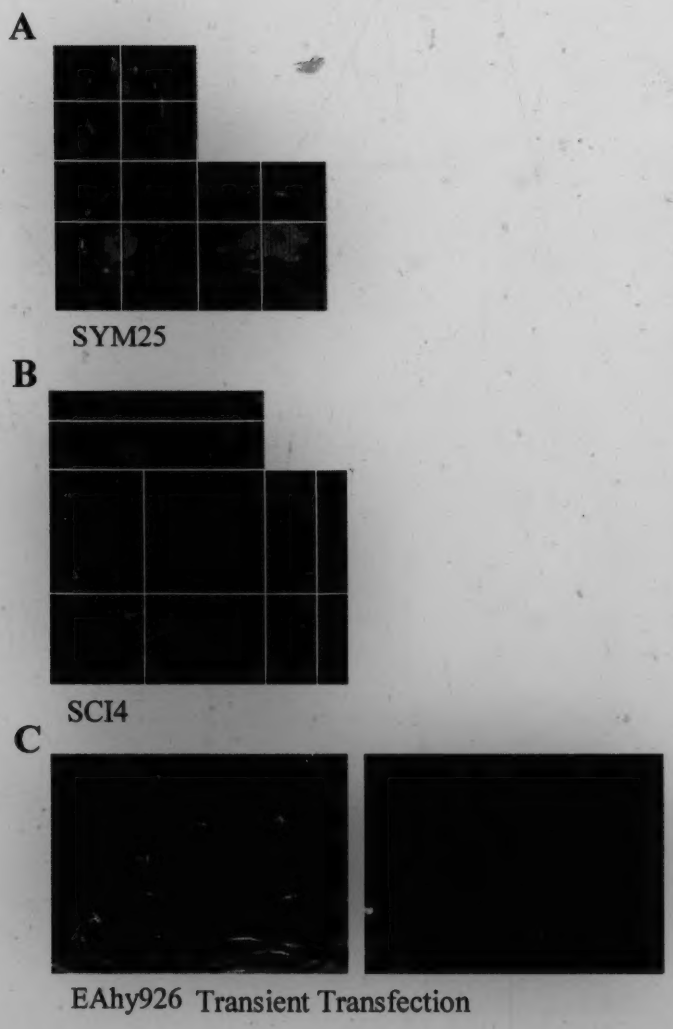

Figure 2.13: Confocal and Fluorescent Microscopy analyses of SYM and SCI transfected cells. (A) Orthogonal representation of the SYM25 subclone by a z-stack of images collected with the YFP filter. The main image (lower left) is a focal plane approximately midway through the z-stack. The images above and to the right of the main image are cross-sections through the z-stack when turned either face down (upper image) or on its left side (image to the right). The white lines represent where each adjacent image cross-sections the other. (B) Orthogonal representation of the SCI4 subclone by a z-stack of images collected with the CFP filter. (C) Single plane DIC and CFP images of SCI transfected EAhy926 cells.

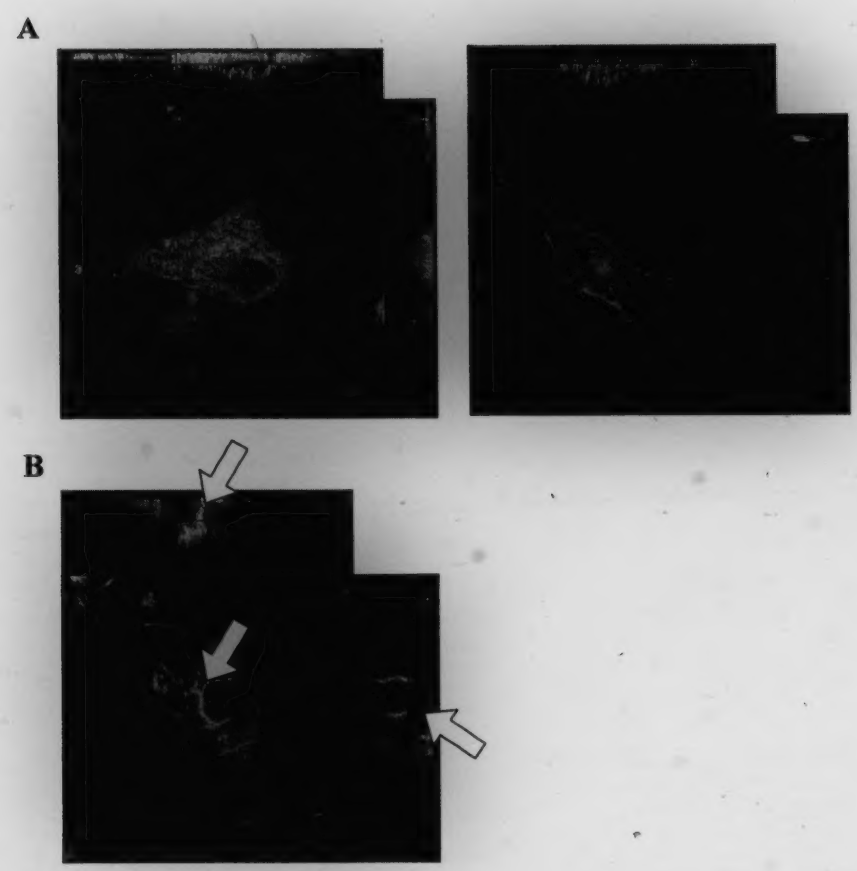

Figure 2.14: A co-localisation signal for YFP-MUC1 and CFP-ICAM-1 is visible with transfected 293T cells. (A) Orthogonal representations from z-stacks of SCI transfected EAhy926 cells interacting with SYM25 cells. YFP-MUC1 is pseudocoloured red, and CFP-ICAM-1 is pseudocoloured green. The main image (lower left) is a focal plane approximately midway through the z-stack. The images above and to the right of the main image are cross-sections through the z-stack when turned either face down (upper image) or on its left side (image to the right). The coloured lines represent where each adjacent image cross-sections the other. (B) Orthagonal representation from a z-stack of SCI4 and SYM25 cells interacting with each other. White arrows indicate yellow pseudocoloured co-localisation signals.

shapes", that is, the tendency to send out pseudopodia and move towards the substratum (Figure 2.15), whereas the SCI cells appeared to retain cuboidal shapes. There may be some concentration of the YFP-labelled MUC1 at the pseuopodial tips (most apparent in Figure 2.15C), however there was no corresponding CFP-ICAM-1 cap. This may indicate that ICAM-1 did not behave in 293T cells in the manner expected in endothelial cells.

2.2.3.4.2 FRET by Acceptor Fluorescence Increase

As described in section 2.1.8.1, an attempt was made to record the spatial and temporal positioning of both MUC1 and ICAM-1 over thirty minutes. Preliminary studies (e.g. Figure 2.15) indicated that at 37°C, 20 minutes was sufficient for SYM cell attachment and the development of obvious migratory behaviour. While observing the FRET data being recorded, a couple of concerns arose. First, the SYM cells remained rounded and moving freely over the coverglass. This may have been due to Brownian motion rather than migration, as no apparent focal adhesions were evident, and the cells appeared to roll. In other preliminary live imaging experiments (not shown), both CFP and YFP-labelled cells behaved differently if they were constantly imaged as compared to a duplicate dish (identical liquid buffer system), in which cells were imaged only at the end of the co-culture period. Specifically, cells exposed repeatedly to the laser light seemed to lose adhesive capability. Thus, the live imaging experiment may not have accurately represented the cell-cell interactions expected to occur in experiments where the co-cultures were performed at 37°C in the dark. Second, the focal planes seemed to shift slightly over time, making it difficult to maintain the correct spatiotemporal region of interest when calculating the FRET values. The lack of morphological change in the SYM2 cells and the shifting of the focal plane over time are evident in Figure 2.16. The FRET values calculated for a region of cell-cell contact in these images were 3.36 for Figure 2.16A and 7.26 for Figure 2.16B, indicating, at least mathematically, that there was indeed an increase in the FRET signal. However, because of the lack of any co-localisation signal in the images and the concerns outlined above, this apparent increase in the FRET signal is most likely artifactual, as such a dramatic increase must surely be visually obvious.

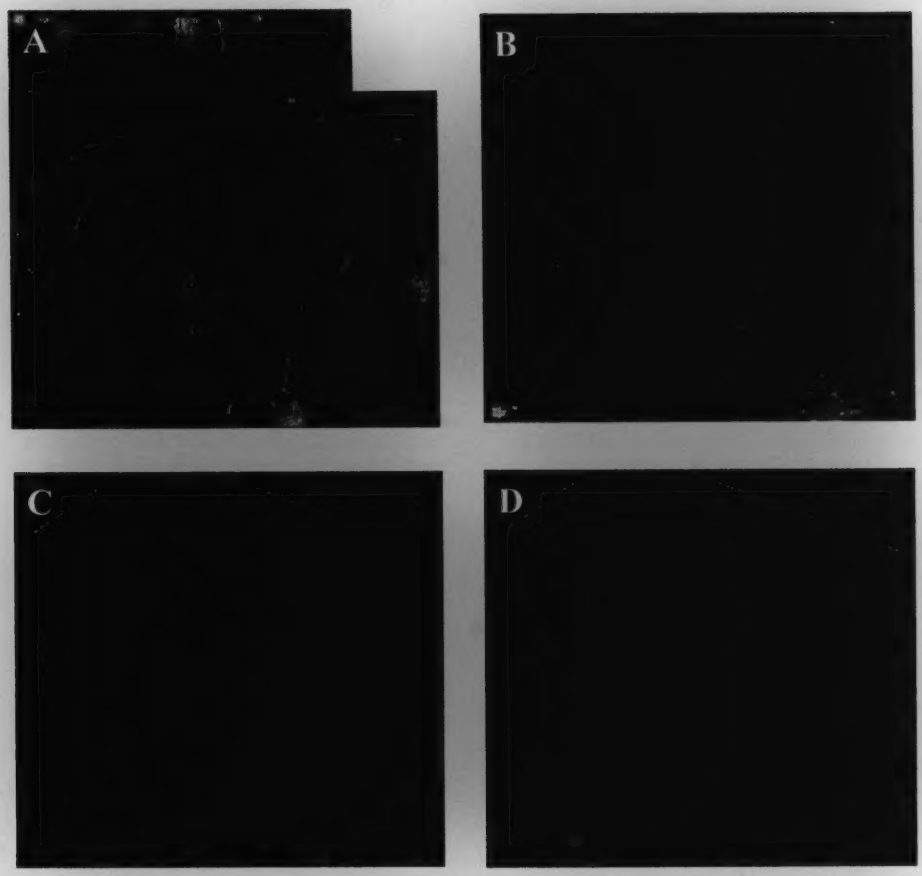

Figure 2.15: Three dimensional projections of an SYM25 cell migrating through SCI4 cells. (A) Orthogonal projection of a z-stack, where YFP-MUC1 is pseudocoloured red, and CFP-ICAM-1 is pseudocoloured green. (B) A three dimensional image generated from every focal plane in the z-stack, using the Imaris software package. (C) The Imaris image rotated ~45° counterclockwise, and ~40° upwards. The CFP channel has been shut off to allow clearer visualisation of the YFP-MUC1 positioning. (D) The Imaris image with the CFP channel turned on.

t = 5 minutes

t = 15 minutes

Figure 2.16: Images taken during the Acceptor Increase FRET experiment. (A) Overlay image of the CFP (green pseudocolour) and YFP (red pseudocolour) channels taken after 5 minutes of co-culture. (B) Overlay image of the CFP and YFP channels taken after 15 minutes of co-culture.

2.2.3.4.3 FRET by Acceptor Photobleaching

Despite obvious photobleaching of the acceptor YFP-MUC1 cells, and obvious co-localisation signals, FRET, as detected by an increase in CFP-ICAM-1 donor fluorescence intensity, was not observed in any of the eighteen trials performed with both the SYM2 and SYM25 subclones (e.g. Figure 2.17). When attempts were made using the transiently transfected SCI EAhy926 cells, there was a slight "bump" in the CFP fluorescence signal (Figure 2.18), however the same thing was seen in the negative control, where CFP-ICAM-1 cells were plated without any SYM cells (Figure 2.19). This was thought to be an artefact of the laser, and not to represent any sort of FRET.

2.3 Discussion

2.3.1 Intracellular Localisation of MUC1 is Important in Prognosis

Our clinical review of MUC1 staining patterns in human breast cancer shows that high MUC1 expression throughout the entire tumour is an indicator of differentiation and associated with good prognostic outcome; in these tumours, MUC1 tended to be present on lumenal or free membrane surfaces not involved in cell-cell contacts. However, specific intracellular localizations of MUC1 are associated with poor prognosis. These are (i) intense cytoplasmic staining, and (ii) "circumferential" staining, or the presence of MUC1 over the entire cell surface. The significance of the extracellular domain of MUC1 appearing in the cytoplasm remains enigmatic, but may be an indication of loss of controlled transport of cellular proteins, which might disregulate other cell processes. The correlation found between circumferential MUC1 staining and the presence of lymph node metastases suggests that the unpolarised localization of this molecule positions it ideally to promote tumour spread. This effect is not a coincidental result of loss of differentiation, as it was shown to be independent of nuclear grade. Previous research in this laboratory, showing that the extracellular domain of MUC1 can bind to the extracellular domain of ICAM-1 raises the possibility that circumferential MUC1 has greater opportunity to bind ICAM-1 expressed on adjacent cells, perhaps fibroblasts which have migrated towards the tumour as part of the desmoplastic reaction. Colonies

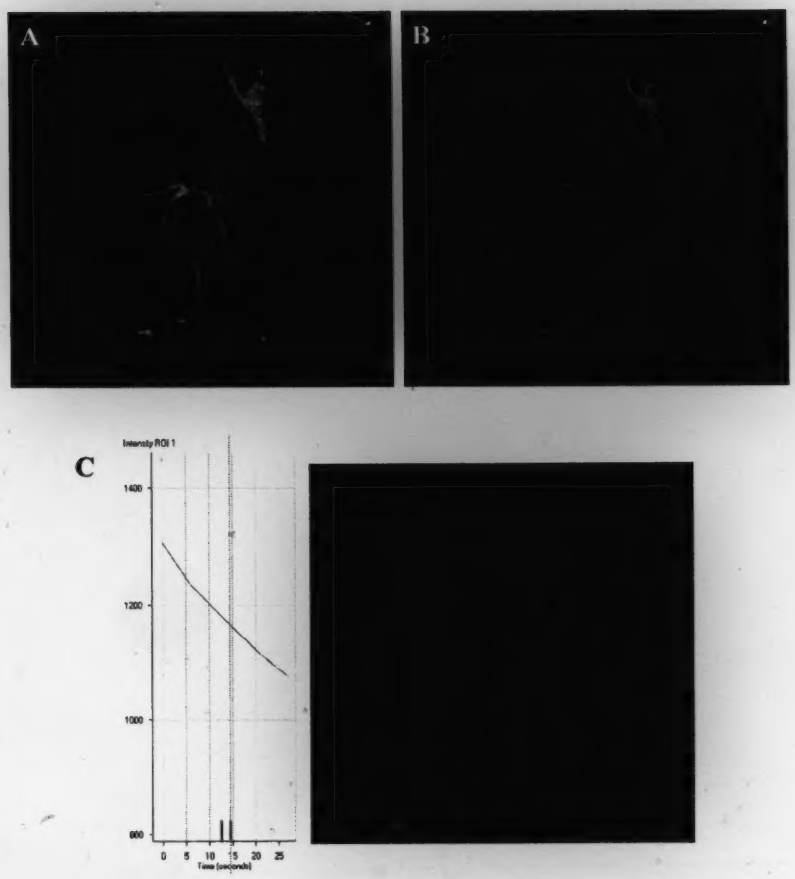

Figure 2.17: Example of FRET attempt made using the SCI4 and SYM25 cells in the Acceptor Photobleaching experiments. (A) Image of the SCI4 cells (CFP-ICAM-1 pseudocoloured green) and the SYM25 cells (YFP-MUC1 pseudocoloured red) before photobleaching. (B) The same field after photobleaching. (C) The measurement of donor fluorescence intensities before and after photobleaching. The region of interest where there had been a yellow co-localisation signal is outlined in red. The CFP fluorescence intensity over time is graphed to the left. No increases were observed.

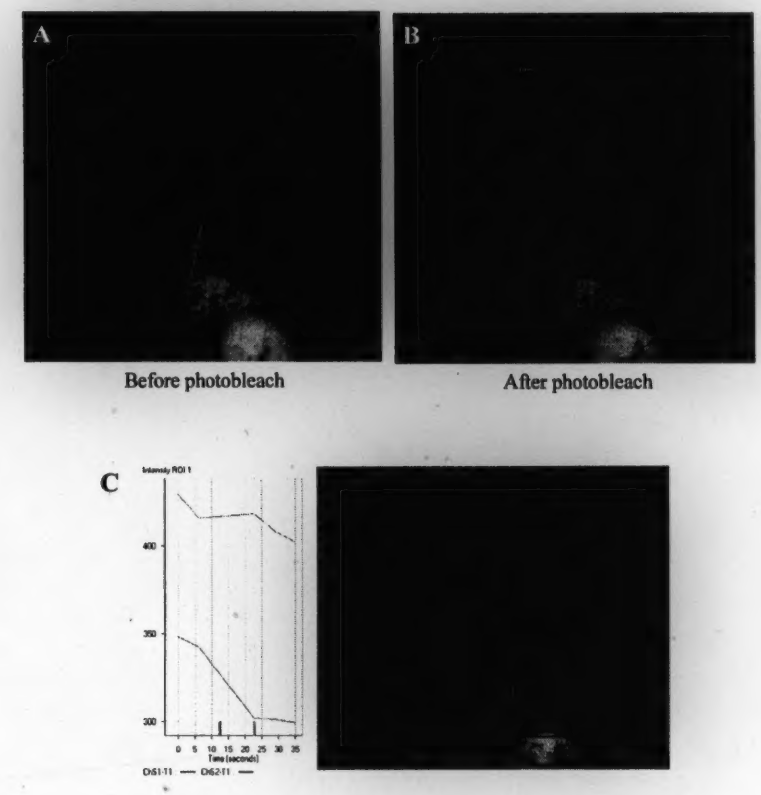

Figure 2.18: Example of FRET attempt made using transiently SCI transfected EAhy926 cells and SYM25 cells in the Acceptor Photobleaching experiments. (A) Image of the EAhy926 cells (CFP-ICAM-1 pseudocoloured green) and the SYM25 cells (YFP-MUC1 pseudocoloured red) before photobleaching. (B) The same field after photobleaching. (C) The measurement of donor fluorescence intensities before and after photobleaching. The region of interest where there had been a yellow co-localisation signal is outlined in red. The CFP fluorescence intensity over time is graphed to the left. A "bump" is apparent in the CFP channel (green).

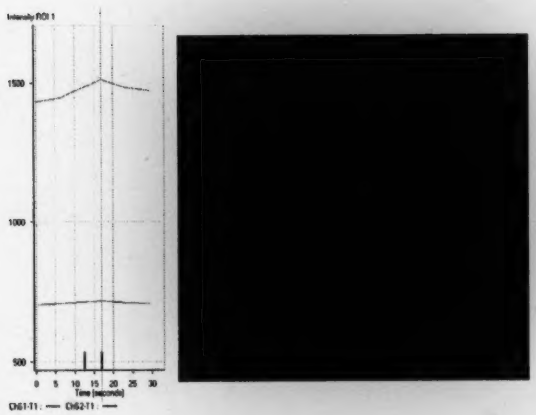

Figure 2.19: Negative control used in the EAhy926 Acceptor Photobleaching FRET Experiment. The measurement made in Figure 2.12 was repeated on a slide plated with only EAhy926 cells, and no SYM cells. The same "bump" is apparent in the CFP channel (green) indicating that this is not an actual FRET signal.

of MCF-7 cells do tend to grow directionally along the body of fibroblasts when co-cultured in three-dimensional collagen gels [83]. The possible explanations for this are examined in Chapter 3, and include the possibility that the presence of ICAM-1 on the fibroblasts may be triggering a pro-migratory signal.

2.3.2 MUC1 and Disruption of Cell-Cell Adhesion

The "steric hindrance" and "electrostatic repulsion" theories do not appear to be supported by the data presented in this chapter. Cells were observed to be aggregated despite circumferential MUC1 distribution, and the membranous MUC1 stain had a diffuse, grainy appearance, in stark contrast to the crisp lines of the β-catenin and E-cadherin stains, almost as if the mucin resides in small membrane invaginations. This suggests that the size or electrostatic charge of the MUC1 extracellular domain does not necessarily disrupt adhesion molecule function. It may be that the large MUC1 molecule pushes into the flexible cell membrane it is embedded in, rather than pushing away an adjacent cell. In terms of electrostatic charge, the glycosylations of MUC1 would have to be unaffected by the presence of charge-neutralizing ions that can reasonably be expected in any buffered, physiological saline solution. Thus, electrostatic repulsion must have a negligible effect on cell adhesion, a conclusion also reached by Wesseling et al. [44].

There is a stronger case for the cytoplasmic domain to affect cell adhesion. *In vitro*, MUC1 CT can compete with E-cadherin for binding to β-catenin, effectively disrupting E-cadherin linking to the cytoskeleton and the tensile strength of the adhesion belt [45,50]. Despite this, in every clinical occurrence of MUC1 and β-catenin co-distribution observed in this study, E-cadherin was also present, and adjacent cells were not visibly disaggregated. It has been reported that if E-cadherin is not "capped" by one of β-catenin, γ-catenin or p120ctn, it is susceptible to processing by E3 ubiquitin ligase, which targets E-cadherin for internalisation and degradation (reviewed in [173]). Although MUC1 and β-catenin could be co-immunoprecipitated from ZR-75-1 cells [50], confocal analysis suggests that the association of these molecules in intact cells may be coincidental, as it only occurs in a subset of cells, and for the most part MUC1 and β-catenin appear segregated. It is noteworthy that lobular carcinomas, which do not have

E-cadherin, and migrate as single cells, have a relatively indolent course of disease when compared to ductal carcinomas. Thus, complete loss of cell-cell adhesion appears to have limited importance in metastasis.

An alternate explanation for how MUC1 may be promoting migration could be related to the observation in two studies that the cytoplasmic domain of MUC1 can affect integrin functions. Application of a β1-integrin activating antibody could reverse the MUC1-induced inhibition of cell-matrix adhesiveness [43], and peptides corresponding to the MUC1 CT could disrupt focal adhesion assembly [55]. Both the cytoplasmic and circumferential membranous distribution of MUC1 that was observed to be associated with poor prognosis and nodal metastases, respectively, could place MUC1 in the correct vicinity to interact with integrins or integrin-associated proteins. This is significant, as integrin function can dominate genotype [79], and clearly mediates cellular motility.

2.3.3 MUC1 and the Intracellular Localisation of β-Catenin

If the function of MUC1 in breast cancer is not to effect homotypic disaggregation by disrupting the β-catenin/E-cadherin complex, does it play a role in modulating the nuclear distribution of β-catenin? Although nuclear MUC1 CT was observed in 2 breast cases, and has reportedly shuttled β-catenin into the nuclei of pancreatic [185] and multiple myeloma cells [184], not one example of nuclear β-catenin was found in any of the breast cancer specimens examined. This finding was confirmed in another lab [55]. The "nuclear shuttling" function of MUC1 appears to be cell type specific, as it does not occur in MUC1-transfected 293T cells [142].

2.3.4 MUC1 and ICAM-1 Co-Localisation at Points of Heterotypic Cell Contact

Fluorescent immunostaining on cultured cells gave a preliminary indication that MUC1 and ICAM-1 could co-localise at points of cell contact. This was also indicated by cells transfected with YFP-MUC1 and CFP-ICAM-1. There was also limited data suggesting that there may have been preferential capping of ICAM-1, and a slight concentration of MUC1 along the filopodia of migrating cells. However, the distance

between apparently co-localised molecules when using dual-colour confocal-microscopy can be as large as 300nm, which lead us to attempt FRET, or fluorescence energy transfer, which has a spatial resolution of ~7nm (discussed in Appendix I).

The FRET study gave minimal information on the distribution of ICAM-1 and MUC1 during heterotypic cell-cell interaction, and no convincing FRET signals were ever obtained. This may have been due to the positioning of the CFP and YFP tags within their respective molecules. The MUC1 YFP tag was situated at the N-terminus of the MUC1 protein core, which is 107 amino acids away from the tandem repeat region, where ICAM-1 is expected to bind. Assuming that the orientation of the two molecules when they interact is antiparallel, and assuming that at least a proportion of the CFP-ICAM-1 expressing cells would bind to the tandem repeats closest to the MUC1 N-terminus, the distance between the CFP and YFP tags can be roughly estimated using programs such as the "Peptide Property Calculator" (http://www.basic.nwu.edu/biotools/ProteinCalc/html). Using this program, the volume of the 107 N-terminal amino acids of MUC1 is estimated as 12603 $Å^3$. As MUC1 is believed to be linear, due in part to the glycosylations along the peptide core, the following hypothetical calculation does not correct for secondary or tertiary structure. The average volume of a single amino acid, estimated as 165.77 Å, would result in an average width and length of 5.5 Å per amino acid (inverse of 165.77^3). If this is the case then the length of the MUC1 N-terminal domain would be estimated as 416.6 Å ($12603/5.5^2$), which would be well outside the ~70 Å distance limit required for measurable FRET energy transfer. If the unlikely assumption is made that the N-terminus is completely globular, the distance would be 23.3 Å (inverse of 12603^3). Despite this, FRET did not occur, even though the interaction between MUC1 and ICAM-1 has been demonstrated by more than one group [2,3,57,58]. Other explanations include the possibilities that (i) the dipole orientation of the fluorophores was incorrect due to the inability of the CFP or YFP β-can structures to rotate freely on the ends of the tagged proteins (discussed in Appendix I), and (ii) attachment of the CFP tag to the ICAM-1 protein may have altered the tertiary structure of the protein. This possibility is based partly on the observation that the CFP-ICAM-1 immunoblot showed weak staining for the ICAM-1 portion of the molecule (Figure 2.12B), despite using a mixture of three different anti-ICAM-1 monoclonal antibodies at

relatively high concentration. ICAM-1, as seen on the NIH 3T3 ICAM-1 control, usually produces fairly dark immunoblots, thus the weak signal was not likely due to a problem with the detection antibodies.

2.3.5 Overview

Intracellular localisation of MUC1 was shown to be important in prognosis, which suggests it may be important in biological activity; (i) cytoplasmic staining was correlated with poor survival, and (ii) "circumferential" staining was correlated with metastasis to the lymph nodes. Either of these staining patterns may allow MUC1 to interfere with adhesion molecules, most likely via its cytoplasmic domain, however there was little evidence that MUC1 displaces E-cadherin from β-catenin. If it does, this may be a transient event that requires a certain threshold of MUC1 at the membrane in order to occur. An alternate possibility is that the changed positioning of MUC1 allowed it to associate with signalling partners from which it would normally be sequestered. The extracellular domain is not yet to be excluded from therories about the ability of MUC1 to promote metastasis, as it may do so by triggering the putative signalling function of its cytoplasmic domain, after ligation by ICAM-1. MUC1 has been shown to localise at the tips of filopodia [140], and our experimental data suggests that there may be interaction with ICAM-1 at points of cell-cell contact. Thus, MUC1 binding to ICAM-1 on adjacent cells, such as fibroblasts, which may have migrated to the primary tumour during the desmoplastic reaction, might have initiated a pro-migratory signal in the tumour cells, that resulted in lymph node metastasis.

Chapter 3: MUC1/ICAM-1 Interactions and Tumour Cell Migration

3.0 Introduction

The experiments presented in this chapter were designed to answer the question if MUC1-bearing tumour cells were stimulated to migrate more in the presence of ICAM-1, which can be expressed on a number of adjacent cells, including the stromal cells at the primary and secondary tumour sites, and endothelial cells, which blood-borne metastases may come in contact with. A secondary question was whether microenviromental influences could affect migration rates, and if this had correlation to ICAM-1 expression levels on endothelial or stromal cells.

Our interest in the extravasation event of the metastatic cascade stems from the recognition in clinical pathology that vascular invasion is a bad prognostic indicator, as the primary cause of mortality in breast cancer is the ability of cancer cells to metastasize which they do via the lymphvascular circulation. Real-time fluorescent video microscopy studies have provided evidence that migration of tumour cells out of the vasculature is rare and adhesion to the endothelium is rate limiting in the formation of metastases [6,7]. There are some similarities between leukocyte and tumour cell transendothelial migration, specifically extravasation (TEM_E) [6,236]. Both leukocytes and MCF-7 human breast carcinoma cells, but not normal mammary cells, bind to endothelial cells, which respond with an intracellular calcium flux, localized disassembly of focal adhesions, and partial cell retraction [203,204,208-210]. These responses are mediated by intercellular adhesion molecule-1 (ICAM-1), as demonstrated by using an ICAM-1 cross-linking antibody [206].

Our specific interest in ICAM-1 is based on previous research in our laboratory demonstrating that breast tumour cell MUC1 is a ligand for endothelial ICAM-1, and can mediate heterotypic adhesion between tumour and endothelial cells under static and physiological fluid flow conditions [2,3,5]. Additionally, tumour MUC1 is underglycosylated [17,237], which might increase the probability that the highly immunogenic protein core, which is the functional binding site for ICAM-1 [3,57], may be exposed to a greater extent. The integration of additional microenvironmental factors into our experimental models came after we realised that stimulating increased ICAM-1 expression on endothelial cells by using inflammatory cytokines had limited effect on

increasing tumour cell TEM_E. We chose to add fibroblasts, as these cells can secrete several factors into the local microenvironment which may well assist metastasis, for example, certain matrix proteins, matrix metalloproteases, or soluble messengers that could act on either the tumour cells or endothelial cells.

The specific questions asked in this chapter were:

i) Did increased ICAM-1 expression increase the TEM_E of MUC1-bearing cells?

ii) Was TEM_E dependent on MUC1?

iii) Could TEM_E be altered by microenvironmental conditions?

iv) Were changes induced by specific microenvironmental factors related to MUC1 or ICAM-1 expression levels?

These issues were addressed by testing the migratory capability of MUC1-expressing epithelial cells through a simulated blood vessel wall that consisted of a Transwell membrane which, where indicated, was plated with ICAM-1-expressing endothelial cells on the upper surface and ICAM-1 expressing fibroblasts on the undersurface. The extravasation step of metastatic spread was chosen, as previous observations made in this laboratory suggested that MUC1-based adhesion to the endothelium may be involved in increasing the opportunity for tumour cells to transmigrate the vasculature, or may even be directly involved in triggering a migratory response.

3.1 Methods and Materials

3.1.1 Assay Development

Selected data from the developmental work appear in Appendix II. Transwell membranes with 8 μm pores were used as supports for basement membrane or stromal matrix-like coatings. The selection of the pore size was based on the average size of epithelial nuclei, to ensure passage of the cells to the underside of the membrane would not be mechanically restricted. Initially, membranes were coated with 50μL of 1:30 Matrigel to mimic the basement membrane, on which EAhy926 cells were plated

(HUVECs immortalized by fusion with A549 lung carcinoma cells). This model gave us preliminary information on the necessity of MUC1 and ICAM-1 to the process of TEM_E. Statistically significant differences were seen when endothelial ICAM-1 expression was increased by the addition of inflammatory cytokines (20 U/mL each of TNF-α and IL-1β), however tumour cell migration rates, although comparable to those in the literature, were still low. Perhaps transit through the Matrigel was rate-limiting in this system, so fibroblasts were added on the undersides of the membranes so that they could secrete the pro-enzyme forms of matrix metalloproteases into the Matrigel, which the migrating tumour cells could then activate. The results showed that Matrigel conditioned by fibroblasts was insufficient to increase tumour cell migration through an endothelial monolayer. Instead, fibroblasts increased tumour cell TEM_E by exerting specific effects on endothelial cells (see below). Later experiments used HUVECs, which were thought to be more physiologically relevant, and gelatin (denatured collagen) for the matrix, since Matrigel stimulates angiogenic-like responses in HUVECs, which formed cord structures on the Transwell membrane, rather than a monolayer. Overall, this model system allowed easy variations of the tumour microenvironment, and testing of which components were important in stimulating TEM_E. The final assay parameters are summarised in Table 3.1 and Figure 3.1. The methods outlined below all relate to the final parameters.

3.1.2 Reagents

Gelatin Type A, fibronectin, MOPC 31C mouse IgG1, B-5-1-2 anti-tubulin antibody, sodium pyruvate, endothelial cell growth supplement, heparin, DMEM, and M199 were from Sigma-Aldrich. Collagen Type I (Vitrogen 100) was from Cohesion Technologies. Matrigel was from BD Biosciences. B27.29 mouse anti-human MUC1 antibody and B67.4 mouse anti-human sialylated Lewis^a antibody were generous gifts from Biomira Inc. 18E3D mouse anti-human ICAM-1 were a kind gift of ICOS Corporation. JB1A, a mouse anti-human integrin antibody that detects an epitope on the β1 subunit, was from the laboratory of Dr. John Wilkins, Department of Medicine, University of Manitoba. FBS, Insulin, L-Glutamine, Penicillin/Streptomycin, Blasticidin

Table 3.1: Optimization of the Final Transwell Model Parameters

Parameter	Trials	Final Selection	Comments
• Tumor Cells	• MCF-7 • ZR-75-1 • HEK 293T ± transfection	• MCF-7 • HEK 293T ± transfection	• ZR-75-1 showed similar migratory responses in comparison to MCF-7 cells, however these were inconsistent, especially when migrating through fibroblasts. • ZR-75-1's are difficult to grow.
• # of Tumor Cells Used	• 100 to 500,000	• 20,000 (200µL at $1x10^5$/mL)	• 20,000 gave an easy number to count and show statistical differences between test conditions, without causing the media to become acidic from having too many cells.
• Duration of Assay	• 5 to 72 hours	• 24 hours	• The doubling time of MCF-7's is 36.8 hours. At 24 hours, an easily quantifiable number of cells had migrated, and cell proliferation would be expected to have minimal impact with this assay duration.
• Endothelial Cells	• EAhy926 (HUVEC fused with A549 lung carcinoma) • HUVECs	• HUVECs	• EAhy926 cells were used for all the development work. • Significantly higher tumor migration responses were seen with HUVECs, which could produce higher levels of ICAM-1. • Since HUVECs are primary cells, they are thought to be more physiologically relevant than the EAhy926 cell line. • Plated at $5x10^5$/mL (200µL), which gives a confluent monolayer, as determined by crystal violet staining.
• Fibroblasts	• Primary human breast • NIH 3T3 (murine) • MRC-5 human lung • Primary human skin	• Primary human breast	• Skin and breast fibroblasts produced similar increases in tumor cell migration, however breast fibroblasts showed synergistic increases in tumor cell migration in the presence of HUVECs and cytokines. • The breast fibroblast stocks we had were of the lowest passage number (second passage after harvest from patient biopsies). • Plated at $6.67x10^4$/mL (75µL), which gave a reasonable # of cells on the membrane, and did not deplete the slowly growing fibroblast stocks.
• Selection of matrix	• Gelatin • Matrigel • Fibronectin • Collagen	• Gelatin	• The results obtained on collagen and gelatin were exactly the same, however gelatin is easier to prepare and sterilize. • Fibronectin inhibited tumor cell migration in the presence of HUVECs and fibroblasts. • Matrigel was used for all the developmental work using EAhy926 cells, however it could not be used with HUVECs, as it sends angiogenic signals into these cells, and they form cords rather than monolayers.
• Selection of assay media	• M199/20% FBS + ECGS • M199/20% FBS	• M199/20% FBS	• M199/20% FBS is the standard media for HUVEC culture. As these were the most sensitive cells, this media was selected. • The presence or absence of ECGS made no difference, and is expensive, so it was left out, since the assay is not long term.
• Cytokine stimulation	• Predetermined by other students.	• 20U/mL each of TNF-α and IL-1β, 4 hrs prior to and during assay.	• After 4 hour cytokine stimulation, E-selectin levels have receded, isolating the ICAM-1 effect, since sialyl groups on MUC1 can also bind to E-selectin. • ICAM-1 levels begin to plateau after 4 hours.

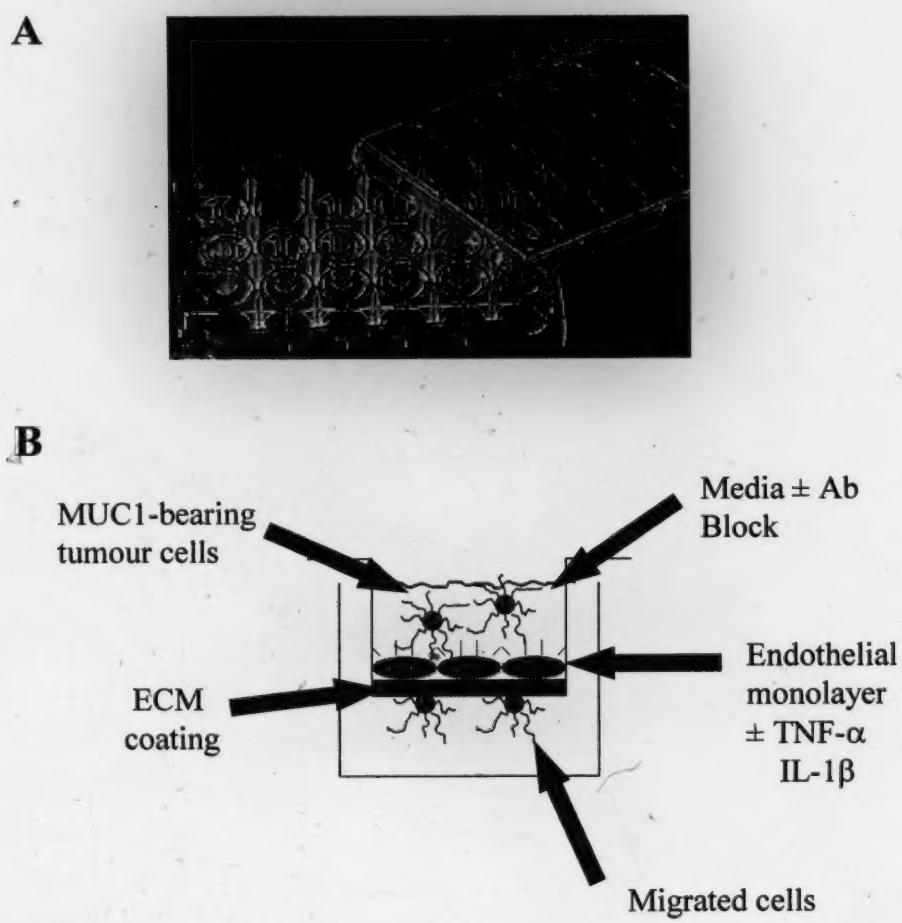

Figure 3.1: Optimized Transwell set up. For routine measurements of epithelial cell TEM_E, the membrane of an 8.0μm pore Transwell insert (shown in a 24-well plate in panel A) was coated on both sides with 0.1% (w/v) gelatin in water and plated on the underside with fibroblasts and on the upper side with endothelial cells (B). Tumour cells were added to the upper chamber after a 4 hour prestimulation of the endothelial cells with cytokines, and allowed to migrate for 24 hours ± cytokines ± monoclonal antibodies against specific test adhesion molecules. Tumour cells were stained for an exclusive marker molecule, and those on the underside of the membranes were counted. Experiments were repeated at least three times in triplicate.

S HCl, non-essential amino acids, and Trypsin were purchased from Invitrogen Canada Inc. Type I Collagenase was from Worthington Biochemical Corporation. Anti- mouse alkaline phosphate or horseradish peroxidase conjugated secondary antibodies (Jackson Immuno Laboratories), TNF-α and IL-1β were purchased from CedarLane Laboratories. NBT/BCIP stock solution was from Roche Diagnostics. ECL Plus Western Blotting Detection Reagents were purchased from Amersham Biosciences.

3.1.3 Primary Cells and Cell Lines

Primary human breast fibroblasts and primary human mammary epithelial cells (1°HMECs) were generous gifts of Dr. Joanne Emerman, University of British Columbia, and were maintained in DMEM media + 10% FBS, 10U penicillin, 10U streptomycin, 2mM L-glutamine and 0.1mM Gibco MEM Non-Essential Amino Acids Solution. Primary human mesothelial cells were isolated by centrifugation of fresh ascites fluid collected from patients with breast cancer, and cultured in DMEM media + 10% FBS. Mesothelial identity was confirmed by phenotyping the cells with a panel of antibodies against ICAM-1, MUC1, cytokeratin, vimentin, Leu M1 and CEA. Primary human umbilical vein endothelial cells (HUVECs) were harvested as described in section 2.1.2. NIH-3T3 murine fibroblasts, and MCF-7, T47D, MDA-MB-468, and Hs578T human breast adenocarcinoma cells were from the ATCC, Manassas, VA, and were maintained in DMEM + 10% FBS (NIH-3T3 cells) or DMEM + 10% FBS + 0.1mg/mL insulin. Human ICAM-1 transfected NIH-3T3 cells and their mock transfected counterparts were a generous gift of Dr. Ken Dimock, University of Ottawa, and were maintained in DMEM + 10% FBS + 2μg/mL Blasticidin S.

3.1.4 Transendothelial Migration Assay

The membranes of Transwell inserts (Corning Costar, 6.5 mm diameter, 8μm pore size) were coated on both sides with 0.1% (w/v) gelatin. If cells were plated on the underside of the membrane, this was done by placing a 75μL drop of cell suspension at 6.67×10^4 cells/mL in the center of a well in a 24 well plate. The Transwell insert was

placed over the drop, the plate was inverted, then left to equilibrate overnight in a 5% CO_2, 37°C incubator. If cells were plated on the upper side of the Transwell membrane, this was done by pipetting 200µL of cell suspension at 5 x 10^5 cells/mL into the upper chamber, 500 µL of media into the lower chamber, then allowing the plate to equilibrate overnight in a 5% CO_2, 37°C incubator. HUVEC confluency at this cell concentration was confirmed by crystal violet staining of designated membranes. To assay tumour cell migration, MCF-7 or 293T MUC1 transfected cells were trypsinized, adjusted to 1 x 10^5 cells/mL in media, and 200µL of this cell suspension was added to the upper chambers of Transwells already coated with gelatin and, where indicated, plated with other cell types. In the "stimulated" conditions, HUVECs or control membranes were treated with 20U/mL of TNF-α and 20U/mL IL-1β in PHEC media, at 37°C for 4 hours prior to the addition of MCF-7 cells. Where indicated, fibroblast conditioned media was prepared by incubation of the routine culture media with fibroblasts at 30 – 50% confluency for 5 days, then used in lieu of other media in the Transwell assay, without dilution. If desired, antibodies or blank vehicle were added to the media at final concentrations of 60µg/mL for B27.29 or MOPC 31C (isotype control), or 20µg/mL for all others. For these blocking experiments, MCF-7 cells were incubated in suspension for 30 minutes at room temperature with the appropriate antibody, while gelatin-coated membranes, with or without fibroblasts, with or without HUVECs, were incubated at 37°C with equivalent concentrations of antibody in media added to both the upper and lower Transwell chambers. Once added, antibodies and/or TNF-α and IL-1β were included in the media for the duration of the assays. 24 hours after the addition of MCF-7 cells, Transwell membranes were washed 1X with PBS, then fixed for 15 minutes in 2% formaldehyde in PBS and washed 3X with PBS. Membranes were blocked overnight in 2% BSA in PBS with 0.05% Tween 20 (BTT), then stained with B27.29, followed by alkaline phosphatase conjugated anti-mouse secondary, and then NBT/BCIP. Cells present on the upper side of the membranes were removed with a cotton swab, and stained cells on the bottom side of the membrane were counted by light microscopy. As the doubling time of MCF-7 cells was measured as ~37 hours in the presence of 0.1 mg/mL insulin (normal culture conditions) and approximately 46 hours in the absence of insulin (routine assay conditions), the number of cells found on the underside of the Transwell membranes after

24 hours is likely to be a direct measure of migration with little or no increase due to proliferation.

3.1.5 Western Blotting and Band Density Analysis

Cells were lysed in 25mM Tris, 150mM NaCl, 5mM EDTA, 1% TritonX-100, pH 7.5, and the insoluble material was pelleted. Supernatants were analysed for protein content, and equal μg of protein from each sample were loaded onto a 7.5% SDS-PAGE gel with a 4% stacking gel. Protein bands were transferred to Immobilon membrane, and visualized by enhanced chemiluminescence. Relative ICAM-1, MUC1 and β1-integrin band densities were compared using NIH Scion Image software and corrected for loading errors by comparison to tubulin band densities.

3.1.6 Statistical Methods

Multiple range comparisons of the mean relative numbers of migrating MCF-7 cells were made using the Newman-Keuls test. Data populations that did not overlap with any other data population ($p = 0.01$) were marked with an asterisk to denote statistical significance. To determine if the endothelial cells, fibroblasts and conditioned media components of the test cultures were acting in an additive or synergistic manner, the numbers of MCF-7's migrating in the presence of each individual component were summed, and compared to test conditions where the components were added in combination. Combinations were designated as synergistic if the summed value was less than the combination value, and the mean of the paired differences were statistically different from zero in a signed rank test.

3.1.7 Ethics

Collection of umbilical cords and ascites fluid and harvesting of HUVECs and mesothelial cells were done according to the approval granted by the Alberta Cancer Board's Research Ethics Board.

3.2 Results

3.2.1 Cytokine Stimulation of ICAM-1 Expression Increased TEM_E in the Developmental Model

The dependency of transendothelial migration on ICAM-1, specifically extravasation (TEM_E), is indicated in Figure 3.2, which shows that migration of MCF-7 human MUC1-positive breast cancer cells through a monolayer of EAhy926 human endothelial hybrid cells is increased when the EAhy926 cells are treated with inflammatory cytokines known to upregulate expression of ICAM-1. This increase was abrogated by the addition of monoclonal antibodies against ICAM-1 (18E3D), but not ICAM-3 (ICR5), indicating specificity of molecular action. The first indication that MUC1 is also important in TEM_E is given by the demonstration that monoclonal antibodies against the peptide core of MUC1 (B27.29) could also reduce MCF-7 migration to basal levels seen with unstimulated EAhy926 cells. It is unlikely that this effect is due only to increased adhesion of tumour cells to endothelium, as this was a static assay, where shear stresses of blood flow were not a factor, and adhesion would be gravity-assisted and not rate limiting.

An initial series of experiments to confirm the involvement of MUC1 was performed using subclones of MCF-7 cells that were shown to have a gradient of MUC1 expression (Figure 3.3). The use of these subclones demonstrated a correlation between the MUC1 expression levels of the subclones and the number of cells that migrated. It was not possible to continue these experiments, as the MUC1 expression levels in these subclones became unstable 4 - 5 passages after this data was collected. Regardless, these early indications that MUC1 and ICAM-1 were important in TEM_E, and therefore metastatic spread, justified further investigation.

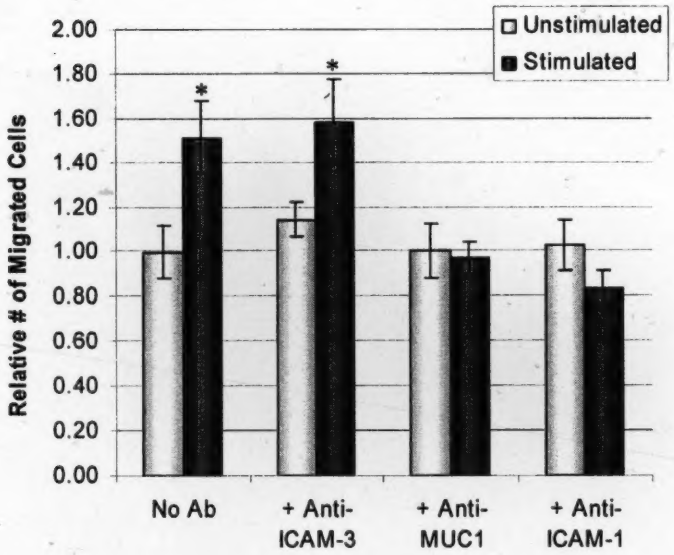

*Indicates statistical significance in Dunnett's multiple range comparison, where "No Ab, Unstimulated" was defined as the baseline control.

Figure 3.2: Addition of ICAM-1-Upregulating cytokines increases MCF-7 migration through an EAhy926 monolayer supported by a Transwell membrane. EAhy926 cells were plated on a Matrigel-coated, 8μm pore Transwell membrane at confluency. They were stimulated with TNF-α and IL-1β for 4 hours prior to the addition of MCF-7 cells. MCF-7 cells were allowed to migrate for 24 hours in the presence (Stimulated) or absence (Unstimulated) of cytokines. MCF-7 cells on the underside of the Transwell membrane were counted. Values shown are the mean ± SEM of three trials in triplicate (n = 9). The data are normalised to the unblocked, unstimulated condition, where 1 = 39 cells.

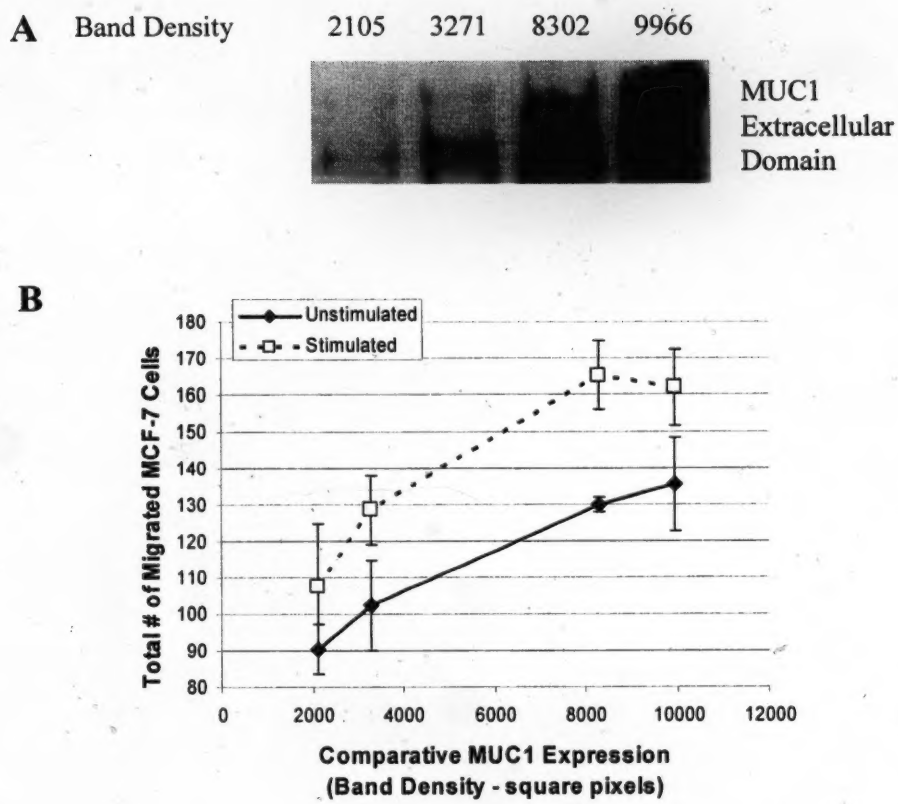

Figure 3.3: Larger numbers of MCF-7 subclones with higher MUC1 expression migrate through a cytokine-stimulated EAhy926 monolayer in comparison to subclones with lower expression. (A) Western blot showing the relative pixel densities of MUC1 expressed on the MCF-7 subclones. (B) Comparison of the relative migratory responses of the MCF-7 subclones through confluent EAhy926 cells plated on a Matrigel-coated Transwell membrane and pre-stimulated with cytokines for 4 hours. MCF-7 cells were added to the upper chamber and allowed to migrate for 24 hours in the presence (Stimulated) or absence (Unstimulated) of cytokines. The numbers of MCF-7 cells on the underside of the Transwell membranes were counted. Values shown are the mean ± SEM of three trials (n = 3).

3.2.2 Synergy Between HUVECs and Primary Fibroblasts in Promoting TEM_E

To investigate if MUC1 and ICAM-1 participate in TEM_E as well as adhesion, MUC1-positive MCF-7 cells were tested in a simulated blood vessel wall with underlying stroma. This model was constructed by plating HUVECs on the upper surface of a gelatin-coated Transwell membrane and/or primary human fibroblasts on the underside of the same membrane.

The addition of either HUVECs or fibroblasts to the Transwell model increased the level of MCF-7 migration to around 1.7 times that seen on membranes only coated with gelatin (Figure 3.4). Addition of the cytokines TNF-α and IL-1β, which are known to increase ICAM-1 expression on HUVECs (reviewed in 25, and shown in Figure 3.7), further promoted MCF-7 migration to a greater extent in the presence of HUVECs (~2.2 times greater). The greatest increase in MCF-7 migration, about 5.5 times that seen with gelatin alone, was observed when HUVECs and fibroblasts were present simultaneously on opposing sides of the same membrane and treated with cytokines. The combination of HUVECs and fibroblasts in cytokine media had a synergistic effect on tumour cell migration, as the resulting number of migrating cells in this condition was significantly higher from the sum of migrating cells when either HUVECs or fibroblasts were used singly, as determined in a signed rank-test, $p < 0.0001$. In unsupplemented media, the corresponding p-value was 0.6095, signifying the importance of cytokines in promoting synergy.

Under the synergy-producing condition, the inclusion of blocking antibodies directed against MUC1 or ICAM-1 reduced MCF-7 TEM_E by around 60-70%, strongly implicating MUC1 and ICAM-1 in MCF-7 migration under these conditions. Neither antibody was able to completely inhibit TEM_E, suggesting that different mechanisms must operate for basal migration. In contrast, an isotype control antibody or one directed against sLe^a antigens had no inhibitory effect, suggesting that the increased migration was not due to adhesion alone.

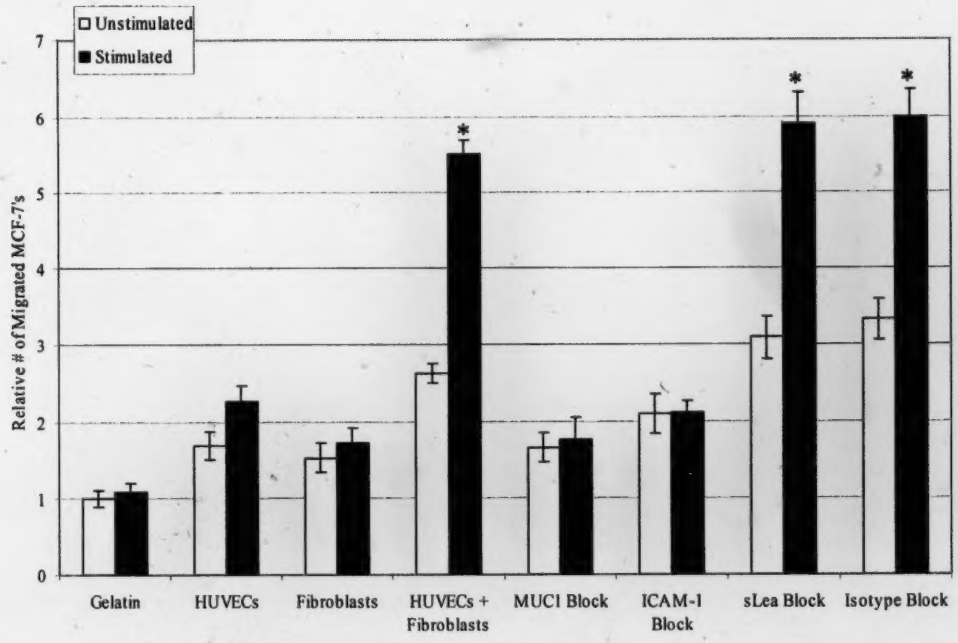

Figure 3.4: The combination of HUVECs and primary human fibroblasts synergistically promote MCF-7 cell TEM_E that is MUC1 and ICAM-1 dependent. MCF-7 cells were allowed to transmigrate for 24 hours through a gelatin-coated Transwell membrane, or through one that had been plated with HUVECs and/or primary fibroblasts. The last five data sets all contained HUVECs and fibroblasts, and where indicated, a blocking antibody. "Stimulated" and "Unstimulated" refer to the presence or absence of 20U/mL each of TNF-α and IL-1β, respectively. The values shown are mean ± SEM of at least three trials performed in triplicate. The asterisks indicate data that were statistically different from the unmarked bars in the Newman-Keuls multiple range comparison test. The data are normalised to the Unstimulated Gelatin only condition, where 1 = 129 cells.

3.2.3 Synergy is Specific to a Particular Microenvironment

To determine if any fibroblast or any ICAM-1 positive cell could increase MCF-7 migration to comparable levels, the primary human fibroblasts on the underside of the Transwell membrane were substituted with either NIH-3T3 mouse fibroblasts (negative for *human* ICAM-1), or primary human mesothelial cells (ICAM-1-positive). NIH-3T3 cells not only failed to promote MCF-7 TEM_E, but also seemed to abrogate HUVEC-induced promotion (Figure 3.5). Mesothelial cells raised MCF-7 migration levels slightly above that seen with gelatin alone, however had no obvious synergistic effect when plated together with HUVECs. This indicated that primary human fibroblasts were essential for providing a specific microenvironment necessary for MCF-7 TEM_E.

3.2.4 Synergy is a Combination of the Physical Presence of ICAM-1 and Fibroblast Secreted Factors Acting on HUVECs

To distinguish whether the large increase in MCF-7 TEM_E observed when both HUVECs and primary human fibroblasts were plated on the Transwell membrane was due to the fibroblasts providing relatively high levels of ICAM-1 on the underside of the membrane or to a secreted chemotactic factor, and whether inflammatory cytokines contributed to this effect, primary human fibroblasts were replaced with NIH-3T3 cells that had been transfected with human ICAM-1 and/or fibroblast conditioned media. By Western Blotting, these NIH-3T3 transfectants had levels of ICAM-1 expression comparable to primary fibroblasts (Figure 3.6A).

Media conditioned by primary human fibroblasts slightly inhibited MCF-7 migration through a gelatin-coated Transwell membrane, and promoted it if HUVECs were present, suggesting that it was not acting as a chemoattractant for MCF-7 cells, but may have been having a direct effect on the HUVECs. There was a synergistic effect between the conditioned media and HUVECs, as the combination of both resulted in higher numbers of migrating tumour cells than the sum of the responses in either agent alone; $p = 0.0078$ and 0.0039 in the absence or presence of cytokines respectively (Figure 3.6B).

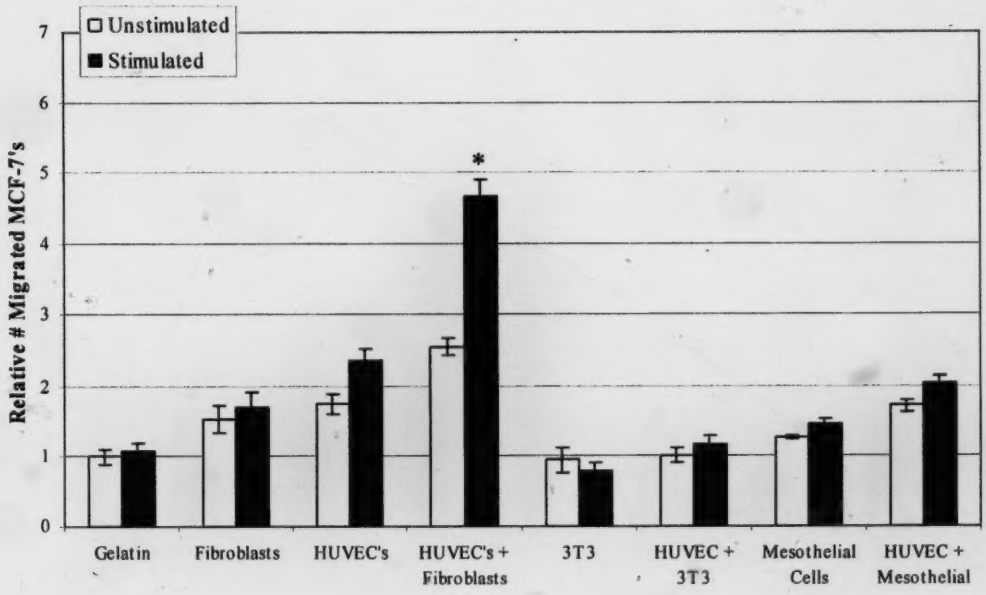

Figure 3.5: The synergy effect is specific to the combination of HUVECs + primary human fibroblasts. Transwells were coated with gelatin and plated with the cell types indicated. 3T3 refers to NIH 3T3 mouse fibroblasts. MCF-7 cells were allowed to transmigrate for 24 hours. "Stimulated" and "Unstimulated" refer to the presence or absence, respectively, of 20U/mL each of TNF-α and IL-1β. The bars represent the mean ± SEM, of at least three trials performed in triplicate. The asterisk indicates data that was statistically different from the unmarked bars in the Newman-Keuls multiple range comparison test. The data are normalised to the Unstimulated Gelatin only condition, where 1 = 129 cells.

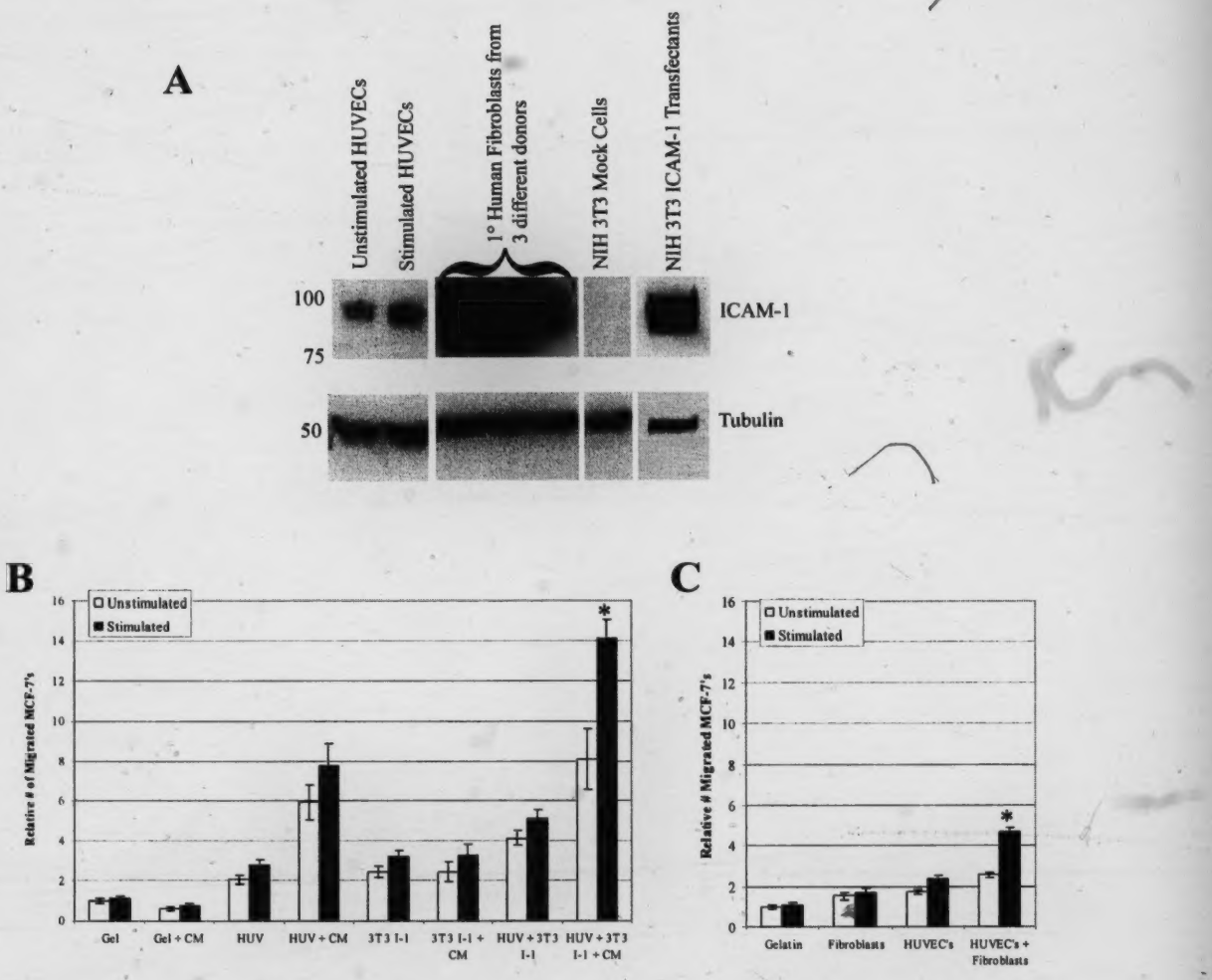

Figure 3.6: The highest levels of MCF-7 TEM_E were observed in the presence of high ICAM-1 expressing cells on either side of the Transwell membrane, inflammatory cytokines, and fibroblast conditioned media. (A) Western blots showing the relative amounts of ICAM-1 and tubulin (loading control) in the indicated cell types. "Unstimulated" and "Stimulated" refer to whether or not TNF-α and IL-1β (20U/mL each) were present. "Mock" refers to mock transfectants. The numbers show the positions of molecular weight standards. (B) Relative levels of MCF-7 cell TEM_E measured through the indicated cell types. "Gel" refers to gelatin coating only, "CM" refers to media conditioned by primary human fibroblasts, "HUV" refers to the presence

Figure 3.6 Continued: of HUVECs, and "3T3 I-1" refers to the presence of human ICAM-1 transfected NIH 3T3 cells. (C) Selected data from Figure 3.5 presented on the same scale for comparison. The white and black bars refer to the presence or absence, respectively, of TNF-α and IL-1β. The data are presented as mean ± SEM, of at least three trials performed in triplicate. The asterisk indicates data that was statistically different from unmarked bars in the Newman-Keuls multiple range comparison. The data are normalised to the Unstimulated Gelatin only condition, where 1 = 129 cells.

The addition of NIH-3T3 ICAM-1 transfectants on the underside of the Transwell membrane, even in the presence of human fibroblast conditioned media, did not increase MCF-7 TEM_E over levels seen with HUVECs alone. Combining HUVECs with NIH-3T3 ICAM-1 transfectants showed an additive effect on promoting MCF-7 migration, suggesting that the effect of each cell type was acting independently. However, the triple combination of HUVECs, NIH-3T3 ICAM-1 transfectants and human fibroblast conditioned media was the most successful in promoting synergy, as the observed relative number of migrating MCF-7's was significantly higher than the expected sum effect generated from adding the results of each individual component; $p = 0.0273$ and 0.0039 in the absence or presence of cytokines respectively.

Taken together, these data suggest that the primary human fibroblasts were secreting some migration regulating factor(s), which exerted their effects primarily on the HUVECs, and this was synergistic with the addition of cytokine stimulation.

3.2.5 The Effect of Fibroblast Secreted Factors on HUVECs is to Further Upregulate ICAM-1 Expression

Since MCF-7 transendothelial migration could be inhibited by blocking either MUC1 or ICAM-1 with antibodies, it was hypothesized that increases in either or both of these molecules would have a promoting effect. Since the addition of a high ICAM-1 expressor on the underside of the membrane by itself was insufficient to promote high levels of TEM_E, it was possible that the level of ICAM-1 on the upper side of the membrane, on the endothelial cells, may have been rate-limiting to the TEM_E effect. Thus, the expression levels of MUC1 and ICAM-1 in the various culture conditions used were examined on MCF-7 cells and HUVECs, respectively.

Incubation of HUVECs with conditioned media from primary human fibroblasts increased HUVEC ICAM-1 expression to approximately 2.5 times that seen with unstimulated HUVECs. In the presence of cytokines, conditioned media increased ICAM-1 expression to around 4 times that seen with unstimulated HUVECs. This effect was restricted to media conditioned by primary human fibroblasts; conditioned media from mouse NIH-3T3 fibroblasts had no detectable effect on HUVEC ICAM-1

expression (Figure 3.7A and C). The fibroblast conditioned media did not cause a general upregulation of all molecules since immunostaining for β1-integrin on the same membranes showed a slight, non-significant decrease. When ICAM-1 expression was plotted as a function of MCF-7 migration, the two events were closely correlated (R^2=0.9967, Figure 3.7D).

When MCF-7 cells were incubated under the same conditions, there was a slight decrease in β1-integrin expression, and an insignificant increase in MUC1 expression with fibroblast conditioned media that appeared to be independent of cytokines. (Figure 3.7B, E and F).

Thus, high ICAM-1 expression on both sides of the Transwell membrane appeared to be instrumental in promoting MCF-7 TEM_E.

3.2.6 Cell Line Specific Migratory Responses are Influenced by the Level of MUC1 Expression

To determine if the influence of the MUC1/ICAM-1 interaction on tumour cell migration could also be observed in other endogenous MUC1-expressing cell lines, T47D, MDA-MB-468, Hs578T human breast cell lines and primary human mammary epithelial cells (1°HMECs) were also tested in the Transwell assay.

The relative numbers of cells that migrated through gelatin alone was cell type specific, and the inclusion cytokines in the media did not have a statistically significant effect (Figure 3.8). When examined in co-culture with fibroblasts and HUVECs, cell lines that expressed relatively high levels of MUC1 (MCF-7 and T47D, Figure 3.9F) appeared to be responsive to culture conditions shown to promote higher levels of ICAM-1 (Figure 3.9A and B). The lower expressors (MDA-MB-468, Hs578T and 1°HMECs) did not show increased migratory responses in the presence of ICAM-1-inducing co-cultures (Figure 3.9C, D and E).

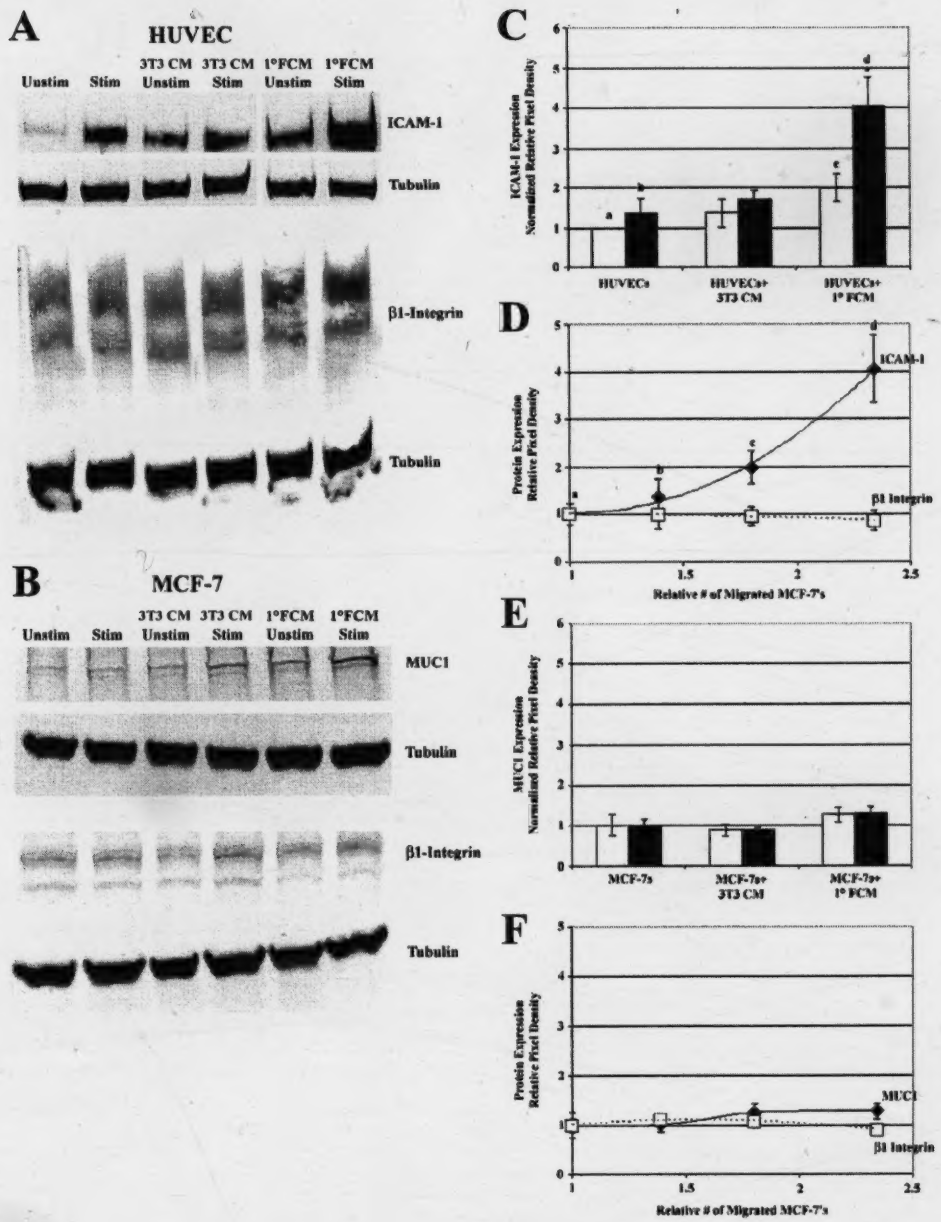

Figure 3.7: Inclusion of inflammatory cytokines and fibroblast conditioned media in co-culture systems results in increased endothelial ICAM-1 and corresponds to high MCF-7 TEM_E. HUVECs (A) or MCF-7 cells (B) were grown on gelatin-coated plastic and incubated with media conditioned by either NIH-3T3 fibroblasts (3T3 CM), or primary human fibroblasts (FCM) for 24 hours with (Stim) or without (Unstim)

Figure 3.7 Continued: TNF-α and IL-1β. Equal protein from the resulting cell lysates were run on SDS-PAGE gels, transferred to Immobilion membranes and immunoblotted for ICAM-1 and α-tubulin, scanned, then reprobed for β1-integrin. (C) The relative band densities from (A) were assessed by Scion Image, and ICAM-1 bands were corrected for loading by comparison to tubulin band densities. Comparisons were made between base media (light bars), and TNF-α and IL-1β containing media (dark bars). (D) The same membranes from (C) were reprobed for β1-integrin and both ICAM-1 (dark diamonds) and β1-integrin (light squares) relative band densities were plotted against MCF-7 migration recorded under similar culture conditions. The lower case letters correspond to similar culture conditions between the two panels. (E) The experiment in panel (C) was performed with MCF-7 cells, and relative levels of MUC1 expression were measured. (F) The membranes from (B) were reprobed for β1-integrin and both MUC1 (dark diamonds) and β1-integrin (light squares) relative band densities were plotted against MCF-7 migration recorded under similar culture conditions. The data are presented as the mean of three separate trials ± SEM. Statistical significance in the Newman-Keuls multiple range comparison is indicated by an asterisk.

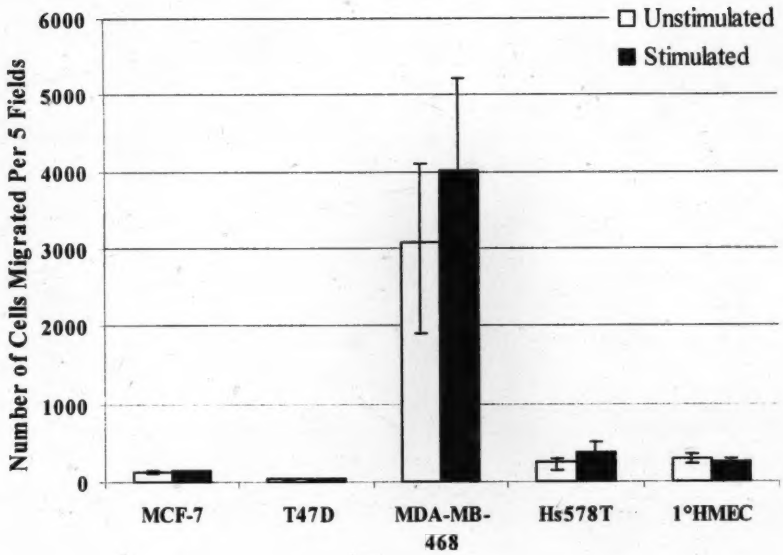

Figure 3.8: Human breast cancer cell lines migrate though gelatin in a cell type-specific manner. Different migratory responses were seen for five different breast cell lines, including benign HMECs from a reduction mammoplasty. Cells were added to the upper chambers of gelatin-coated Transwell inserts and allowed to migrate for 24 hours. Unstimulated and Stimulated refer to the absence or presence of 20 U/mL each of TNF-α and IL-1β, respectively.

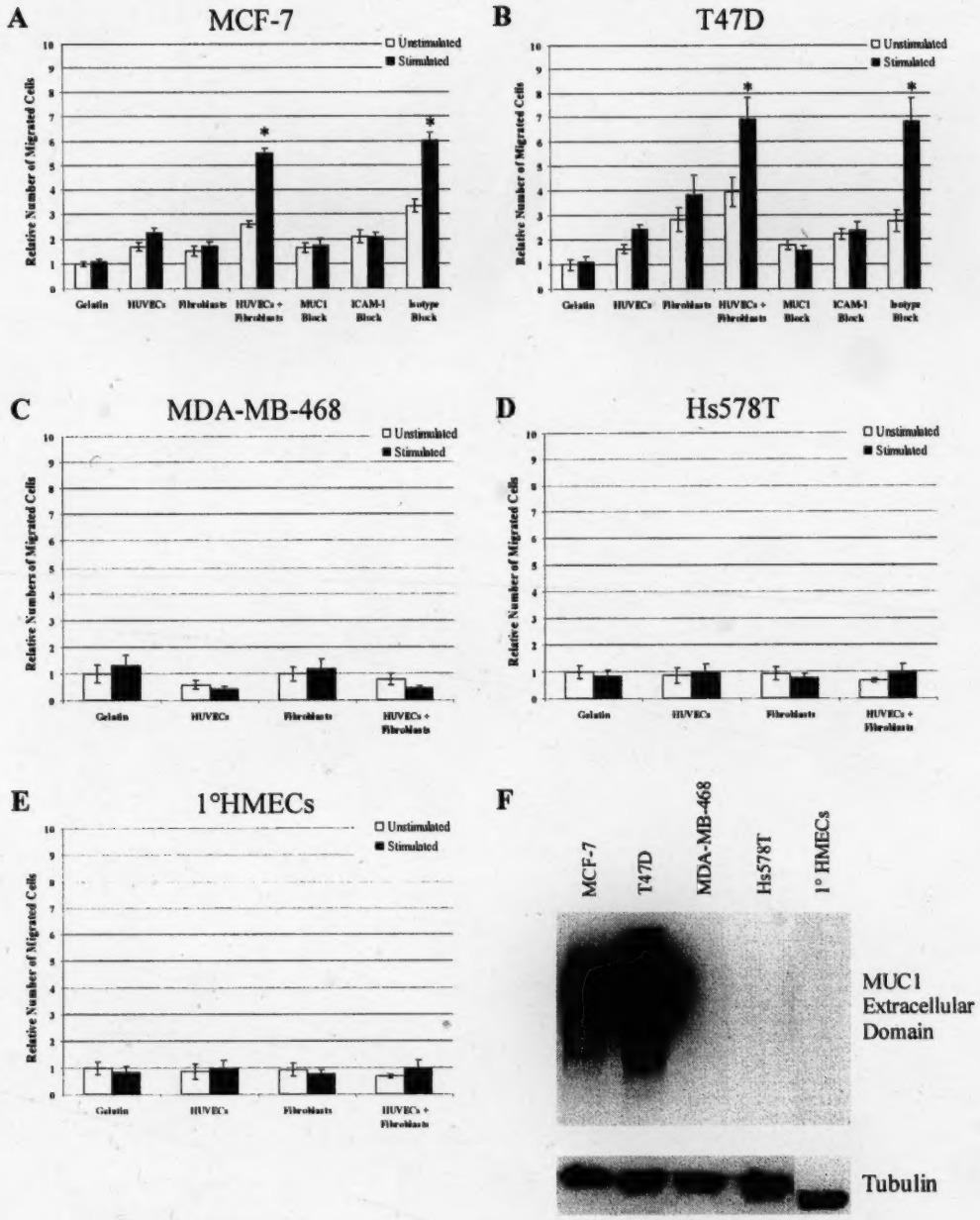

Figure 3.9: MUC1-expressing cell lines have higher migratory responses in culture-conditions shown to increase endothelial ICAM-1 expression. (A) Repitition of the MCF-7 data from Figure 3.4, included for comparison. (B) Migratory responses of T47D, (C) MDA-MB-468, (D) Hs578T and 1°HMECs (E) in the Transwell assay. The last four data sets in (A) and (B) all contained HUVECs and fibroblasts, and where

Figure 3.9 Continued: indicated, a blocking antibody. (F) Western blot showing relative amounts of MUC1 expression. Tubulin was used as a loading control. "Stimulated" and "Unstimulated" refer to the presence or absence of 20U/mL each of TNF-α and IL-1β, respectively. The values shown are mean ± SEM of at least three trials performed in triplicate. The asterisks indicate data that were statistically different from the unmarked bars in the Newman-Keuls multiple range comparison test ($p=0.01$). The data are normalised to the Unstimulated Gelatin only condition, where 1 = 129 for MCF-7 cells, 38 for T47D cells, 3091 for MDA-MB-468 cells, 259 for Hs578T cells, and 291 for 1°HMECs.

3.2.7 The MUC1/ICAM-1 Requirement for TEM_E Holds True with MUC1 Transfected Cells

To address whether the effects of the MUC1/ICAM-1 interactions are generally applicable, two subclones of human embryonic kidney epithelial 293T cells transfected with MUC1 (SYM1 and 25), and one reverse mutant subclone (SYM3), were assessed in the Transwell system. As with the endogenous MUC1 expressors, the relative migratory responses of the SYM1 and SYM25 subclones through a gelatin-coated Transwell membrane appeared to be subclone specific (Figure 3.10). The patterns of migratory responses of the MUC1-expressing cells (Figure 3.11A, B and D) were similar to those observed with the cell lines that endogenously expressed MUC1 (Figure 3.9), in that they appeared to have higher migratory responses in the presence of increased ICAM-1 expression, and these responses were sensitive to MUC1 and ICAM-1 antibody blockade. The SYM3 cells did not show any pattern that might be expected to correlate with ICAM-1 expression levels (Figure 3.11C).

3.3 Discussion

Earlier work in our laboratory showed that the protein backbone of MUC1 mediates tumour-to-endothelial cell adhesion by binding to ICAM-1, representing a novel co-receptor pairing [2,3]. In normal breast tissue, MUC1 is restricted to the apical surface of epithelial cells, however in breast cancers its expression is increased and variable in location. We found that although overall MUC1 expression was associated with a better prognosis, non-apical or aberrant expression was associated with a worse prognosis. In particular, non-apical membrane expression was associated with a higher incidence of lymph node metastases [1], perhaps because such positioning may facilitate interaction with stromal and/or endothelial ICAM-1. Furthermore, recent intravital and *ex vivo* microscopy studies have indicated that adhesion of blood-borne metastases to the vasculature of target organs is independent of mechanical trapping and is crucial to the formation of secondary tumours [7,116]. This supports the doubt [115] surrounding an earlier posit that all tumour cells from a heterogenous source are capable of vascular

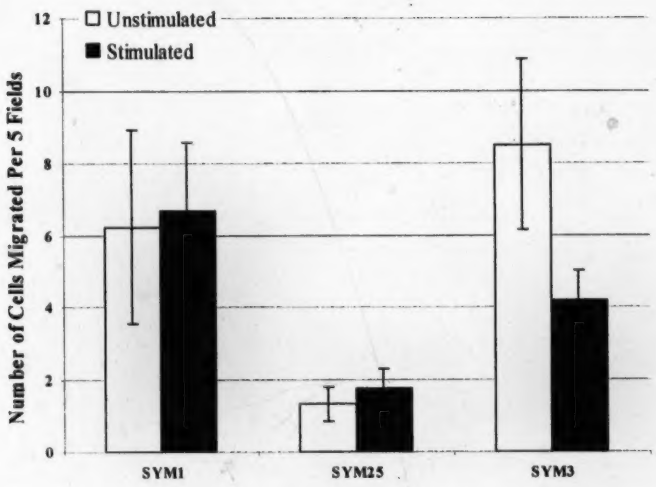

Figure 3.10: Basal rates of migration through a gelatin-coated Transwell membrane appear to be subclone specific. Different migratory responses were seen for three different MUC1-transfected 293T subclones. Cells were added to the upper chambers of gelatin-coated Transwell inserts and allowed to migrate for 24 hours. Unstimulated and Stimulated refer to the absence or presence of 20 U/mL each of TNF-α and IL-1β, respectively.

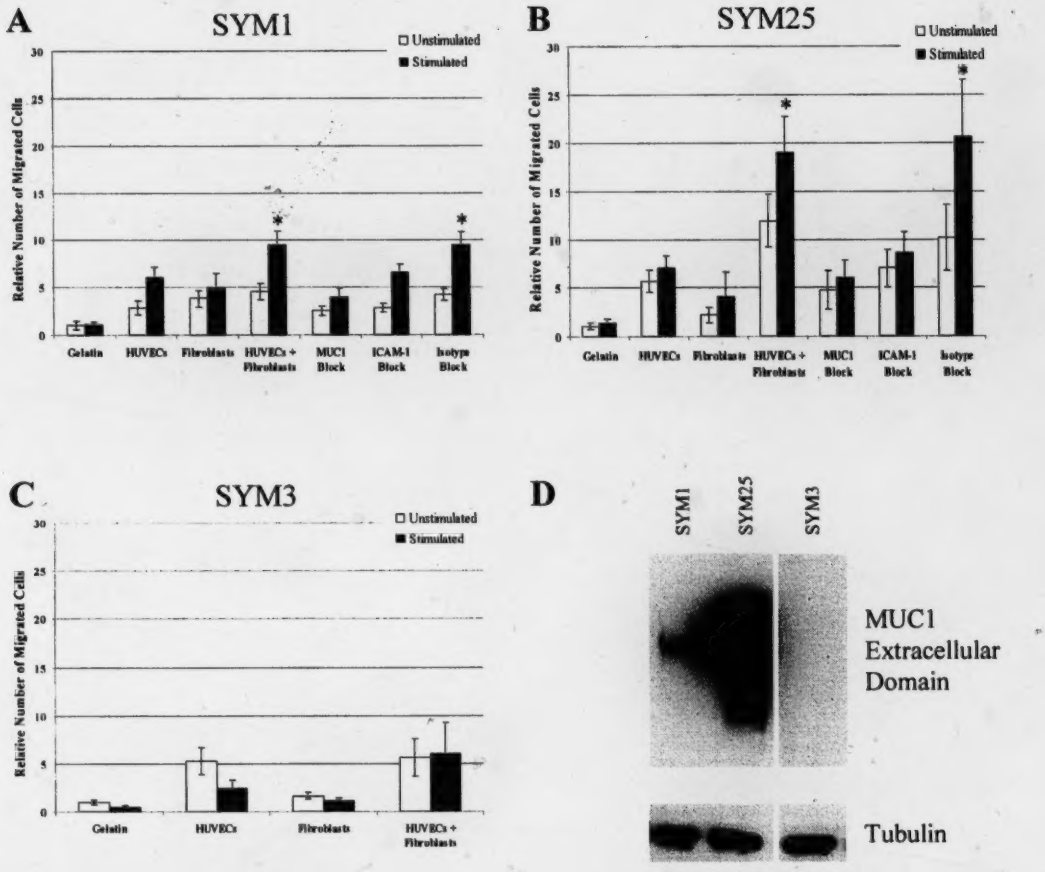

Figure 3.11: The migratory responses of MUC1-expressing 293T subclones appear to be sensitive to ICAM-1 expression. (A) Migratory responses of SYM1, (B) SYM25, (C) SYM3 293T subclones. The last four data sets in (A) and (B) all contained HUVECs and fibroblasts, and where indicated, a blocking antibody. (D) Western blot showing relative amounts of MUC1 expression. Tubulin was used as a loading control. "Stimulated" and "Unstimulated" refer to the presence or absence of 20U/mL each of TNF-α and IL-1β, respectively. The values shown are mean ± SEM of at least three trials performed in triplicate. The asterisks indicate data that were statistically different from the unmarked bars in the Newman-Keuls multiple range comparison test (p=0.05). The data are normalised to the Unstimulated Gelatin only condition, where 1 = 6 for SYM1 cells, 1 for SYM25 cells, and 8 for SYM3 cells.

adhesion and exit [238]. This current study shows that in addition to initial adhesion, tumour cell extravasation is also mediated in part by MUC1/ICAM-1 interactions.

3.3.1 Both MUC1 and ICAM-1 are Involved in Epithelial Cell TEM_E

The involvement of the MUC1/ICAM-1 interaction in TEM_E is supported by our data showing that the augmented migration of MCF-7 cells was proportional to the level of ICAM-1 expression along the migration route and that migration could be reduced to baseline levels by antibody blockade of MUC1 and ICAM-1 binding sites. The involvement of MUC1 was confirmed by the demonstration that cell lines or transfected 293T cells expressing MUC1 migrated more than those which did not. The highest level of TEM_E was achieved when ICAM-1 expression was greatest on both the upper and under surfaces of the Transwell membrane. Replacing the under surface primary human fibroblasts with NIH-3T3 ICAM-1 transfectants that expressed high levels of ICAM-1, increased MCF-7 TEM_E from 5.5 to 14 times baseline migration. However, this increase was dependent on concomitant presence of cytokine/fibroblast conditioned media, which induced increased HUVEC ICAM-1 on the upper side of the membrane, suggesting that migration through the HUVEC monolayer was rate-limiting.

3.3.2 Specific Microenvironmental Factors Can Further Promote TEM_E in an ICAM-1-Dependent Manner

The necessity of using primary human fibroblasts (instead of mouse fibroblasts or human "non-fibroblasts"/mesothelial cells) or their conditioned media to cause HUVEC upregulation of ICAM-1 and very high levels of MCF-7 TEM_E, emphasizes the importance of the *in vivo* microenvironment in promoting metastatsis. Several excellent reviews have described the significance of the microenvironment in modulating tumour behaviour [77,85,239]. Fibroblasts are key components of the stroma or microenvironment, and are known to assist in epithelial migration in situations such as wound healing (reviewed in [66]). The use of co-culture in our experiments to systematically add components that are arguably of physiologic importance has resulted

in one of the highest levels of MCF-7 migration reported in a Transwell system (Table 3.2). Although the fibroblast secreted factor(s) that induce HUVEC ICAM-1 expression have not been identified, the data supports the notion that even a cell line generally considered to be poorly metastatic (i.e. MCF-7 cells) can migrate given the appropriate set of conditions.

3.3.3 Endothelial Cell TEM_E Bears Resemblances to Leukocyte TEM_E

MUC1 has previously been implicated in tumour-to-endothelial cell adhesion, as the tumour-specific carbohydrate moieties contain sialylated Lewis a and x antigens, which are known to bind to endothelial selectins and mediate the initial adhesion and recruitment of leukocytes from the circulation [240-242]. However, the MUC1 mediated increase in TEM_E is unlikely to be caused by sLe^a-selectin binding, since TEM_E was not inhibited by antibodies against sLe^a, and the 24 hour course of the migration assay exceeds the usual transient expression of selectins. Thus, both selectins and ICAM-1 are also involved in tumour cell TEM_E.

The current results are expected to hold true under shear stresses, as a preliminary study done in our laboratory determined that the MUC1/ICAM-1 interaction is strong enough to enable tumour cell binding to endothelium under physiological fluid flow conditions, as recreated using a parallel plate flow chamber [5].

3.3.4 Overview

Using Transwell inserts, we have created an easily manipulated culture model, which allowed selective inclusion of cells or soluble factors, thereby defining specific, physiologically relevant microenvironments. This has allowed us to dissect the contribution of these various elements to the extravasation of blood borne metastases. In this way we have shown the crucial role of ICAM-1 in promoting transendothelial migration of the MCF-7 human breast carcinoma cell line, which in the absence of co-operating cells appears poorly metastatic. The fact that human fibroblasts were specifically needed in order to realize the maximum migratory response of MUC1-

Table 3.2 Comparison of MCF-7 Migration Using the Transwell Method

Total # of Cells Added	% Migrated	Membrane Coating	Culture Additions	Migration Time (hrs)	Reference
15,000	1.1%*	Fibronectin	1ng/mL MIP-1α, 0.1ng/mL pertussis toxin	5	[243]
100,000	0.5%	FBS/Vitronectin	10nM sc-uPA	24	[244]
15,000	~2.5%*	Fibronectin	0.01mg/mL MIP-1α, or 0.001ng/mL RANTES	5	[245]
60,000	~1%	Vitronectin or Collagen IV	10 ng/mL IGF-I	4	[246]
60,000	~1%*	Laminin 5	None	18	[247]
20,000	~9%	Gelatin	HUVECs, 20UmL TNF-1α, 20U/mL IL-1β, NIH 3T3 ICAM-1 cells, fibroblast conditioned media	24	This study

*Assumes that one microscopic field is ~1/10 of the total membrane area.

expressing cells, underscores the necessity of using components of physiological relevance *in vitro*. These experiments extend our previous findings and suggest MUC1-mediated tumour cell adhesion is followed by a pro-migratory response, including transendothelial migration. The possibility that MUC1 triggers an intracellular signal is supported by several studies showing that MUC1 has several putative tyrosine phosphorylation sites, and certain kinases, for example GSK3β, *src* and PKCδ, not only phosphorylate the cytoplasmic tail of MUC1 [48,49,142], but also appear to regulate its association with other signalling molecules or adapters, such as β-catenin or Grb2/Sos [48,51,143]. Furthermore, MUC1 associates with EGFR [54,143], which is known to trigger a migratory response [181], and may participate in the activation of the ERK/MAPK signalling pathway, an effect also observed after forced clustering of CD8 chimeras carrying MUC1 cytoplasmic tails [52,53]. In this context, ERK activation was not associated with increased proliferation (PCNA activation) [54], suggesting that it may be part of the other known ERK1/2 pathway, which regulates migration [248,249]. The MUC1 CT in particular, has been shown to interfere with intracellular components of cell-cell and cell-matrix adhesions.

The MUC1 CT competes with E-cadherin for binding to β-catenin [45,48-50,55,142,143,185,250], and peptides corresponding to the MUC1 CT binding sequences for β-catenin, GKS3β and *src* disrupted focal adhesion structure and increased migratory behaviour in MDA-MB-468 cells [55]. Alternately, MUC1 may be acting through association with p120ctn (discussed in Section 1.2.3.3). These observations support the idea that the MUC1 signal is related to a shift towards a motile phenotype. Thus, ICAM-1 may serve as a stimulatory ligand for the MUC1 extracellular domain.

The idea that MUC1 initiates a pro-migratory signal is compatible with recent *in vitro* evidence. MUC1 is found in lipid rafts [251], suggesting that it participates in signalling. Our data adds to the current knowledge by clearly identifying ICAM-1 as a clinically relevant, physiological ligand that may trigger a MUC1-dependent pro-migratory signal. The current report, combined with those describing MUC1 signalling function(s) [47-54,144,184], suggest that MUC1 should perhaps be considered as tumorigenic, rather than a simple, passive facilitator of metastasis.

Chapter 4: Microenvironmental Influences on MCF-7 Integrin Expression

4.0 Introduction

In the Transwell experiments, we found that antibody blockade of MUC1 or ICAM-1 inhibited the ICAM-1-induced increases in MCF-7 TEM_E, and raised the possibility that ligation of MUC1 must be activating a shift towards a motile phenotype. The highest levels of TEM_E, were dependent on the presence of fibroblasts on the underside of the membranes, and the effect of these cells was two-fold; first, they expressed additional ICAM-1 themselves, thus increasing the duration of ICAM-1 exposure as the tumour cells moved along the migratory track, and second, they secreted a factor that acted synergistically with inflammatory cytokines to increase endothelial ICAM-1 expression. There is one other question, however, which is whether the fibroblasts or their secreted factors may have had any effect on the tumour cells themselves, an idea supported in the literature [252,253].

The data in Figure 3.6 makes it clear that the fibroblast conditioned media (FCM) is not in itself a chemoattractant (test condition "Gel+CM"). Panels E and F in Figure 3.7 show that FCM may be having some direct effect on the MCF-7 cells, as not only did it produce a slight increase in MUC1 expression, which was independent of cytokines, but it also induced a slight downward trend in total cell β1-integrin expression (as detected by Western Blotting of whole cell lysates). While neither of these observations held statistical significance, it was not unreasonable to expect that these culture conditions may have induced some changes in the integrin state(s), as these molecules are well known to be involved in modulating changes in polarity as well as generating contractile forces necessary for migration [246,254-259].

MCF-7 cells express relatively high levels of α2β1 integrins in comparison to other integrin pairs (Figure 4.1, [246]). This particular integrin receptor regulates the differentiation state of epithelial cells, and also tends to decrease as normal luminal epithelia changes into invasive carcinoma, favouring a switch to the α6β4 integrin (Table 4.1, [260]). Further to this, Gui et al., have reported that in a clinical setting, 70% of patients with positive lymph node metastases had no detectable β1-integrin expression

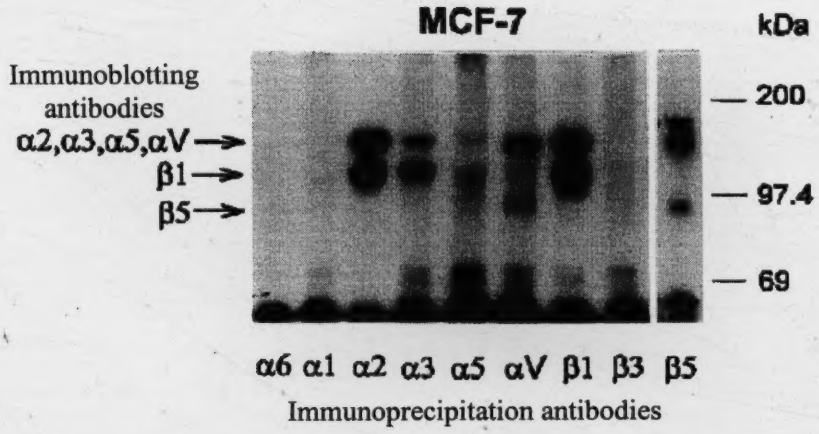

Figure 4.1: Integrin expression profile of MCF-7 cells. Expression of the α2β1 integrin appears to be the most prevalent. Based on Doerr, ME, et al. [246]

Table 4.1: β1-Integrins Show a Tendency to Decrease Expression as Transformed Epithelia Develop into Invasive Carcinomas.

Integrin Receptor	Luminal Epithelial Cells	Invasive Carcinoma	Proposed Function in Carcinoma
α1β1	-	-	Not expressed
α2β1	+	+/-	Regulates epithelial differentiation
α3β1	+	+/-	Unknown
α5β1	+	+/-	Unknown
α6β1	+	+/++	Promotes growth and survival
α6β4	+	+	Promotes invasion

Based on Shaw, LM et al. [260]

[261], suggesting that such a phenotypic change is a part of tumour cells perhaps becoming de-differentiated as they change to a migratory state.

To follow up on our initial observation that total β1-integrin expression was showing a slight decrease in MCF-7 cells under conditions that induced the highest migratory response of these cells, we asked the following specific questions:

i) Did the co-culture conditions used to produce the syngergistic TEM_E effect alter the β1- or β4-integrin profile of MCF-7 cells?

ii) Did this alteration have anything to do with ICAM-1?

We investigated these questions by recreating large scale versions of the Transwell co-cultures, and examining the MCF-7 surface expression of β1- and β4 integrins by flow cytometry. HUVECs were substituted with NIH 3T3 ICAM-1 and Mock transfectants, so that the effect of ICAM-1 could be separated from the cytokine effects, and fibroblast conditioned media was used instead of fibroblasts, again to separate the ICAM-1 effect from the soluble factors effect. Thus, each component that may have altered MCF-7 integrin expression could be examined singly, or in combination.

4.1 Methods and Materials

4.1.1 Reagents

The green fluorescent vital stain BCECF-AM, cell permeant, was purchased from Molecular Probes, and prepared as a 5mM stock in DMSO. Gelatin Type A, Tween 20, MOPC 31C mouse IgG1, DNase I and $MgCl_2 \cdot 6H_2O$ were from Sigma-Aldrich. HUTS-21 mouse anti-human activated β1 integrin antibody was purchased from BD Biosciences. JB1A antibody, which detects an epitope on the β1-integrin subunit, was from the laboratory of Dr. John Wilkins, Department of Medicine, University of Manitoba. A9 antibody against β4-integrin was purchased from Santa Cruz Biotechnology. BSA, fraction IV was from Fisher Scientific. Goat anti-mouse phycoerythrin secondary antibody was purchased from Southern Biotechnology Associates, Inc., and used at a 1/250 dilution. TNFα and IL-1β were purchased from

CedarLane Laboratories.

4.1.2 Cells

MCF-7 human breast adenocarcinoma cells were from the ATCC, and were maintained in DMEM + 10% FBS + 0.1mg/mL insulin. Human ICAM-1 transfected NIH-3T3 cells and their mock transfected counterparts were generous gifts of Dr. Ken Dimock, University of Ottawa, and were maintained in DMEM + 10% FBS + 2μg/mL Blasticidin S. Primary human fibroblasts were provided by Dr. Joanne Emerman, University of British Columbia, and were maintained in DMEM media + 10% FBS, 10U penicillin, 10U streptomycin, 2mM L-glutamine, 10mM sodium pyruvate and 0.1mM Gibco MEM Non-Essential Amino Acids Solution.

4.1.3 Co-Culture

T75 Tissue culture flasks were coated with 0.1% (w/v) gelatin prepared in water, and plated with (i) no cells, (ii) NIH 3T3-ICAM-1 transfectants, or (iii) NIH 3T3 Mock transfectants at confluency (10mL of cell suspension at 5×10^5/mL). NIH 3T3 cells were loaded with BCECF-AM by adding 6mL of a 2nM solution of BCECF-AM in Dulbecco's PBS for 30 minutes at 37°C. Excess BCECF-AM was removed by two washes with Dulbecco's PBS. MCF-7 cells, grown to ~60% confluency in separate T75 tissue culture flasks, were trypsinized and added to the gelatin-coated flasks with or without the before mentioned NIH 3T3 transfectants (Figure 4.2). For each co-culture condition, one of the following was added: (i) base media (DMEM + 10% FBS, 10U penicillin, 10U streptomycin, 2mM L-glutamine, 10mM sodium pyruvate and 0.1mM Gibco MEM Non-Essential Amino Acids Solution, i.e. unconditioned primary fibroblast culture media), (ii) base media with 20U/mL each of TNF-α and IL-1β, (iii) fibroblast conditioned media, or (iv) fibroblast conditioned media with 20U/mL each of TNF-α and IL-1β. Co-cultures were incubated at 37°C, 5% CO_2 for 24 hours.

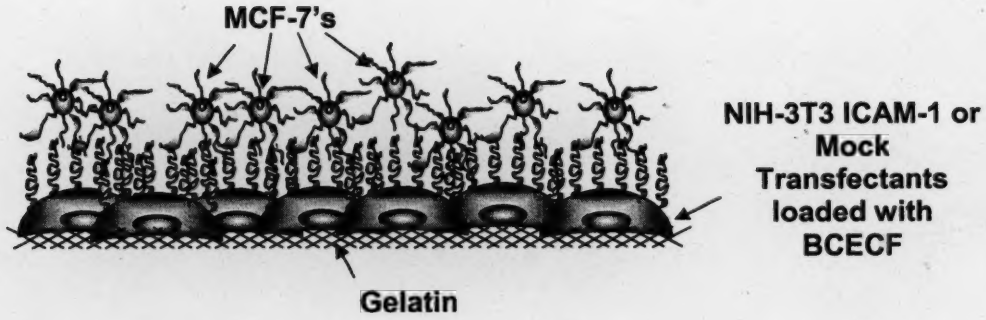

Figure 4.2: Schematic diagram of the co-culture model. Tissue culture flasks were coated with gelatin, on which NIH 3T3 ICAM-1 or mock transfectants were plated at confluency. These were loaded with the green fluorescent vital stain, BCECF. MCF-7 cells were plated over top of the adhered NIH 3T3 cells at ~60% confluency, with the intention that this procedure would allow maximum probability of contact between ICAM-1 expressed by the NIH 3T3 cells, and MUC1 expressed by the MCF-7 cells, in a close approximation of the cell-cell interactions occurring in the Transwell model.

4.1.4 Flow Cytometry

Cells in co-culture were trypsinized, washed 1X in FBS-containing media, then divided into 4 aliquots, each of which was incubated with one of BTT (2% BSA, 0.02% Tween 20, in Tris Buffered Saline, unlabeled control), 5μg/mL MOPC 31C in BTT (isotype control), 20μg/mL HUTS-21 in BTT, 8μg/mL of A9 in BTT or 5μg/mL JB1A in BTT, on ice for 1 hour in a volume of 30μL. Cells were washed in a 50X volume of cold PBS, then resuspended in 30 μL BTT (unlabeled control) or 30μL of phycoerythrin secondary, 2μg/mL in BTT, for a further 1 hour, in the dark, on ice. Cells were again washed in a 50X volume of cold PBS, then resuspended in 300μL PBS, and treated with final concentrations of 120U/mL DNase I and 4.2mM $MgCl_2$, for 15 minutes at room temperature. Samples were stored at 4°C in the dark until analysed by flow cytometry. Data collection gates were set so that the green (BCECF) labelled NIH 3T3 cells were not included, and 10,000 events (specific to MCF-7 cells) were recorded on the FL2 (phycoerythrin or red fluorescence) channel (Figure 4.3). This permitted separation of integrins stained on the NIH 3T3 cells from those on the MCF-7 cells. As cells were neither fixed nor allowed to warm up, only surface antigens should have been labelled.

4.2 Results

4.2.1 MCF-7 Cells Do Not Express Significant Levels of Surface β4-Integrins, Regardless of Culture Conditions

The percentage of MCF-7 cells staining positively with the A9 antibody was not appreciably greater than the unlabelled and isotype control samples in any of the test conditions (Figure 4.4). This result may have been specific to MCF-7 cells, or it may suggest that MCF-7 cells still exhibit some features of normal, polarised breast epithelia, and have not made the phenotypic switch from mainly α2β1 integrins to α6β4 integrins.

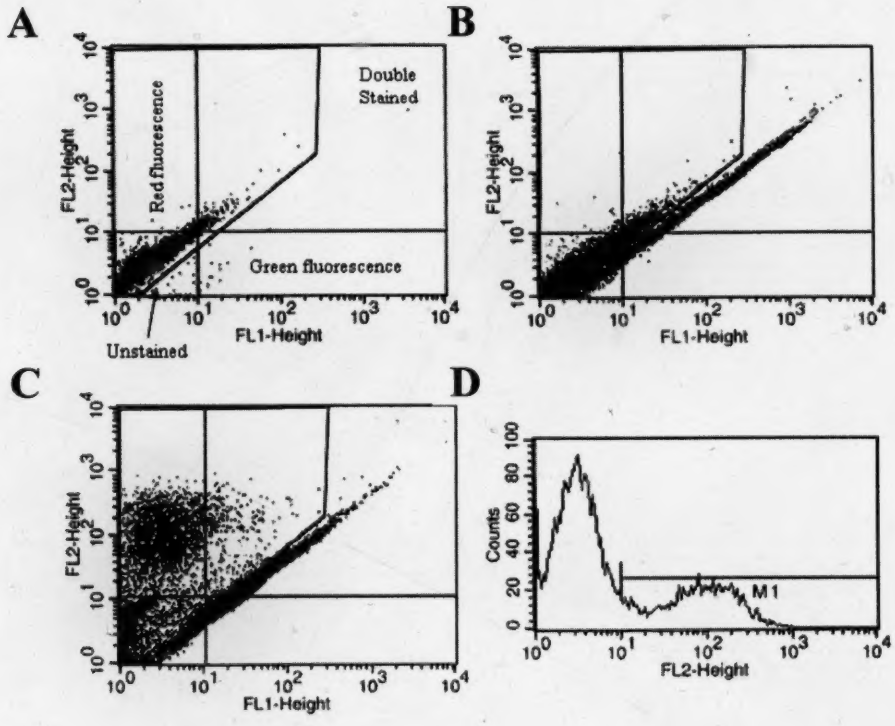

Figure 4.3: Mode of flow cytometry data collection. (A) Example of the two-colour acquisition dot plot used for data collection. The lower left chamber represents the plotting area for unstained cells, the upper left for red fluorescently stained cells (FL2 channel), the lower right for green fluorescently stained cells (FL1 channel), and the upper right for double stained cells. The settings on the flow cytometer were adjusted so that the majority of unstained MCF-7 cells were plotted in the lower left quadrant. (B) Example of MCF-7 and BCECF-labelled NIH 3T3 cells analysed together. Although there is no red stain added, the intrinsic properties of the NIH 3T3 cells resulted in this population appearing in the upper right quadrant. Note that there is clear separation between the two cell populations, allowing a gate to be drawn around the MCF-7 cells. (C) Example of MCF-7 cells stained red for β1-integrins. Note that a percentage of the cells have shifted into the upper left quadrant. (D) An example of a histogram plotted only for the FL2 channel of the gated data shown in the dot plot to the left, allowing easier visualisation of the number of cells showing an increase in fluorescent intensity.

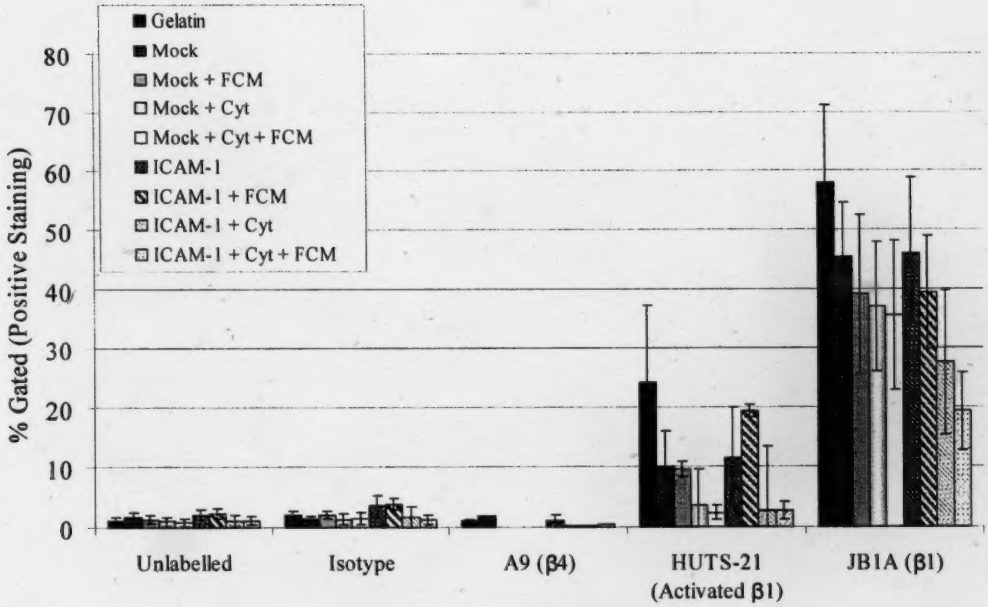

Figure 4.4: MCF-7 cells cultured under conditions that resulted in high levels of transendothelial migration in the Transwell assay show decreased surface β1-integrin expression. The graph shows the percentages of MCF-7 cells within a test population that stained positively for each of the antibodies listed on the x-axis, as explained in Figure 4.4. MCF-7 cells showed no appreciable β4-integrin expression under any of the conditions tested. However, surface expression of β1-integrins decreased with addition of cytokines (Cyt) and fibroblast conditioned media (FCM). The presence of ICAM-1 expressing cells augmented this effect.

4.2.2 Decreases in MCF-7 Surface Expression of β1-Integrins is Independent of ICAM-1 Unless both Cytokines and Fibroblast Conditioned Media are Present

The mean percentages of MCF-7 cells presenting the activated β1-integrin epitope showed a tendency to drop with sequential addition of fibroblast conditioned media and cytokines, however, the numbers were variable, and there was no notable difference when comparing the NIH 3T3 mock data with that collected from the NIH 3T3 ICAM-1 co-cultures (Figure 4.4). A similar trend was noted for total surface β1-integrins, with the expression levels decreasing the most under the same culture conditions that produced the highest levels of MCF-7 migration in the Transwell assay, that being when the MCF-7 cells were presented with a combination of ICAM-1, cytokines and fibroblast conditioned media. When the total surface β1-integrin data was plotted as a pair of line graphs comparing the NIH 3T3 mock and NIH 3T3 ICAM-1 co-cultures, the expression levels were clearly decreased more when ICAM-1 was present (Figure 4.5). The numbers were again variable, and t-tests performed between the mock and ICAM-1 conditions for the "+ cytokines" and the "+ fibroblast conditioned media + cytokines" data points, showed no significant differences ($p = 0.295$ and $p = 0.153$, respectively). When comparing the first data point (base media) with the last data point (+ cytokines + fibroblast conditioned media) for a given NIH 3T3 feeder layer, the decrease in β1-integrins observed on the NIH 3T3 ICAM-1 cells was statistically significant ($p = 0.047$). Whereas that of the NIH 3T3 Mock cells was not ($p = 0.277$). This suggests that ICAM-1 can further the effect of cytokines and fibroblast conditioned media, but is not a major influence on its own.

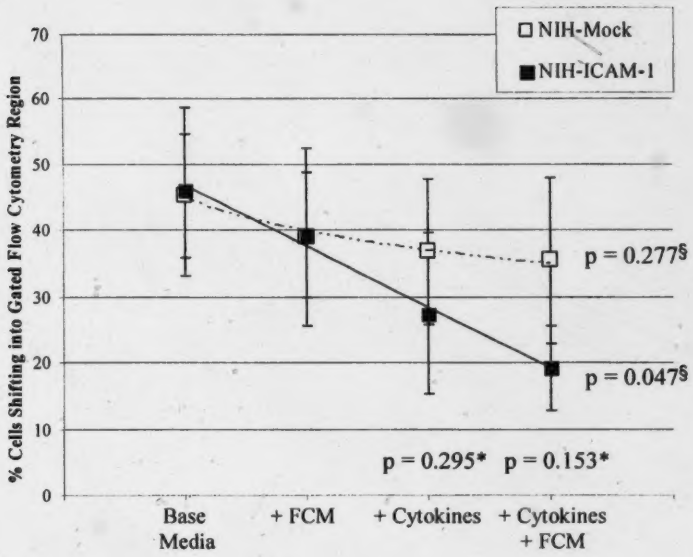

*Comparison of NIH 3T3 Mock and NIH 3T3 ICAM-1 data points.

§Comparison of first and last data points within either the NIH 3T3 Mock or ICAM-1 data sets.

Figure 4.5: Line graphs of surface β1-integrin expression on MCF-7 cells with statistical analyses done on specific data pairs. The graph shows a comparison of the surface MCF-7 β1-integrin expression levels on cells co-cultured with either NIH 3T3 Mock or ICAM-1 transfected cells. FCM refers to fibroblast conditioned media. In the presence of ICAM-1, the decreases observed with the addition of cytokines and fibroblast conditioned media are more pronounced. There were no statistical differences between the NIH 3T3 Mock or ICAM-1 data sets when examining the final two data points ("+ Cytokines" and "+ Cytokines + FCM"). However, there was a borderline statistically significant difference between the "Base Media" and "+ Cytokines + FCM" data points within the NIH 3T3 ICAM-1 data set ($p = 0.047$). Data shown are means ± SEM, $n = 4$.

4.3 Discussion

The results suggested that the culture condition which produced the highest levels of MCF-7 cell TEM_E, also seemed to decrease the surface expression of β1-integrins on MCF-7 cells. As in the Transwell experiments, a combination of ICAM-1, inflammatory cytokines and fibroblast secreted factors was necessary to see the maximum effect. The change seen in the surface expression of β1-integrins on MCF-7 cells was reminiscent of observations made in clinical breast cancer specimens that were associated with metastasis to the lymph node (reviewed in [260,261]). However, clinical specimens are examined mainly by immunohistochemistry performed on sectioned tumours, a technique that gives an indication of total cellular expression of a particular protein. The flow cytometry used herein was performed without permeabilization, which should have measured integrin molecules only on the surface of the cells. The drop in total β1-integrin expression, as shown by Western Blotting in Figure 3.7B and F, was much less. This may indicate that the downregulation of the β1-integrins begins at the cell surface, and the total cellular levels may drop later, or that the integrins are being turned over at the cell surface.

Clinical breast cancer specimens also show an increase in β4-integrin expression, which has been implicated in the cells adopting a motile phenotype. This was not seen on the MCF-7 cells. One possible explanation is that the actual shift to β4-integrin expression may have occurred outside of the 24 hour time point examined. Another possibility is that MCF-7 cells may not use this particular receptor to migrate, or may need to accumulated further mutations in order to become more metastatically agressive.

4.3.1 The Potential Significance of the β1-Integrin Drop

Antibody blockade of β1-integrins leads to the induction of apoptosis in normal mammary epithelial cells, but not malignant breast cells [262]. As breast carcinomas tend to downregulate their expression of β1-integrins, it is tempting to speculate that by doing so, they may be able to escape anoikis or switch to adhesion-independent growth. If so, the experimental data presented herein may indicate that this switch is encouraged

by specific microenvironmental elements. Since ICAM-1, inflammatory cytokines and fibroblast secreted factors were involved, and all of these can reasonably be expected to normally function to encourage wound healing, another interesting possibility may be that the tumour cells are opportunisitically using a normal mechanism to promote the migration of epithelial cells into a wound bed, in order to metastasize.

4.3.2 Overview

MCF-7 cells express high levels of $\alpha 2\beta 1$ integrins [246], which suggests that they are still relatively well differentiated [260]. This may, in part, explain the observations made in the Transwell assay. MCF-7 cells did not migrate to the undersides of the Transwell membranes, unless exposed to the combination of ICAM-1-expressing cells on both sides of the membrane, inflammatory cytokines, and fibroblast conditioned media, which appeared to be concurrent with a change in the surface expression of $\beta 1$-integrins on the MCF-7 cells. Thus, the effects of the fibroblast conditioned media + inflammatory cytokines combination appear to be two fold: i) they stimulate higher ICAM-1 expression on the endothelial cells, and ii) they work in combination with ICAM-1 to trigger MCF-7 cells to shift to what may be a more motile phenotype.

Chapter 5: MUC1/ICAM-1 Interactions and Calcium Signalling[2]

[2] A version of this chapter has been published. Rahn JJ, et al. 2004. J Biol Chem. 279:29386-90. Data appearing in the publication which were not directly generated by J. Rahn have been excluded from this thesis.

5.0 Introduction

The data presented in Chapters 2-4 have thus far suggested that depolarised MUC1 on the surface of a breast tumour cells is situated ideally to interact with ICAM-1 on adjacent cells. Not only does MUC1 bind to ICAM-1, but the MUC1-expressing tumour cell appears to shift towards a motile phenotype, and the amount of tumour cell TEM_E correlated with the amount of endothelial ICAM-1. The latter was dependent on the presence of cytokines and soluble fibroblast-secreted factors, which acted on both the endothelial cells and the tumour cells. It seems logical, that some signal is needed to spur the tumour cell to migrate, and that this signal is triggered by ICAM-1 binding to MUC1.

Considering that calcium-based signalling is important in nearly every aspect of cell migration [181,263-265], it seemed worthwhile to determine if any such signal might be initiated by the MUC1/ICAM-1 interaction. In addition to the possibility of MUC1 sending a calcium-based signal into the tumour cell, it has been reported that ICAM-1 can send a calcium-based signal into endothelial cells, after contact with cross-linking anti-ICAM-1 antibodies [201,206], activated leukocytes [201], or MCF-7 cells [203].

The specific questions asked in this chapter were:

i) Was the hypothesized ICAM-1 triggered MUC1-mediated signal calcium based?

ii) Was this signal specific to MUC1 and ICAM-1?

iii) Was this signal bi-directional, i.e. was it sent within both the MUC1 expressing cell and the ICAM-1 expressing cell?

These questions were addressed by loading cells with the fluorescent calcium indicator dye Fluo-3, allowing MUC1 and ICAM-1 expressing cells to come into contact with each other, and measuring the changes in intracellular calcium.

5.1 Methods and Materials

5.1.1 Assay Development

The details of the development of the calcium oscillation assay appear in Table

5.1, and selected data in Appendix III. The assay was designed to specifically measure oscillatory response in a population of unsynchronised cells, not intracellular calcium concentrations, and allow comparisons between different culture conditions.

5.1.2 Reagents

The CT2 antibody against the MUC1 cytoplasmic domain was generously provided by Dr. Sandra Gendler, Mayo Clinic, Scottsdale. Pluronic F-127, MOPC C31 mouse IgG1 isotype control antibody, anti-tubulin B-5-1-2 antibody and gelatin were from Sigma-Aldrich. B27.29 antibody against the MUC1 extracellular domain was a gift from Biomira, Inc. ICR5 antibody against human ICAM-3 was a gift of ICOS Corporation. Goat anti-mouse phycoerythrin secondary antibody was purchased from Southern Biotechnology Associates, Inc. Goat anti-mouse or anti-Armenian hamster peroxidase conjugated antibodies were purchased from Jackson ImmunoResearch. ECL Plus was from Amersham Pharmacia. FBS and culture media were from Gibco.

5.1.3 Cells

293T human embryonic kidney epithelial cells were from the ATCC and were transfected with pEYFP-N1/MUC1. These were designated SYM, followed by a number indicating subclone identity (the development of these cells is described in Chapter 2). For this particular study, five subclones were selected. Cells expressing the YFP tag were not sufficiently fluorescent to interfere with Fluo-3 imaging. T47D, MCF-7, MDA-MB-468 and Hs578T human breast cancer cells were also from the ATCC. Mock and ICAM-1 transfected NIH 3T3 mouse fibroblast cells were a generous gift of Dr. Ken Dimock, University of Ottawa, Ontario. HUVECs were isolated and cultured as described in section 2.1.2.

Table 5.1: Development of the Calcium Oscillation Assay

Parameter	Trials	Final Selection	Comments
• Type of culture support	• Plastic Petri Dish • MatTek Uncoated Glass Bottomed Dish, No.0 Coverglass	• MatTek Uncoated Glass Bottomed Dish, No.0 Coverglass	• The optical resolution of the calcium images taken on tissue culture plastic were too poor for publication purposes. • The thin glass coverslip allowed sharper focus on the cells and did not interfere with transmission of fluorescent light.
• Order of cell addition	• Addition of Fluo-3-loaded MUC1 cells in suspension over adherent ICAM-1 cells • Addition of ICAM-1 cells in suspension over adherent Fluo-3 loaded MUC1 cells	• Addition of ICAM-1 cells in suspension over adherent Fluo-3 loaded MUC1 cells	• Dropping MUC1 cells on adherent ICAM-1 cells would have been closer to the Transwell assay, but this was impractical, as we had to guess where the Fluo-3 cells would be after they were dropped, and focus the microscope on that plane • MUC1 cells oscillated regardless of adhesion • The selected method allowed us to focus the microscope on the Fluo-3 loaded cells prior to adding the drop cells, thus ensuring that the entire calcium event was imaged on a single focal plane with higher clarity • It allowed us to take "before" images that would allow us to keep track of where the MUC1 cells were before addition of the secondary cell types • It allowed us to take an "after" image to ensure all cells were covered by the drop cells
• Matrix used to coat glass coverslips	• No coating • 0.1% (w/v) gelatin in water • FBS • Matrigel • Poly-L-Lysine • Collagen	• 0.1% gelatin for 293T cells • FBS for MCF-7 cells • Collagen for HUVECs	• Cells did not adhere easily to uncoated glass. • The matrix selected for a particular cell type was based on the combination that produced the most easily measurable results; e.g. 293T cells hardly oscillate on Matrigel.
• Method of coating coverslips	• Air dry at room temperature • Heat to 60°C for 1 hour	• Air dry for Matrigel, FBS and poly-L-lysine • Heat for gelatin and collagen	• The method chosen for each matrix was based on what resulted in even coating with minimal "peeling up". • Cover slips were sterilized after coating under UV light for 30 minutes.

Table 5.1 Continued: Development of the Calcium Oscillation Assay

Parameter	Trials	Final Selection	Comments
• Volume of cell suspension to drop over adherent cells	• 100µL over 100µL of imaging buffer covering cells • 100µL over adherent cells after removing the buffer from the dish	• 100µL over adherent cells after removing the buffer from the dish	• If the buffer over the adherent cells was not removed first, the volume of the drop cell suspension tended to either form a dome of liquid over the coverslip, or spill out onto the surrounding plastic, and the drop cells would not make efficient contact with the adherent cells.
• How to drop the ICAM-1 cells	• In a high density suspension • Grown on beads	• In a high density suspension	• The beads were intended to force the cells to make contact more quicky, via their weight, but the bead matrix diffracted the laser light too much, making measurements difficult. A high density of drop cells in a small volume worked much better.
• Temperature	• Room Temperature • 37°C (Microscope stage warmer)	• 37°C (Microscope stage warmer)	• More oscillations were recorded when the cells were warm
• Cell Confluency	• Totally confluent • ~60% confluent • Low confluency (>50%)	• ~60% confluent	• Oscillations tended to disappear from cells known to oscillate if the cell confluency varied greatly from ~60%.
• Data Comparisons	• Amplitude only • Frequency only • Amplitude (from trendline) x Frequency	• Amplitude (from trendline) x Frequency	• Amplitude only: Cells could have a large calcium influx without oscillating, and amplitude comparisons with genuinely oscillating cells would show no difference. • Frequency only: Cells could have shallow oscillations and appear to be no different from those with strong oscillations • Taking the amplitude from a trendline compensated for differences in background; e.g. such as may come from differential loading of Fluo-3, which is difficult to avoid.

5.1.4 Calcium Oscillation Assay

3cm glass bottomed dishes were purchased from MatTek. The glass bottoms were coated with 100 μL FBS (for untransfected cell lines) or a solution of 0.1% (w/v) gelatin in water (for 293T cells). 293T cells would not oscillate on FBS, however the endogenous MUC1-expressing cells perhaps required fibronectin that may have been present in the serum [266]. 100μL of untransfected cell suspension at 1 x 10^5/ml or MUC1-transfected 293T cells at 5 x 10^4/mL were plated onto coated cover glasses and allowed to equilibrate overnight. This generally resulted in ~60% cell confluency the next day. The media was aspirated from plated cells, and 1:1 mixture of 5mM Fluo-3 in DMSO:20% (w/v) Pluronic F-127 in DMSO, diluted 1/1000 in DMEM + 10% FBS was pipetted over the cells. The plated cells were then incubated with Fluo-3 for 1 hour at 37°C, 5% CO_2. Cells were washed once in 37°C Imaging Buffer (152mM NaCl, 5.4mM KCl, 0.8mM $MgCl_2$, 1.8mM $CaCl_2$, 10mM HEPES, 5.6 mM glucose, pH 7.2 [267]), then left in Imaging Buffer at 37°C for 30-45 minutes until imaged. For the antibody blockade experiments, this buffer contained either B27.29 (MUC1 block) or ICR5 (Irrelevant block) at 120μg/mL for 293T MUC1-transfectants, and either B27.29 or MOPC C31 (Irrelevant block) at 60μg/mL for T47D cells. NIH 3T3 ICAM-1 or mock transfectants were trypsinized and resuspended in Imaging Buffer at ~1.2 x 10^7/mL. Immediately before photographing, the Imaging Buffer was decanted, and if blocking antibodies were used, the cells were gently rinsed with warmed Imaging Buffer. The MatTek dish was then placed in a microscope stage warmer set to 37°C, on a Zeiss Axioscope Digital Imaging Microscope. Using Metamorph software (Universal Imaging Corporation), a DIC image was recorded, then 60 images at 3 second intervals were recorded under the FITC filter. 100μL of NIH-3T3 cell suspension was added to the plated cells immediately after the first FITC image was taken, so that the calcium flux response of the plated cells was recorded in the remaining 59 images. A final DIC image was taken at the end of the time course to ensure that all plated cells had been covered by the NIH 3T3 cells (Figure 5.1).

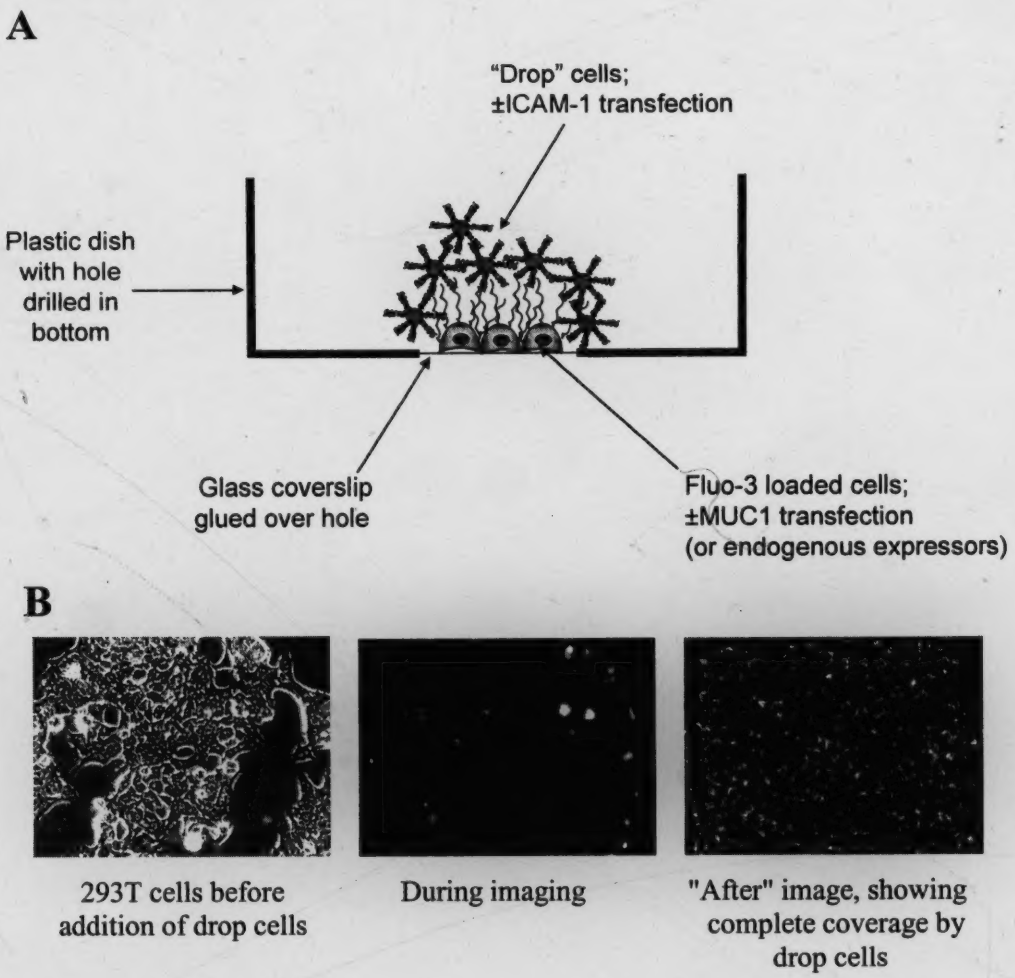

Figure 5.1: The calcium oscillation assay experimental set up. (A) Schematic diagram of the glass-bottomed dishes used for imaging. MUC1 expressing or transfected cells were adherent on the matrix-coated glass surface, and drop cells that did or did not express ICAM-1 were added during imaging. (B) Example photographs of MUC1-transfected 293T cells, taken before, during and after imaging.

5.1.5 Data Analysis

Using Metamorph software, the images taken for each test condition were built into a stack, and 40 random cells per condition were circled (circled areas = regions of interest, or ROI). The changes in average fluorescence intensity for each ROI were graphed over time and exported to MS Excel. Each condition was repeated at least 3 times, n = a minimum of 120.

MS Excel was used to plot the data and calculate the "Oscillation Factors" which are defined as the number of oscillation cycles multiplied by the "amplitude factor" for each ROI (Figure 5.2). The number of oscillation cycles was counted manually from the plotted data. The "amplitude factors" were calculated by plotting an Excel "LOGEST" trend line ($y = \text{intercept} \cdot \text{slope}^x$) from the start of the oscillatory portion of the data to the last recorded data point, then calculating the absolute value of the difference between the actual plotted data and the trend line and for each data point; the sum of these differences was defined as the amplitude factor.

5.1.6 Western Blotting

Cells were lysed in RIPA buffer (150mM NaCl, 1% NP40, 0.5% deoxycholic acid, 0.1% SDS, 5µl/mL Sigma-Aldrich Protease Inhibitor Cocktail, 50mM Tris pH 7.6 [169]) and subjected to shearing with a 26G needle. Insoluble materials were pelleted, and the supernatant was assessed for protein concentration using the BioRad DC Assay Kit. Equal amounts of protein for each test sample were loaded onto polyacrylamide gels. Resolved gels were transferred to Immobilon P or PSQ membranes and probed with B27.29 or CT2 antibodies, respectively, followed by a peroxidase conjugated secondary antibody. Specific labeling was visualized with ECL Plus, and imaged using a Typhoon 9400 Variable Mode Imager and ImageQuant 5.2 Software (Molecular Dynamics). Membranes were re-probed for tubulin as a loading control.

Oscillation Factor = number of oscillation cycles x "amplitude factor"

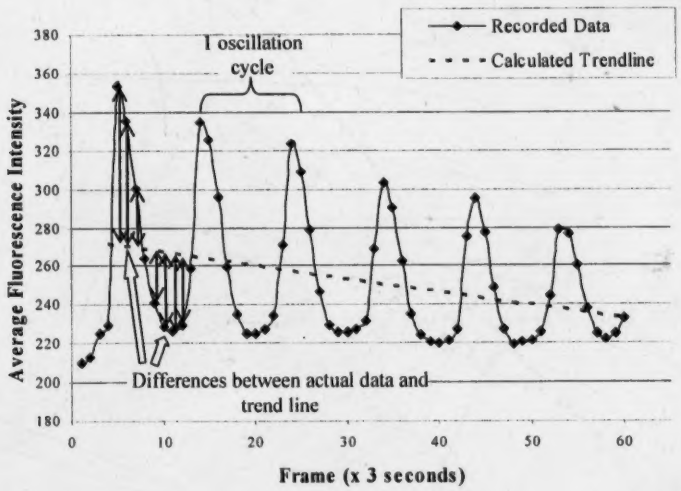

Trendline ➔ pre-programmed "LOGEST" function in Excel ➔ $y= b \cdot m^x$

Figure 5.2: The Oscillation Factor Calculation. The number of oscillation cycles was counted manually for each tracing. Single peaks with no obvious secondary increase in intracellular calcium were scored as zero. The amplitude factor was calculated by drawing an Excel LOGEST trendline through the data, beginning with the first oscillation, then summating the absolute values of the differences between the actual data points and the trendline. The frequency of oscillation was then multiplied by the amplitude factor, resulting in the oscillation factor. Based on [8].

5.1.7 Flow Cytometry

Cells were trypsinized, washed 1X in FBS-containing media, then divided into 3 aliquots, each of which was incubated with one of 2% BSA, 0.02% Tween 20 in Tris buffered saline (BTT, unlabeled control), 5μg/mL MOPC 31C in BTT (isotype control), or 5μg/mL B27.29 in BTT, on ice for 1 hour in a volume of 30μL. Cells were washed in a 50X volume of cold PBS, then resuspended in 30 μL BTT (unlabeled control) or 30μL of phycoerythrin secondary, 2μg/mL in BTT, for a further 1 hour, in the dark, on ice. Cells were again washed in a 50X volume of cold PBS, then resuspended in 300μL PBS, and treated with final concentrations of 120U/mL DNase I and 4.2mM $MgCl_2$, for 15 minutes at room temperature. Samples were stored at 4°C in the dark until analysed by flow cytometry. At least 10,000 events were recorded on the FL2 (phycoerythrin) channel. As the cells were chilled, unfixed and unpermeabilized, only surface MUC1 was stained.

5.1.8 Statistical Analysis

The Newman-Keuls multiple range comparison was used to determine statistical differences in data sets where there were more than two conditions. Otherwise, the Student's t-test was used.

5.2 Results

5.2.1 Human ICAM-1 Transfected NIH 3T3 Cells can Induce Calcium Oscillations in Human Breast Cancer Cell Lines

Using the adherent calcium oscillation assay, four human breast cancer cell lines were tested for their calcium-based oscillatory responses when exposed to NIH 3T3 ICAM-1 or mock transfected cells. Two of these, T47D and MCF-7 cells, showed statistically significant increases in the oscillatory response when exposed to ICAM-1 as opposed to mock transfectants (Figure 5.3A, t-test, $p = 2.6 \times 10^{-8}$ and 8.8×10^{-4}

respectively). When these cells were screened for relative levels of MUC1 expression by immunoblotting (Figure 5.3B), there was a correlation between the amount of cellular MUC1 expression and tendency to oscillate. This was strengthened by comparing the oscillation factors to surface expression of MUC1 as tested by flow cytometry analysis of cells stained without permeabilization (Figure 5.3C).

5.2.2 Human ICAM-1 Transfected NIH 3T3 Cells can Induce Calcium Oscillations in Human MUC1-Transfected 293T Cells

Figure 5.4A shows a schematic of the MUC1 construct used to transfect 293T cells. Five subclones, designated SYM, were shown to have a range of oscillatory responses on contact with NIH 3T3 ICAM-1 cells (Figure 5.4B). As seen with the endogenous MUC1 expressors, contact with NIH 3T3 ICAM-1 cells produced statistically higher responses in the subclones shown to be positive for MUC1 expression by immunoblotting, in comparison to when the cells were contacted by NIH 3T3 mock transfectants (Figure 5.4B, $p = 4.6x10^{-26}$, $1.4x10^{-14}$ and $1x10^{-16}$, respectively). With this set of cells, there does not appear to be a consistent trend between levels of MUC1 expression and intensity of oscillatory response, as SYM25 clearly expresses more MUC1 than SYM1, yet oscillates less. However, when these cells are analysed by flow cytometry without permeabilization (Figure 5.4D), the level of surface MUC1 on SYM1 was higher than that on SYM25. This suggests that only surface MUC1 is available for induction of the calcium oscillations, which is consistent with the idea that it must bind extracellular ICAM-1 in order for an oscillatory response to be generated. Supporting this idea, there appeared to be a correlation between surface MUC1 expression and oscillatory response (Figure 5.4E; $R^2=0.9946$). There does appear to be some cell specificity in terms of the level of response, as the SYM1 cells seem to express MUC1 at a lower level than the T47D or MCF-7 cells, yet have a much greater oscillatory response. There may also be a cell specific "threshold" of MUC1 expression needed in order for any measurable response to occur.

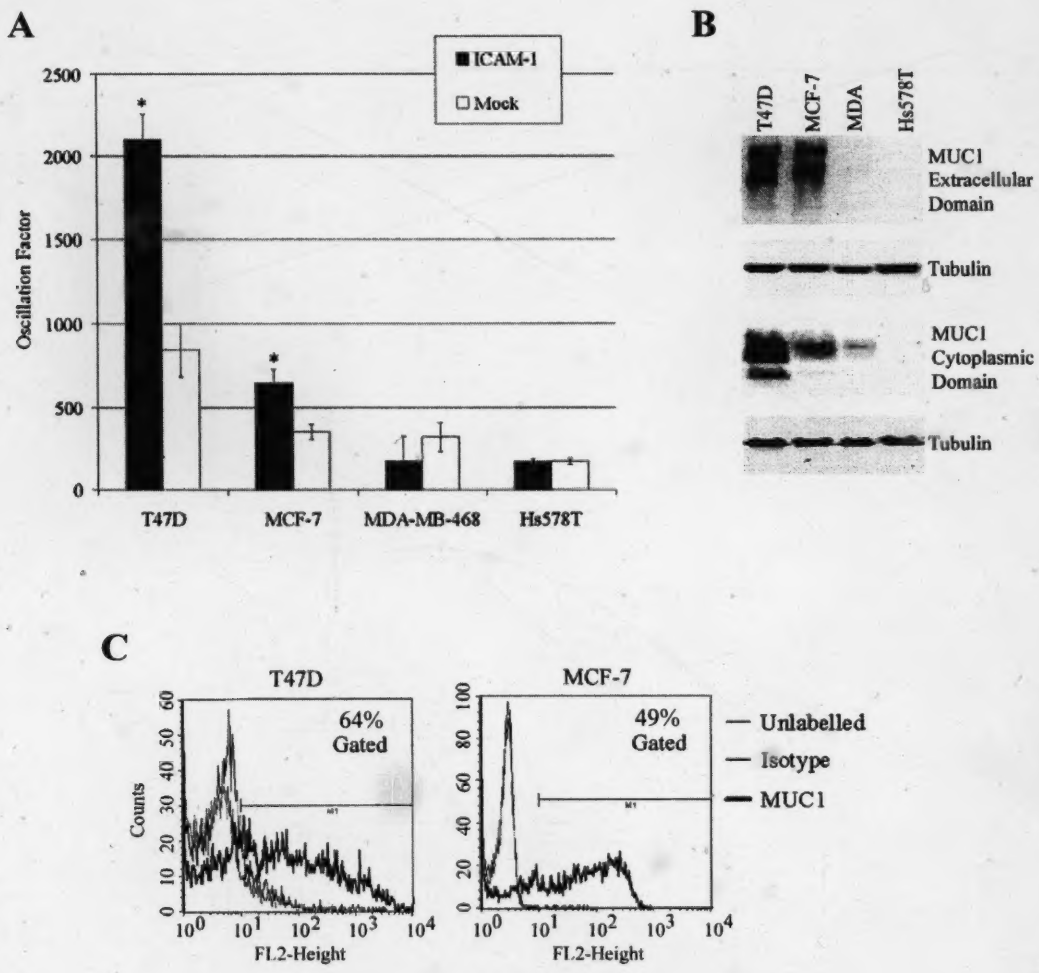

Figure 5.3: Contact with ICAM-1 expressing cells induces calcium oscillations in MUC1-expressing human breast cancer cell lines. (A) Mean oscillation factors ± SEM calculated for 120 individual cells from four cell lines derived from human breast cancers, after exposure to NIH 3T3 ICAM-1 or mock cells. Statistical differences (t-test) are denoted by an asterisk. (B) Western blots for total cellular expression of MUC1 in each cell line. (C) Flow cytometry measurements of surface MUC1 expression on cell lines displaying relatively high total cellular MUC1 expression. Based on [8].

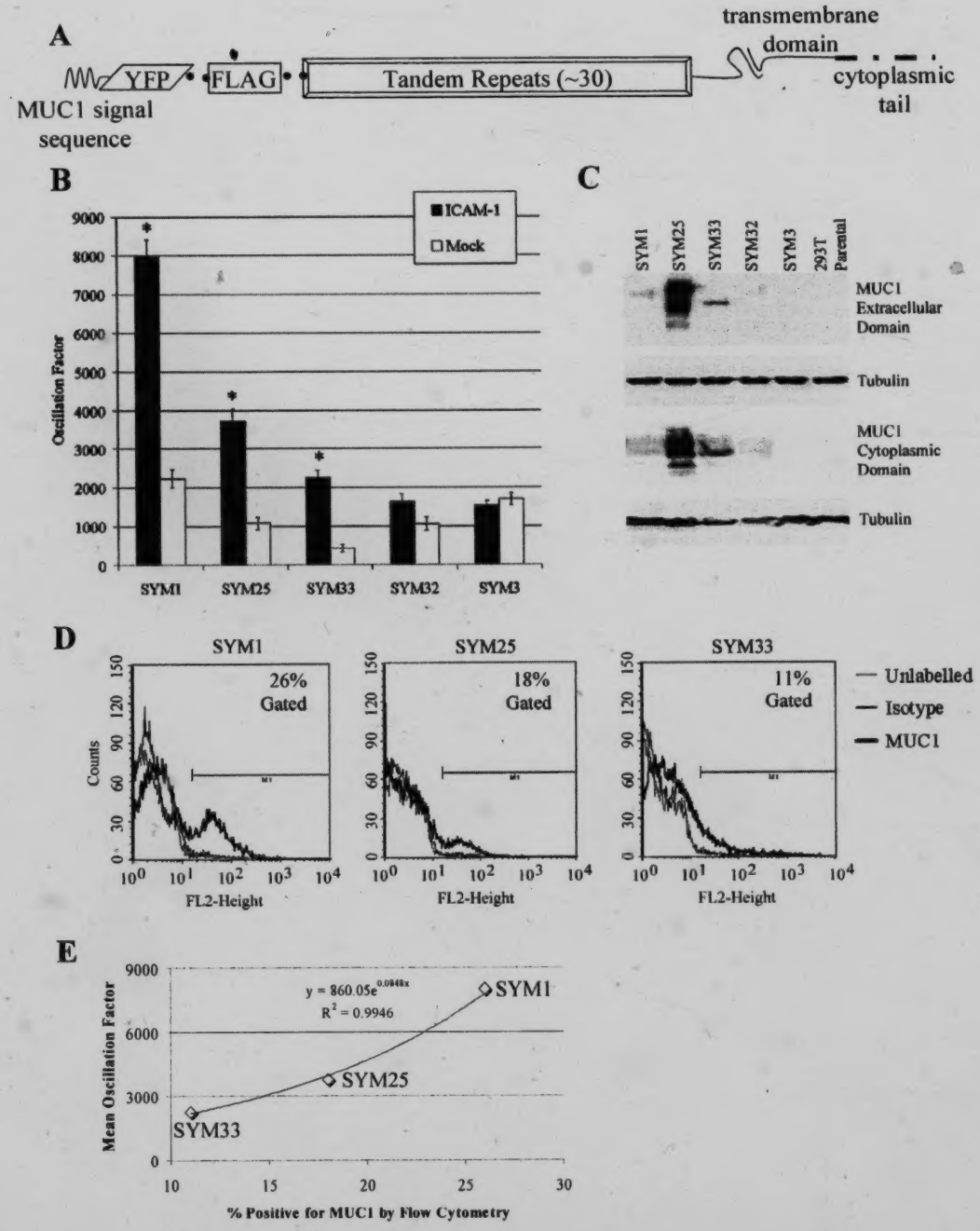

Figure 5.4: Contact with ICAM-1 expressing cells induces calcium oscillations in MUC1-expressing 293T transfectants. (A) Schematic of the SYM plasmid used for transfection. (B) Mean oscillation factors ± SEM calculated for 120 individual cells from five subclones of MUC1-transfected 293T cells. Statistical differences (t-test) are

Figure 5.4 Continued: denoted by an asterisk. (C) Western blots for total cellular expression of MUC1 in each subclone. (D) Flow cytometry measurements of surface MUC1 expression on subclones displaying relatively high total cellular MUC1 expression. (E) Exponential trendline fit of MUC1 surface expression on the SYM subclones when compared to oscillatory response. Based on [8].

5.2.3 Antibodies Against the MUC1 Extracellular Domain that are Known to Block Interaction with ICAM-1 can Diminish the Oscillatory Response

The cell types shown to have relatively high oscillatory responses to ICAM-1 were pre-treated with either an irrelevant antibody or B27.29, which is known to block the MUC1/ICAM-1 interaction [2,3]. In all three cell lines, SYM1, SYM25 and T47D, B27.29 pre-incubation resulted in a statistically significant drop in the oscillatory responses, while pre-incubation with an irrelevant antibody did not decrease the oscillatory response from that seen with untreated cells (Figure 5.5). In the SYM1 and SYM25 cells, the decrease matched the responses seen when NIH 3T3 mock cells were used, however in the T47D cells the decrease was intermediate.

5.2.4 MUC1 Positive Cells can Induce a Mild Oscillatory Response in HUVECs Stimulated with Cytokines Known to Upregulate ICAM-1 Expression

The calcium-based oscillatory response in HUVECs on contact with SYM1 cells, was typically not more than one cycle in cells that oscillated at all (Figure 5.6A). Results from cell to cell were markedly variable, and many cells demonstrated transient increases in intracellular calcium with no definite pattern. This was not unreasonable, as observed calcium oscillations were minimal when leukocytes were used to trigger calcium-based responses in HUVECs [202]. The results again suggested that both MUC1 and ICAM-1 were necessary to obtain a relatively high oscillation factor, as a MUC1-expressing transfectant (SYM1) had to be dropped on HUVECs pre-stimulated with 20U/mL each of TNF-α and IL-1β in order to obtain this result. If the HUVECs were not stimulated to upregulate their ICAM-1 expression, the results were similar to those seen when a non-MUC1 expressing transfectant was used as the drop cell (SYM3).

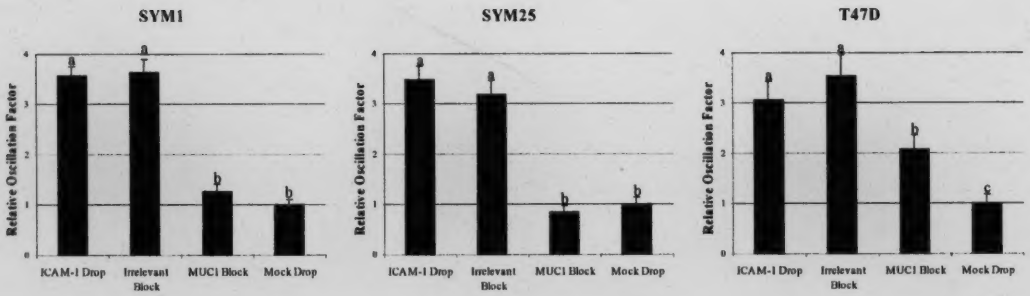

Figure 5.5: Antibody Blockade of the ICAM-1 binding site on the MUC1 molecule inhibits the calcium-based oscillatory response. Antibody blockade was performed on cells that demonstrated relatively high oscillatory responses. Cells were pre-treated either with an irrelevant or MUC1-blocking antibody, then exposed to NIH 3T3 ICAM-1 cells. Untreated cells exposed to NIH 3T3 ICAM-1 or mock cells are included for comparison. Data are normalized to the Mock Drop condition. Statistically distinct populations, as determined in the Newman-Keuls multiple range comparison, are denoted by lower case letters ($p = 0.01$ for SYM1 and SYM25, $p = 0.05$ for T47D). Based on [8].

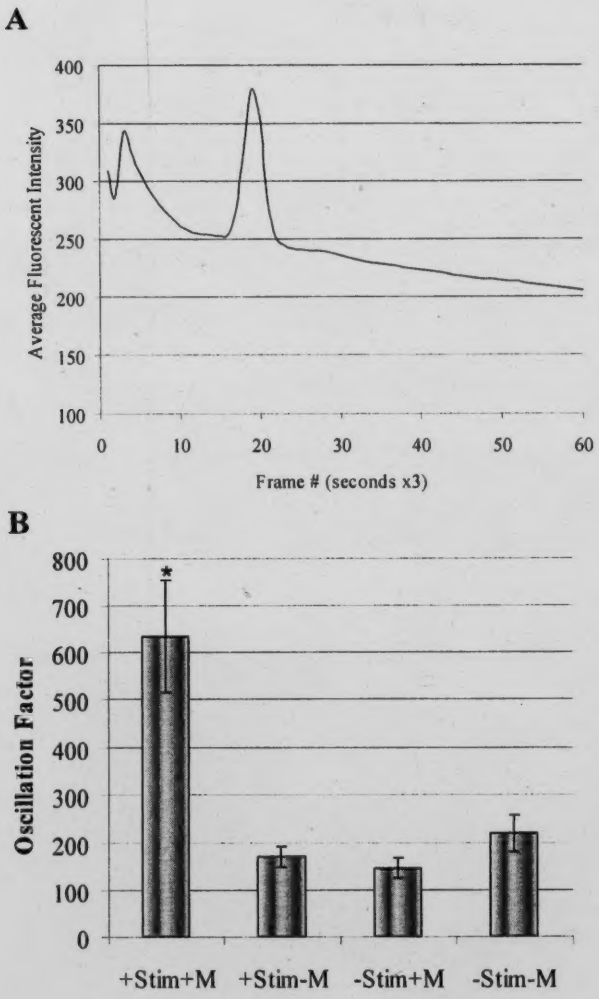

Figure 5.6: MUC1 positive cells can induce an ICAM-1 dependent, intracellular calcium-based response in HUVECs, with minor oscillations. (A) A typical oscillatory response seen in HUVECs showing one oscillation cycle. (B) A relatively high oscillation factor occurred in HUVECs only when the drop cells were MUC1 positive (+M), and the HUVECs were stimulated with 20U/mL each of TNF-α and IL-1β to upregulate ICAM-1 expression (+Stim). The asterisk indicates a data population that is statistically different from the other data according to the Newman-Keuls test.

5.3 Discussion

The data in earlier chapters have described the promoting effect that the presence and placement of MUC1 appeared to have on transendothelial migration. As the Transwell assay was performed under static conditions (i.e. not under shear stresses induced by fluid flow), it seemed unlikely that the increased levels of migration seen were due to increased adhesion, since all cells were in contact with the endothelial cells by gravity, and thus should have had equal opportunity to migrate. Furthermore, tumour cells migrated less through a gelatin-coated membrane, despite the presence of fibroblast conditioned media, as compared to a membrane plated specifically with ICAM-1 expressing cells, suggesting that the presence of an endothelial "barrier" was irrelevant, and ICAM-1 itself might be triggering the migration of the tumour cells by initiating a MUC1-based signal.

5.3.1 The MUC1/ICAM-1 Triggered Signal is Calcium Based, Oscillatory, Specific and Bi-Directional

The Fluo-3 measurements of intracellular calcium have demonstrated that on contact with ICAM-1 bearing cells, MUC1 positive cells exhibit calcium oscillations. This was different from calcium fluxes observed when either MUC1 or ICAM-1 was absent. In the latter scenario, the Fluo-3-loaded cells sometimes demonstrated shallow oscillations, or transient rises in intracellular calcium without oscillations, resulting in overall low oscillation factors. These may have been the result of the weight of the drop cells causing pressure-induced deformations of the cell membrane, as they were similar to "poke-induced" [268] calcium responses, which are characterised by a transient rise in intracellular calcium without oscillations. Thus the responses seen in the absence of MUC1 or ICAM-1 may have been non-specific.

Oscillations are strongly indicative of an intentional signal, rather than spurious fluctuations in intracellular calcium concentrations, which may occur from membrane leakage. Other reports have demonstrated that oscillations of specific frequency or amplitude can trigger the activation of particular kinases (e.g. calcium/calmodulin-

dependent kinase II) [269] or transcription factors [270]. In our study, the specificity of MUC1 and ICAM-1 in inducing the calcium oscillations was shown through the use of transfectants in factorial combinations, and by antibody blockade of MUC1.

The data also suggest that the MUC1/ICAM-1 interaction can initiate bi-directional signals; into a carcinoma cell via MUC1, and into an endothelial cell via ICAM-1. This pertains to metastasis at the point of tumour cell exit from the circulation by adhesion and subsequent migration through the endothelial lining, as calcium signals are expected to be necessary for tumour cell diapedesis and motility, as well as localised endothelial retraction. The ability of ICAM-1 to initiate a calcium signal in HUVECs has been previously described [201,202,271]. This appears to trigger endothelial retraction [206,208], which is generally believed to be part of the mechanism coupled to the tri-cellular corner phenomenon, wherein leukocytes are "guided" by a concentration of specific adhesion molecules, to tri-cellular corners of an endothelial monolayer, where the tight junctions are discontinuous [209,210]. Leukocytes are thus allowed to extravasate without compromising the integrity of the endothelial barrier to fluids or solutes.

It has also been shown that MCF-7 cells can induce a transient increase in endothelial cell intracellular calcium, and initiate localised retraction [203,204] much as leukocytes do [206], whereas normal mammary epithelial cells do not [204]. There are most likely several differences between normal mammary cells and MCF-7 cells, however as the reaction of the HUVECs is similar to that seen with antibody crosslinking of ICAM-1 [201], and MUC1 is a known ligand of ICAM-1 [2,3,57], it stands to reason that tumour-specific characteristics of the MUC1 on MCF-7 cells may be the cause of the observed differences in endothelial response. MUC1 on tumour cells as opposed to normal cells may differ in amount, membrane distribution [1] and glycosylation status [14,272,273], all of which may confer enhanced ability of MUC1 to bind endothelial ICAM-1. Thus, MUC1 may be involved at least partially in modulating signals transmitted into endothelial cells, perhaps by incorporation into different signalling platforms on the tumour cell, where it might bring a specific complement of adhesion molecules in close proximity to putative endothelial co-receptors.

5.3.2 Possible Signal Mediators and Downstream Targets

There are seven putative tyrosine phosphorylation sites in the MUC1 cytoplasmic tail, and some of these have already been shown to recruit Grb2/Sos [51] and src [48,143,147], which have been implicated in Ras/MAPK signalling. Activation of MAPK is a downstream result of MUC1 phosphorylation by EGFR [54], and has been shown to be involved in motility [68,249,274,275]. In the case of MUC1, a pro-migratory signal is more likely than a proliferative one, as Schroeder et al., showed that increased MAPK activation via MUC1 was not associated with increased activation of PCNA (proliferative cell nuclear antigen) [54]. Other work in our lab (thesis project of Qiang Shen, [8]) has shown that the calcium-based signal induced by MUC1 releases calcium from internal stores, and involves lipid rafts, phosphoinositol-3-kinase (PI3K), phospholipase C (PLC) and src, but not MAPK, as disruptors of lipid rafts or chemical inhibitors of all the signalling molecules except MAPK, could decrease the oscillatory responses in SYM1 cells. Therefore, it is possible that the MAPK and calcium-based responses are two separate signals that may work alternatively or in tandem to promote migration. We have been unable to show any clear relationship between calcium signalling and phosphorylation of the MUC1 cytoplasmic tail, whether one event is upstream of the other, or if they are mutually exclusive (thesis project of Danny Au).

Possible differences in membrane distribution of MUC1 is of particular interest, since it has recently been reported that MUC1 partitions into lipid rafts [251], and it is possible that in tumour cells it can partner with an entirely different set of signalling molecules as it might in normal cells.

One of our current hypotheses is that on ligation with ICAM-1, MUC1 undergoes a conformational shift which may allow it to partition into lipid rafts. Here, it may be brought into close proximity with src, which can associate with the unphosphorylated cytoplasmic domain of MUC1 via its SH3 domain [48]. Src can be upstream of both PI3K and PLC [276-278]. There is a possible PI3K binding site on the MUC1 cytoplasmic domain (Figure 1.6), and overexpression of MUC1 has been shown to activate the PI3K/Akt survival pathway [189]. Inhibition of PI3K with wortmannin [8] could still inhibit the MUC1/ICAM-1 induced calcium oscillations. PI3K generates the

membrane binding site for phospholipase C, by the conversion of PI(4,5)P to PI(3,4,5)P, which allows recruitment of phospholipase C to the membrane by its PH domain [279]. Although the PH domains of some isotypes of PLC, for example PLCδ_1, bind preferentially to phosphatidyl inositol (4,5) P_2 [280], it is PLCγ that many studies have implicated in tumour cell migration, through techniques such as dominant mutants or pharmacological inhibitors [181,281-284]. Activation of PLCγ appears to require three separate components: (i) binding to a receptor via its SH2 and SH3 domains, which may cause unfolding of the molecule, (ii) phosphorylation of specific tyrosine residues, and (iii) binding to phosphoinositol (3,4,5) P_3 [279,281,282]. This last requirement has suggested an absolute requirement for the activity of PI3K in PLCγ activation [281,282]. As MUC1 may have binding sites for PI3K, src and PLCγ (Figure 1.6), it may serve as scaffolding for the initiation of such a signal.

The role of PLC in this signal seems more apparent, as once it is activated by src, it can be expected to cleave PIP2 to diacylglycerol and IP3 (Figure 5.7, [285]), the latter being responsible for release of calcium from the endoplasmic reticulum. This, along with the observation that 2-APB, an inhibitor of calcium release from the endoplasmic reticulum, also prevented oscillations [8], suggested that the MUC1/ICAM-1 signal was dependent on internal calcium stores. The the recruitment of src may be to phosphorylate the MUC1 cytoplasmic tail and thereby recruit Grb2/Sos [48,51,143], which may subsequently activate MLCK through the Ras/ERK pathway [180]. This may be assisted by calcium activated calmodulin and calmodulin kinase II [286] (Figure 5.8).

MUC1-initiated signalling could also theoretically be involved in the regulation of calcium-sensitive proteins. Possible calcium regulated proteins involved in motility include: (i) gelsolin [287], which mediates depolymerisation of actin to allow remodelling, while (ii) troponin C [288,289] and calmodulin [263] which mediate activation of myosin light chain kinase and allow formation of myosin/actin crossbridges, and contraction of the cell body, and (iii) calpain [290], a protease known to cleave integrins, which would be needed to disassemble adhesions at the trailing edge of the cell (Figure 5.7).

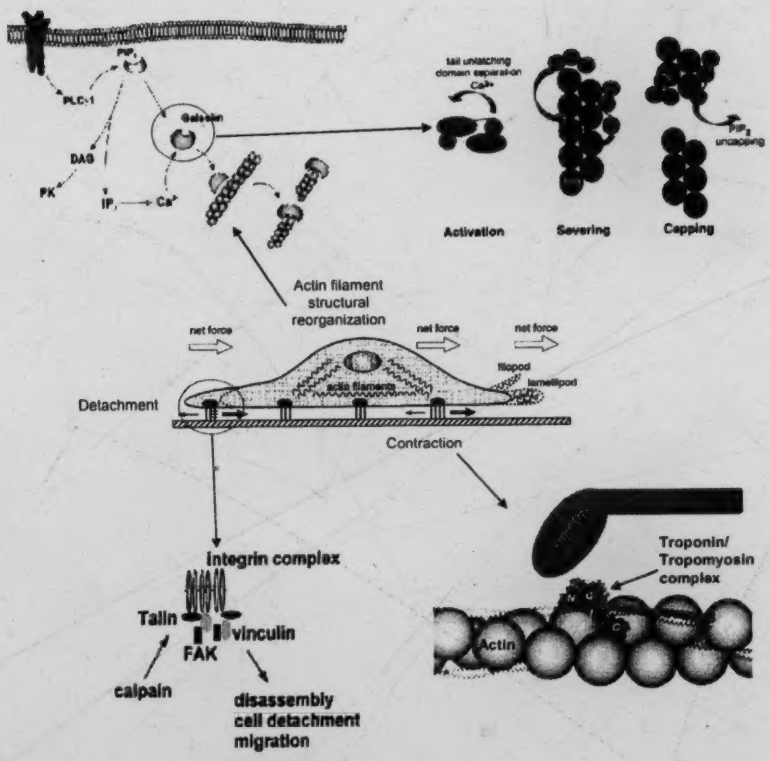

Figure 5.7: Schematic of selected calcium-sensitive migratory processes. On an appropriate extracellular signal, phospholipase C cleaves PIP2 in the plasma membrane. This can release sequestered gelsolin, and initiate release of calcium from the endoplasmic reticulum. Calcium binding to gelsolin induces a conformational change to its activated state, in which it can sever and cap actin monomers, allowing changes in cell shape. When PIP2 is regenerated, gelsolin releases actin monomers and is again sequestered at the membrane. Calcium also enables crossbridge formation between myosin and actin filaments via troponin C (TnC), and activation of calmodulin kinase, which phosphorylates myosin light chain kinase. With the hydrolysis of ATP, myosin and actin slide past each other, making the cell contract. Detachment of the trailing edge of the cell is facilitated by the calcium-sensitive protease, calpain, which digests integrins, allowing disassembly of focal adhesions. Based on [181,287,290,291] and http://www.le.ac.uk/biochem/mp84/ teaching/figures/camfig25.gif

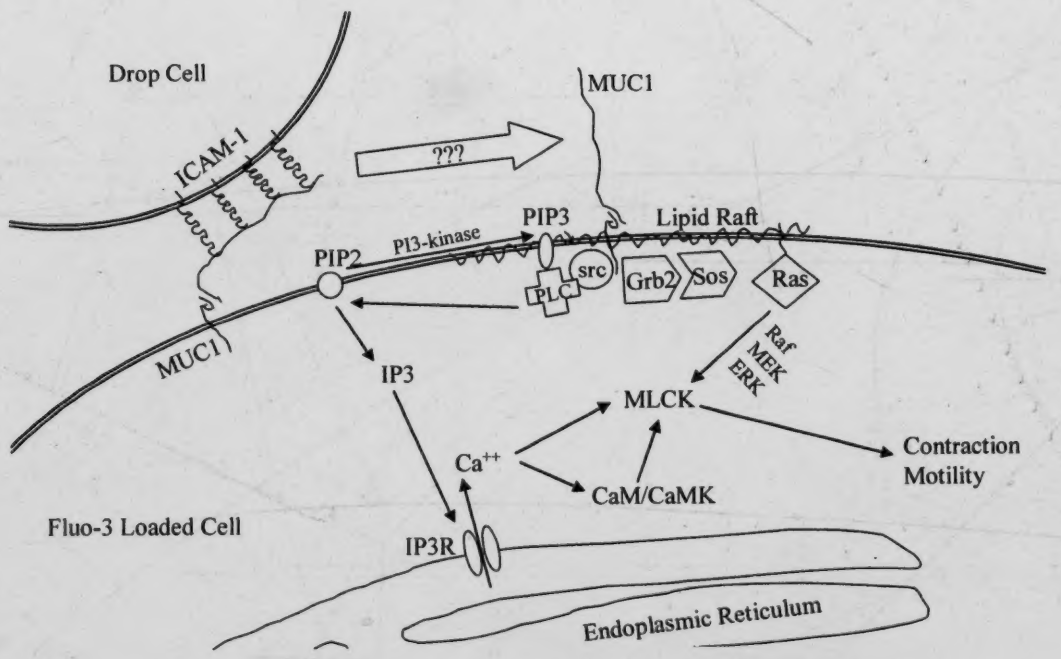

Figure 5.8: Schematic of how the MUC1/ICAM-1 initiated signal may occur. Binding of ICAM-1 to the tandem repeat domain of MUC1, may cause MUC1 to shift into lipid rafts, where it may come into contact with src, phospholipase C (PLC), Grb2/Sos and Ras. Inhibitors of src, PLC, PI-3-kinase and the inositol-3-phosphate receptor (IP3R) have confirmed their involvement in this signal. Although MUC1 is known to activate the MAPK pathway, inhibition of MAPK had no effect on calcium oscillations. This pathway may be parallel or complementary to the suggested pro-migratory signal.

5.3.3 Overview

The experiments presented in Chapter 3 (Transwell Data), showed that ICAM-1 could promote the migration of MUC1-positive cells. The data from this chapter shows that ICAM-1 can induce relatively strong calcium oscillations in MUC1-positive cells. Since calcium is frequently involved in pro-migratory signals, it appears that the MUC1/ICAM-1 signal is also involved in triggering cell motility. However, it would be unlikely that the MUC1/ICAM-1 interaction is the only co-receptor pairing involved in these processes. Muller et al., clearly implicated the CXCR4 and CCR7 cytokine receptors in the metastasis of blood-borne breast cancer cells to every preferred target organ except the brain [113]. Additionally, many tumour cell carbohydrate epitopes and adhesion molecules present on endothelial cells can be involved in tumour cell to endothelial cell interactions [112,292-297]. As such, the MUC1/ICAM-1 interaction must be part of a complex cascade of adhesions and signals that may be complementary or redundant in nature.

Chapter 6: Discussion

6.0 Thesis Overview

This thesis has focused on the extravasation step of the metastatic cascade. Vascular invasion is a bad prognostic indicator, as the circulation can provide tumour cells with access to the entire body. Colonization of secondary organs by carcinoma cells eventually leads to disruption of organ function and death. If the extravasation of tumour cells can be inhibited, this may not only delay the formation of secondary tumours, but may "trap" metastasizing tumour cells in a compartment that is easily accessible to chemotherapeutic agents.

The study objectives stated in the introduction of this thesis were:

i) To determine if a correlation exists between MUC1 localisation in clinical specimens and the propensity to metastasize

ii) To determine if MUC1 and ICAM-1 can co-localise *in vitro* during heterotypic interactions between cells expressing either MUC1 or ICAM-1

iii) To determine if the functional consequence of MUC1 expression in an environment where adjacent cells express ICAM-1 is the adoption of a migratory phenotype

iv) To determine if a specific microenvironmental context can impact the migratory behaviour of MUC1-expressing cells

v) To begin characterising the intracellular events within the MUC1 expressing cell that may connect the initiation of the putative ICAM-1 induced signal at the cell surface to the actual motility of the cell.

The clinical review in Chapter 2 contained data indicating a statistical correlation between MUC1 expression around the entire cell membrane, and the presence of nodal metastases [1], suggesting that depolarised expression of MUC1 at the plasma membrane may be indicative of a propensity of tumour cells to migrate.

The fluorescent microscopy data showed that MUC1 and ICAM-1 expressed on opposing cells could co-localise at sites of heterotypic cell-cell contact, however, with the exception of endogenously expressed ICAM-1, there was no convincing evidence that

these molecules were concentrated at these sites, and observed ICAM-1 capping was rare. Since we know that the MUC1/ICAM-1 interaction does occur [2,3,57], it may be that these interactions are transient, and/or trigger the recruitment of other co-receptor pairs.

MUC1 and ICAM-1 appeared to be of great importance in mediating TEM_E in our Transwell model. Increases in endothelial ICAM-1 expression correlated with increased TEM_E, and these increases could be abrogated by antibody blockade of either MUC1 or ICAM-1. Furthermore, 293T cells transfected with human MUC1 migrated more than transfectants that did not express the mucin.

The microenvironmental context also appeared to be significant in modulating TEM_E, as the addition of fibroblasts contributed in three different ways to the promotion of MCF-7 migration: i) they provided ICAM-1 on the underside of the Transwell membranes, ii) they acted synergistically with inflammatory cytokines to boost endothelial ICAM-1 expression on the upper surface of the Transwell membranes, and iii) they secreted a factor that acted on the MCF-7 cells to change their surface expression of β1-integrins. Although the functional consequence of this phenotypic change was not fully investigated in this thesis, the change appears to be at least partly consistent with clinical specimens exhibiting migratory behaviour [260,298].

Finally, the signalling event connecting the MUC1/ICAM-1 interaction at the cell surface with the change to a migratory phenotype was identified as being calcium-based. Although much work remains to fully characterise this signalling pathway, calcium is a known mediator of cell motility [181,285]. Experiments to demonstrate that the MUC1/ICAM-1 interaction can induce cytoskeletal changes are underway (thesis project of Qiang Shen).

6.1 Properties of MUC1 that May be Related to Metastasis

6.1.1 Distribution

Expression of MUC1 at the plasma membrane, or surface MUC1, appears to be important in two ways. First, "circumferential" staining correlated with nodal metastases in clinical samples (Chapter 2; [1]), and surface MUC1 was also required for initiation of

the calcium-based signal, as SYM25 cells, although having higher overall MUC1 expression in comparison to SYM1 cells, had lower surface MUC1, and a lower oscillation factor (Chapter 5; [8]). Our current hypothesis surrounding these observations is that surface MUC1 that is not apically restricted is ideally positioned to interact with ICAM-1 on adjacent cells, and may have access to signalling partners it would normally be sequestered from, thus triggering what we suggest is a pro-migratory signal.

Other explanations include the possibility that depolarised MUC1 may contact and disrupt the E-Cadherin/β-catenin complex [44,45,50], or alter integrin/matrix adhesions [43,55]. Current literature reports seem to attribute this ability to the cytoplasmic domain of MUC1 rather than the extracellular domain. The importance of disrupting the E-Cadherin/β-catenin complex in breast cancer is unclear for three reasons; i) in our clinical review, in cases where we saw co-distribution of MUC1 and β-catenin, E-cadherin was always present, ii) when E-cadherin was not present (lobular carcinomas), MUC1 and β-catenin still did not show a preference for co-distribution, and iii) ductal carcinomas still metastasize as emboli, despite having apparently intact E-cadherin at the cell membranes.

Finally, depolarisation of MUC1 may be indicative of cell status, and one of the first signs that genetic changes have occurred which are causing de-differentiation. The MUC1-mediated events are probably occurring secondarily.

The significance of cytoplasmically distributed MUC1 is also still unclear. Although this staining pattern was clinically associated with a lowered probability of survival, we found that this distribution of MUC1, as represented by the SYM25 cell line, was associated with lower calcium-based signalling, which we are proposing is a pro-migratory signal. One possible explanation is that such cells have other altered characteristics that make them unable to respond to growth control or polarisation signalling. Whether such a state may be induced by the accumulation of cytoplasmic MUC1 remains an open question.

Also not explained, is the significance of the MUC1 cytoplasmic tail in the nuclei of breast cancers. Other reports have suggested that MUC1 may be capable of shuttling β-catenin into the nucleus [184,185,299], however, we were unable to demonstrate this [1,186]. This may suggest that MUC1 is capable of entering the nucleus on its own, or it

may be able to shuttle molecules other than β-catenin. As the observation of the MUC1 cytoplasmic tail in the nuclei of breast cancers was only made twice, we have insufficient information for further speculation.

6.1.2 Adhesion and Dysadhesion

The steric hindrance theory of MUC1 function suggested that the extreme length of this rigid mucin sterically blocked other adhesion molecules from reaching their receptors [39,43,44]. This theory was already questionable (please see Section 1.2.3.3), and the Transwell data seems to add to its being unlikely. There was no evidence that increased MUC1 expression, in either our clinical samples or cell lines, lead to dysaggregation of tumour masses. Furthermore, if MUC1 were blocking integrin/matrix adhesion, then the addition of an antibody against the MUC1 tandem repeat domain (mAb B27.29), should have theoretically capped MUC1, allowing the integrins to be exposed, and perhaps more cells should have migrated to the undersides of the Transwell membranes. Instead, B27.29 inhibited MCF-7 cell migration (Chapter 3). It is entirely possible that the interaction of the native MUC1 protein with integrins may be regulated by its size and glycosylations, limiting contact of the MUC1 CT with either lateral membrane signalling complexes, for example focal adhesions, that may contain motility signalling partners. Baruch et al. have shown that MUC1/Y is clearly upregulated in tumour tissue, and is distinctly more tumourigenic in mice than the full length protein [154]. This raises the possibility that the shorter isoform may not be as inhibited in diffusing, or otherwise shifting through the membrane, and may be more readily able to contact focal adhesions and reduce binding to the matrix proteins, as it lacks both the long tandem repeat region, and all the accompanying glycosylations. Correspondingly, full-length MUC1 may also have similar properties upon shedding the extracellular domain, or acquiring depolarised localisation.

Thus, MUC1 appears to be an adhesive molecule with much more than passive involvement. Contrary to the negative repulsion or steric hindrance theories, it can mediate firm adhesion of tumour cells to the endothelium by binding to ICAM-1, and initiate events to promote transmigration.

6.1.3 Signalling

MUC1 has been found in lipid rafts [251], which are currently thought to be signalling platforms, where the scaffolding of signalling complexes stands ready, with perhaps a key element for signal initation missing (reviewed in [300]). When an appropriate stimulus is applied, certain proteins that had remained sequestered from these platforms are released, relocated to the lipid rafts, and the signal occurs.

Early experimentation in this lab has suggested that MUC1 does not partition preferentially into lipid rafts, but is found in both raft and non-raft fractions (work of Qiang Shen), however, certain molecules such as src may be recruited to MUC1-containing rafts after stimulation with ICAM-1. This notion was strengthened by the observation that PP2, a src inhibitor, and methyl-β-cyclodextrin, a lipid raft disruptor, could lessen the oscillatory calcium signal [8]. Thus, our current hypothesis is that on contact with ICAM-1, a specific population of MUC1 partitions into lipid rafts, where it complexes with src and PLC to initiate the calcium signal (Figure 5.8). Alternately, since the fluorescence microscopy data did not show any apparent shifts of MUC1 on contact with ICAM-1 positive cells, ICAM-1 may trigger the calcium oscillations from MUC1 that is already present in lipid rafts.

We do not yet know the contribution of tyrosine phosphorylation of the MUC1 cytoplasmic tail in this signalling modality. It may be involved in a completely different signal, a complementary one, or a redundant one. Site-directed mutagenesis experiments are currently underway to determine which tyrosine residues, if any, are significant in the MUC1/ICAM-1 initiated calcium signal (work of Qiang Shen).

6.2 Possible Contributions of Endothelial and Stromal Cells to Metastasis

Several reports indicate that mechanical entrapment is not necessary for tumour cell adhesion to the vasculature, and that tumour cells do adhere to vessels of larger diameter than the circulating cells or emboli [6,7,114]. Tumour cells may undergo a series of weak adhesions which allow them to roll along the vasculature, much in the same way leukocytes do, before becoming firmly adhered or arrested on the endothelium

[122,292]. There appears to be some controversy over whether extravasation automatically occurs for all tumour cells, or is a selective process [114-116]. Regardless, without TEM_E, or some other method of exiting the circulation, colonisation of secondary organs is unlikely to occur.

Transendothelial migration appears to be a cooperative process between malignant and normal cells. MCF-7 cells have been shown to cause endothelial retraction [203], which is also induced by leukocytes, and is a result of ICAM-1 based calcium signalling [201-204,206,208]. Thus, any cell expressing an ICAM-1 ligand may have the potential to coordinate their extravasation with endothelial cells. Since our data suggests that MUC1 can indeed trigger an endothelial calcium flux in ICAM-1-expressing HUVECs (Chapter 5), it may be that any breast cancer cell expressing MUC1 on its surface should be able to exit the vasculature by this method. Additionally, our data suggests that the endothelial cells contribute to metastasis by providing an ICAM-1 mediated pro-migratory signal.

Fibroblasts also have a significant contribution to TEM_E, which appears to be heavily dependent on their ability to increase ICAM-1 expression along the migratory track, by expressing it on their own cell body, and increasing its expression on endothelial cells (Chapter 3). In our particular model system, this appeared to have a greater impact than the other known ways in which fibroblasts can induce carcinoma cell migration, namely the secretion of fibronectins and matrix metalloproteases. In our developmental data (Appendix II, Figure AppII.5) the physical presence of fixed fibroblasts had a greater effect on MCF-7 cell migration than "conditioning" the matrix with fibroblasts. Also, in the final assay configuration the matrix would have provided very little resistance to tumour cell migration, as it consisted of a thin coating of 0.1% gelatin. Despite this, tumour cell migration through the gelatin alone was very low, and high migratory responses required high levels of ICAM-1.

Fibroblasts are known to secrete factors that can promote tumour cell proliferation and migration, such as bFGF and HGF [252,301,302]. These were not considered as possible explanations for the increases in TEM_E observed in the Transwell experiments, since fibroblast conditioned media by itself did not appear to have chemotactic properties within the duration of the assay (Figure 3.6). Any effects the fibroblast secreted factors

may have had on MCF-7 proliferation appeared to be irrelevant; there was no evidence that increased proliferation corresponded to increased migration (Figure 3.6), and despite tumour cells always being added in excess, only about 9% of them ever migrated (Table 3.2). This may be an indication of the vast heterogeneity that may be present even in an established cell line.

The combination of fibroblast secreted factors and ICAM-1 also had the greatest effect in lowering β1-integrin surface expression on the MCF-7 cells. In Chapter 4 it was speculated tumour cells may use this as a mechanism to escape anoikis. Alternately, the fibroblasts and ICAM-1 may produce this effect on normal epithelial cells as part of the epithelial-to-mesenchymal transition that occurs during wound healing. That it may also occur around a tumour, perhaps during the desmoplastic reaction, or in response to tumour cell adhesion to the endothelium, may be an example of how healthy, normal tissues inadvertently cooperate in the metastatic process.

6.3 Relative Importance of the MUC1/ICAM-1 Interaction to Metastasis

The MUC1/ICAM-1 interaction has been demonstrated to have a significant impact on TEM_E in this thesis. It also shows that TEM_E is to a large extent similar to leukocyte extravastion, which may offer partial or complementary explanation as to why anti-inflammatory drugs such as NSAIDs reportedly delay the onset of secondary tumour formation [303-305]. In addition to inhibiting cyclooxygenases, which can promote tumour growth, NSAIDs can also downregulate ICAM-1 expression [306,307].

Although it has been suggested that the MUC1/ICAM-1 triggered calcium oscillations lead to increased TEM_E, there are scenarios that are not explained by this hypothesis. For example, cytoplasmic distribution of MUC1 is prognostically bad, yet in Chapter 5, it appeared that cells which did not have MUC1 on the surface could not trigger this signal on contact with ICAM-1-bearing cells. Additionally, many cell types with low or null MUC1 expression still show high levels of migration through Transwells, for example, MDA-MB-231 cells [308,309]. Considering that there are many other known mediators of cell migration, such as EGFR [181] and CXCR4 [310], it may be that the MUC1/ICAM-1 interaction contributes in part to TEM_E, or is only

relevant in certain breast cancers. Also, not all of the MCF-7 cells migrated (~9%, Table 3.2), even after 24 hours exposure to elements identified as pro-migratory. It is likely that there must be a shift in the balance of signals a cell will receive before it will migrate. Alternately, the expression levels of MUC1 can be heterogenous in a given cell line or population (Chapter 2), thus only a subset of the cells added to the Transwell assay may have been able to respond. Regardless, only a few cells need to successfully metastasize in order for the disease to progress.

6.4 Closing Remarks

The work in this thesis has demonstrated that tumour-to-endothelial cell adhesion mediated by the MUC1/ICAM-1 interaction is followed by TEM_E mediated by the same co-receptor pair. We have also found that the microenvironment has a significant impact on TEM_E via its influence on the expression of ICAM-1 and β1-integrins on endothelial and tumour cells, respectively. A novel, calcium-based signal has also been identified, which may link the MUC1/ICAM-1 binding event on the tumour cell surface to the functional, migratory response.

It stands to reason that the MUC1/ICAM-1 signal is one that exists for a specific purpose, however, as with many phenomena in cancer, it may be a process that is opportunistically 'hijacked' by tumour cells to promote the disease state. Understanding the MUC1/ICAM-1 signal is part of understanding the mechanisms of cancer spread, and may finally provide explanation of why aberrant MUC1 levels and distribution is so frequently observed in tumours that have metastasized.

References:

1. Rahn JJ, Dabbagh L, Pasdar M, Hugh JC: **The importance of MUC1 cellular localization in patients with breast carcinoma: an immunohistologic study of 71 patients and review of the literature**. *Cancer* 2001, **91**:1973-1982.
2. Regimbald LH, Pilarski LM, Longenecker BM, Reddish MA, Zimmermann G, Hugh JC: **The breast mucin MUCI as a novel adhesion ligand for endothelial intercellular adhesion molecule 1 in breast cancer**. *Cancer Res* 1996, **56**:4244-4249.
3. Kam JL, Regimbald LH, Hilgers JH, Hoffman P, Krantz MJ, Longenecker BM, Hugh JC: **MUC1 synthetic peptide inhibition of intercellular adhesion molecule-1 and MUC1 binding requires six tandem repeats**. *Cancer Res* 1998, **58**:5577-5581.
4. Kuby J: *Immunology* edn 3rd. New York: W.H. Freeman; 1997.
5. Horne G: **The Role of Breast Cancer Associated MUC1 in Tumor Cell Recruitment to Vascular Endothelium During Physiological Fluid Flow. [Masters Thesis]**. Edmonton, AB: University of Alberta: 1999.
6. Glinskii OV, Huxley VH, Turk JR, Deutscher SL, Quinn TP, Pienta KJ, Glinsky VV: **Continuous real time ex vivo epifluorescent video microscopy for the study of metastatic cancer cell interactions with microvascular endothelium**. *Clin Exp Metastasis* 2003, **20**:451-458.
7. Glinsky VV, Glinsky GV, Glinskii OV, Huxley VH, Turk JR, Mossine VV, Deutscher SL, Pienta KJ, Quinn TP: **Intravascular metastatic cancer cell homotypic aggregation at the sites of primary attachment to the endothelium**. *Cancer Res* 2003, **63**:3805-3811.
8. Rahn JJ, Shen Q, Mah BK, Hugh JC: **MUC1 initiates a calcium signal after ligation by intercellular adhesion molecule-1**. *J Biol Chem* 2004, **279**:29386-29390.
9. Apostolopoulos V, McKenzie IF: **Cellular mucins: targets for immunotherapy**. *Crit Rev Immunol* 1994, **14**:293-309.
10. Bieche I, Lidereau R: **A gene dosage effect is responsible for high overexpression of the MUC1 gene observed in human breast tumors**. *Cancer Genet Cytogenet* 1997, **98**:75-80.
11. Bon GG, van Kamp GJ, Verstraeten RA, von Mensdorff-Pouilly S, Hilgers J, Kenemans P: **Quantification of MUC1 in breast cancer patients. A method comparison study**. *Eur J Obstet Gynecol Reprod Biol* 1999, **83**:67-75.
12. Croce MV, Colussi AG, Price MR, Segal-Eiras A: **Expression of tumour associated antigens in normal, benign and malignant human mammary epithelial tissue: a comparative immunohistochemical study**. *Anticancer Res* 1997, **17**:4287-4292.
13. Croce MV, Isla-Larrain MT, Rua CE, Rabassa ME, Gendler SJ, Segal-Eiras A: **Patterns of MUC1 tissue expression defined by an anti-MUC1 cytoplasmic tail monoclonal antibody in breast cancer**. *J Histochem Cytochem* 2003, **51**:781-788.
14. Ciborowski P, Finn OJ: **Non-glycosylated tandem repeats of MUC1 facilitate attachment of breast tumor cells to normal human lung tissue and**

immobilized extracellular matrix proteins (ECM) in vitro: potential role in metastasis. *Clin Exp Metastasis* 2002, **19**:339-345.

15. Burchell J, Taylor-Papadimitriou J: **Effect of modification of carbohydrate side chains on the reactivity of antibodies with core-protein epitopes of the MUC1 gene product.** *Epithelial Cell Biol* 1993, **2**:155-162.
16. Ho JJ, Cheng S, Kim YS: **Access to peptide regions of a surface mucin (MUC1) is reduced by sialic acids.** *Biochem Biophys Res Commun* 1995, **210**:866-873.
17. Brockhausen I, Yang JM, Burchell J, Whitehouse C, Taylor-Papadimitriou J: **Mechanisms underlying aberrant glycosylation of MUC1 mucin in breast cancer cells.** *Eur J Biochem* 1995, **233**:607-617.
18. Poland PA, Kinlough CL, Rokaw MD, Magarian-Blander J, Finn OJ, Hughey RP: **Differential glycosylation of MUC1 in tumors and transfected epithelial and lymphoblastoid cell lines.** *Glycoconj J* 1997, **14**:89-96.
19. Spicer AP, Duhig T, Chilton BS, Gendler SJ: **Analysis of mammalian MUC1 genes reveals potential functionally important domains.** *Mamm.Genome* 1995, **6**:885-888.
20. Ding L, Lalani EN, Reddish M, Koganty R, Wong T, Samuel J, Yacyshyn MB, Meikle A, Fung PY, Taylor-Papadimitriou J, et al.: **Immunogenicity of synthetic peptides related to the core peptide sequence encoded by the human MUC1 mucin gene: effect of immunization on the growth of murine mammary adenocarcinoma cells transfected with the human MUC1 gene.** *Cancer Immunol Immunother* 1993, **36**:9-17.
21. Apostolopoulos V, Pietersz GA, Xing PX, Lees CJ, Michael M, Bishop J, McKenzie IF: **The immunogenicity of MUC1 peptides and fusion protein.** *Cancer Lett* 1995, **90**:21-26.
22. Kontani K, Taguchi O, Ozaki Y, Hanaoka J, Sawai S, Inoue S, Abe H, Hanasawa K, Fujino S: **Dendritic cell vaccine immunotherapy of cancer targeting MUC1 mucin.** *Int J Mol Med* 2003, **12**:493-502.
23. Mukherjee P, Madsen CS, Ginardi AR, Tinder TL, Jacobs F, Parker J, Agrawal B, Longenecker BM, Gendler SJ: **Mucin 1-specific immunotherapy in a mouse model of spontaneous breast cancer.** *J Immunother* 2003, **26**:47-62.
24. Holmberg LA, Sandmaier BM: **Theratope vaccine (STn-KLH).** *Expert Opin Biol Ther* 2001, 1:881-891.
25. Miles DW, Taylor-Papadimitriou J: **Therapeutic aspects of polymorphic epithelial mucin in adenocarcinoma.** *Pharmacol Ther* 1999, **82**:97-106.
26. Akagi J, Hodge JW, McLaughlin JP, Gritz L, Mazzara G, Kufe D, Schlom J, Kantor JA: **Therapeutic antitumor response after immunization with an admixture of recombinant vaccinia viruses expressing a modified MUC1 gene and the murine T-cell costimulatory molecule B7.** *J Immunother* 1997, **20**:38-47.
27. Watanabe H: **Significance of mucin on the ocular surface.** *Cornea* 2002, **21**:S17-22.
28. Yoon JH, Park IY: **Mucin gene expression and mucin secretion in human airway epithelium.** *Rhinology* 1998, **36**:146-152.
29. Patton S, Gendler SJ, Spicer AP: **The epithelial mucin, MUC1, of milk, mammary gland and other tissues.** *Biochim Biophys Acta* 1995, **1241**:407-423.

30. Van Klinken BJ, Dekker J, Buller HA, Einerhand AW: **Mucin gene structure and expression: protection vs. adhesion**. *Am J Physiol* 1995, **269**:G613-627.
31. Gum JR, Jr.: **Mucin genes and the proteins they encode: structure, diversity, and regulation**. *Am J Respir Cell Mol Biol* 1992, **7**:557-564.
32. Carraway KL, Hull SR: **Cell surface mucin-type glycoproteins and mucin-like domains**. *Glycobiology* 1991, **1**:131-138.
33. Snyder JD, Walker WA: **Structure and function of intestinal mucin: developmental aspects**. *Int Arch Allergy Appl Immunol* 1987, **82**:351-356.
34. Clamp JR, Creeth JM: **Some non-mucin components of mucus and their possible biological roles**. *Ciba Found Symp* 1984, **109**:121-136.
35. Patton S: **MUC1 and MUC-X, epithelial mucins of breast and milk**. *Adv Exp Med Biol* 2001, **501**:35-45.
36. Spicer AP, Duhig T, Chilton BS, Gendler SJ: **Analysis of mammalian MUC1 genes reveals potential functionally important domains**. *Mamm Genome* 1995, **6**:885-888.
37. Soler M, Desplat-Jego S, Vacher B, Ponsonnet L, Fraterno M, Bongrand P, Martin JM, Foa C: **Adhesion-related glycocalyx study: quantitative approach with imaging-spectrum in the energy filtering transmission electron microscope (EFTEM)**. *FEBS Lett* 1998, **429**:89-94.
38. Hilkens J: **Episialin/CA15-3: its structure and involvement in breast cancer progression**. *Ned Tijdschr Klin Chem* 1995, **20**:293-298.
39. Hilkens J, Vos HL, Wesseling J, Boer M, Storm J, van der Valk S, Calafat J, Patriarca C: **Is episialin/MUC1 involved in breast cancer progression?** *Cancer Lett* 1995, **90**:27-33.
40. Hayes DF, Silberstein DS, Rodrique SW, Kufe DW: **DF3 antigen, a human epithelial cell mucin, inhibits adhesion of eosinophils to antibody-coated targets**. *J Immunol* 1990, **145**:962-970.
41. van de Wiel-van Kemenade E, Ligtenberg MJ, de Boer AJ, Buijs F, Vos HL, Melief CJ, Hilkens J, Figdor CG: **Episialin (MUC1) inhibits cytotoxic lymphocyte-target cell interaction**. *J Immunol* 1993, **151**:767-776.
42. Hilkens J, Wesseling J, Vos HL, Storm J, Boer B, van der Valk SW, Maas MC: **Involvement of the cell surface-bound mucin, episialin/MUC1, in progression of human carcinomas**. *Biochem Soc Trans* 1995, **23**:822-826.
43. Wesseling J, van der Valk SW, Vos HL, Sonnenberg A, Hilkens J: **Episialin (MUC1) overexpression inhibits integrin-mediated cell adhesion to extracellular matrix components**. *J Cell Biol* 1995, **129**:255-265.
44. Wesseling J, van der Valk SW, Hilkens J: **A mechanism for inhibition of E-cadherin-mediated cell-cell adhesion by the membrane-associated mucin episialin/MUC1**. *Mol Biol Cell* 1996, **7**:565-577.
45. Kondo K, Kohno N, Yokoyama A, Hiwada K: **Decreased MUC1 expression induces E-cadherin-mediated cell adhesion of breast cancer cell lines**. *Cancer Res* 1998, **58**:2014-2019.
46. Wreschner DH, Zrihan-Licht S, Baruch A, Sagiv D, Hartman ML, Smorodinsky N, Keydar I: **Does a novel form of the breast cancer marker protein, MUC1, act as a receptor molecule that modulates signal transduction?** *Adv Exp Med Biol* 1994, **353**:17-26.

47. Zrihan-Licht S, Baruch A, Elroy-Stein O, Keydar I, Wreschner DH: **Tyrosine phosphorylation of the MUC1 breast cancer membrane proteins. Cytokine receptor-like molecules**. *FEBS Lett* 1994, **356**:130-136.
48. Li Y, Kuwahara H, Ren J, Wen G, Kufe D: **The c-Src tyrosine kinase regulates signaling of the human DF3/MUC1 carcinoma-associated antigen with GSK3 beta and beta-catenin**. *J Biol Chem* 2001, **276**:6061-6064.
49. Ren J, Li Y, Kufe D: **Protein kinase C delta regulates function of the DF3/MUC1 carcinoma antigen in beta-catenin signaling**. *J Biol Chem* 2002, **277**:17616-17622.
50. Yamamoto M, Bharti A, Li Y, Kufe D: **Interaction of the DF3/MUC1 breast carcinoma-associated antigen and beta-catenin in cell adhesion**. *J Biol Chem* 1997, **272**:12492-12494.
51. Pandey P, Kharbanda S, Kufe D: **Association of the DF3/MUC1 breast cancer antigen with Grb2 and the Sos/Ras exchange protein**. *Cancer Res* 1995, **55**:4000-4003.
52. Meerzaman D, Xing PX, Kim KC: **Construction and characterization of a chimeric receptor containing the cytoplasmic domain of MUC1 mucin**. *Am J Physiol Lung Cell Mol Physiol* 2000, **278**:L625-629.
53. Meerzaman D, Shapiro PS, Kim KC: **Involvement of the MAP kinase ERK2 in MUC1 mucin signaling**. *Am J Physiol Lung Cell Mol Physiol* 2001, **281**:L86-91.
54. Schroeder JA, Thompson MC, Gardner MM, Gendler SJ: **Transgenic MUC1 interacts with epidermal growth factor receptor and correlates with mitogen-activated protein kinase activation in the mouse mammary gland**. *J Biol Chem* 2001, **276**:13057-13064.
55. Schroeder JA, Adriance MC, Thompson MC, Camenisch TD, Gendler SJ: **MUC1 alters beta-catenin-dependent tumor formation and promotes cellular invasion**. *Oncogene* 2003, **22**:1324-1332.
56. Fontenot JD, Tjandra N, Bu D, Ho C, Montelaro RC, Finn OJ: **Biophysical characterization of one-, two-, and three-tandem repeats of human mucin (muc-1) protein core**. *Cancer Res.* 1993, **53**:5386-5394.
57. Hayashi T, Takahashi T, Motoya S, Ishida T, Itoh F, Adachi M, Hinoda Y, Imai K: **MUC1 mucin core protein binds to the domain 1 of ICAM-1**. *Digestion* 2001, **63 Suppl 1**:87-92.
58. McDermott KM, Crocker PR, Harris A, Burdick MD, Hinoda Y, Hayashi T, Imai K, Hollingsworth MA: **Overexpression of MUC1 reconfigures the binding properties of tumor cells**. *Int J Cancer* 2001, **94**:783-791.
59. Treon SP, Raje N, Tai YT, Hideshima T, Shima Y, Davies FE, Hilgers J, Hoffman P, Anderson KC: **Expression of MUC1 core protein on multiple myeloma plasma cells permits binding to ICAM-1.** *41st Annual Meeting of the American Society of Hematology* 1999.
60. Hovey RC, Trott JF, Vonderhaar BK: **Establishing a framework for the functional mammary gland: from endocrinology to morphology**. *J Mammary Gland Biol Neoplasia* 2002, **7**:17-38.
61. Neville MC, McFadden TB, Forsyth I: **Hormonal regulation of mammary differentiation and milk secretion**. *J Mammary Gland Biol Neoplasia* 2002, **7**:49-66.

62. Kenney NJ, Smith GH, Lawrence E, Barrett JC, Salomon DS: **Identification of Stem Cell Units in the Terminal End Bud and Duct of the Mouse Mammary Gland.** *J Biomed Biotechnol* 2001, **1**:133-143.
63. Stem Cells in Mammary Glands on World Wide Web URL: http://mammary.nih.gov/reviews/development/Chepko001/index.html
64. Merker HJ: **Morphology of the basement membrane.** *Microsc Res Tech* 1994, **28**:95-124.
65. Leblond CP, Inoue S: **Structure, composition, and assembly of basement membrane.** *Am J Anat* 1989, **185**:367-390.
66. Powell DW, Mifflin RC, Valentich JD, Crowe SE, Saada JI, West AB: **Myofibroblasts. I. Paracrine cells important in health and disease.** *Am J Physiol* 1999, **277**:C1-9.
67. Ronnov-Jessen L, Petersen OW, Koteliansky VE, Bissell MJ: **The origin of the myofibroblasts in breast cancer. Recapitulation of tumor environment in culture unravels diversity and implicates converted fibroblasts and recruited smooth muscle cells.** *J Clin Invest* 1995, **95**:859-873.
68. McBain VA, Forrester JV, McCaig CD: **HGF, MAPK, and a small physiological electric field interact during corneal epithelial cell migration.** *Invest Ophthalmol Vis Sci* 2003, **44**:540-547.
69. Miller WR: **Aromatase inhibitors: mechanism of action and role in the treatment of breast cancer.** *Semin Oncol* 2003, **30**:3-11.
70. Ronnov-Jessen L, Petersen OW, Bissell MJ: **Cellular changes involved in conversion of normal to malignant breast: importance of the stromal reaction.** *Physiol Rev* 1996, **76**:69-125.
71. Dick JE: **Breast cancer stem cells revealed.** *Proc Natl Acad Sci U S A* 2003, **100**:3547-3549.
72. Anderson E, Clarke RB: **Epithelial stem cells in the mammary gland: casting light into dark corners.** *Breast Cancer Res* 1999, **1**:11-13.
73. Gudjonsson T, Villadsen R, Nielsen HL, Ronnov-Jessen L, Bissell MJ, Petersen OW: **Isolation, immortalization, and characterization of a human breast epithelial cell line with stem cell properties.** *Genes Dev* 2002, **16**:693-706.
74. Al-Hajj M, Wicha MS, Benito-Hernandez A, Morrison SJ, Clarke MF: **Prospective identification of tumorigenic breast cancer cells.** *Proc Natl Acad Sci U S A* 2003, **100**:3983-3988.
75. Desai KV, Kavanaugh CJ, Calvo A, Green JE: **Chipping away at breast cancer: insights from microarray studies of human and mouse mammary cancer.** *Endocr Relat Cancer* 2002, **9**:207-220.
76. Miyakis S, Spandidos DA: **Allelic loss in breast cancer.** *Cancer Detect Prev* 2002, **26**:426-434.
77. Radisky D, Hagios C, Bissell MJ: **Tumors are unique organs defined by abnormal signaling and context.** *Semin Cancer Biol* 2001, **11**:87-95.
78. Wang F, Hansen RK, Radisky D, Yoneda T, Barcellos-Hoff MH, Petersen OW, Turley EA, Bissell MJ: **Phenotypic reversion or death of cancer cells by altering signaling pathways in three-dimensional contexts.** *J Natl Cancer Inst* 2002, **94**:1494-1503.

79. Weaver VM, Petersen OW, Wang F, Larabell CA, Briand P, Damsky C, Bissell MJ: **Reversion of the malignant phenotype of human breast cells in three-dimensional culture and in vivo by integrin blocking antibodies.** *J Cell Biol* 1997, **137**:231-245.
80. Elston CW: **Grading of invasive carcinoma of the breast.** In *Diagnostic histopathology of the breast*. Edited by Page DL, Anderson TJ: Churchill Livingstone; 1990:300-311.
81. Love S: *Dr. Susan Love's Breast Book* edn 2nd ed. Reading, Mass.: Addison-Wesley; 1995.
82. Cozier GE, Lockyer PJ, Reynolds JS, Kupzig S, Bottomley JR, Millard TH, Banting G, Cullen PJ: **GAP1IP4BP contains a novel group I pleckstrin homology domain that directs constitutive plasma membrane association.** *J Biol Chem* 2000, **275**:28261-28268.
83. Ronnov-Jessen L, Van Deurs B, Nielsen M, Petersen OW: **Identification, paracrine generation, and possible function of human breast carcinoma myofibroblasts in culture.** *In Vitro Cell Dev Biol* 1992, **28A**:273-283.
84. Bissell MJ, Radisky D: **Putting tumours in context.** *Nat Rev Cancer* 2001, **1**:46-54.
85. Park CC, Bissell MJ, Barcellos-Hoff MH: **The influence of the microenvironment on the malignant phenotype.** *Mol Med Today* 2000, **6**:324-329.
86. Ruoslahti E, Rajotte D: **An address system in the vasculature of normal tissues and tumors.** *Annu Rev Immunol* 2000, **18**:813-827.
87. Schonherr E, Schaefer L, O'Connell BC, Kresse H: **Matrix metalloproteinase expression by endothelial cells in collagen lattices changes during co-culture with fibroblasts and upon induction of decorin expression.** *J Cell Physiol* 2001, **187**:37-47.
88. Halama T, Groger M, Pillinger M, Staffler G, Prager E, Stockinger H, Holnthoner W, Lechleitner S, Wolff K, Petzelbauer P: **Platelet endothelial cell adhesion molecule-1 and vascular endothelial cadherin cooperatively regulate fibroblast growth factor-induced modulations of adherens junction functions.** *J Invest Dermatol* 2001, **116**:110-117.
89. Sieweke MH, Bissell MJ: **The tumor-promoting effect of wounding: a possible role for TGF-beta-induced stromal alterations.** *Crit Rev Oncog* 1994, **5**:297-311.
90. Pujuguet P, Hammann A, Moutet M, Samuel JL, Martin F, Martin M: **Expression of fibronectin ED-A+ and ED-B+ isoforms by human and experimental colorectal cancer. Contribution of cancer cells and tumor-associated myofibroblasts.** *Am J Pathol* 1996, **148**:579-592.
91. Greiling D, Clark RA: **Fibronectin provides a conduit for fibroblast transmigration from collagenous stroma into fibrin clot provisional matrix.** *J Cell Sci* 1997, **110 (Pt 7)**:861-870.
92. Midulla M, Verma R, Pignatelli M, Ritter MA, Courtenay-Luck NS, George AJ: **Source of oncofetal ED-B-containing fibronectin: implications of production by both tumor and endothelial cells.** *Cancer Res* 2000, **60**:164-169.
93. Matsumoto-Taniura N, Matsumoto K, Nakamura T: **Prostaglandin production in mouse mammary tumour cells confers invasive growth potential by inducing**

hepatocyte growth factor in stromal fibroblasts. *Br J Cancer* 1999, **81**:194-202.

94. Brown LF, Guidi AJ, Schnitt SJ, Van De Water L, Iruela-Arispe ML, Yeo TK, Tognazzi K, Dvorak HF: **Vascular stroma formation in carcinoma in situ, invasive carcinoma, and metastatic carcinoma of the breast.** *Clin Cancer Res* 1999, **5**:1041-1056.
95. Sonohara S, Mira-y-Lopez R, Brentani MM: **Laminin and estradiol regulation of the plasminogen-activator system in MCF-7 breast-carcinoma cells.** *Int J Cancer* 1998, **76**:77-85.
96. Reiss M, Barcellos-Hoff MH: **Transforming growth factor-beta in breast cancer: a working hypothesis.** *Breast Cancer Res Treat* 1997, **45**:81-95.
97. Tang B, Vu M, Booker T, Santner SJ, Miller FR, Anver MR, Wakefield LM: **TGF-beta switches from tumor suppressor to prometastatic factor in a model of breast cancer progression.** *J Clin Invest* 2003, **112**:1116-1124.
98. Dumont N, Arteaga CL: **Transforming growth factor-beta and breast cancer: Tumor promoting effects of transforming growth factor-beta.** *Breast Cancer Res* 2000, **2**:125-132.
99. Danforth DN, Jr., Sgagias MK: **Tumor necrosis factor alpha enhances secretion of transforming growth factor beta2 in MCF-7 breast cancer cells.** *Clin Cancer Res* 1996, **2**:827-835.
100. Benbow U, Schoenermark MP, Mitchell TI, Rutter JL, Shimokawa K, Nagase H, Brinckerhoff CE: **A novel host/tumor cell interaction activates matrix metalloproteinase 1 and mediates invasion through type I collagen.** *J Biol Chem* 1999, **274**:25371-25378.
101. Bogetto L, Gabriele E, Cariati R, Dolcetti R, Spessotto P, Doglioni C, Boiocchi M, Perris R, Colombatti A: **Bidirectional induction of the cognate receptor-ligand alpha4/VCAM-1 pair defines a novel mechanism of tumor intravasation.** *Blood* 2000, **95**:2397-2406.
102. Jain RK: **Tumor angiogenesis and accessibility: role of vascular endothelial growth factor.** *Semin Oncol* 2002, **29**:3-9.
103. Carmeliet P, Jain RK: **Angiogenesis in cancer and other diseases.** *Nature* 2000, **407**:249-257.
104. Hendrix MJ, Seftor EA, Kirschmann DA, Seftor RE: **Molecular biology of breast cancer metastasis. Molecular expression of vascular markers by aggressive breast cancer cells.** *Breast Cancer Res* 2000, **2**:417-422.
105. Folberg R, Hendrix MJ, Maniotis AJ: **Vasculogenic mimicry and tumor angiogenesis.** *Am J Pathol* 2000, **156**:361-381.
106. Bissell MJ: **Tumor plasticity allows vasculogenic mimicry, a novel form of angiogenic switch. A rose by any other name?** *Am J Pathol* 1999, **155**:675-679.
107. Fausto N: **Vasculogenic mimicry in tumors. Fact or artifact?** *Am J Pathol* 2000, **156**:359.
108. McDonald DM, Munn L, Jain RK: **Vasculogenic mimicry: how convincing, how novel, and how significant?** *Am J Pathol* 2000, **156**:383-388.
109. Brandtzaeg P, Farstad IN, Haraldsen G: **Regional specialization in the mucosal immune system: primed cells do not always home along the same track.** *Immunol Today* 1999, **20**:267-277.

110. Mebius RE, Schadee-Eestermans IL, Weissman IL: **MAdCAM-1 dependent colonization of developing lymph nodes involves a unique subset of CD4+CD3- hematolymphoid cells**. *Cell Adhes Commun* 1998, **6**:97-103.
111. Ruoslahti E: **Targeting tumor vasculature with homing peptides from phage display**. *Semin Cancer Biol* 2000, **10**:435-442.
112. Orr FW, Wang HH: **Tumor cell interactions with the microvasculature: a rate-limiting step in metastasis**. *Surg Oncol Clin N Am* 2001, **10**:357-381, ix-x.
113. Muller A, Homey B, Soto H, Ge N, Catron D, Buchanan ME, McClanahan T, Murphy E, Yuan W, Wagner SN, et al.: **Involvement of chemokine receptors in breast cancer metastasis**. *Nature* 2001, **410**:50-56.
114. Chambers AF, Groom AC, MacDonald IC: **Dissemination and growth of cancer cells in metastatic sites**. *Nat Rev Cancer* 2002, **2**:563-572.
115. Vlems FA, Ruers TJ, Punt CJ, Wobbes T, van Muijen GN: **Relevance of disseminated tumour cells in blood and bone marrow of patients with solid epithelial tumours in perspective**. *Eur J Surg Oncol* 2003, **29**:289-302.
116. Al-Mehdi AB, Tozawa K, Fisher AB, Shientag L, Lee A, Muschel RJ: **Intravascular origin of metastasis from the proliferation of endothelium-attached tumor cells: a new model for metastasis**. *Nat Med* 2000, **6**:100-102.
117. Akhmedkhanov A, Toniolo P, Zeleniuch-Jacquotte A, Kato I, Koenig KL, Shore RE: **Aspirin and epithelial ovarian cancer**. *Prev Med* 2001, **33**:682-687.
118. Wong BC, Jiang X, Fan XM, Lin MC, Jiang SH, Lam SK, Kung HF: **Suppression of RelA/p65 nuclear translocation independent of IkappaB-alpha degradation by cyclooxygenase-2 inhibitor in gastric cancer**. *Oncogene* 2003, **22**:1189-1197.
119. Moyad MA: **An introduction to aspirin, NSAIDs, and COX-2 inhibitors for the primary prevention of cardiovascular events and cancer and their potential preventive role in bladder carcinogenesis: part I**. *Semin Urol Oncol* 2001, **19**:294-305.
120. Moyad MA: **An introduction to aspirin, NSAids, and COX-2 inhibitors for the primary prevention of cardiovascular events and cancer and their potential preventive role in bladder carcinogenesis: part II**. *Semin Urol Oncol* 2001, **19**:306-316.
121. von Andrian UH, Mackay CR: **T-Cell Function and Migration: Two Sides of the Same Coin**. *The New England Journal of Medicine* 2000, **343**:1020-1034.
122. Orr FW, Wang HH, Lafrenie RM, Scherbarth S, Nance DM: **Interactions between cancer cells and the endothelium in metastasis**. *J Pathol* 2000, **190**:310-329.
123. Thurin M, Kieber-Emmons T: **SA-Lea and tumor metastasis: the old prediction and recent findings**. *Hybrid Hybridomics* 2002, **21**:111-116.
124. Kannagi R: **Carbohydrate-mediated cell adhesion involved in hematogenous metastasis of cancer**. *Glycoconj J* 1997, **14**:577-584.
125. Moniaux N, Escande F, Porchet N, Aubert JP, Batra SK: **Structural organization and classification of the human mucin genes**. *Front Biosci* 2001, **6**:D1192-1206.
126. Devine PL, McKenzie IF: **Mucins: structure, function, and associations with malignancy**. *Bioessays* 1992, **14**:619-625.

127. Correa I, Plunkett T, Vlad A, Mungul A, Candelora-Kettel J, Burchell JM, Taylor-Papadimitriou J, Finn OJ: **Form and pattern of MUC1 expression on T cells activated in vivo or in vitro suggests a function in T-cell migration**. *Immunology* 2003, **108**:32-41.
128. Dekker J, Rossen JWA, Buller HA, Einerhand AW: **The MUC1 family:an obituary**. *TIBS* 2002.
129. Wreschner DH, McGuckin MA, Williams SJ, Baruch A, Yoeli M, Ziv R, Okun L, Zaretsky J, Smorodinsky N, Keydar I, et al.: **Generation of ligand-receptor alliances by "SEA" module-mediated cleavage of membrane-associated mucin proteins**. *Protein Sci* 2002, **11**:698-706.
130. Bork P, Patthy L: **The SEA module: a new extracellular domain associated with O-glycosylation**. *Protein Sci* 1995, **4**:1421-1425.
131. Hilkens J, Buijs F: **Biosynthesis of MAM-6, an epithelial sialomucin. Evidence for involvement of a rare proteolytic cleavage step in the endoplasmic reticulum**. *J Biol Chem* 1988, **263**:4215-4222.
132. Altschuler Y, Kinlough CL, Poland PA, Bruns JB, Apodaca G, Weisz OA, Hughey RP: **Clathrin-mediated endocytosis of MUC1 is modulated by its glycosylation state**. *Mol Biol Cell* 2000, **11**:819-831.
133. Scheiffele P, Peranen J, Simons K: **N-glycans as apical sorting signals in epithelial cells**. *Nature* 1995, **378**:96-98.
134. Litvinov SV, Hilkens J: **The epithelial sialomucin, episialin, is sialylated during recycling**. *J Biol Chem* 1993, **268**:21364-21371.
135. Dekker J, Rossen JW, Buller HA, Einerhand AW: **The MUC family: an obituary**. *Trends Biochem Sci* 2002, **27**:126-131.
136. Brockhausen I, Yang JM, Burchell J, Whitehouse C, Taylor-Papadimitriou J: **Mechanisms underlying aberrant glycosylation of MUC1 mucin in breast cancer cells**. *Eur.J.Biochem.* 1995, **233**:607-617.
137. Altschuler Y, Kinlough CL, Poland PA, Bruns JB, Apodaca G, Weisz OA, Hughey RP: **Clathrin-mediated endocytosis of MUC1 is modulated by its glycosylation state**. *Mol.Biol.Cell* 2000, **11**:819-831.
138. Pemberton LF, Rughetti A, Taylor-Papadimitriou J, Gendler SJ: **The epithelial mucin MUC1 contains at least two discrete signals specifying membrane localization in cells**. *J Biol Chem* 1996, **271**:2332-2340.
139. Parry G, Li J, Stubbs J, Bissell MJ, Schmidhauser C, Spicer AP, Gendler SJ: **Studies of Muc-1 mucin expression and polarity in the mouse mammary gland demonstrate developmental regulation of Muc-1 glycosylation and establish the hormonal basis for mRNA expression**. *J.Cell Sci.* 1992, **101 (Pt 1)**:191-199.
140. Bennett R, Jr., Jarvela T, Engelhardt P, Kostamovaara L, Sparks P, Carpen O, Turunen O, Vaheri A: **Mucin MUC1 is seen in cell surface protrusions together with ezrin in immunoelectron tomography and is concentrated at tips of filopodial protrusions in MCF-7 breast carcinoma cells**. *J Histochem Cytochem* 2001, **49**:67-77.
141. Wang H, Lillehoj EP, Kim KC: **Identification of four sites of stimulated tyrosine phosphorylation in the MUC1 cytoplasmic tail**. *Biochem Biophys Res Commun* 2003, **310**:341-346.

142. Li Y, Bharti A, Chen D, Gong J, Kufe D: **Interaction of glycogen synthase kinase 3beta with the DF3/MUC1 carcinoma-associated antigen and beta-catenin.** *Mol Cell Biol* 1998, **18**:7216-7224.
143. Li Y, Ren J, Yu W, Li Q, Kuwahara H, Yin L, Carraway KL, 3rd, Kufe D: **The epidermal growth factor receptor regulates interaction of the human DF3/MUC1 carcinoma antigen with c-Src and beta-catenin.** *J Biol Chem* 2001, **276**:35239-35242.
144. Li Y, Kufe D: **The Human DF3/MUC1 carcinoma-associated antigen signals nuclear localization of the catenin p120(ctn).** *Biochem Biophys Res Commun* 2001, **281**:440-443.
145. Li Y, Yu WH, Ren J, Chen W, Huang L, Kharbanda S, Loda M, Kufe D: **Heregulin targets gamma-catenin to the nucleolus by a mechanism dependent on the DF3/MUC1 oncoprotein.** *Mol Cancer Res* 2003, **1**:765-775.
146. Hattrup CL, Fernandez-Rodriguez J, Schroeder JA, Hansson GC, Gendler SJ: **MUC1 can interact with adenomatous polyposis coli in breast cancer.** *Biochem Biophys Res Commun* 2004, **316**:364-369.
147. Gonzalez-Guerrico AM, Cafferata EG, Radrizzani M, Marcucci F, Gruenert D, Pivetta OH, Favaloro RR, Laguens R, Perrone SV, Gallo GC, et al.: **Tyrosine kinase c-Src constitutes a bridge between cystic fibrosis transmembrane regulator channel failure and MUC1 overexpression in cystic fibrosis.** *J Biol Chem* 2002, **277**:17239-17247.
148. Wreschner DH, Zrihan-Licht S, Baruch A, Sagiv D, Hartman ML, Smorodinsky N, Keydar I: **Does a novel form of the breast cancer marker protein, MUC1, act as a receptor molecule that modulates signal transduction?** *Adv.Exp.Med.Biol.* 1994, **353**:17-26.
149. Baruch A, Hartmann M, Yoeli M, Adereth Y, Greenstein S, Stadler Y, Skornik Y, Zaretsky J, Smorodinsky NI, Keydar I, et al.: **The breast cancer-associated MUC1 gene generates both a receptor and its cognate binding protein.** *Cancer Res* 1999, **59**:1552-1561.
150. Zrihan-Licht S, Vos HL, Baruch A, Elroy-Stein O, Sagiv D, Keydar I, Hilkens J, Wreschner DH: **Characterization and molecular cloning of a novel MUC1 protein, devoid of tandem repeats, expressed in human breast cancer tissue.** *Eur J Biochem* 1994, **224**:787-795.
151. Analysis of the Secreted Novel Breast-Cancer-Associated MUC1/Zs Cytokine on World Wide Web URL: http://www.stormingmedia.us/cgi-bin/43/4386/A438693.php
152. Thathiah A, Blobel CP, Carson DD: **Tumor necrosis factor-alpha converting enzyme/ADAM 17 mediates MUC1 shedding.** *J Biol Chem* 2003, **278**:3386-3394.
153. Borrell-Pages M, Rojo F, Albanell J, Baselga J, Arribas J: **TACE is required for the activation of the EGFR by TGF-alpha in tumors.** *Embo J* 2003, **22**:1114-1124.
154. Baruch A, Hartmann M, Zrihan-Licht S, Greenstein S, Burstein M, Keydar I, Weiss M, Smorodinsky N, Wreschner DH: **Preferential expression of novel MUC1 tumor antigen isoforms in human epithelial tumors and their tumor-potentiating function.** *Int J Cancer* 1997, **71**:741-749.

155. Oosterkamp HM, Scheiner L, Stefanova MC, Lloyd KO, Finstad CL: **Comparison of MUC-1 mucin expression in epithelial and non-epithelial cancer cell lines and demonstration of a new short variant form (MUC-1/Z)**. *Int J Cancer* 1997, **72**:87-94.
156. Obermair A, Schmid BC, Stimpfl M, Fasching B, Preyer O, Leodolter S, Crandon AJ, Zeillinger R: **Novel MUC1 splice variants are expressed in cervical carcinoma**. *Gynecol Oncol* 2001, **83**:343-347.
157. MUC1 (CD227) on World Wide Web URL: http://www.ncbi.nlm.nih.gov/PROW/guide/921344893_g.htm
158. McGuckin MA, Walsh MD, Hohn BG, Ward BG, Wright RG: **Prognostic significance of MUC1 epithelial mucin expression in breast cancer**. *Hum Pathol* 1995, **26**:432-439.
159. Bresalier RS, Byrd JC, Brodt P, Ogata S, Itzkowitz SH, Yunker CK: **Liver metastasis and adhesion to the sinusoidal endothelium by human colon cancer cells is related to mucin carbohydrate chain length**. *Int.J.Cancer* 1998, **76**:556-562.
160. Fujita K, Denda K, Yamamoto M, Matsumoto T, Fujime M, Irimura T: **Expression of MUC1 mucins inversely correlated with post-surgical survival of renal cell carcinoma patients**. *Br.J.Cancer* 1999, **80**:301-308.
161. Hiraga Y, Tanaka S, Haruma K, Yoshihara M, Sumii K, Kajiyama G, Shimamoto F, Kohno N: **Immunoreactive MUC1 expression at the deepest invasive portion correlates with prognosis of colorectal cancer**. *Oncology* 1998, **55**:307-319.
162. Suwa T, Hinoda Y, Makiguchi Y, Takahashi T, Itoh F, Adachi M, Hareyama M, Imai K: **Increased invasiveness of MUC1 and cDNA-transfected human gastric cancer MKN74 cells**. *Int.J.Cancer* 1998, **76**:377-382.
163. Suwa T, Hinoda Y, Makiguchi Y, Takahashi T, Itoh F, Adachi M, Hareyama M, Imai K: **Increased invasiveness of MUC1 and cDNA-transfected human gastric cancer MKN74 cells**. *Int J Cancer* 1998, **76**:377-382.
164. He TC, Sparks AB, Rago C, Hermeking H, Zawel L, da Costa LT, Morin PJ, Vogelstein B, Kinzler KW: **Identification of c-MYC as a target of the APC pathway**. *Science* 1998, **281**:1509-1512.
165. Tetsu O, McCormick F: **Beta-catenin regulates expression of cyclin D1 in colon carcinoma cells**. *Nature* 1999, **398**:422-426.
166. Huber O, Korn R, McLaughlin J, Ohsugi M, Herrmann BG, Kemler R: **Nuclear localization of beta-catenin by interaction with transcription factor LEF-1**. *Mech Dev* 1996, **59**:3-10.
167. Spicer AP, Rowse GJ, Lidner TK, Gendler SJ: **Delayed mammary tumor progression in Muc-1 null mice**. *J.Biol.Chem.* 1995, **270**:30093-30101.
168. Hirasawa Y, Kohno N, Yokoyama A, Inoue Y, Abe M, Hiwada K: **KL-6, a human MUC1 mucin, is chemotactic for human fibroblasts**. *Am J Respir Cell Mol Biol* 1997, **17**:501-507.
169. Quin RJ, McGuckin MA: **Phosphorylation of the cytoplasmic domain of the MUC1 mucin correlates with changes in cell-cell adhesion**. *Int J Cancer* 2000, **87**:499-506.
170. Mareel MM, Behrens J, Birchmeier W, De Bruyne GK, Vleminckx K, Hoogewijs A, Fiers WC, Van Roy FM: **Down-regulation of E-cadherin expression in Madin**

Darby canine kidney (MDCK) cells inside tumors of nude mice. *Int J Cancer* 1991, **47**:922-928.

171. Satoh S, Hinoda Y, Hayashi T, Burdick MD, Imai K, Hollingsworth MA: **Enhancement of metastatic properties of pancreatic cancer cells by MUC1 gene encoding an anti-adhesion molecule**. *Int J Cancer* 2000, **88**:507-518.
172. Hudson MJ, Stamp GW, Chaudhary KS, Hewitt R, Stubbs AP, Abel PD, Lalani EN: **Human MUC1 mucin: a potent glandular morphogen**. *J Pathol* 2001, **194**:373-383.
173. Kowalczyk AP, Reynolds AB: **Protecting your tail: regulation of cadherin degradation by p120-catenin**. *Curr Opin Cell Biol* 2004, **16**:522-527.
174. Kelly KF, Spring CM, Otchere AA, Daniel JM: **NLS-dependent nuclear localization of p120ctn is necessary to relieve Kaiso-mediated transcriptional repression**. *J Cell Sci* 2004, **117**:2675-2686.
175. Anastasiadis PZ, Moon SY, Thoreson MA, Mariner DJ, Crawford HC, Zheng Y, Reynolds AB: **Inhibition of RhoA by p120 catenin**. *Nat Cell Biol* 2000, **2**:637-644.
176. Grosheva I, Shtutman M, Elbaum M, Bershadsky AD: **p120 catenin affects cell motility via modulation of activity of Rho-family GTPases: a link between cell-cell contact formation and regulation of cell locomotion**. *J Cell Sci* 2001, **114**:695-707.
177. Noren NK, Liu BP, Burridge K, Kreft B: **p120 catenin regulates the actin cytoskeleton via Rho family GTPases**. *J Cell Biol* 2000, **150**:567-580.
178. Aho S, Levansuo L, Montonen O, Kari C, Rodeck U, Uitto J: **Specific sequences in p120ctn determine subcellular distribution of its multiple isoforms involved in cellular adhesion of normal and malignant epithelial cells**. *J Cell Sci* 2002, **115**:1391-1402.
179. Reynolds AB, Daniel JM, Mo YY, Wu J, Zhang Z: **The novel catenin p120cas binds classical cadherins and induces an unusual morphological phenotype in NIH3T3 fibroblasts**. *Exp Cell Res* 1996, **225**:328-337.
180. Reddy KB, Nabha SM, Atanaskova N: **Role of MAP kinase in tumor progression and invasion**. *Cancer Metastasis Rev* 2003, **22**:395-403.
181. Feldner JC, Brandt BH: **Cancer cell motility--on the road from c-erbB-2 receptor steered signaling to actin reorganization**. *Exp Cell Res* 2002, **272**:93-108.
182. Yamashita YM, Jones DL, Fuller MT: **Orientation of asymmetric stem cell division by the APC tumor suppressor and centrosome**. *Science* 2003, **301**:1547-1550.
183. Ohkubo T, Ozawa M: **p120(ctn) binds to the membrane-proximal region of the E-cadherin cytoplasmic domain and is involved in modulation of adhesion activity**. *J Biol Chem* 1999, **274**:21409-21415.
184. Li Y, Chen W, Ren J, Yu WH, Li Q, Yoshida K, Kufe D: **DF3/MUC1 signaling in multiple myeloma cells is regulated by interleukin-7**. *Cancer Biol Ther* 2003, **2**:187-193.
185. Wen Y, Caffrey TC, Wheelock MJ, Johnson KR, Hollingsworth MA: **Nuclear Association of the Cytoplasmic Tail of MUC1 and {beta}-Catenin**. *J Biol Chem* 2003, **278**:38029-38039.

186. Rahn JJ, Hugh JC: **Comments on: Involvement of adenomatous polyposis coli (APC) beta-catenin signalling in human breast cancer, Johnsson M, Borg A, Nilbert M, Andersson, T. Eur.J. Cancer 2000, 36, 242-248.** *Eur J Cancer* 2001, **37**:668-670.

187. Huang L, Ren J, Chen D, Li Y, Kharbanda S, Kufe D: **MUC1 cytoplasmic domain coactivates Wnt target gene transcription and confers transformation.** *Cancer Biol Ther* 2003, **2**:702-706.

188. Yin L, Li Y, Ren J, Kuwahara H, Kufe D: **Human MUC1 carcinoma antigen regulates intracellular oxidant levels and the apoptotic response to oxidative stress.** *J Biol Chem* 2003, **278**:35458-35464.

189. Raina D, Kharbanda S, Kufe D: **The MUC1 Oncoprotein Activates the Anti-apoptotic Phosphoinositide 3-Kinase/Akt and Bcl-xL Pathways in Rat 3Y1 Fibroblasts.** *J Biol Chem* 2004, **279**:20607-20612.

190. Hakimelahi S, Parker HR, Gilchrist AJ, Barry M, Li Z, Bleackley RC, Pasdar M: **Plakoglobin regulates the expression of the anti-apoptotic protein BCL-2.** *J Biol Chem* 2000, **275**:10905-10911.

191. van de Stolpe A, van der Saag PT: **Intercellular adhesion molecule-1.** *J Mol Med* 1996, **74**:13-33.

192. Carpen O, Pallai P, Staunton DE, Springer TA: **Association of intercellular adhesion molecule-1 (ICAM-1) with actin-containing cytoskeleton and alpha-actinin.** *J Cell Biol* 1992, **118**:1223-1234.

193. Barreiro O, Yanez-Mo M, Serrador JM, Montoya MC, Vicente-Manzanares M, Tejedor R, Furthmayr H, Sanchez-Madrid F: **Dynamic interaction of VCAM-1 and ICAM-1 with moesin and ezrin in a novel endothelial docking structure for adherent leukocytes.** *J Cell Biol* 2002, **157**:1233-1245.

194. Romero IA, Amos CL, Greenwood J, Adamson P: **Ezrin and moesin co-localise with ICAM-1 in brain endothelial cells but are not directly associated.** *Brain Res Mol Brain Res* 2002, **105**:47-59.

195. Li Y, Liu D, Chen D, Kharbanda S, Kufe D: **Human DF3/MUC1 carcinoma-associated protein functions as an oncogene.** *Oncogene* 2003, **22**:6107-6110.

196. Jun CD, Carman CV, Redick SD, Shimaoka M, Erickson HP, Springer TA: **Ultrastructure and function of dimeric, soluble intercellular adhesion molecule-1 (ICAM-1).** *J Biol Chem* 2001, **276**:29019-29027.

197. Jun CD, Shimaoka M, Carman CV, Takagi J, Springer TA: **Dimerization and the effectiveness of ICAM-1 in mediating LFA-1-dependent adhesion.** *Proc Natl Acad Sci U S A* 2001, **98**:6830-6835.

198. Reilly PL, Woska JR, Jr., Jeanfavre DD, McNally E, Rothlein R, Bormann BJ: **The native structure of intercellular adhesion molecule-1 (ICAM-1) is a dimer. Correlation with binding to LFA-1.** *J Immunol* 1995, **155**:529-532.

199. Bradley JR, Pober JS: **Prolonged cytokine exposure causes a dynamic redistribution of endothelial cell adhesion molecules to intercellular junctions.** *Lab Invest* 1996, **75**:463-472.

200. Braddock M, Schwachtgen JL, Houston P, Dickson MC, Lee MJ, Campbell CJ: **Fluid Shear Stress Modulation of Gene Expression in Endothelial Cells.** *News Physiol Sci* 1998, **13**:241-246.

201. Clayton A, Evans RA, Pettit E, Hallett M, Williams JD, Steadman R: **Cellular activation through the ligation of intercellular adhesion molecule-1**. *J Cell Sci* 1998, **111 (Pt 4)**:443-453.
202. Huang AJ, Manning JE, Bandak TM, Ratau MC, Hanser KR, Silverstein SC: **Endothelial cell cytosolic free calcium regulates neutrophil migration across monolayers of endothelial cells**. *J Cell Biol* 1993, **120**:1371-1380.
203. Lewalle JM, Bajou K, Desreux J, Mareel M, Dejana E, Noel A, Foidart JM: **Alteration of interendothelial adherens junctions following tumor cell-endothelial cell interaction in vitro**. *Exp Cell Res* 1997, **237**:347-356.
204. Lewalle JM, Cataldo D, Bajou K, Lambert CA, Foidart JM: **Endothelial cell intracellular Ca2+ concentration is increased upon breast tumor cell contact and mediates tumor cell transendothelial migration**. *Clin Exp Metastasis* 1998, **16**:21-29.
205. Durieu-Trautmann O, Chaverot N, Cazaubon S, Strosberg AD, Couraud PO: **Intercellular adhesion molecule 1 activation induces tyrosine phosphorylation of the cytoskeleton-associated protein cortactin in brain microvessel endothelial cells**. *J Biol Chem* 1994, **269**:12536-12540.
206. Etienne S, Adamson P, Greenwood J, Strosberg AD, Cazaubon S, Couraud PO: **ICAM-1 signaling pathways associated with Rho activation in microvascular brain endothelial cells**. *J Immunol* 1998, **161**:5755-5761.
207. Tilghman RW, Hoover RL: **The Src-cortactin pathway is required for clustering of E-selectin and ICAM-1 in endothelial cells**. *Faseb J* 2002, **16**:1257-1259.
208. Phan C, McMahon AW, Nelson RC, Elliott JF, Murray AG: **Activated lymphocytes promote endothelial cell detachment from matrix: a role for modulation of endothelial cell beta 1 integrin affinity**. *J Immunol* 1999, **163**:4557-4563.
209. Burns AR, Bowden RA, MacDonell SD, Walker DC, Odebunmi TO, Donnachie EM, Simon SI, Entman ML, Smith CW: **Analysis of tight junctions during neutrophil transendothelial migration**. *J Cell Sci* 2000, **113 (Pt 1)**:45-57.
210. Burns AR, Walker DC, Brown ES, Thurmon LT, Bowden RA, Keese CR, Simon SI, Entman ML, Smith CW: **Neutrophil transendothelial migration is independent of tight junctions and occurs preferentially at tricellular corners**. *J Immunol* 1997, **159**:2893-2903.
211. Ozaki H, Ishii K, Horiuchi H, Arai H, Kawamoto T, Okawa K, Iwamatsu A, Kita T: **Cutting edge: combined treatment of TNF-alpha and IFN-gamma causes redistribution of junctional adhesion molecule in human endothelial cells**. *J Immunol* 1999, **163**:553-557.
212. Tucker EL, Pignatelli M: **Catenins and their associated proteins in colorectal cancer**. *Histol Histopathol* 2000, **15**:251-260.
213. Brock R, Hamelers IH, Jovin TM: **Comparison of fixation protocols for adherent cultured cells applied to a GFP fusion protein of the epidermal growth factor receptor**. *Cytometry* 1999, **35**:353-362.
214. Rasmussen BB, Pedersen BV, Thorpe SM, Hilkens J, Hilgers J, Rose C: **Prognostic value of surface antigens in primary human breast carcinomas, detected by monoclonal antibodies**. *Cancer Res.* 1985, **45**:1424-1427.

215. Ellis IO, Hinton CP, MacNay J, Elston CW, Robins A, Owainati AA, Blamey RW, Baldwin RW, Ferry B: **Immunocytochemical staining of breast carcinoma with the monoclonal antibody NCRC 11: a new prognostic indicator**. *Br.Med.J.(Clin.Res.Ed)* 1985, **290**:881-883.

216. Lundy J, Thor A, Maenza R, Schlom J, Forouhar F, Testa M, Kufe D: **Monoclonal antibody DF3 correlates with tumor differentiation and hormone receptor status in breast cancer patients**. *Breast Cancer Res.Treat.* 1985, **5**:269-276.

217. Angus B, Napier J, Purvis J, Ellis IO, Hawkins RA, Carpenter F, Horne CH: **Survival in breast cancer related to tumour oestrogen receptor status and immunohistochemical staining for NCRC 11**. *J.Pathol.* 1986, **149**:301-306.

218. Helle M: **The prognostic significance of the monoclonal antibody III D 5 to human milk fat globule antigen in breast cancer**. *Acta Pathol.Microbiol.Immunol.Scand.[A]* 1986, **94**:375-380.

219. Krohn K, Helle M: **Recognition with a monoclonal antibody of a cytoplasmic mammary carcinoma antigen, correlated to the estrogen receptor status**. *Int.J.Cancer* 1986, **37**:43-47.

220. Ellis IO, Bell J, Todd JM, Williams M, Dowle C, Robins AR, Elston CW, Blamey RW, Baldwin RW: **Evaluation of immunoreactivity with monoclonal antibody NCRC 11 in breast carcinoma**. *Br.J.Cancer* 1987, **56**:295-299.

221. Wright C, Angus B, Napier J, Wetherall M, Udagawa Y, Sainsbury JR, Johnston S, Carpenter F, Horne CH: **Prognostic factors in breast cancer: immunohistochemical staining for SP1 and NCRC 11 related to survival, tumour epidermal growth factor receptor and oestrogen receptor status**. *J.Pathol.* 1987, **153**:325-331.

222. Helle M, Helin H, Antonen J, Krohn K: **Human milk fat globule antigen III D 5, steroid receptors and histopathologic parameters in breast cancer**. *APMIS* 1988, **96**:415-420.

223. Arnerlov C, Ellis IO, Emdin SO: **Monoclonal antibody NCRC 11 reactivity with advanced breast carcinoma: lack of prognostic value**. *Histopathology* 1988, **13**:695-697.

224. Baildam AD, Howell A, Barnes DM, Turnbull L, Sellwood RA: **The expression of milk fat globule antigens within human mammary tumours: relationship to steroid hormone receptors and response to endocrine treatment**. *Eur.J.Cancer Clin.Oncol.* 1989, **25**:459-467.

225. Walker RA: **Assessment of milk fat globule membrane antibodies and lectins as markers of short-term prognosis in breast cancer**. *Br.J.Cancer* 1990, **62**:462-466.

226. Muir IM, Reed RG, Stacker SA, Alexander AI, McKenzie IF, Bennett RC: **The prognostic value of immunoperoxidase staining with monoclonal antibodies NCRC-11 and 3E1.2 in breast cancer**. *Br.J.Cancer* 1991, **64**:124-127.

227. Byrne J, Horgan PG, England S, Callaghan J, Given HF: **An evaluation of the usefulness of primary tumour expression of MCA and CA15-3 as prognostic indicators in breast carcinoma**. *Eur.J.Surg.Oncol.* 1992, **18**:230-234.

228. Wilkinson MJ, Howell A, Harris M, Taylor-Papadimitriou J, Swindell R, Sellwood RA: **The prognostic significance of two epithelial membrane antigens expressed by human mammary carcinomas**. *Int.J.Cancer* 1984, **33**:299-304.

229. Berry N, Jones DB, Smallwood J, Taylor I, Kirkham N, Taylor-Papadimitriou J: **The prognostic value of the monoclonal antibodies HMFG1 and HMFG2 in breast cancer**. *Br.J.Cancer* 1985, **51**:179-186.
230. Ohuchi N, Page DL, Merino MJ, Viglione MJ, Kufe DW, Schlom J: **Expression of tumor-associated antigen (DF3) in atypical hyperplasias and in situ carcinomas of the human breast**. *J.Natl.Cancer Inst.* 1987, **79**:109-117.
231. Parham DM, Slidders W, Robertson AJ: **Quantitation of human milk fat globule (HMFG1) expression in breast carcinoma and its association with survival**. *J.Clin.Pathol.* 1988, **41**:875-879.
232. Parham DM, Coghill G, Robertson AJ: **Critical evaluation of monoclonal antibody staining in breast carcinoma**. *J.Clin.Pathol.* 1989, **42**:810-813.
233. Hayes DF, Mesa-Tejada R, Papsidero LD, Croghan GA, Korzun AH, Norton L, Wood W, Strauchen JA, Grimes M, Weiss RB: **Prediction of prognosis in primary breast cancer by detection of a high molecular weight mucin-like antigen using monoclonal antibodies DF3, F36/22, and CU18: a Cancer and Leukemia Group B study [see comments]**. *J.Clin.Oncol.* 1991, **9**:1113-1123.
234. Ceriani RL, Chan CM, Baratta FS, Ozzello L, DeRosa CM, Habif DV: **Levels of expression of breast epithelial mucin detected by monoclonal antibody BrE-3 in breast-cancer prognosis**. *Int.J.Cancer* 1992, **51**:343-354.
235. McGuckin MA, Walsh MD, Hohn BG, Ward BG, Wright RG: **Prognostic significance of MUC1 epithelial mucin expression in breast cancer**. *Hum.Pathol.* 1995, **26**:432-439.
236. Khaldoyanidi SK, Glinsky VV, Sikora L, Glinskii AB, Mossine VV, Quinn TP, Glinsky GV, Sriramarao P: **MDA-MB-435 human breast carcinoma cell homo- and heterotypic adhesion under flow conditions is mediated in part by Thomsen-Friedenreich antigen-galectin-3 interactions**. *J Biol Chem* 2003, **278**:4127-4134.
237. Burchell JM, Mungul A, Taylor-Papadimitriou J: **O-linked glycosylation in the mammary gland: changes that occur during malignancy**. *J Mammary Gland Biol Neoplasia* 2001, **6**:355-364.
238. Chambers AF, MacDonald IC, Schmidt EE, Koop S, Morris VL, Khokha R, Groom AC: **Steps in tumor metastasis: new concepts from intravital videomicroscopy**. *Cancer Metastasis Rev* 1995, **14**:279-301.
239. Weaver VM, Fischer AH, Peterson OW, Bissell MJ: **The importance of the microenvironment in breast cancer progression: recapitulation of mammary tumorigenesis using a unique human mammary epithelial cell model and a three-dimensional culture assay**. *Biochem Cell Biol* 1996, **74**:833-851.
240. Sawada T, Ho JJ, Chung YS, Sowa M, Kim YS: **E-selectin binding by pancreatic tumor cells is inhibited by cancer sera**. *Int J Cancer* 1994, **57**:901-907.
241. Zhang K, Baeckstrom D, Brevinge H, Hansson GC: **Secreted MUC1 mucins lacking their cytoplasmic part and carrying sialyl-Lewis a and x epitopes from a tumor cell line and sera of colon carcinoma patients can inhibit HL-60 leukocyte adhesion to E-selectin-expressing endothelial cells**. *J Cell Biochem* 1996, **60**:538-549.
242. Beum PV, Singh J, Burdick M, Hollingsworth MA, Cheng PW: **Expression of core 2 beta-1,6-N-acetylglucosaminyltransferase in a human pancreatic cancer**

cell line results in altered expression of MUC1 tumor-associated epitopes. *J Biol Chem* 1999, **274**:24641-24648.

243. Youngs SJ, Ali SA, Taub DD, Rees RC: **Chemokines induce migrational responses in human breast carcinoma cell lines.** *Int J Cancer* 1997, **71**:257-266.

244. Nguyen DH, Hussaini IM, Gonias SL: **Binding of urokinase-type plasminogen activator to its receptor in MCF-7 cells activates extracellular signal-regulated kinase 1 and 2 which is required for increased cellular motility.** *J Biol Chem* 1998, **273**:8502-8507.

245. Prest SJ, Rees RC, Murdoch C, Marshall JF, Cooper PA, Bibby M, Li G, Ali SA: **Chemokines induce the cellular migration of MCF-7 human breast carcinoma cells: subpopulations of tumour cells display positive and negative chemotaxis and differential in vivo growth potentials.** *Clin Exp Metastasis* 1999, **17**:389-396.

246. Doerr ME, Jones JI: **The roles of integrins and extracellular matrix proteins in the insulin-like growth factor I-stimulated chemotaxis of human breast cancer cells.** *J Biol Chem* 1996, **271**:2443-2447.

247. Plopper GE, Domanico SZ, Cirulli V, Kiosses WB, Quaranta V: **Migration of breast epithelial cells on Laminin-5: differential role of integrins in normal and transformed cell types.** *Breast Cancer Res Treat* 1998, **51**:57-69.

248. Moon A, Kim MS, Kim TG, Kim SH, Kim HE, Chen YQ, Kim HR: **H-ras, but not N-ras, induces an invasive phenotype in human breast epithelial cells: a role for MMP-2 in the H-ras-induced invasive phenotype.** *Int J Cancer* 2000, **85**:176-181.

249. Kim MS, Lee EJ, Kim HR, Moon A: **p38 kinase is a key signaling molecule for H-Ras-induced cell motility and invasive phenotype in human breast epithelial cells.** *Cancer Res* 2003, **63**:5454-5461.

250. Yang SZ, Kohno N, Yokoyama A, Kondo K, Hamada H, Hiwada K: **Decreased E-cadherin augments beta-catenin nuclear localization: studies in breast cancer cell lines.** *Int J Oncol* 2001, **18**:541-548.

251. Handa K, Jacobs F, Longenecker BM, Hakomori SI: **Association of MUC-1 and SPGL-1 with low-density microdomain in T-lymphocytes: a preliminary note.** *Biochem Biophys Res Commun* 2001, **285**:788-794.

252. Arihiro K, Oda H, Kaneko M, Inai K: **Cytokines facilitate chemotactic motility of breast carcinoma cells.** *Breast Cancer* 2000, **7**:221-230.

253. Kunz-Schughart LA, Heyder P, Schroeder J, Knuechel R: **A heterologous 3-D coculture model of breast tumor cells and fibroblasts to study tumor-associated fibroblast differentiation.** *Exp Cell Res* 2001, **266**:74-86.

254. Gao B, Saba TM, Tsan MF: **Role of alpha(v)beta(3)-integrin in TNF-alpha-induced endothelial cell migration.** *Am J Physiol Cell Physiol* 2002, **283**:C1196-1205.

255. Urbich C, Dernbach E, Reissner A, Vasa M, Zeiher AM, Dimmeler S: **Shear stress-induced endothelial cell migration involves integrin signaling via the fibronectin receptor subunits alpha(5) and beta(1).** *Arterioscler Thromb Vasc Biol* 2002, **22**:69-75.

256. Hagios C, Lochter A, Bissell MJ: **Tissue architecture: the ultimate regulator of epithelial function?** *Philos Trans R Soc Lond B Biol Sci* 1998, **353**:857-870.
257. Schmeichel KL, Weaver VM, Bissell MJ: **Structural cues from the tissue microenvironment are essential determinants of the human mammary epithelial cell phenotype.** *J Mammary Gland Biol Neoplasia* 1998, **3**:201-213.
258. Gunst SJ, Tang DD: **The contractile apparatus and mechanical properties of airway smooth muscle.** *Eur Respir J* 2000, **15**:600-616.
259. Arthur WT, Petch LA, Burridge K: **Integrin engagement suppresses RhoA activity via a c-Src-dependent mechanism.** *Curr Biol* 2000, **10**:719-722.
260. Shaw LM: **Integrin function in breast carcinoma progression.** *J Mammary Gland Biol Neoplasia* 1999, **4**:367-376.
261. Gui GP, Wells CA, Browne PD, Yeomans P, Jordan S, Puddefoot JR, Vinson GP, Carpenter R: **Integrin expression in primary breast cancer and its relation to axillary nodal status.** *Surgery* 1995, **117**:102-108.
262. Howlett AR, Bailey N, Damsky C, Petersen OW, Bissell MJ: **Cellular growth and survival are mediated by beta 1 integrins in normal human breast epithelium but not in breast carcinoma.** *J Cell Sci* 1995, **108 (Pt 5)**:1945-1957.
263. Ranta-Knuuttila T, Kiviluoto T, Mustonen H, Puolakkainen P, Watanabe S, Sato N, Kivilaakso E: **Migration of primary cultured rabbit gastric epithelial cells requires intact protein kinase C and Ca2+/calmodulin activity.** *Dig Dis Sci* 2002, **47**:1008-1014.
264. Piccolo E, Innominato PF, Mariggio MA, Maffucci T, Iacobelli S, Falasca M: **The mechanism involved in the regulation of phospholipase Cgamma1 activity in cell migration.** *Oncogene* 2002, **21**:6520-6529.
265. Cullen PJ, Lockyer PJ: **Integration of calcium and Ras signalling.** *Nat Rev Mol Cell Biol* 2002, **3**:339-348.
266. Marks PW, Hendey B, Maxfield FR: **Attachment to fibronectin or vitronectin makes human neutrophil migration sensitive to alterations in cytosolic free calcium concentration.** *J Cell Biol* 1991, **112**:149-158.
267. Oosawa Y, Imada C, Furuya K: **Temperature dependency of calcium responses in mammary tumour cells.** *Cell Biochem Funct* 1997, **15**:113-117.
268. Sigurdson WJ, Sachs F, Diamond SL: **Mechanical perturbation of cultured human endothelial cells causes rapid increases of intracellular calcium.** *Am J Physiol* 1993, **264**:H1745-1752.
269. Putney JW, Jr.: **Calcium signaling: up, down, up, down...what's the point?** *Science* 1998, **279**:191-192.
270. Dolmetsch RE, Xu K, Lewis RS: **Calcium oscillations increase the efficiency and specificity of gene expression.** *Nature* 1998, **392**:933-936.
271. Etienne-Manneville S, Manneville JB, Adamson P, Wilbourn B, Greenwood J, Couraud PO: **ICAM-1-coupled cytoskeletal rearrangements and transendothelial lymphocyte migration involve intracellular calcium signaling in brain endothelial cell lines.** *J Immunol* 2000, **165**:3375-3383.
272. Graham RA, Burchell JM, Taylor-Papadimitriou J: **The polymorphic epithelial mucin: potential as an immunogen for a cancer vaccine.** *Cancer Immunol Immunother* 1996, **42**:71-80.

273. Grinstead JS, Koganty RR, Krantz MJ, Longenecker BM, Campbell AP: **Effect of glycosylation on MUC1 humoral immune recognition: NMR studies of MUC1 glycopeptide-antibody interactions**. *Biochemistry* 2002, **41**:9946-9961.
274. Li W, Nadelman C, Henry G, Fan J, Muellenhoff M, Medina E, Gratch NS, Chen M, Han J, Woodley D: **The p38-MAPK/SAPK pathway is required for human keratinocyte migration on dermal collagen**. *J Invest Dermatol* 2001, **117**:1601-1611.
275. Klekotka PA, Santoro SA, Zutter MM: **alpha 2 integrin subunit cytoplasmic domain-dependent cellular migration requires p38 MAPK**. *J Biol Chem* 2001, **276**:9503-9511.
276. Ozdener F, Dangelmaier C, Ashby B, Kunapuli SP, Daniel JL: **Activation of phospholipase Cgamma2 by tyrosine phosphorylation**. *Mol Pharmacol* 2002, **62**:672-679.
277. Tokmakov AA, Sato KI, Iwasaki T, Fukami Y: **Src kinase induces calcium release in Xenopus egg extracts via PLCgamma and IP3-dependent mechanism**. *Cell Calcium* 2002, **32**:11-20.
278. Shu L, Shayman JA: **Src kinase mediates the regulation of phospholipase C-gamma activity by glycosphingolipids**. *J Biol Chem* 2003, **278**:31419-31425.
279. Katan M, Rodriguez R, Matsuda M, Newbatt YM, Aherne GW: **Structural and mechanistic aspects of phospholipase Cgamma regulation**. *Adv Enzyme Regul* 2003, **43**:77-85.
280. Irvine R: **Inositol lipids: to PHix or not to PHix?** *Curr Biol* 2004, **14**:R308-310.
281. Bobe R, Wilde JI, Maschberger P, Venkateswarlu K, Cullen PJ, Siess W, Watson SP: **Phosphatidylinositol 3-kinase-dependent translocation of phospholipase Cgamma2 in mouse megakaryocytes is independent of Bruton tyrosine kinase translocation**. *Blood* 2001, **97**:678-684.
282. Falasca M, Logan SK, Lehto VP, Baccante G, Lemmon MA, Schlessinger J: **Activation of phospholipase C gamma by PI 3-kinase-induced PH domain-mediated membrane targeting**. *Embo J* 1998, **17**:414-422.
283. Wells A, Kassis J, Solava J, Turner T, Lauffenburger DA: **Growth factor-induced cell motility in tumor invasion**. *Acta Oncol* 2002, **41**:124-130.
284. Kassis J, Moellinger J, Lo H, Greenberg NM, Kim HG, Wells A: **A role for phospholipase C-gamma-mediated signaling in tumor cell invasion**. *Clin Cancer Res* 1999, **5**:2251-2260.
285. Berridge MJ, Lipp P, Bootman MD: **The versatility and universality of calcium signalling**. *Nat Rev Mol Cell Biol* 2000, **1**:11-21.
286. Agell N, Bachs O, Rocamora N, Villalonga P: **Modulation of the Ras/Raf/MEK/ERK pathway by Ca(2+), and calmodulin**. *Cell Signal* 2002, **14**:649-654.
287. Sun HQ, Yamamoto M, Mejillano M, Yin HL: **Gelsolin, a multifunctional actin regulatory protein**. *J Biol Chem* 1999, **274**:33179-33182.
288. White SP, Cohen C, Phillips GN, Jr.: **Structure of co-crystals of tropomyosin and troponin**. *Nature* 1987, **325**:826-828.
289. Yamada K: **Calcium binding to troponin C as a primary step of the regulation of contraction. A microcalorimetric approach**. *Adv Exp Med Biol* 2003, **538**:203-212; discussion 213.

290. Perrin BJ, Huttenlocher A: **Calpain**. *Int J Biochem Cell Biol* 2002, **34**:722-725.
291. Lauffenburger DA, Horwitz AF: **Cell migration: a physically integrated molecular process**. *Cell* 1996, **84**:359-369.
292. Burdick MM, McCaffery JM, Kim YS, Bochner BS, Konstantopoulos K: **Colon carcinoma cell glycolipids, integrins, and other glycoproteins mediate adhesion to HUVECs under flow**. *Am J Physiol Cell Physiol* 2003, **284**:C977-987.
293. Fujii Y, Yoshida M, Chien LJ, Kihara K, Kageyama Y, Yasukochi Y, Oshima H: **Significance of carbohydrate antigen sialyl-Lewis X, sialyl-Lewis A, and possible unknown ligands to adhesion of human urothelial cancer cells to activated endothelium**. *Urol Int* 2000, **64**:129-133.
294. Goetz DJ, Ding H, Atkinson WJ, Vachino G, Camphausen RT, Cumming DA, Luscinskas FW: **A human colon carcinoma cell line exhibits adhesive interactions with P-selectin under fluid flow via a PSGL-1-independent mechanism**. *Am J Pathol* 1996, **149**:1661-1673.
295. Goetz DJ, Brandley BK, Hammer DA: **An E-selectin-IgG chimera supports sialylated moiety dependent adhesion of colon carcinoma cells under fluid flow**. *Ann Biomed Eng* 1996, **24**:87-98.
296. Hosono J, Narita T, Kimura N, Sato M, Nakashio T, Kasai Y, Nonami T, Nakao A, Takagi H, Kannagi R: **Involvement of adhesion molecules in metastasis of SW1990, human pancreatic cancer cells**. *J Surg Oncol* 1998, **67**:77-84.
297. Iwai K, Ishikura H, Kaji M, Sugiura H, Ishizu A, Takahashi C, Kato H, Tanabe T, Yoshiki T: **Importance of E-selectin (ELAM-1) and sialyl Lewis(a) in the adhesion of pancreatic carcinoma cells to activated endothelium**. *Int J Cancer* 1993, **54**:972-977.
298. Gui GP, Wells CA, Yeomans P, Jordan SE, Vinson GP, Carpenter R: **Integrin expression in breast cancer cytology: a novel predictor of axillary metastasis**. *Eur J Surg Oncol* 1996, **22**:254-258.
299. Baldus SE, Monig SP, Huxel S, Landsberg S, Hanisch FG, Engelmann K, Schneider PM, Thiele J, Holscher AH, Dienes HP: **MUC1 and nuclear beta-catenin are coexpressed at the invasion front of colorectal carcinomas and are both correlated with tumor prognosis**. *Clin Cancer Res* 2004, **10**:2790-2796.
300. Pike LJ: **Lipid rafts: bringing order to chaos**. *J Lipid Res* 2003, **44**:655-667.
301. Seeger H, Wallwiener D, Mueck AO: **Influence of stroma-derived growth factors on the estradiol-stimulated proliferation of human breast cancer cells**. *Eur J Gynaecol Oncol* 2004, **25**:175-177.
302. Okunieff P, Fenton BM, Zhang L, Kern FG, Wu T, Greg JR, Ding I: **Fibroblast growth factors (FGFS) increase breast tumor growth rate, metastases, blood flow, and oxygenation without significant change in vascular density**. *Adv Exp Med Biol* 2003, **530**:593-601.
303. Vane JR, Botting RM: **Anti-inflammatory drugs and their mechanism of action**. *Inflamm Res* 1998, **47 Suppl 2**:S78-87.
304. Beauparlant P, Hiscott J: **Biological and biochemical inhibitors of the NF-kappa B/Rel proteins and cytokine synthesis**. *Cytokine Growth Factor Rev* 1996, **7**:175-190.

305. Ruegg C, Zaric J, Stupp R: **Non steroidal anti-inflammatory drugs and COX-2 inhibitors as anti-cancer therapeutics: hypes, hopes and reality**. *Ann Med* 2003, **35**:476-487.
306. Voisard R, Fischer R, Osswald M, Voglic S, Baur R, Susa M, Koenig W, Hombach V: **Aspirin (5 mmol/L) inhibits leukocyte attack and triggered reactive cell proliferation in a 3D human coronary in vitro model**. *Circulation* 2001, **103**:1688-1694.
307. Tozawa K, Sakurada S, Kohri K, Okamoto T: **Effects of anti-nuclear factor kappa B reagents in blocking adhesion of human cancer cells to vascular endothelial cells**. *Cancer Res* 1995, **55**:4162-4167.
308. Heylen N, Baurain R, Remacle C, Trouet A: **Effect of MRC-5 fibroblast conditioned medium on breast cancer cell motility and invasion in vitro**. *Clin Exp Metastasis* 1998, **16**:193-203.
309. Lee TH, Avraham HK, Jiang S, Avraham S: **Vascular endothelial growth factor modulates the transendothelial migration of MDA-MB-231 breast cancer cells through regulation of brain microvascular endothelial cell permeability**. *J Biol Chem* 2003, **278**:5277-5284.
310. Scotton CJ, Wilson JL, Milliken D, Stamp G, Balkwill FR: **Epithelial cancer cell migration: a role for chemokine receptors?** *Cancer Res* 2001, **61**:4961-4965.

Appendix I: The FRET Technique

Appendix I: The FRET Technique

FRET, or Fluorescence Resonance Energy Transfer, is considered to be an advancement on the dual-colour confocal imaging technique, in which two distinct molecules can be immunolabelled with fluorophores that are detected at different emission light wavelengths. The intracellular positioning of each fluorophore relative to each other has been used to detect "co-localisation" or the positioning of two proteins in relatively close proximity to each other. Co-localisation is not indicative of actual physical contact, however, as the maximum spatial resolution of fluorescent microscopy, even on the confocal system is about 300nm. Considering that a globular protein of ~30kDa is estimated to be 3nm in diameter, it would be impossible to show protein-protein interaction with another such molecule using this method [1].

As MUC1 and ICAM-1 have already been shown to functionally interact with each other [2,3], we hoped that the concept could be furthered by using FRET to not only show the spatial relationship of MUC1 to ICAM-1 during heterotypic cell-cell adhesion, but also demonstrate the physical interaction of these molecules in a three dimensional reconstructed image.

FRET is based on the concept that a pair of fluorophores with overlapping emission and excitation wavelengths, for example cyan fluorescent protein (CFP) and yellow fluorescent protein (YFP) (Figure AppI.1A), can indicate physical association of two proteins, if each protein is labelled with one of the fluorophores [1]. In other words if ICAM-1 is labelled with CFP, and MUC1 is labelled with YFP, then the physical interaction of these two molecules should bring the CFP and YFP tags in close proximity to each other. If this proximity is within ~7nm [4] (or ~70Å [5,6]), and the CFP is excited with a laser set to a wavelength of ~436nm, instead of releasing the absorbed energy as fluorescent light at a longer wavelength (~474nm), the CFP will transfer energy to the YFP fluorophore (absorption at ~514nm), which will then release energy at its specific emission wavelength (~530nm) (Figure AppI.1B and www.zeiss.de). The reason why such close proximity is required for the energy transfer to occur, is that the efficiency ("E") of the energy transfer is dependent on the distance separating the two fluorophores ("Ro"). The Forster radius ("R") is the distance at which

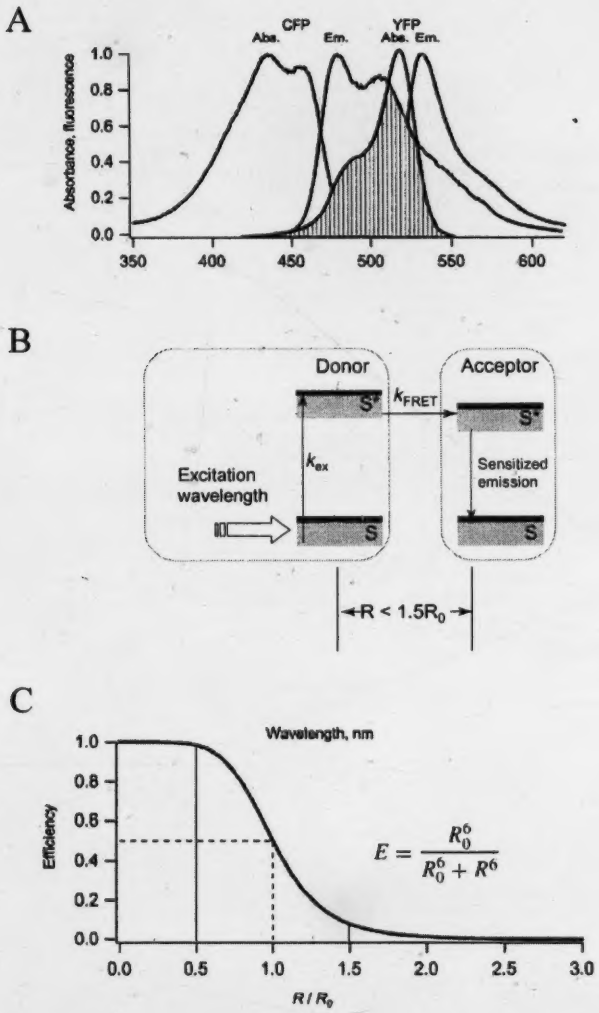

Figure AppI.1: Fundimental Concepts in FRET. (A) Diagram showing the overlapping emission and absorption spectra of CFP and YFP, which makes FRET possible between these two fluorophores. (B) Energy transfer between matched fluorophores. The donor fluorophore is excited with a specific wavelength of light, and the energy, instead of being released as fluorescence, is transferred to an acceptor fluorophore, which releases light at its own specific emission wavelength. (C) Representation of how distance between fluorophores (Ro) affects efficiency of energy transfer (E). "R" represents the Forster radius, or where the efficiency of energy transfer is at 50%. The maximum distance for FRET to occur is at 1.5 R/Ro, where the efficiency of energy transfer is ~1%, and typically calculates as ~7nm. Modified from [1,4].

energy transfer is ~50% efficient (Figure AppI.1C), and when Ro=R, the fluorophores are typically calculated to be 2-7nm apart (reviewed in [1,4-8]). Additionally, the efficiency of energy transfer is also affected by the positioning of the CFP and YFP dipoles in relation to each other, that is, they are assumed to be parallel. However, if the final conformation of the fluorphore-tagged protein is such that the fluorophore cannot rotate freely, or is locked at an angle where the dipoles of the CFP and YFP structures cannot align, FRET may not occur despite physical interaction of the two proteins being examined [1,6,7].

In this thesis, two FRET methodologies were used: (i) Acceptor fluorescence increase, in which the intensity of the YFP fluorescence was monitored (Figure AppI.2A), and (ii) Acceptor photobleaching and donor fluorescence increase, in which the acceptor fluorophore is destroyed by an intense laser light while it is in the excited state. As the YFP fluorophore can no longer accept energy from the donor fluorophore, the fluorescence intensity of the donor increases (Figure 2.3B). There are caveats to either method. The acceptor fluorescence method is mathematically challenging, as there is considerable "specific bleed through" of the donor fluorescence in the acceptor channel, and vice versa, as well as the donor and acceptor fluorescence in the FRET channel. These must be corrected for, as well as the background fluorescence that occurs in the raw images. Although the Metamorph software package handles the final calculation the background corrections must be handled manually, and great care must be taken to ensure the correct mathematical manipulations are being performed.

The relevant equations are:

FRET = RawFRET – [Acceptor - (Donor in Acceptor * Donor)] * [Acceptor in FRET]
–[Donor - (Acceptor in Donor * Acceptor)] * [Donor in FRET]
(From reference [9])

Or

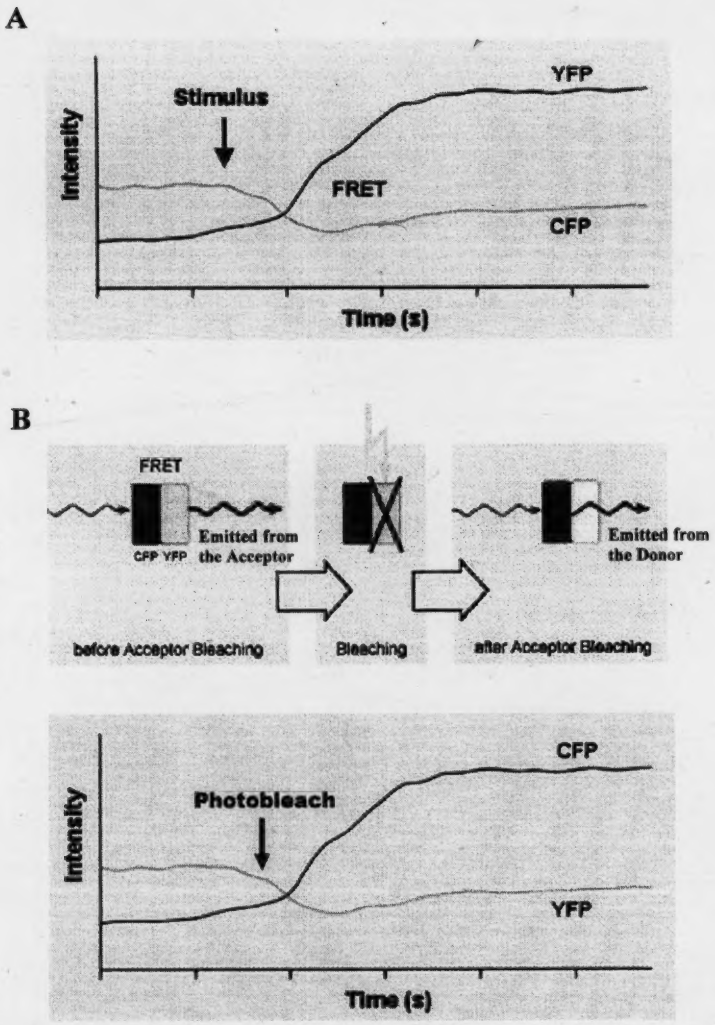

Figure AppI.2: Comparison of the Acceptor Fluorescence and the Acceptor Photobleaching FRET methods. (A) In the Acceptor Fluorescence method, the close proximity of the CFP fluorophore transfers energy to the YFP fluorophore, which subsequently fluoresces more intensely. Care must be taken to ensure that bleed through from other channels is not mistaken as a FRET signal. (B) In the Acceptor Photobleaching method, the fluorescence intensity of the donor fluorophore is monitored as FRET is abolished by destroying the acceptor fluorophore. The energy that is no longer being transferred to the acceptor by FRET is visualised as light at the emission wavelength of the acceptor. Modified from www.zeiss.de.

RawFRET = Bleed through of CFP + Bleed through of YFP + Actual FRET signal

Therefore, in order to obtain the actual FRET signal, corrections must be made for the bleed through.
[Conversations with Dr. Sun.]

The main drawback of the acceptor photobleaching method is that the acceptor fluorophore is destroyed. As such, it cannot be used to monitor living cells over time [6].

Taken together, it appears that the acceptor fluorescence method is more appropriate for live cell imaging over time, while the acceptor photobleaching method is simpler, as the increases in acceptor fluorescence intensity is monitored directly, without correction and the results are immediately visible, but only appropriate for fixed time points.

References:

1. Hink MA, Bisselin T, Visser AJ: **Imaging protein-protein interactions in living cells**. *Plant Mol Biol* 2002, **50**:871-883.
2. Kam JL, Regimbald LH, Hilgers JH, Hoffman P, Krantz MJ, Longenecker BM, Hugh JC: **MUC1 synthetic peptide inhibition of intercellular adhesion molecule-1 and MUC1 binding requires six tandem repeats**. *Cancer Res* 1998, **58**:5577-5581.
3. Regimbald LH, Pilarski LM, Longenecker BM, Reddish MA, Zimmermann G, Hugh JC: **The breast mucin MUCI as a novel adhesion ligand for endothelial intercellular adhesion molecule 1 in breast cancer**. *Cancer Res* 1996, **56**:4244-4249.
4. Bastiaens PI, Squire A: **Fluorescence lifetime imaging microscopy: spatial resolution of biochemical processes in the cell**. *Trends Cell Biol* 1999, **9**:48-52.
5. Emptage NJ: **Fluorescent imaging in living systems**. *Curr Opin Pharmacol* 2001, **1**:521-525.
6. Kenworthy AK: **Imaging protein-protein interactions using fluorescence resonance energy transfer microscopy**. *Methods* 2001, **24**:289-296.
7. De Angelis DA: **Why FRET over genomics?** *Physiol Genomics* 1999, **1**:93-99.
8. Heyduk T: **Measuring protein conformational changes by FRET/LRET**. *Curr Opin Biotechnol* 2002, **13**:292-296.
9. Universal-Imaging-Corporation: *Meta Imaging Series MetaMorph FRET Analysis Drop-In Manual*. USA: Molecular Devices; 2003.

Appendix II: Transwell Development Data

Appendix II: Transwell Development Data

Much of the early work using the Transwell system was done using the EAhy926 cell line, which allowed multiple "survey" experiments to be done relatively quickly, without the complications of primary cell culture; primary endothelial cells must constantly be harvested from fresh umbilical cords, as their phenotype alters after the fifth passage, and need special growth supplements. However, questions were raised as to whether this cell line was properly representative of *in vivo* endothelial cells, as it is a fusion hybrid of HUVECs and the A549 lung carcinoma cell line. While convenient for the initial studies, the EAhy926 cells appeared to have a different complement of cell-surface adhesion molecules in comparison to HUVECs, and ultimately did not produce the same dramatic differences when comparing tumour cell migration through unstimulated endothelial cells and those treated with inflammatory cytokines.
Another key difference between the developmental work and the final experimental paradigm was whether Matrigel or gelatin was used for coating the Transwell membranes. Ideally, Matrigel would have better represented the *in vivo* situation, as it is generally considered to be similar in composition to the physiological basement membrane found underneath endothelial cells, and expected to send relevant integrin-based signals into the cells plated over it. However, Matrigel is frequently used in angiogenesis assays, where the integrin signals tell endothelial cells to form cord-like growths in preparation of vascular development. While EAhy926 cells grew as monolayers over Matrigel, HUVECs formed cords; no tumour cells could be dropped on the endothelial "luminal" surfaces. Gelatin, or denatured collagen, was used routinely to culture HUVECs on tissue culture plastic, and seemed to have little effect on MCF-7 cell morphology. Thus, it was deemed an appropriate matrix to use in the final assay, if for no other reason than to ensure endothelial adhesion to the Transwell membranes.

AppII.1 Selected Methods

AII.1.1 Selection of Transwell Inserts to use.

These are available in many diameters and many pore sizes. In general, use the 6.5 mm diameter membrane insert, with 8 μm pores. This accommodates passage of epithelial cell nuclei. For cells with smaller nuclei, such as leukocytes, 3 μm pore sizes can be used. These inserts may be purchased from Fisher Scientific (Corning Costar Brand).

AII.1.2 Coating Transwell Membranes with Matrix

The choice of matrix depends on what cell types are to be used, and what is being tested. Matrigel (available from BD Biosciences, or Sigma as EHS matrix) is approximately equivalent to the mixture of proteins one would expect to be in a basement membrane. Collagen I or III would be more like stromal matrix, and gelatin, or denatured collagen, is a basic generic matrix which just gives sensitive cell types something to hold on to. While Matrigel seems to be the best choice, it sends very specific integrin signals into the cells layered on it, for example, it appears to instruct HUVECs to form "cords", perhaps in preparation for vascularization. This effect can be adjusted by diluting the Matrigel, or adding other matrix protein, but that does take some tweaking.

Method for Matrigel:

- Unpack the 24 well plate containing the inserts and place in a tissue culture hood.
- Soak a pair of tweezers in 70% EtOH for 30 minutes, or have the tweezers autoclaved.
- Thaw the Matrigel at 4°C, and always keep the solution on ice. Failure to do this will result in the polymerization of the Matrigel inside the bottle, and it will be impossible to pipette. Aliquot the Matrigel and store at -20°C for the long term. Keep one aliquot at 4°C for short term use.

- In a small sterile Petri dish, which is on ice, dilute the Matrigel 1:100 in sterile PBS. One at a time, pick up a Transwell with the tweezers and dip the bottom of it into the Matrigel. Give it a quick tap to shake of excess fluid and then place it back into the 24 well plate.
- Push the 24 well plate to the back of the hood and let the Transwells dry.
- In a small sterile Petri dish, again on ice, dilute the Matrigel 1:30 in sterile PBS. Pipette 50μL of this solution into the upper chamber of each Transwell. Gently tap the side of the 24 well plate to make sure the Matrigel coats the entire surface of the membranes. At this point it can be seen that there is a significant meniscus effect. This can be minimized by carefully overlaying 200 μL of sterile water over the Matrigel.
- Push the plate to the back of the hood and let the water and Matrigel dry completely. This may take a few days depending on the air flow.
- Once dry, the coated membranes can be stored at 4°C for a few days until they are needed. Prior to use, the Matrigel must be rehydrated in culture media. Simply add about 100μL into the upper chamber, and let it sit for 30 minutes at room temperature. This media is aspirated prior to cell addition.

Method for Gelatin:

- Gelatin is prepared as a 0.1% (w/v) solution in water (Sigma Cat# G-1890). It must be heated to 37°C for about 30 minutes to initially dissolve it, then it is autoclaved to sterilize it.
- Working in a tissue culture hood, a small volume of gelatin is transferred into a sterile Petri dish.
- One at a time, transwells are picked up using sterile tweezers, and the bottoms are dipped into the gelatin. They are given a quick tap to shake off excess fluid, are replaced into the 24 well dish, then allowed to dry.
- 50 μL of gelatin are pipetted into the upper chamber of each transwell, and the side of the 24 well plate is gently tapped to ensure proper coating of the membrane.
- The gelatin is allowed to dry.

- The coated Transwells can be stored at 4°C for a few days until needed.

AII.1.3 Plating Cells.

Method for Plating Cells on the Bottom of a Transwell:

Note: This doesn't work so well for larger diameter membranes.

- Dilute the cells in media so that the final total number of cells desired on the bottom of each membrane will be contained in a volume of 75μL.
- Using sterile tweezers, lift the Transwell out of its well, and carefully pipette the 75μL drop into the middle of the well. DO NOT allow it to touch the sides of the well, or it will spread everywhere, and be impossible to fix.
- Quickly place the Transwell back in the well, over the drop, so that the fluid is held in place by surface tension between the Transwell and bottom of the 24 well plate.
- Quickly finish plating all the other Transwells, as desired.
- Put the lid on the 24 well plate, and flip it upside down.
- Put the 24 well plate, upside down, into a 37°C incubator and leave it there overnight. If the surface tension is insufficient to prevent the media from leaking away from the Transwell surface, either shorten the time the plate is upside down (at least long enough for gravity to pull the cells to the membrane, and for the cells to attach), or decrease the volume of the drop. If the cells dry out, they will die.
- The next day, flip the plate back over, and proceed with the experiment.

Method for Plating Cells on the Upper membrane surface of a Transwell:

- Dilute the cells in media so that the final total number of cells desired on the membrane will be in a volume of 200 μL. In general, 5 x 10^5/mL will produce a confluent monolayer. This may have to be adjusted according to how fast the cells grow. If they overgrow, they may peel up and take the matrix coating with them. Also be aware, that if the 8μL pore size is used, there really is no way to

prevent cells seeded on the upper membrane surface from migrating to the lower membrane surface.

- Pipette 200 µL of cell suspension into the upper chambers of each Transwell.
- Pipette 500 µl of media into the lower chamber of each Transwell.

Let the system equilibrate at 37°C overnight. The next day, proceed with the experiment.

AII.1.4 Detection of Migratory Test Cells.

The number of cells added is arbitrary, but in general, remove the media in the upper chamber, then add 200µL of test cell suspension, at 1 x 10^5/mL. If desired, the media in the lower chamber can also be removed, and replaced with media containing chemoattractants, etc. Usually, the plate is put back in the incubator for 24 hours, and again, this time will vary based on the cells used. It is a good idea to measure the doubling time of the cells, and factor that into consideration, since one wants to be relatively sure that the increased number of cells on the bottom of the Transwell membrane is due to migration only, and not division of migrated cells. Proper controls to measure any inadvertent cell division will also minimize this effect on the data.

There are several published methods for cell quantitation. One option is to pre-load the test cells with a fluorescent vital stain, so that they can be distinguished from other cells in the system. Examples of such stains are BCECF (good for about 4 hours of incubation) and Cell Tracker Green (good for a few generations), available from Molecular Probes. The fluorescence can then be quantitated either by counting the cells on the underside of the membrane (after swabbing the tops with a Q-Tip), or by lysing the cells and determining the relative fluorescence in a fluorescent plate reader. Cells may also be colourimetrically immunostained and manually counted. This is not practical for cell counts above 1000 (extreme eyestrain), but also allows visualization of the molecule of interest.

Basic Method:

- When the predetermined incubation time is over, remove the 24 well plate from the incubator and aspirate the media from both the upper and lower Transwell chambers.
- Wash both sides of the membranes 1X with PBS.
- Fix the cells by adding 200µL of 2% Formaldehyde in PBS into the bottom chamber of each Transwell. Let sit for 15 minutes.
- Wash both sides of the Transwell membranes 3X with PBS.
- Block the cells with 2% BSA in Tris Buffered Saline (TBS) with 0.05% Tween 20, at 4°C, overnight.
- Choose a primary antibody against a molecule of interest on the test cells, that will not be on any other cell type. Dilute the antibody to its working concentration in the 2% BSA solution. Add 200µL into the bottom chamber of each Transwell. Check to make sure the antibody solution is contacting the undersides of each Transwell. Incubate at room temperature for at least an hour.
- Wash both sides of the Transwell membrane 3X with TBS.
- Dilute an alkaline phosphatase conjugated secondary antibody in the 2% BSA solution. Add 200µL of this to the bottom chamber of each Transwell. Incubate at room temperature for at least an hour.
- Wash both sides of the Transwell membrane 3X with TBS.
- Add 200 µL of NBT/BCIP colourimetric substrate to the bottom of each Transwell membrane. Roche (Cat # 1 681 451).
- Watch the colour reaction develop. Checking the plate with a microscope may help. Do not let it go so long that background staining occurs, or this will cause problems with quantitation. In general, this will produce a very good stain. The optics of the microscope can be fiddled with if there isn't good contrast.
- When the desired level of staining is achieved, wash out the 24 well dish with tap water. Be careful not to flush the Transwells out of the dish, because if they fall into the sink, the impact will make the membranes crack.
- Working one Transwell at a time, take a Q-Tip, and pinch the cotton so that there is a bit of a flat edge to it. Pick up a Transwell and swab the upper membrane

surface, using the flattened edge of the cotton to get into the corners. Be gentle enough so that the membranes are not stretched and weakened, as that will limit their lifespan. The Transwells can be allowed to dry at this point, and can be stored at room temperature for a few days until they are counted.

- Place a microscope slide over the objective of an inverted microscope.
- Put a Transwell on top of the slide.
- Count all the stained cells in at least 5 microscopic fields, or 50% of the membrane. The data can be presented as raw, converted to total membrane, or converted to relative numbers, where a selected condition = 1.

AII.1.5 Cleaning the Transwells for Re-Use.

- Swab both sides of the membrane with 1% SDS.
- Soak the Transwells in 1% SDS overnight in a 24 well plate, as taking them out and putting them in a beaker results in damaged membranes.
- Swab both sides of the membranes again with 1% SDS.
- Rinse out the SDS with tap water. Rinse the Transwells 2X in Nanopure water. Let them soak for an hour in nanopure water.
- Rinse the Transwells in 70% EtOH.
- Rinse the Transwells in Nanopure water.
- Let the Transwells dry under UV in a tissue culture hood. Inspect the membranes for any that may have cracked. Pick them out and throw them away.
- They are now ready for re-use. Tape the lid shut to prevent contamination during storage. Transfer them to a fresh 24 well plate when they are next coated with matrix.

AII.1.6 Embedding Cells in Collagen Gels

Vitrogen 100, which is acid solubilized bovine collagen I, was kept at 4°C during handling to prevent premature gelling. A $1/10^{th}$ volume of 10X culture media was added, and the pH adjusted with NaOH until the phenol red indicator was around 7.0. This was

confirmed by pipetting a small volume of the sterile solution onto a pH indicator strip. Trypsinized and media-quenched cells were dispersed in the collagen by adding the total number of cells required in a small volume to the collagen, then gently pipetting up and down, avoiding the formation of bubbles. 0.5 to 1mL volumes were added to each well of a 24 well plate, and put into a 37°C incubator for half an hour. At this time, the gels were again gently pipetted to re-suspend cells which may have settled to the bottom of the well before either allowing the gels to completely set at 37°C for 2 hours. If desired, the collagen could be added to Transwell chambers. Media was pipetted over the set gels to maintain hydration.

AppII.2 Selection of Tumour Cell Line

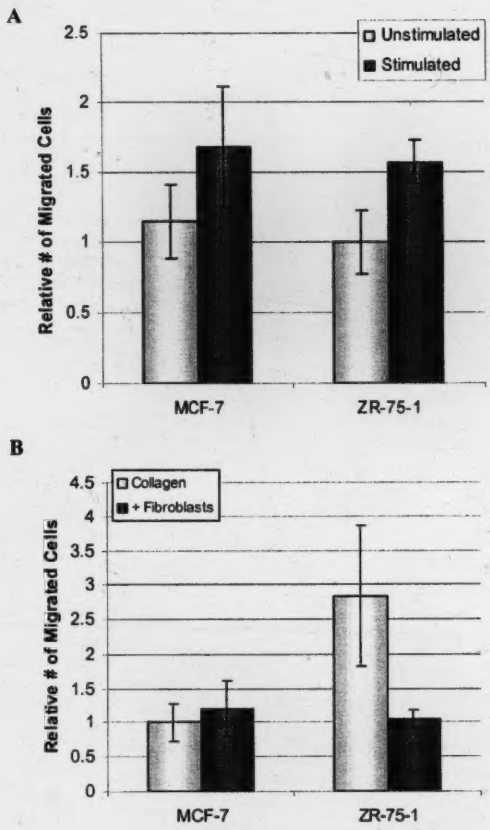

MCF-7 Cells were selected for later experiments since their migration did not appear to be inhibited by primary fibroblasts. When tested for migration through a monolayer of EAhy926 cells plated over Matrigel in the Transwell system, EAhy926 and MCF-7 cells exhibited similar behaviours (A). However, when these cell types were tested for invasion through collagen gels seeded with primary breast fibroblasts (B; also on a Transwell membrane), the ZR-75-1 cells appeared to be inhibited. ZR-75-1 cells carry mutations such as PTEN, and do not appear well-polarised on tissue culture plastic, thus the explanation for their migration being inhibited by fibroblasts would be difficult to ascertain. As this would have confounded later analyses, it was decided that MCF-7 cells would be easier to use. "Stimulated" refers to the presence of TNF-α and IL-1β.

AppII.3 Effect of MCF-7 Concentration and Migration Time

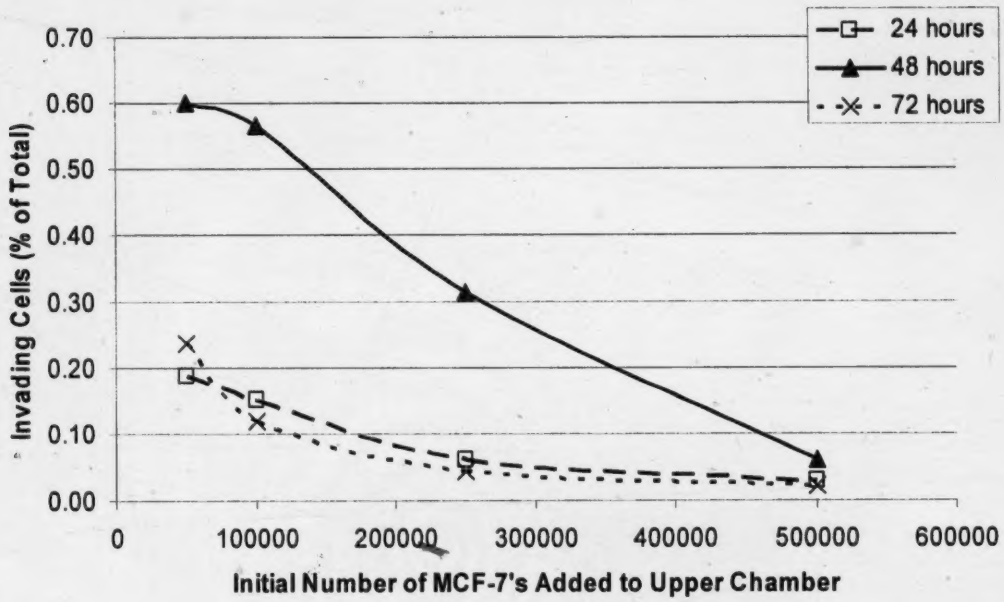

The most reliable cell counts appeared to be generated by adding lower numbers of cells to the upper chambers of Transwell inserts, and allowing the cells 24 hours to transmigrate cytokine stimulated EAhy926 monolayers plated on Matrigel. At 72 hours, the media had grown considerably acidic, and the low numbers may be a result of cell death. Although there appears to be very high migration at 48 hours, for all cell concentrations tested, the doubling time for MCF-7 cells in this culture system was measured as 36.8 hours. Thus, the final numbers would have to be adjusted for cell division, a complicated and difficult to justify calculation at best. At 24 hours, enough cells had migrated through to make the counts significant, and the effect of cell proliferation would have been minimized.

AppII.4 Placement of Primary Fibroblasts in the Transwell System

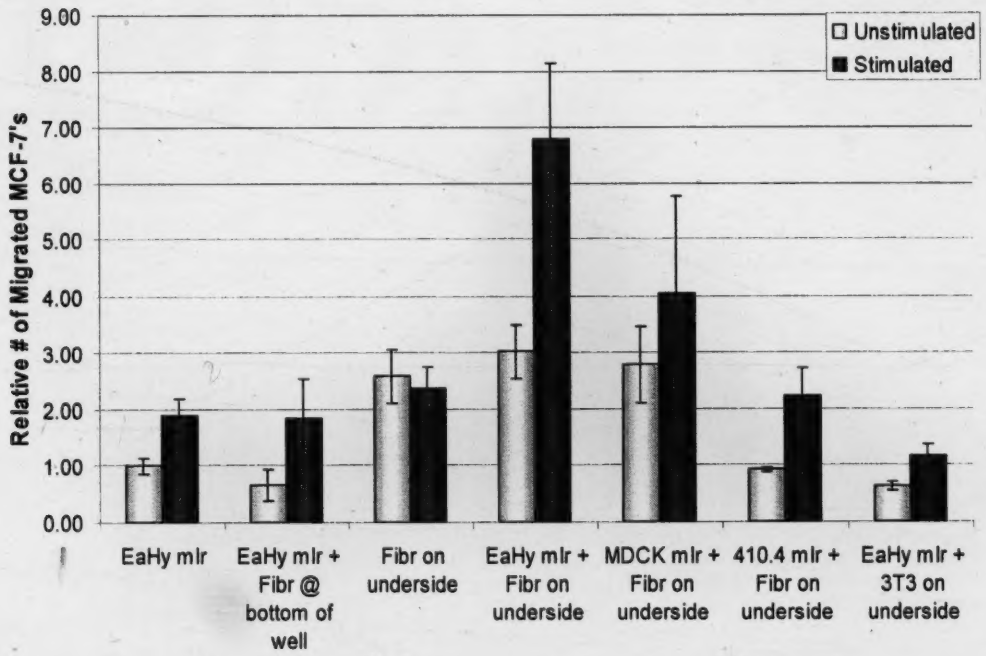

Primary human fibroblasts required close proximity to the endothelial cells in order to influence MCF-7 cell TEM_E. Fibroblasts plated directly on the underside of the Transwell membrane, immediately adjacent to the endothelial cells, had a greater effect on tumour cell migration in comparison to fibroblasts on the bottom of the wells of the 24 well plate. Also, endothelial cells were absolutely required to trigger high levels of TEM_E. Primary human fibroblasts could not be substituted with murine fibroblasts (NIH 3T3 cells). At first it seemed that the fibroblasts needed physical contact with the endothelial cells to exert their effect, however later experiments indicated that the close proximity of the fibroblasts was most likely causing higher local concentrations of secreted factors that were stimulating ICAM-1 expression on the endothelial cells, as fibroblast conditioned media + human ICAM-1 transfected NIH 3T3 cells could mimic this effect. "Stimulated" refers to the presence of TNF-α and IL-1β.

AppII.5 Physical Presence of Fibroblasts vs. Matrix Conditioning

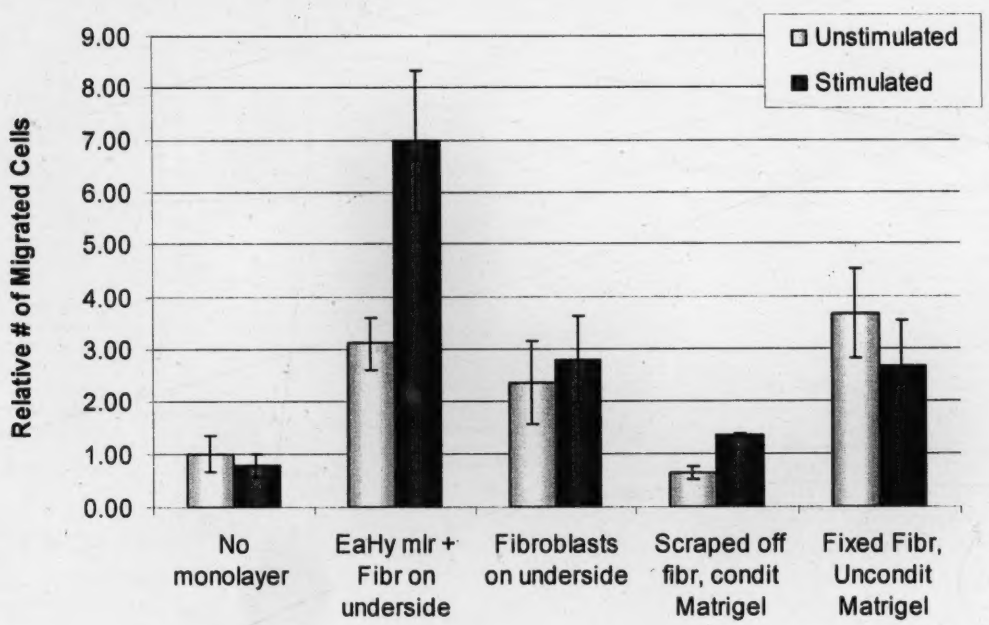

The physical presence of the fibroblasts appears to be more important that factors that may have been secreted into the Matrigel. The original goal of this experiment was to test for any indications that fibroblasts might be acting by secreting matrix metalloproteases (for example) into the Matrigel. The physical presence of the fibroblasts was separated from factors they might be secreting, by scraping them off the underside of the Transwell membrane after incubating them with Matrigel coated on the top of the membrane, or by allowing them to adhere and fixing them (ethanol at -20°C, followed by complete dehydration) before coating the Matrigel on top. Since the latter technique produced results similar to having live fibroblasts and presumed conditioned Matrigel together, it was concluded that something present on the fibroblast surfaces was important in regulating TEM_E. This effect appeared to be separate from the fibroblasts' effect on the EAhy926 cells. "Stimulated" refers to the presence of TNF-α and IL-1β.

AppII.6 Selection of Fibroblasts

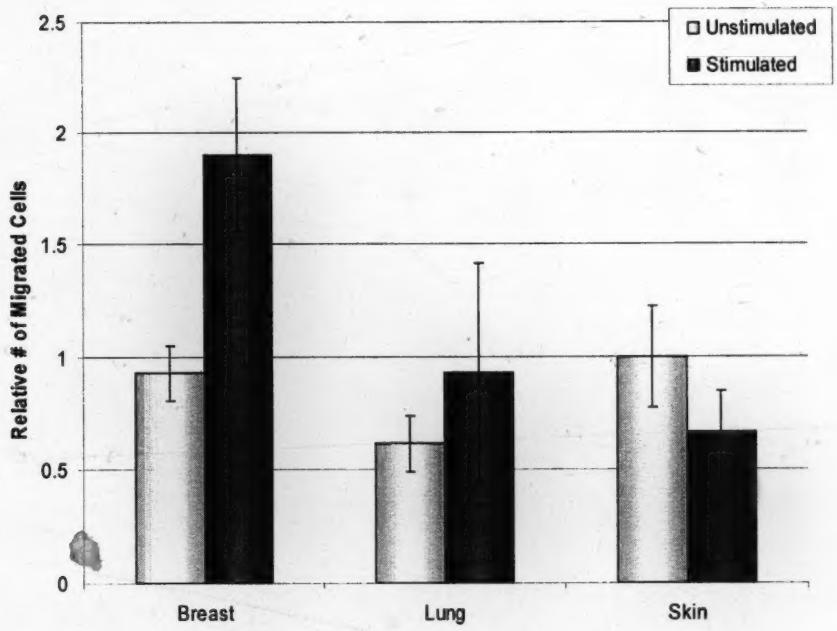

Primary Human Breast Fibroblasts produced the most measurable effects on TEM_E. Consideration was given to the possible implications the fibroblast effect might have on the preference of breast cancer to metastasize to particular tissues. The lung fibroblasts were the MRC-5 human male embryonic cell line and the skin fibroblasts were primary cells purchased from the ATCC (gift of Dr. Michael Hendzel). As breast cancer tends to metastasize to the lung more than to the skin, yet this was not reflected by the fibroblasts used, it was decided to perform future experiments using primary breast fibroblasts, and focus the study on the adhesion molecules involved, specifically, the contribution of ICAM-1 to TEM_E. "Stimulated" refers to the presence of TNF-α and IL-1β.

AppII.7 Selection of Matrix

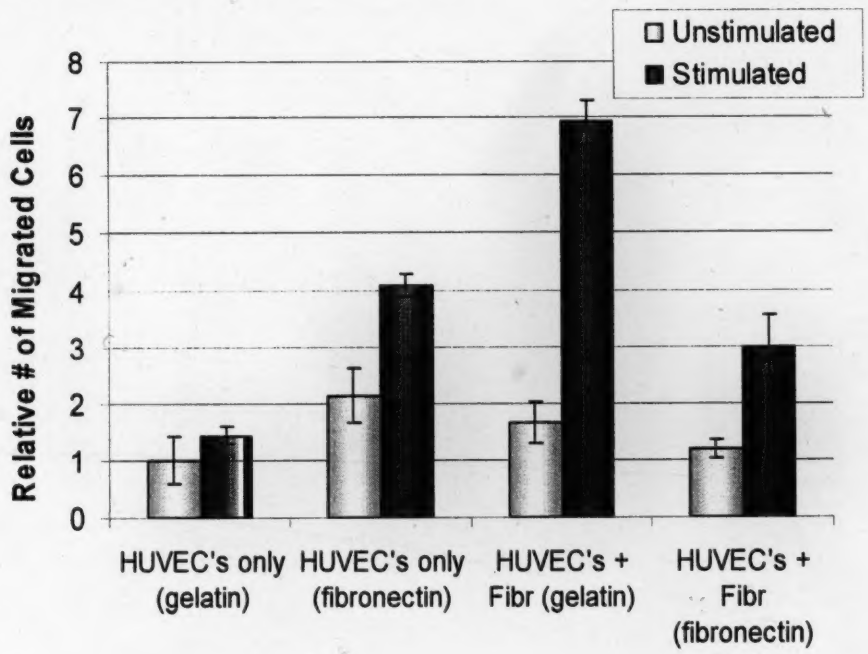

Gelatin does not appear to interfere with TEM_E. Plasma fibronectin was tested as an alternate to Matrigel when the system was changed over to HUVECs instead of EAhy926 cells. Since fibronectin is often described as promoting cell migration, for example in wound healing, it was considered as a possible coating for the Transwell membranes. However, it seemed to inhibit the synergistic effect of HUVECs and fibroblasts on MCF-7 cell TEM_E, that was seen on gelatin. Collagen (Vitrogen 100) also could not be used as it promoted the contraction of the fibroblasts into clumps (visualised directly on the Transwell membrane after Ponceau S staining; not shown), rather than allowing them to be distributed evenly over the Transwell surface. "Stimulated" refers to the presence of TNF-α and IL-1β.

AppII.7 Inclusion of Endothelial Cell Growth Supplement

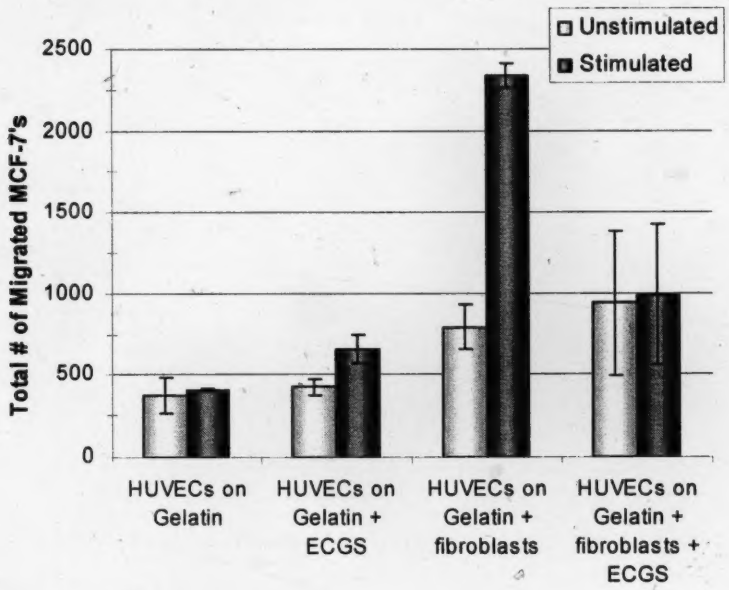

Endothelial Cell Growth Supplement (ECGS) was not included in the Transwell Assay. ECGS is an extract of bovine brain that is routinely used in HUVEC cell culture, and usually promotes HUVEC growth. However, it appeared to interfere in the synergistic effect of co-culturing HUVECs with fibroblasts. Instead of including it in the assay, HUVECs were plated at high density (5 x 10^5/mL, 200μL added to the upper chamber of the Transwell) to ensure a confluent monolayer. "Stimulated" refers to the presence of TNF-α and IL-1β.

Appendix III: Calcium Oscillation Development Data

Appendix III: Calcium Oscillation Development Data

AIII.1 MUC1 Cells Oscillate on Contact with ICAM-1 Cells, Regardless of their Adhesive State

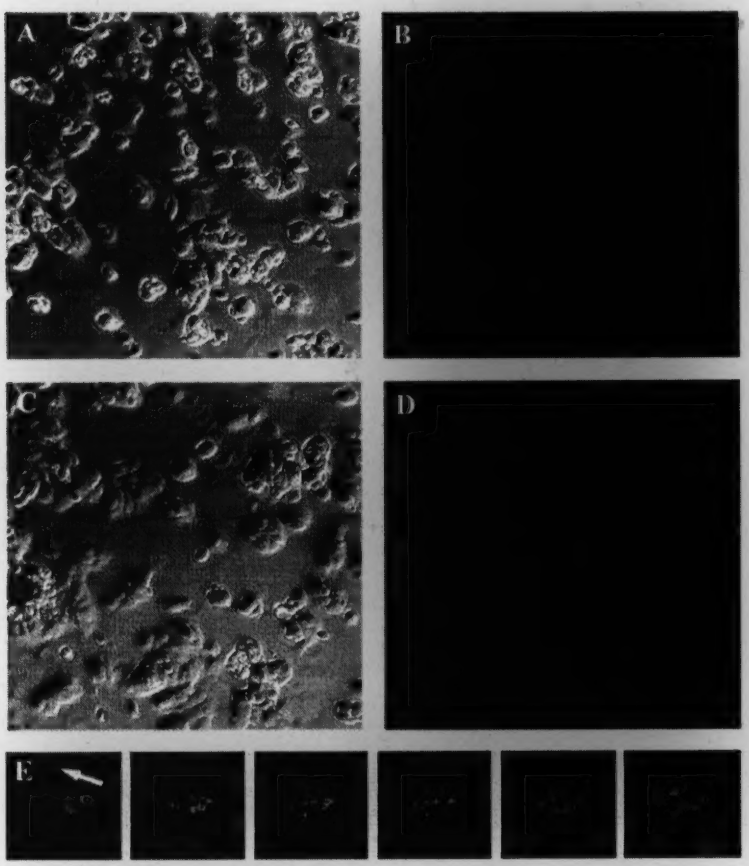

The calcium oscillation assay was routinely performed with adherent, Fluo-3 loaded, MUC1-positive cells, as this allowed the microscope to be properly focussed on the responding cells during the entire assay. However, in the Transwell model, the ICAM-1 bearing cells were adherent, and the MUC1 bearing cells were added as a cell suspension. To confirm that non-adherent MCF-7 cells would also display an oscillatory response on contact with ICAM-1 bearing cells, NIH ICAM's were plated on tissue culture plastic, and MCF-7 cells were trypsinized after loading with Fluo-3, and pipetted

over the NIH's. Not only did the MCF-7 cells oscillate on contact with NIH ICAM's, but not NIH Mocks, the calcium signal also appeared to propagate as a wave through clustered MCF-7 cells, perhaps indicating communication via IP3 and gap junctions. This raises the possibility that once the putative MUC1 signal is triggered, it can be transmitted to other cells in a tumour embolus that are not necessarily in contact with ICAM-1 on an opposing cell. (A) DIC image of MCF-7 cells plated on glass. (B) Fluorescent image of intracellular calcium detected in MCF-7 cells after being in contact with NIH 3T3 ICAM-1 cells for 130 seconds. Magnification = 20X. (C and D) DIC and fluorescent images of MCF-7 cells before and after 130 seconds contact with NIH 3T3 mock cells. (E) Pseudocolored images of calcium fluorescence intensity over time in clustered MCF-7 cells added to plated NIH 3T3 ICAM-1 cells. This demonstrated that adhesion of MCF-7 cells to the dish was not necessary for a calcium-based response to occur. Intensity of fluorescence is indicated by the color change, and following the order of wavelength in the visible spectrum, where red is the most intense, and violet the least. The white arrow indicates the direction of the calcium wave propagation through the cluster, and each frame was taken 6 seconds after the previous image.

AIII.2 Calcium Oscillations Appear to be Affected by Adhesion Substrate

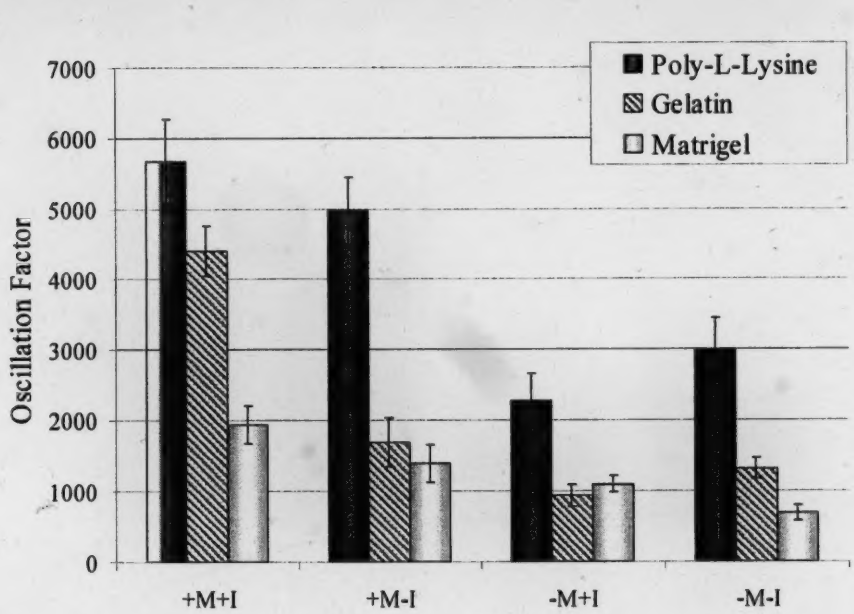

The calcium-based oscillatory response to ICAM-1 in MUC1-transfected 293T cells varies with adhesion substrate. Although we were only looking for a suitable adhesion substrate, we found that the oscillatory responses of cells differed, depending on which matrix was used. MCF-7 cells had an absolute requirement for FBS, and did not oscillate on any other matrix. MUC1-transfected 293T cells were less stringent in their requirements, however these cells would not oscillate significantly on FBS-coated glass. Interestingly, the matrices on which MUC1-transfected 293T cells did respond, there was an apparent correlation between the intensity of oscillation and the degree to which integrin signalling would be predicted. Specifically, the highest oscillations were seen on

poly-L-lysine, which is traditionally thought to allow cells to adhere by charge rather than integrin activation . Moderate oscillatory responses were observed on gelatin, which is denatured collagen, and perhaps could be considered to be "stromal-like". In our Transwell experiments (Chapter 3), gelatin was an ideal matrix that on its own, appeared to neither inhibit nor promote 293T migration. Matrigel, which is frequently described as reconstituted basement membrane, contains many proteins shown to promote polarisation of epithelial cells, for example, laminins [1,2]. On this adhesion substrate, the oscillatory response of the MUC1-transfected 293T cells was significantly suppressed. It is tempting to speculate that a microenviroment which favours migration or does not actively promote cellular polarisation is more permissive for what we believe to be a pro-migratory signal triggered by the MUC1/ICAM-1 interaction. (A) 293T cells plated on the different matrices display cell morphologies consistent with the assumptions of how the cells may be adhering to the coatings. Poly-L-lysine, assumed to promote cell adhesion by charge rather than integrin binding, shows clumped cells that did not spread out over the glass. Cells spread on gelatin and Matrigel, suggesting some degree of integrin engagement. (B) Relatively high oscillatory responses were seen on poly-L-lysine, regardless of the presence of transfected MUC1 (M) or ICAM-1 (I). Calcium-based responses are suppressed on Matrigel. Intermediate responses were seen on gelatin. This substrate not only produced the greatest differences between the +M+I condition, and those where M and/or I were missing, but also most closely matched the Transwell experimental conditions. Data are means ± SEM, n = 120.

AIII.3 Development of the Oscillation Factor.

A

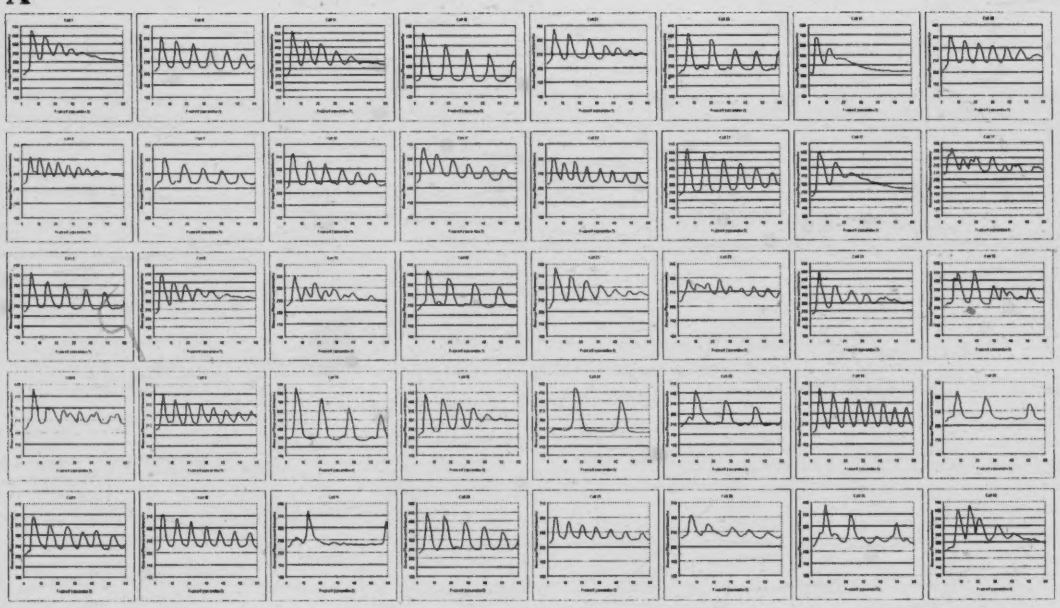

B

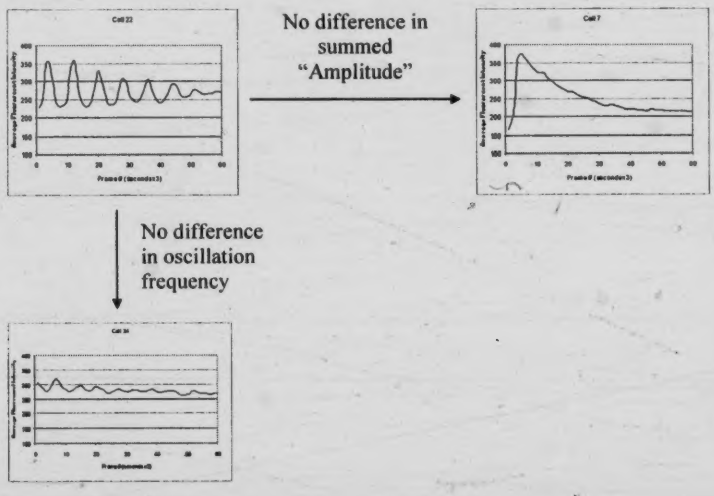

The Oscillation Factor allows comparisons between non-synchronised cell populations, and differentiates oscillatory responses from non-oscillating calcium flux. Although we did notice a wave of calcium-based response in suspended MCF-7 cells, the oscillations were never synchronized in suspended or adherent cells, and tracings of fluorescent intensities over time varied greatly from cell to cell. This

presented a problem for quantitation and comparisons between different experimental conditions. In the literature, other authors either averaged data points and plotted them with error bars, a tactic that only worked with synchronized populations, such as cardiac muscle cells, or selected representative tracings from single cells, which we felt would introduce too much subjective bias in our data. Comparisons of amplitude or frequencies did not adequately reflect obvious differences in the data. Consequently, we multiplied an "amplitude factor", which was the sum of the deviations of actual data points from a "LOGEST" trendline automatically calculated by MS Excel, by the frequency, or number of oscillation cycles. Using a trendline plotted through the data, rather than the actual summed amplitude, eliminated bias introduced by the sometimes large variations in background fluorescence (i.e. baseline readings could vary from 200 to 500 fluorescence intensity units) that may have occurred from slight differences in loading, removal of extracellular Fluo-3, or inter-operator technique, and also allowed us to use an Excel template to rapidly convert the tracings from 120 individual cells into a single mean "oscillation factor" ± SEM, and perform statistical comparisons between different test conditions. (A) Fluorescence intensity tracings of 40 individual cells. The cells are not synchronized, and there are differences in both the amplitude and frequencies of the oscillatory responses. Selection of a "representative" tracing could introduce bias. (B) Demonstration of why the oscillation factor is necessary for comparisons. Although all three tracings are clearly different, if only the frequencies or amplitudes are compared, the numerical results may show very little difference.

References:

1. Bissell MJ, Bilder D: **Polarity determination in breast tissue: desmosomal adhesion, myoepithelial cells, and laminin 1**. *Breast Cancer Res* 2003, **5**:117-119.
2. Muschler J, Lochter A, Roskelley CD, Yurchenco P, Bissell MJ: **Division of labor among the alpha6beta4 integrin, beta1 integrins, and an E3 laminin receptor to signal morphogenesis and beta-casein expression in mammary epithelial cells**. *Mol Biol Cell* 1999, **10**:2817-2828.